

**PHARMACOMETRICS FOR TREATMENT  
OPTIMIZATION AND  
DRUG DEVELOPMENT IN ONCOLOGY**

Aurelia H.M. de Vries Schultink

The research in this thesis was performed at the Departments of Pharmacy & Pharmacology of the Netherlands Cancer Institute – Antoni van Leeuwenhoek hospital, Amsterdam, the Netherlands and in collaboration with other institutes.

Printing of this thesis was financially supported by:

The Netherlands Cancer Institute  
Merus N.V.

**ISBN**

978-94-6323-566-2

**Design/lay-out**

Suzan Crijns

**Print**

Gildeprint, Enschede

© Aurelia H.M. de Vries Schultink, 2019

**Pharmacometrics for treatment  
optimization and drug development  
in oncology**

*Farmacometrie voor optimalisatie van behandelingen en  
geneesmiddelontwikkeling in de oncologie  
(met een samenvatting in het Nederlands)*

**Proefschrift**

ter verkrijging van de graad van doctor aan de Universiteit Utrecht op gezag van de rector magnificus, prof. dr. H.R.B.M. Kummeling, ingevolge het besluit van het college voor promoties in het openbaar te verdedigen op woensdag 29 mei 2019 des middags te 2.30 uur

door

**Aurelia Hanneke Maria de Vries Schultink**

geboren op 16 januari 1988

te Rotterdam

Promotoren: Prof. dr. A.D.R. Huitema  
Prof. dr. J.H. Beijnen

Copromotor: Dr. T.P.C. Dorlo



## CONTENTS

Preface		9
<b>CHAPTER 1</b>	<b>PHARMACOKINETICS AND PHARMACODYNAMICS: TAMOXIFEN</b>	<b>13</b>
1.1	Effects of pharmacogenetics on the pharmacokinetics and pharmacodynamics of tamoxifen. (review) <i>Clin Pharmacokinet. 2015 Aug;54(8):797-810</i>	15
1.2	An Antiestrogenic Activity Score for tamoxifen and its metabolites is associated with breast cancer outcome. <i>Breast Cancer Res Treat. 2017 Feb;161(3):567-574</i>	49
1.3	Therapeutic Drug Monitoring of endoxifen as an alternative for CYP2D6 genotyping in individualizing tamoxifen therapy. <i>Breast. 2018 Aug 22;42:38-40 [Epub ahead of print]</i>	71
1.4	Prospective evaluation of Therapeutic Drug Monitoring of Endoxifen: feasibility of observational and randomized trials. <i>To be submitted</i>	81
<b>CHAPTER 2</b>	<b>PHARMACOKINETICS AND PHARMACODYNAMICS: MCLA-128</b>	<b>101</b>
2.1	Translational PK-PD modeling analysis of MCLA-128, a HER2/HER3 bispecific monoclonal antibody, to predict clinical efficacious exposure and dose. <i>Invest New Drugs. 2018 Dec;36(6):1006-1015</i>	103
2.2	Populations pharmacokinetics of MCLA-128, a HER2/HER3 bispecific monoclonal antibody, in patients with solid tumors. <i>Submitted</i>	127

<b>CHAPTER 3</b>	<b>PHARMACODYNAMICS: TOXICITY</b>	<b>149</b>
3.1	Pharmacodynamic modeling of adverse effects of anti-cancer drug treatment. (review) <i>Eur J Clin Pharmacol. 2016 Jun;72(6):645-53.</i>	<b>151</b>
3.2	Pharmacodynamic modeling of cardiac biomarkers in breast cancer patients treated with anthracycline and trastuzumab regimens. <i>J Pharmacokinet Pharmacodyn. 2018 Jun;45(3):431-442</i>	<b>175</b>
3.3	Neutropenia and exposure to docetaxel in metastatic castration resistance prostate cancer patients: a meta-analysis and evaluation of a clinical cohort. <i>Cancer Med. 2019 Feb 22 [Epub ahead of print]</i>	<b>201</b>
3.4	Age-associated hematological toxicity in metastatic castration-resistant prostate cancer patients treated with docetaxel in clinical practice. <i>Drugs Aging. 2018 Feb 8 [Epub ahead of print]</i>	<b>223</b>
<b>CHAPTER 4</b>	<b>CONCLUSIONS &amp; SUMMARY</b>	<b>239</b>
	Conclusions & Perspectives	<b>241</b>
	Summary	<b>251</b>
	Nederlandse samenvatting	<b>259</b>
<b>APPENDICES</b>		<b>267</b>
	List of author affiliations	<b>269</b>
	Dankwoord	<b>274</b>
	List of publications	<b>276</b>
	Curriculum vitae	<b>279</b>





## PREFACE

In 2018 an estimated number of 18 million people worldwide were diagnosed with cancer and, in the same year, an estimated 9.6 million people died as a consequence of the disease.<sup>1</sup> Given the high mortality and incidence of cancer, extensive efforts are increasingly being made to develop new and better drugs and to improve treatment with existing drugs. Data and data analysis are essential for the drug development process, and even beyond registration and clinical use of the drug, collection and analysis of data continue, to further optimize treatment. Data on pharmacokinetic (PK) and pharmacodynamic (PD) properties of a drug provide information on the dynamics of drug concentrations in the body over time (PK) and on both the desired and undesired (toxic) effects of a drug (PD). Identification and quantification of PK-PD relationships is the cornerstone of quantitative clinical pharmacology research, also known as pharmacometrics. In the field of pharmacometrics, mathematical and computational sciences are intertwined with pharmacology, biology and physiology. It entails the development of mathematical and statistical models to describe, characterize and predict (simulate) the PK and PD properties of drugs in different populations.<sup>2</sup> Pharmacometrics is being used increasingly to improve the clinical application of drugs and support drug development decision making.<sup>3</sup>

In this thesis the application of modeling and simulation methods to support drug development and to improve application of existing therapies in the area of oncology is described.

**Chapter 1** describes different aspects of treatment optimization of tamoxifen, an anti-estrogenic drug, used to treat estrogen receptor-positive breast cancer. The focus of this research is on how tamoxifen doses can be individualized using Therapeutic Drug Monitoring (TDM) of its active metabolite endoxifen. **Chapter 1.1** provides an introduction to the subject and an overview of available literature regarding the effects of pharmacogenetics on the PK and PD of tamoxifen. In **chapter 1.2** an anti-estrogenic activity score is developed and presented to evaluate whether endoxifen can serve as a proxy for the anti-estrogenic effect of tamoxifen and three of its metabolites. In **chapter 1.3** we share our view

on therapy individualization of tamoxifen treatment, where genotyping of metabolizing enzymes is compared to TDM of endoxifen. **Chapter 1.4** gives insight into the feasibility of observational and randomized controlled trials, aiming to prospectively validate TDM of endoxifen, by conducting clinical trial simulations to determine study power.

**Chapter 2** demonstrates how PK-PD modeling can be used to support decision making in drug development. The PK-PD modeling of a bispecific monoclonal antibody (MCLA-128) in development to treat solid tumors expressing HER2 and HER3, is described. **Chapter 2.1** describes the preclinical PK-PD modeling framework, which was utilised to determine a safe and efficacious starting dose for a First-in-Human trial. **Chapter 2.2** reports on the clinical PK characteristics of MCLA-128 in patients included in the First-in-Human clinical phase I/II trial, including the evaluation of the predictive value of the preclinical PK model.

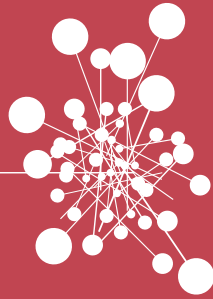
**Chapter 3** focusses on modeling toxicity of classical cytotoxic and newer anti-cancer drugs. **Chapter 3.1** is an introduction to the subject of toxicity modeling and provides a perspective of how adverse effects of anti-cancer drugs can be quantified in mathematical models. It also reports on several model structures of adverse effect models that describe relationships between drug concentrations and toxicity. In **Chapter 3.2** the kinetics and exposure-response relationships of left ventricular ejection fraction (LVEF) and troponine T in breast cancer patients receiving both anthracyclines and trastuzumab are quantified, to identify patients that are more likely to exhibit an LVEF decline during trastuzumab treatment. **Chapter 3.3** and **chapter 3.4** focus on the toxicity of docetaxel in metastatic castration-resistant prostate cancer (mCRPC) patients. More specifically, **chapter 3.3** describes the difference in exposure to docetaxel and incidence of neutropenia in patients with mCRPC compared to patients with other solid tumors. **Chapter 3.4** reports the differences in docetaxel-induced hematological toxicity in elderly patients compared to younger patients with mCRPC.

This thesis represents the application of pharmacometrics to optimize treatment and support drug development of new drugs in oncology.

## REFERENCES

1. Bray, F. et al. *Global Cancer Statistics 2018 : GLOBOCAN Estimates of Incidence and Mortality Worldwide for 36 Cancers in 185 Countries*. *CA Cancer J Clin* 68, 394-424 (2018).
2. Ette, E. & Williams, P. *Pharmacometrics: The Science of Quantitative Pharmacology*. (Wiley-Interscience, 2007).
3. Derendorf, H. et al. *Pharmacokinetic/pharmacodynamic modeling in drug research and development*. *J Clin Pharmacol* 40, 1399-1418 (2000).





# CHAPTER 1

PHARMACOKINETICS AND  
PHARMACODYNAMICS:  
TAMOXIFEN



## CHAPTER 1.1

### Effects of Pharmacogenetics on the Pharmacokinetics and Pharmacodynamics of Tamoxifen

*Clinical Pharmacokinet.* 2015 Aug;54(8):797-810

A.H.M. de Vries Schultink  
W. Zwart  
S.C. Linn  
J.H. Beijnen  
A.D.R. Huitema

## ABSTRACT

### Introduction

The antiestrogenic drug tamoxifen is widely used in the treatment of estrogen receptor- $\alpha$ -positive breast cancer and substantially decreases recurrence and mortality rates. However, high interindividual variability in response is observed, calling for a personalized approach to tamoxifen treatment. Tamoxifen is bioactivated by cytochrome P450 (CYP) enzymes such as CYP2B6, CYP2C9, CYP2C19, CYP2D6 and CYP3A4/5, resulting in the formation of active metabolites, including 4-hydroxy-tamoxifen and endoxifen. Therefore, polymorphisms in the genes encoding these enzymes are proposed to influence tamoxifen and active tamoxifen metabolites in the serum and consequently affect patient response rates. To tailor tamoxifen treatment, multiple studies have been performed to clarify the influence of polymorphisms on its pharmacokinetics and pharmacodynamics. Nevertheless, personalized treatment of tamoxifen based on genotyping has not yet met consensus.

### Methods

This article critically reviews the published data on the effect of various genetic polymorphisms on the pharmacokinetics and pharmacodynamics of tamoxifen, and reviews the clinical implications of its findings. For each CYP enzyme, the influence of polymorphisms on pharmacokinetic and pharmacodynamic outcome measures is described throughout this review.

### Results

No clear effects on pharmacokinetics and pharmacodynamics were seen for various polymorphisms in the CYP encoding genes *CYP2B6*, *CYP2C9*, *CYP2C19* and *CYP3A4/5*. For *CYP2D6*, there was a clear gene-exposure effect that was able to partially explain the interindividual variability in plasma concentrations of the pharmacologically most active metabolite endoxifen; however, a clear exposure-response effect remained controversial.



## **Conclusion**

These controversial findings and the partial contribution of genotype in explaining interindividual variability in plasma concentrations of, in particular, endoxifen, imply that tailored tamoxifen treatment may not be fully realized through pharmacogenetics of metabolizing enzymes alone.

## INTRODUCTION

Tamoxifen is an antiestrogenic drug, widely used for the treatment of estrogen receptor- $\alpha$  (ER $\alpha$ )-positive breast cancer. Adjuvant tamoxifen treatment substantially reduces breast cancer relapse and mortality rates.<sup>1</sup> Recently, the Adjuvant Tamoxifen: Longer Against Shorter (ATLAS) and adjuvant Tamoxifen-To offer more? (aTTom) trials have suggested the extension of tamoxifen treatment duration from 5 years to 10 years for a subpopulation of premenopausal patients, to further lower recurrence rates.<sup>2,3</sup> Both pre- and postmenopausal patients are treated with tamoxifen; however, in postmenopausal patients or patients who underwent ovarian ablation, treatment with aromatase inhibitors is effective, either in a sequence, before or after tamoxifen, or for 5 years.<sup>4</sup> Aromatase inhibition does not work in women with active ovarian function, like in premenopausal women.<sup>5</sup> Inhibition of aromatase reduces feedback of estrogens to the hypothalamus-pituitary-ovary axis, leading to an increased stimulation of the ovaries via gonadotropin secretion.<sup>6</sup> This stimulation overrules the effect of aromatase inhibitors. Therefore, tamoxifen is currently the only drug of choice in this subpopulation. Even though a differentiation between ER $\alpha$ -positive and ER $\alpha$ -negative tumors is made prior to treatment, a high interindividual variability in response to adjuvant treatment with tamoxifen is observed.<sup>7</sup> Tailoring tamoxifen therapy was the main focus of an extensive number of studies with emphasis on germline genotyping as a tool to guide treatment. Bioactivation of tamoxifen is mediated by polymorphic cytochrome P450 (CYP) enzymes and may therefore be an important process causally involved in response variability.<sup>8</sup> Bioactivation of tamoxifen results in the formation of metabolites that have different affinity and potency towards ER $\alpha$ .<sup>9,10</sup> The ER $\alpha$  receptor is known to be the main target in anti-estrogen therapy, while the role of ER $\beta$  is still under investigation.<sup>11</sup> The formation of the two major primary metabolites of tamoxifen, *N*-desmethyl-tamoxifen and 4-hydroxy-tamoxifen, is predominantly catalyzed by CYP3A4/5 and CYP2D6, respectively. The formation of the secondary metabolite 4-hydroxy-*N*-desmethyltamoxifen (endoxifen) is generated from *N*-desmethyl-tamoxifen by CYP2D6, and less substantially from 4-hydroxy-tamoxifen by CYP3A4/5.<sup>8</sup> Endoxifen and 4-hydroxy-tamoxifen are potent antiestrogenic metabolites, with a 100-fold higher affinity for ER and a 30- to 100-fold higher potency in suppressing cell proliferation compared with tamoxifen, pointing towards key roles for CYP2D6

and CYP3A4/5 in the bioactivation of tamoxifen.<sup>9,10</sup> Since plasma concentrations of endoxifen exceed plasma concentrations of 4-hydroxy-tamoxifen, endoxifen is proposed to be the most important metabolite of tamoxifen.<sup>9</sup> Nevertheless, tamoxifen metabolism has shown to be more complex than solely transformation to endoxifen via CYP2D6, depending on other factors such as serum abundance and the activity of other CYP enzymes such as CYP2B6, CYP2C9, CYP2C19 and CYP3A4/5, as depicted in Fig 1.<sup>8</sup>

Currently, only CYP2D6 genotyping is proposed to guide tamoxifen treatment, and an AmpliChip® CYP450 test for determination of the genotype has been approved by the US Food and Drug Administration (FDA). The FDA Advisory Committee recommended including pre-treatment genotyping in the drug label of tamoxifen<sup>12</sup>; however, such a recommendation is not included in the current label. Determination of the genotype is suggested to make treatment decisions for both postmenopausal and premenopausal women. Postmenopausal women with low metabolic activity are expected to have lower exposure to an active tamoxifen metabolite and could therefore derive more benefit from either aromatase inhibitors or a higher dose of tamoxifen, as opposed to the standard dose of 20 mg/day. Likewise, premenopausal patients can benefit from a higher dose of tamoxifen when experiencing low metabolic activity since tamoxifen is currently the only drug of choice in the premenopausal setting.

However, controversial findings of various studies, to be discussed in this review, have led to conflicting views on pharmacogenotyping as a tool to guide tamoxifen treatment. Therefore, this article critically reviews the published data regarding the effect of various genetic polymorphisms on the pharmacokinetics and pharmacodynamics of tamoxifen, and aims to review the clinical implications of these findings.

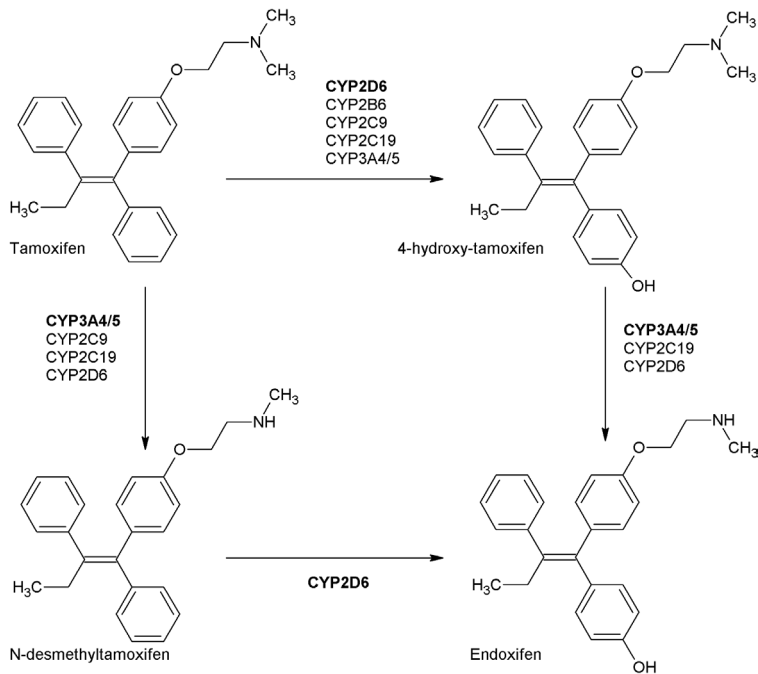


**Figure 1** Part of the tamoxifen metabolic pathway. Bold enzymes illustrate a higher extent of contribution to the formation of the metabolite.<sup>8</sup> CYP cytochrome P450

## LITERATURE SEARCH

A literature search was performed using the PubMed/MEDLINE database. The following terms were searched in October and November 2014: [(Tamoxifen AND CYP2B6) OR (Tamoxifen AND CYP2C9) OR (Tamoxifen AND CYP2C19) OR (Tamoxifen AND CYP3A4) OR (Tamoxifen AND CYP3A5) OR (Tamoxifen AND CYP2D6)]. Studies including patients with ER $\alpha$ -positive breast cancer undergoing adjuvant treatment with tamoxifen for early-stage breast cancer and investigating an effect of polymorphisms in genes encoding the metabolizing enzymes CYP2B6, CYP2C9, CYP2C19, CYP3A4, CYP3A5, and/or CYP2D6 on pharmacokinetic and/or pharmacodynamic outcome measures were selected. Pharmacokinetic outcome measures included steady-state plasma concentrations of tamoxifen and its metabolites and/or associated metabolic ratios.

Pharmacodynamic outcome measures included survival outcomes such as overall survival (OS), (distant or invasive) disease-free survival (DFS), (distant) recurrence-free survival (RFS), (distant) recurrence-free interval (RFI), breast cancer-free interval (BCFI), or any other measurement of breast cancer recurrence risk.

Search results were limited to studies conducted in humans and full-text articles available in the English language. Various characteristics of studies and study populations were identified, such as number of patients, dose, concomitant use of CYP2D6 inhibitors and if this was accounted for, deviation from Hardy-Weinberg equilibrium, DNA derived tissue, and menopausal status.

## **RESULTS OF THE LITERATURE SEARCH**

The described search terms identified 451 papers, 36 of which were found to be eligible for inclusion. Of 451 papers, 102 were reviews, 10 investigated effects in animals, 60 studies were in vitro studies or investigated the metabolism of tamoxifen, 104 studies did not investigate previously described pharmacokinetic or pharmacodynamic outcome measurements, 6 studies were on bioanalytic methods, 23 studies investigated genotyping methods or tumorgenetics, 30 studies investigated drugs other than tamoxifen, and 52 hits consisted of author replies, comments, errata, or editorials. The remaining 64 studies analyzed an effect of polymorphisms on pharmacokinetics and/or pharmacokinetics. Eleven studies investigated effects in non-adjuvant-treated patients, in three studies it was unclear if receptor status was accounted for, and 13 studies did not investigate previously described pharmacokinetic or pharmacodynamic outcome measurements after reading full texts, were of poor methodological quality, or provided an insufficient amount of information; these studies were excluded from the review. Survival outcomes included mainly DFS, RFS and RFI, which were specified as time from surgery or randomization to recurrence. Event-free survival (EFS) was defined as the time from surgery or randomization to occurrence of a defined event; events were specified differently among studies. Characteristics of the 36 included studies are depicted in Table 1.<sup>13-48</sup>

Table 1 Characteristics of included studies

REFE-REN-CE	YEAR	PK/PD	STUDY TYPE	N	MENOPAUSAL STATUS	DOSE (MG)	CYP2D6 INHI-BITORS <sup>A</sup>	HWQ	DNA <sup>B</sup>
14	2006	PK	Cohort	158	Both	20	++	-	G
15	2013	PD	Ca-Co	57	Both	20	++	++	G
16	2013	PK	Cohort	135	Both	20	++	++	G
17	2005	PD	Cohort	223	Post	20	--	-	G+T
18	2013	PD	Ca-Co	319	Post	20	--	++	G+T
19	2005	PK	Cohort	80	Both	20	++	+	G
20	2008	PD	Cohort	67	Both	20	++	-	G
21	2010	PK/PD	Cohort	282	Both	20	++	++	G
22	2011	PD	Ca-Co	494	Post	-	++	++	G
23	2011	PK	Cohort	165	Both	20	++	++	G
24	2011	PK	Cohort	1370	Both	-	++	++	G
25	2011	PD	Cohort	190	Post	20	++	++	T
26	2011	PK	Cohort	236	Post	20	++	+	G
27	2014	PD	Cohort	99	Both	-	-	++	G
28	2005	PD	Cohort	162	Both	-	--	-	T
29	2009	PD	Cohort	173	Both	20	++	-	G
30	2012	PD	Cohort	588	Post	20	++	+	T
31	2012	PD	Cohort	1243	Post	20	--	-	T
32	2014	PK/PD	Cohort	548	Pre	20	-	++	G
33	2007	PD	Cohort	206	Both	-	--	+	T
34	2009	PD	Cohort	1325	Both	20	--	-	T
35	2013	PD	Cohort	30	Both	-	++	++	G
36	2013	PK/PD	Cohort	132	Both	-	++	++	G
37	2005	PK/PD	Cohort	98	Post	20	--	++	G
38	2005	PD	RCT	50	Post	40	-	-	T
39	2007	PD	Cohort	119	Post	20/40	++	-	T
40	2008	PK/PD	Ca-Co	152	Both	20	++	-	G
41	2013	PK	Cohort	90	Both	20	++	++	G
42	2008	PK	Cohort	151	Both	20	++	++	-
43	2009	PD	Cohort	156	Both	20	--	++	T
44	2010	PD	Cohort	493	Both	20	--	++	G
45	2010	PD	Cohort	3155	Both	20	++	+	G
46	2012	PK/PD	Cohort	716	Both	20	-	-	G

**Table 1 continued**

<sup>47</sup>	2011	PD	Cohort	110	Both	20	++	-	G
<sup>48</sup>	2011	PK	Cohort	117	Both	20	++	++	G

*PK = pharmacokinetic outcomes, PD = pharmacodynamic outcomes, RCT = randomized controlled trial, Ca-Co = case-control study, Post = postmenopausal, Pre = premenopausal, Both = postmenopausal and premenopausal, CYP = cytochrome P450, HWQ = Hardy-Weinberg equilibrium, G = germline DNA, T = tumor tissue extracted DNA, ++ indicates yes, + indicates in part, - indicates unknown, -- indicates not, <sup>4</sup>Accounted for CYP2D6 inhibitors, <sup>8</sup>Source of DNA*

## Study Designs

As depicted in Table 1, a variety of study designs were used to determine the effects of polymorphisms in metabolic enzymes on pharmacokinetic and pharmacodynamic outcomes. Studies investigating the effect of polymorphisms on plasma concentrations were mostly well-designed, prospective cohort studies, while studies investigating the effect of polymorphisms on survival outcome were predominantly designed as retrospective cohort studies and, to a lesser extent, as case-control studies. Cohort studies solely included patients treated with tamoxifen and analyzed whether polymorphisms had an impact on survival in this patient group. Case-control studies compared incidences of recurrences in patients carrying variant alleles (cases) and patients carrying the wild-type genotype (controls) or compared hazard ratios (HRs) of both groups. Cases and controls were both treated with tamoxifen. Since prognosis can differ between patients, most analyses were multivariate analyses correcting for nodal status and tumor grade and stage because these factors are known to influence survival outcome. What is not known is whether CYP variant alleles can also influence prognosis. In most studies described throughout this review, only tamoxifen-treated patients have been studied. This precludes any definitive conclusion regarding either prognostic or predictive value of the CYP variant because outcome after tamoxifen is a combination of prognosis and treatment effect (prediction). In studies where the CYP variant group had a multivariate corrected, poorer outcome than the CYP wild-type group after tamoxifen treatment, any conclusion that this CYP variant was causal in lower endoxifen concentrations and therefore reduced efficacy of tamoxifen is premature. To discern the predictive effect from the prognostic effect of polymorphisms in CYP enzymes on survival outcome, a randomized controlled trial (RCT) or case-control design should be used, with four patient subgroups<sup>49</sup>: patients with and without the

CYP polymorphism of interest, and patients with and without the treatment of interest. Studies by Beelen et al. and Wegman et al.<sup>13,38</sup> investigated the prognostic value of the *CYP2C19*\*2 and *CYP2D6*\*4 variant alleles, respectively. Interestingly, the *CYP2C19*\*2 variant conferred an adverse prognosis in the absence of treatment, while patients with this variant allele derived significantly more benefit from adjuvant tamoxifen than patients without this variant.<sup>13</sup> While reading this review, it is crucial to keep in mind that if the four subgroups are not included in the study design, conclusions regarding prognosis and/or prediction will not have any influence on patient care.

### **Effect of Polymorphisms on Pharmacokinetic and Pharmacodynamic Outcome Measures**

For each CYP enzyme, the effect of various polymorphisms on pharmacokinetic and pharmacodynamic outcome measures will be described.

#### *CYP2B6*

*CYP2B6* plays a role in the formation of the primary metabolites 4-hydroxy-tamoxifen. *CYP2B6* enzymes can show different metabolic activities based on their polymorphic state.<sup>8</sup> Over 50 allelic variations of *CYP2B6* are described, but not all associated metabolic activities are known. *CYP2B6*\*4 shows an increased in vivo metabolic activity, and *CYP2B6*\*6, \*16 and \*26 allelic variations show a decreased metabolic activity.<sup>50</sup> Regarding pharmacokinetic outcome measures, no association between the *CYP2B6*\*6 genotype and endoxifen concentrations, 4-hydroxy-tamoxifen concentrations, or the metabolic ratio of tamoxifen concentration over 4-hydroxy-tamoxifen concentration ( $MR_{\text{TAM}/4\text{OHT}}$ ) was found.<sup>26,36</sup> Additionally, *CYP2B6*\*6 polymorphism was not associated with significantly different relapse-free time (RFT).<sup>27</sup>

The definition of RFT was in line with the definition of RFI, as described by Hudis et al.<sup>51</sup> In addition, no association was found between the *CYP2B6* genotype and EFS or OS.<sup>11</sup>



## CYP2C9

CYP2C9 contributes to the formation of the primary tamoxifen metabolites N-desmethyl-tamoxifen and 4-hydroxy-tamoxifen, albeit to a lesser extent than CYP2D6 and CYP3A5 isoforms.<sup>52</sup> The metabolic activity of CYP2C9 can be normal (\*1A), decreased (\*3, \*5, \*8, \*11A, \*13), or absent (\*6).<sup>50</sup>

Regarding pharmacokinetics, in the studies by Teft et al. (no *p*-values reported) and Jin et al. (*p*-values >0.05) no significant difference was found in mean plasma concentrations of tamoxifen or its metabolites between patients carrying two wild-type alleles or carriers of either heterozygous or homozygous variant alleles of CYP2C9\*2 and CYP2C9\*3.<sup>19,36</sup> Lim et al.<sup>23</sup> found similar results regarding CYP2C9\*3 and the influence on tamoxifen and metabolite concentrations. In contrast, a significant difference in the formation of 4-hydroxy-tamoxifen from tamoxifen (*p* = 0.007) between homozygous wild-type carriers and carriers of CYP2C9\*2 and/or \*3 alleles and significant lower plasma concentrations of 4-hydroxy-tamoxifen (*p* = 0.0006) and endoxifen (*p* = 0.0024) were found.<sup>26,32</sup>

Regardless of the significant difference in formation of 4-hydroxy-tamoxifen and endoxifen and 4-hydroxy-tamoxifen concentration, no association between genotypes and treatment outcome, survival, or RFT has been reported.<sup>27,33</sup> The definition of RFT was in line with the definition of RFI, as described by Hudis et al.<sup>51</sup>

## CYP2C19

CYP2C19 activity could alter tamoxifen metabolism and exposure to its metabolites via catalyzation of the conversion of tamoxifen into 4-hydroxy-tamoxifen.<sup>8</sup> CYP2C19\*2 and \*3 variant alleles showed no metabolic activity, whereas CYP2C19\*17 showed increased metabolic activity due to increased transcriptional activity.<sup>50</sup>

No significant correlation between CYP2C19 genotypes and concentrations of tamoxifen or its metabolites (*p* > 0.05) were found by Lim et al.<sup>23</sup> Mürdter et al.<sup>26</sup> underlined these results, finding no correlation between CYP2C19\*3 or CYP2C19\*17 and plasma concentrations of endoxifen and 4-hydroxy-tamoxifen or associated metabolic ratios.

Regarding survival outcome measures, Okishiro et al.<sup>29</sup> found no significant difference between genotypes of *CYP2C19* and RFS in Japanese patients with breast cancer treated with adjuvant tamoxifen [HR 0.37, 95 % confidence interval (CI) 0.08–176;  $p = 0.19$ ]. In addition, no significant impact on RFT was found for *CYP2C19* variant allele carriers<sup>27</sup>, and heterozygous carriers of a *CYP2C19* variant allele did not significantly impact DFS (HR 0.93 95 % CI 0.47–1.84;  $p = 0.82$ ).<sup>14</sup> In addition, Moyer et al.<sup>25</sup> did not find a significant difference between the *CYP2C19*\*17 genotype and DFS.

The study by Schroth et al.<sup>33</sup> investigated the impact of single nucleotide polymorphisms (SNPs) on RFT, EFS, and OS, but found no significant correlations between *CYP2C19*\*2 and/or \*3 carriers and these survival outcomes. However, in carriers of *CYP2C19*\*17, improvement in RFT was found (HR 0.45, 95 % CI 0.21–0.92;  $p = 0.03$ ) but this was not significant for EFS (HR 0.58, 95 % CI 0.32–1.01;  $p = 0.05$ ) and OS (HR 0.61, 95 % CI 0.29–1.26;  $p = 0.18$ ).

Beelen et al.<sup>13</sup> investigated the prognostic value of the *CYP2C19*\*2 variant allele, comparing patients using tamoxifen with patients not using tamoxifen for both *CYP2C19*\*2 carriers and patients with wild-type genotype. Patients carrying at least one *CYP2C19*\*2 variant allele showed an improved RFI (HR 0.26;  $p = 0.001$ ), while patients without this allele derived less benefit (HR 0.68;  $p = 0.18$ ). Interestingly, breast-cancer patients carrying the *CYP2C19*\*2 variant allele had a poor prognosis in the absence of adjuvant tamoxifen (HR 2.5) compared with patients without a variant allele. As explained by the authors, *CYP2C19* exposure affects the metabolism of tamoxifen as well as estrogen catabolism. The non-functional *CYP2C19*\*2 causes higher exposure to estrogens, leading to a possible higher susceptibility to tumors that are dependent on estrogen signaling.

Therefore, these patients could be more sensitive to estrogen-inhibiting therapy, explaining the more beneficial HR in the *CYP2C19*\*2 subgroup.

## CYP3A4/5

CYP3A4/5 enzymes catalyze the formation of tamoxifen into different active metabolites, of which transformation into *N*-desmethyl-tamoxifen from tamoxifen and endoxifen from 4-hydroxy-tamoxifen are the most important.<sup>8</sup> The CYP3A4\*22 polymorphism shows decreased metabolic activity, and CYP3A5\*3 and CYP3A5\*6 polymorphisms show no metabolic activity; therefore, lower endoxifen and *N*-desmethyl-tamoxifen concentrations leading to decreased response are expected to be associated with these polymorphisms.<sup>50</sup>

Regarding the influence of CYP3A4/5 polymorphisms on the pharmacokinetics of tamoxifen, various studies have been conducted. Teft et al. unexpectedly found higher endoxifen ( $p < 0.05$ ) concentrations for CYP3A4\*22 carriers, as well as higher concentrations of tamoxifen ( $p < 0.0001$ ), *N*-desmethyl-tamoxifen, 4-hydroxy-tamoxifen and other, less relevant, metabolites. Since CYP3A4\*22 polymorphism shows a decreased metabolic activity, higher metabolite concentrations are not expected; however, tamoxifen concentrations were also elevated. Therefore, it is suggested that intestinal CYP3A4 activity was decreased, leading to reduced first-pass metabolism, increasing the concentration of tamoxifen and subsequently its metabolites. The study also investigated the combination of CYP2D6 and CYP3A4 polymorphisms. In patients with low CYP2D6 metabolic activity, the CYP3A4\*22 allele carriers had endoxifen concentrations above a set threshold of 6.72 ng/ml compared with subtherapeutic concentrations in patients with low CYP2D6 metabolic activity and CYP3A4 wild-type. These findings indicate that CYP3A4\*22 polymorphism is more important in CYP2D6 poor metabolizer.<sup>36</sup> This threshold was based on the 20th percentile of endoxifen concentrations in the enrolled patients because, in the study by Madlensky et al., patients with endoxifen concentrations in the lowest quintile were at the highest risk of recurrence.<sup>24,36</sup>

In the study by Tucker et al.<sup>37</sup> no significant differences were seen for tamoxifen, *N*-desmethyl-tamoxifen, or 4-hydroxy-tamoxifen concentrations in patients carrying at least one variant CYP3A5\*3 or CYP3A5\*6 allele. The influence of CYP3A5 polymorphisms on endoxifen concentrations was not investigated and possible other polymorphisms were not taken into account.

Although the study by Jin et al.<sup>19</sup> found higher steady-state mean plasma concentrations of endoxifen in patients with at least one functional allele (82.0 nM; range 56.2–107.8) compared with patients with no functional alleles (58.1 nM; range 49.3–66.9), no significant associations were found between *CYP3A5*\*3 homozygous carriers and any of the metabolite concentrations (tamoxifen,  $p = 0.98$ ; 4-hydroxy-tamoxifen,  $p = 0.57$ ; *N*-desmethyl-tamoxifen,  $p = 0.99$ ). Additional studies did not find a correlation between carriers of *CYP3A5*\*3 alleles and tamoxifen or tamoxifen metabolite steady-state concentrations or their metabolic ratios.<sup>8,22,29</sup>

Considering pharmacodynamic survival outcomes, the study by Goetz et al.<sup>17</sup> found that the *CYP3A5*\*3 variant was not associated with RFS, DFS, or OS. Furthermore, no associations between the *CYP3A5*\*3 variant allele and treatment outcome or survival were found in the study by Schroth et al.<sup>33</sup>

Both multivariate and univariate analyses by Wegman et al.<sup>39</sup> showed unexpected improved RFS (multivariate: HR 0.13, 95 % CI 0.02–0.86;  $p = 0.03$ ) in homozygous carriers of *CYP3A5*\*3 treated with tamoxifen for 5 years.

The gene-exposure effect for *CYP3A4/5* polymorphisms and tamoxifen is less clear than that for *CYP2D6*. The study by Teft et al.<sup>36</sup> investigated the relevance of the *CYP3A4*\*22 polymorphism in different *CYP2D6* genotype groups, indicating that the *CYP3A* pathway becomes more relevant if *CYP2D6* metabolic activity is decreased.

#### *CYP2D6*

Two of the most potent metabolites of tamoxifen, 4-hydroxy-tamoxifen and endoxifen, are predominantly generated by *CYP2D6*.<sup>8</sup> More than 100 allelic variants of *CYP2D6* with different metabolic activities are currently known.

Metabolic activity can either be normal (\*1, \*2, \*33, \*35), decreased (\*9, \*10, \*17, \*29, \*41, \*69), absent (\*3, \*4, \*6, \*7, \*8, \*11–\*15, \*18–\*21, \*31, \*38, \*40, \*42, \*44) or increased (\*2XN, \*35X2).<sup>50</sup> To facilitate comparison, the predicted phenotype is derived from the genotype, enabling classification of metabolizers into four different groups: poor metabolizer (PM), intermediate metabolizer (IM), extensive metabolizer (EM), or

ultrarapid metabolizer (UM).

Study results regarding the effect of CYP2D6 polymorphisms on pharmacokinetic and pharmacodynamic parameters are depicted in Tables 2 and 3, respectively.

**Table 2 Results for CYP2D6 polymorphisms and their effect on pharmacokinetic parameters.**

VARIANT ALLELES	REF	OUTCOME	COMPARISON	SIGNIFICANCE
3-8,11,14A, 15,19,20,40,4x	24	C <sub>ss</sub> T + M <sub>1-3</sub>	EM/EM vs. Various comb	T (NS); M <sub>1-3</sub> (p < 0.001) M <sub>3</sub> 45% explained by genotype
3,4,5,6	19	C <sub>ss</sub> T+M <sub>1-3</sub>	wt/wt vs. wt/* or */*	M <sub>3</sub> (p=0.003)
3,4,6,7,8,9, 10,41	26	C <sub>ss</sub> T+M <sub>1-3</sub> MR <sub>DMTAM/END</sub>	EM/EM vs. Various comb	M: 39% explained by genotype M: 9% explained by genotype
3-6,9,10,41,14,15,17	32	MR <sub>DMTAM/END</sub>	CYP2D6 activity score	p < 10 <sup>-77</sup>
3,4,8,10,41	36	C <sub>ss</sub> T+M <sub>1-3</sub>	EM/EM vs. Various comb	M <sub>3</sub> significant
5, 10, 41	23	C <sub>ss</sub> T+M <sub>1-3</sub>	wt/wt vs. wt/*5, wt/*10 : *10/*10,*5/*10	M <sub>1</sub> (p=0.077) and (p=0.006) M <sub>3</sub> (p<0.001); M <sub>1</sub> (*10) (p=0.011)
			wt/* vs. *5/*10	M <sub>3</sub> (p=0.001)
2-6,10,41	41	C <sub>ss</sub> T+M <sub>1-3</sub>	EM vs. PM	M <sub>1,3</sub> (p < 0.001)
3-6, 9,10,17,41	16	C <sub>ss</sub> T+M <sub>1-3</sub>	EM/EM vs. PM/PM	M <sub>3</sub> (p < 0.001)
33 alleles	14	MR <sub>END/DMTAM</sub>	wt/wt vs. wt/* vs */*	(p < 0.001)
4,5,10,36,41,21	21	C <sub>ss</sub> T+M <sub>1-3</sub>	wt/wt vs. wt/* or */*	M <sub>2,3</sub> ( p < 0.01) both
2-6	42	C <sub>ss</sub> T+M <sub>1-3</sub>	EM/* vs.PM vs.UM	M <sub>1</sub> (p=0.001); M <sub>3</sub> (p=0.001)
5,10,41	46	C <sub>ss</sub> T+M <sub>1-3</sub>	wt/wt, wt/* vs. */*	M <sub>2,3</sub> (p < 0.001)
2,2A,2AxN,4-6,9,10, 17,41	48	M <sub>1-3</sub>	CYP2D6 activity score	M <sub>3</sub> (p = 0.0009), Z-endoxifen (p < 0.0001)

CYP = cytochrome P450, C<sub>ss</sub> = steady-state concentration, comb = combinations, T = tamoxifen, M = tamoxifen metabolite; M<sub>1</sub> = N-desmethyl-tamoxifen, M<sub>2</sub> = 4-hydroxy-tamoxifen, M<sub>3</sub> = endoxifen, MR = metabolic ratio, EM = extensive metabolizer, PM = poor metabolizer, UM = ultrarapid metabolizer, NS = not significant, MR<sub>DMTAM/END</sub> = metabolic ratio of N-desmethyl-tamoxifen concentration over endoxifen concentration, MR<sub>END/DMTAM</sub> = metabolic ratio of endoxifen concentration over N-desmethyl-tamoxifen concentration, wt/wt = two wildtype alleles, wt/\* = one wildtype allele and one polymorphic allele, \*/\* = two polymorphic allele

Table 3 Results for CYP2D6 polymorphisms and their effect on pharmacodynamic parameters.

VARIANT ALLELES	REF	OUTCOME	COMPARISON	SIGNIFICANCE <sup>A</sup>	REMARKS <sup>B</sup>
<b>No significant results</b>					
4	39	RFS	wt/wt vs. wt/* + */*	NS	Only result for the 5 year tamoxifen treatment arm are included in this table
3-6,10,41	27	RFT	wt/wt vs. wt/* and/or */*	NS	-
10	29	RFS	wt/wt, wt/* vs. *10/*10	NS	Lack of statistical power
4	44	TTP,PFS	wt/wt vs. wt/*4 or *4/*4	NS	-
5,10,41	46	RFS	wt/wt vs. wt/* or */*	NS	Possible misclassification of genotypes
4	22	Recurrence	wt/wt vs. *4/*4 or *4/*1	NS	-
4	28	OS, RFS	wt/wt vs. wt/* + */*	NS	Heterogeneous study population
4	17	RFT,DFS,OS	wt/wt, wt/* vs. *4/*4	NS	In the univariate analysis RFT and DFS were significantly worse for the CYP2D6 *4/*4 genotype
10	43	DFS,DDFS,BCSS, OS	wt/wt vs. wt/* or */*	NS	-
4-6,9,10,41,UM	45	BCSS, OS	wt/wt vs. Any genotype	NS	In the unadjusted analysis CYP2D6*6 (PM) were at increased risk of BCSS: HR 2.14 (95%CI 1.05-4.36)
2-5,10,14,18,21,41,49,52,60	47	RFS, OS	EM and IM vs. PM	NS	Univariate analysis showed some significance in OS and RFS; potential lack of statistical power
<b>Significant results</b>					
4,5,10,41	33	RFT,EFS,OS	EM/EM vs. wt/* or */*	RFT, EFS (p = 0.02); OS (NS)	Note: OS is not significant
3-6,9,10,41,14,15,17	32	DRFS	CYP2D activity score	P = 0.013	Potential lack of power, potential selection bias

4,5,10,36,41	15	DFS	wt/wt	vs.	wt/* or /*/* (*10)	DFS postmeno (p=0.046)	Potential lack of power
4,5,10,41,21	20	RFS	wt/wt	vs.	*10/*10	(p=0.0057)	Potential selection bias
4,5,10,36,41,21	21	RFS	wt/wt	vs.	wt/* or /*/*	(p=0.00036)	Potential bias in time of inclusion, cross-sectional design
10	40	RFS	wt/wt, */wt	vs.	*//*	(p=0.04)	Potential bias
4	38	DRFS	wt/* or /*/* tamoxifen	vs.	wt/* or /*/* no tamoxifen	(p=0.0089) longer DRFS	Potential selection bias; different comparison
<b>Most recent trials</b>							
3,4,6,10, 41	18	IDFS	EM/EM	vs.	PM/IM or PM/ EM	(p = 0.04) and (p = 0.07)	ABCSG 8 trial
3,4,5,10,41	34	TTR, EFS,DFS, OS	EM EM	vs.	EM/IM and PM	TTR (p < 0.001) EFS (p=0.003) DFS (p=0.005)	-
2,3,4,6,10,41	30	Recurrence	EM	vs.	PM	NS	ATAC trial
2,3,4,6,7,10,17, 41	31	BCFI	EM	vs.	PM or + and IM	NS	BIG 1-98 trial

CYP = cytochrome P450, IDFS = invasive disease-free survival, TTR = time to recurrence, BCFI = breast cancer-free interval, RFT relapse-free time, EFS event-free survival, OS overall survival, RFS recurrence-free survival, DRFS = distant recurrence-free survival, DFS = disease-free survival, DDFS = distant disease-free survival, BCSS = breast cancer-specific survival, PFS = progression-free survival, TTP = time to tumor progression, EM = extensive metabolizer, IM = intermediate metabolizer, PM = poor metabolizer, UM = ultrarapid metabolizer, NS = not significant, HR = hazard ratio, CI = confidence interval, ABCSG = Austrian Breast and Colorectal Cancer Study Group, ATAC = Arimidex, Tamoxifen, Alone or in Combination, BIG = Breast International Group, wt/wt = two wildtype alleles, wt/\* = one wildtype allele and one polymorphic allele, \*/\* = two polymorphic alleles

<sup>a</sup>Outcomes of multivariate analysis, if available

<sup>b</sup>In addition to the characteristics in Table 1.

All 13 reports investigating the associations between *CYP2D6* polymorphisms and pharmacokinetics found a significant effect of genotype on endoxifen concentrations and/or the formation of endoxifen from *N*-desmethyl-tamoxifen.<sup>14,16,19,21,23,24,26,32,36,41,42,46,48</sup> For *N*-desmethyl-tamoxifen and 4-hydroxy-tamoxifen a significant effect of *CYP2D6* variant alleles was indicated by four and three studies, respectively.<sup>21,23,24,41,42,46</sup> None of the studies indicated a correlation between genotype and tamoxifen concentrations.

Four studies<sup>24,26,32,36</sup> estimated to what extent *CYP2D6* polymorphisms could explain the variability in endoxifen concentrations by testing *CYP2D6* activity as a covariate using linear models. Mürdter et al.<sup>26</sup> found that *CYP2D6* polymorphisms explained 39% of variability in endoxifen concentrations. Teft et al.<sup>36</sup> found a similar contribution of 30%, Saladores et al.<sup>32</sup> found a contribution of 53%, and Madlensky et al.<sup>24</sup> indicated that the *CYP2D6* genotype, together with age and body mass index (BMI), explained 46% of the variability in endoxifen concentrations.

Madlensky et al. indicated a threshold of 5.97 ng/ml for endoxifen. Patients with endoxifen concentrations above 5.97 ng/ml had lower recurrence rates (HR 0.74, 95% CI 0.55–1.00) based on patient plasma concentrations of endoxifen and associated DFS times. Even though the majority of PMs had low endoxifen concentrations, 24% were still able to generate endoxifen concentrations above the threshold of 5.97 ng/ml.<sup>24</sup> The study by Teft et al.<sup>36</sup> used a comparable threshold of 6.72 ng/ml. This threshold was based on the 20th percentile of endoxifen concentrations in enrolled patients, since patients with endoxifen concentrations in the lowest quintile were at highest risk of recurrence in the study conducted by Madlensky et al. The majority of PMs failed to generate an endoxifen concentration above a threshold of approximately 6.72 ng/ml.

With regard to pharmacodynamic outcomes, findings are more controversial. Various studies were conducted to clarify the influence of different polymorphisms of *CYP2D6* on the pharmacodynamics of tamoxifen. The results of these studies are categorized and presented in Table 2. The first 11 studies showed no significant association between *CYP2D6* polymorphisms and different types of survival outcome.<sup>17,22,27–29,39,43–47</sup>



In contrast, seven studies indicated a significant association between *CYP2D6* polymorphisms and different survival outcomes.<sup>15,20,21,32,33,38,40</sup>

Only six studies investigated an effect of *CYP2D6* polymorphisms on OS; however, none of these studies showed significant results.<sup>17,28,33,43,45,47</sup>

Four trials and a meta-analysis were of great importance in settling the controversy between positive and negative findings for an effect of *CYP2D6* polymorphisms on clinical outcome: the Breast International Group (BIG)1-98 trial<sup>31</sup>, the Armidex, Tamoxifen, Alone or in combination (ATAC) trial<sup>30</sup>, the Austrian Breast and Colorectal cancer Study Group (ABCSG) 8 trial<sup>18</sup>, and the International Tamoxifen Pharmacogenomics Consortium (ITPC) meta-analysis.<sup>53</sup> The BIG1-98 trial<sup>31</sup> and the ATAC trial<sup>30</sup> demonstrated no evidence for an association between *CYP2D6* genotype and recurrence. However, both studies have been criticized: the BIG1-98 trial showed strong deviation from Hardy-Weinberg equilibrium, and the ATAC trial had a lack of statistical power since less than 19% of patients randomized to tamoxifen were analyzed. However, the relevance of meeting Hardy-Weinberg equilibrium in a study reflecting clinical practice is questioned in an editorial by Berry.<sup>54</sup> In contrast, the ABCSG 8 trial showed that *CYP2D6* PMs had a significantly higher rate of recurrence and death in patients treated with tamoxifen monotherapy for 5 years. For patients carrying two PM alleles this effect was significant (odds ratio [OR] 2.45, 95% CI 1.05–5.73;  $p = 0.04$ ), and for patients carrying one PM allele (OR 1.67, 95% CI 0.95–2.93;  $p = 0.07$ ) a trend was observed.<sup>18</sup> Schroth et al. found similar results; patients with reduced *CYP2D6* activity, carrying either one or two PM alleles, had significantly shorter time to recurrence (HR 1.40, 95% CI 1.04–1.90, and HR 1.90, 95% CI 1.10–3.28, respectively). In addition, the effects on EFS (HR 1.33, 95% CI 1.06–1.68) and DFS (HR 1.29, 95% CI 1.03–1.61) showed significance, but the effect on OS was not significant (HR 1.15, 95% CI 0.88–1.51), comparing EMs with heterozygous and homozygous carries of PM alleles together.<sup>34</sup> The ITPC meta-analysis by Provence et al. defined three groups of inclusion criteria, of which criteria 1 was the most restrictive (including ER-positive breast-cancer patients receiving tamoxifen 20 mg daily for 5 years). In this subgroup, *CYP2D6* PM status was associated with shorter DFS (HR 1.25, 95% CI 1.06–1.47;  $p = 0.009$ ).

However, when tamoxifen duration, menopausal status, and annual follow-up were not specified, no significant association was seen (HR 1.17, 95% CI 0.90–1.52;  $p = 0.25$ ) [criteria 2] and non-significance remained when no exclusions were applied (HR 1.07, 95% CI 0.92–1.26;  $p = 0.38$ ) [criteria 3]. The meta-analysis concluded that high restrictiveness of patient groups validates *CYP2D6* genotyping<sup>53</sup>; however, the credibility of this study has been questioned, in part due to the lack of prospectively defining the endpoint, selection bias, and omitting OS.<sup>55</sup>

The study by Wegman et al.<sup>38</sup> investigated whether or not the *CYP2D6*\*4 variant allele was of prognostic value. Patients carrying at least one *CYP2D6*\*4 allele had significantly improved benefit from tamoxifen treatment ( $p = 0.0089$ ); for the wild-type *CYP2D6*, this benefit was not significant.

Thus, based on these studies it can be concluded that *CYP2D6* activity has a clear effect on endoxifen concentrations, advocating a gene-exposure effect. However, interindividual variability in endoxifen concentrations can only, in part, be explained by *CYP2D6* genotypes or predicted phenotypes. Whether this also translates into less efficacy of tamoxifen in *CYP2D6* PMs remains controversial. As depicted in Tables 1 and 3, included studies investigating the effect of polymorphisms on survival outcome had various weaknesses and differences regarding characteristics, statistical power, methodological quality, and study design. Therefore, combining results of different studies and drawing a clear conclusion is challenging. Potential biases in a subset of studies are more extensively described in a previous review.<sup>56</sup>

## DISCUSSION

Review of the published data on the effect of various genetic polymorphisms shows that interindividual variability in response to tamoxifen treatment cannot sufficiently be explained by genotype variability. A conclusive answer to whether genotyping is of clinical value for patients to be treated with tamoxifen is currently not available, which is mainly caused by the controversial outcomes of multiple studies, partially explained by high interstudy heterogeneity and methodological flaws in different studies.

Different factors contribute to interstudy heterogeneity, such as differences in quantification of tamoxifen and metabolites, registration of co-medication, administered dose, time on tamoxifen treatment, compliance, genotype comparison, tissue used for genotyping, deviation from Hardy-Weinberg equilibrium, specification of survival outcome, statistical power, methodology, and study design. Additionally, studies are selective on what polymorphisms are taken into account, leading to potential misclassification of phenotypes.

Regardless of the extensive heterogeneity between studies, none of the conducted trials reported consistent evidence for an effect of polymorphisms in *CYP2B6*, *CYP2C9*, and *CYP2C19* encoding genes on the pharmacokinetics and/or pharmacodynamics of tamoxifen. For *CYP3A5* polymorphisms, there was no clear gene-exposure effect, but *CYP3A4\*22* showed significantly higher concentrations of endoxifen, probably attributed to higher tamoxifen concentrations. In addition, *CYP2D6* PMs benefited from *CYP3A4\*22*, resulting in higher endoxifen concentrations compared with *CYP2D6* PMs lacking this genomic variation. No studies linked *CYP3A4* polymorphisms to outcome. No association between *CYP3A5* polymorphisms and survival outcome was found, except for the unexpected association between *CYP3A5\*3* homozygous carriers and improved RFS.<sup>39</sup> Nevertheless, further investigation is needed to determine if the *CYP3A4/5* pathway in tamoxifen metabolism, and therefore its polymorphic state, becomes more important with decreasing *CYP2D6* activity.

For *CYP2D6*, all indicated studies clearly show a significant gene-exposure effect. However, interindividual variability in endoxifen concentrations can only, in part, be attributed to the *CYP2D6* genotype. This partial contribution might be a reason for the controversy seen in trials aimed at finding an association between variant allele carriers of *CYP2D6* and survival outcomes. In addition, CYP enzymes are also known to play a role in estrogen metabolism. *CYP3A4*, for example, catalyzes the conversion of estradiol to 2-hydroxyestradiol (E2). E2 inhibits cellular proliferation, therefore SNP-induced alterations in *CYP3A4* activity can affect tumor development itself, apart from its effect on tamoxifen metabolism and outcome.<sup>57,58</sup> *CYP2C19* polymorphisms are also known to affect estrone (E1) and E2 catabolism.

High concentrations of E1 were seen in patients carrying either one or two *CYP2C19\*2* variant alleles, and low E2 concentrations were associated with the *CYP2C19\*17* genotype.<sup>59</sup> *CYP2C19\*2* variant allele carriers have been shown to be at a higher risk of developing breast cancer, and the prognosis in these patients in the absence of treatment is poor. However, these tumors are more sensitive to anti-estrogen treatment, rendering their prognosis after adjuvant tamoxifen treatment similar to breast-cancer patients with wild-type *CYP2C19*.<sup>13</sup>

While the debate continues on whether or not genotyping of *CYP2D6* prior to adjuvant treatment with tamoxifen should be implemented, further validation for genotyping and other approaches to personalize treatment with tamoxifen should be explored.

To truly settle controversy on whether or not to use genotyping, previously described factors contributing to interstudy heterogeneity should be addressed in future attempts. Some selected points to consider are discussed shortly. For pharmacokinetic-oriented studies, discrepancies in quantitative analysis of tamoxifen and metabolite concentrations should be addressed. Lack of bioanalytical method selectivity can result in misinterpreting plasma concentrations. A selective liquid chromatography–tandem mass spectrometry (LC-MS/MS) method for the quantification of tamoxifen and metabolites is preferred.<sup>60</sup> Coadministration of *CYP2D6* inhibitors, such as antidepressants, can alter exposure to active metabolites of tamoxifen and subsequently alter survival outcomes.<sup>61</sup> Therefore, patients using medication that interferes with *CYP2D6* metabolism should be excluded, or co-medication should be registered. In addition, it is not preferable to use tumor tissue as a source for germline DNA since loss of heterozygosity at the *CYP2D6* locus in breast tumors has been described.<sup>62</sup> Using an insensitive technique to analyse tumor tissue-derived DNA can cause misclassification of genotypes.<sup>62</sup> In order to prevent misclassification through incomprehensive allele coverage, validated tests should be used to ensure accurate *CYP2D6* genotyping.<sup>63</sup> A major drawback for all studies testing an effect of polymorphisms on clinical outcome is the retrospective study design. Prospective studies, with prospectively defined endpoints and sufficient sample size, are needed to validate further recommendations.<sup>55,64</sup> Post hoc analyses of

prospective RCTs and case-control studies including four subgroups can be a valuable alternative for prospective studies. Since polymorphisms in metabolic enzymes can also be of prognostic value, a distinction between the prognostic and predictive value of a polymorphism in a metabolic enzyme should be made. A post hoc analysis of an RCT including an untreated control group can identify such a distinction. Once a prognostic biomarker is identified, it can be corrected for in a multivariate analysis.<sup>49</sup>

In addition to optimization of future trials, two effects should be validated to decide upon the clinical value of genotyping: (1) a clear gene-exposure effect, and (2) a clear exposure-response effect. For *CYP2D6*, a clear gene-exposure effect is reported for endoxifen, as described in this review. However, the variability in plasma concentrations of endoxifen can be partially attributed to the *CYP2D6* genotype, and the residual variability remains unexplained. Therefore, genotyping of *CYP2D6* might not sufficiently predict exposure and, consequently, might not be applicable as a biomarker for tamoxifen treatment response. Other factors, contributing to metabolite concentration variability, should be identified and quantified. Subsequently, these factors, and the genotype, could be of clinical value to tailor tamoxifen treatment. In addition, tamoxifen and other active metabolites have different pharmacological activities and could contribute, in other extents, to treatment outcomes.<sup>48</sup>

An exposure-response effect can be validated by studies linking tamoxifen or metabolite concentrations to clinical outcome. This has been investigated retrospectively by Madlensky et al.<sup>24</sup> where endoxifen concentrations below 5.97 ng/ml correlated with more recurrences, while Saladores et al.<sup>32</sup> indicated that patients with endoxifen concentrations below a threshold of approximately 5.<sup>30</sup> ng/ml were at higher risk for distant relapse or death. Additional prospective research is preferred to further validate an exposure-response relationship; however, conducting a prospective trial in the adjuvant setting is nearly impossible. Therefore, evidence from different trial settings, such as post hoc analyses of RCTs, prospectively collected cohort data in the metastatic setting, and case-control studies, should be combined in order to support an exposure-response effect.

Since there is, as yet, no conclusive predictor for exposure, measurement of plasma concentrations of tamoxifen and active metabolites could be suggested to establish exposure, ensuring the true phenotype of patients. Therapeutic Drug monitoring (TDM) has advantages over the measurement of factors contributing to endoxifen exposure, such as genotype. TDM can identify EMs, or even UMs, with endoxifen concentrations below the threshold, which would have stayed unexposed using genotyping. On the other hand, not all PMs have endoxifen concentrations under the proposed threshold. This is supported by Madlensky et al.<sup>24</sup> who indicated that 24% of the PMs were still able to generate therapeutic concentrations of endoxifen, and Teft et al.<sup>36</sup> who indicated that PMs were able to generate endoxifen, despite the lack of metabolic activity of CYP2D6. Therefore, a risk of unnecessarily high dosing might exist if treatment is only based on genotyping. In addition, TDM could identify non-compliance. However, endoxifen steady-state concentrations are only met after 1-4 months of treatment. Since steady-state endoxifen plasma concentrations are used to tailor tamoxifen treatment, a risk-period of suboptimal treatment exists between the start of treatment and the time of steady state. This short timeframe of risk will not be of clinical relevance since tamoxifen is indicated to reduce recurrence and mortality rates after years of treatment. Nevertheless, this problem could potentially be addressed by using a population pharmacokinetic model to predict steady-state plasma concentrations of endoxifen in an early stage of tamoxifen treatment.<sup>65</sup> Moreover, a population pharmacokinetic model could guide tamoxifen dosing from an early stage.

Both genotyping and TDM rely on the assumption that exposure is correlated with survival outcome. To anticipate either low concentrations or low metabolic activities of CYP2D6, a dose-exposure effect needs to be validated. Previous studies provide evidence for such a dose-exposure effect. An increase of tamoxifen dose from 20 mg daily to 30 or 40 mg daily, increases endoxifen concentrations.<sup>48,66,67</sup> In addition, endoxifen concentrations in CYP2D6 PMs and IMs treated with 40 mg of tamoxifen were comparable to CYP2D6 EMs treated with 20 mg, outlining the feasibility of dose adjustment based on TDM measurements.<sup>68</sup> Regardless of its feasibility, safety of dose adjustments should also be investigated. Several studies have investigated the toxicity of a dose increase of tamoxifen, but no data on long-term toxicity were included.<sup>69,70</sup>

## CONCLUSIONS

No clear effects on pharmacokinetics and pharmacodynamics were seen for various polymorphisms in the CYP encoding genes *CYP2B6*, *CYP2C9*, *CYP2C19*, and *CYP3A4/5*, based on the reviewed data. For *CYP2D6*, there was a clear gene-exposure effect that was able to partially explain the interindividual variability in endoxifen plasma concentration; however, a clear exposure-response effect remained controversial. Even though the effects of polymorphisms on the pharmacokinetics and pharmacodynamics of tamoxifen are rationalized by its well-understood metabolism, the genotype remains a surrogate parameter for the plasma concentration of tamoxifen and its metabolites, hampering the clinical applicability of genotyping. Based on existing evidence for a link between exposure and response to tamoxifen, TDM seems to be the best approach for tailored tamoxifen treatment at the moment. However, to truly validate genotyping or any other tailored treatment of tamoxifen, additional studies linking metabolite concentrations to clinical outcome, as well as studies on toxicity, are needed, in addition to studies investigating to what extent tamoxifen and other metabolites contribute to the antiestrogenic effect of tamoxifen.

## REFERENCES

1. Early Breast Cancer Trialists' Collaborative Group. Effects of chemotherapy and hormonal therapy for early breast cancer on recurrence and 15-year survival: an overview of the randomised trials. *Lancet* 365, 1687-717 (2005).
2. Davies, C. et al. Long-term effects of continuing adjuvant tamoxifen to 10 years versus stopping at 5 years after diagnosis of oestrogen receptor-positive breast cancer: ATLAS, a randomised trial. *Lancet* 381, 805-816 (2013).
3. Gray, R., Rea, D. & Handley, K. ATTom: Long-term effects of continuing adjuvant tamoxifen to 10 years versus stopping at 5 years in 6,953 women with early breast cancer. *J Clin Oncol* 31: suppl; (2013).
4. Regan, M. M. et al. Assessment of letrozole and tamoxifen alone and in sequence for postmenopausal women with steroid hormone receptor-positive breast cancer: the BIG 1-98 randomised clinical trial at 8.1 years median follow-up. *Lancet Oncol.* 12, 1101-8 (2011).
5. Winer, E. P. et al. American Society of Clinical Oncology technology assessment on the use of aromatase inhibitors as adjuvant therapy for postmenopausal women with hormone receptor-positive breast cancer: status report 2004. *J. Clin. Oncol.* 23, 619-29 (2005).
6. Smith, I. E. & Dowsett, M. Aromatase Inhibitors in Breast Cancer. *N Engl J Med* 348, 2431-2442 (2003).
7. Early Breast Cancer Trialists' Collaborative Group. Relevance of breast cancer hormone receptors and other factors to the efficacy of adjuvant tamoxifen: patient-level meta-analysis of randomised trials. *Lancet* 378, 771-784 (2011).
8. Desta, Z., Ward, B. A., Soukhova, N. V & Flockhart, D. A. Comprehensive Evaluation of Tamoxifen Sequential Biotransformation by the Human Cytochrome P450 System in Vitro: Prominent Roles for CYP3A and CYP2D6. *J. Pharmacol. Exp. Ther.* 310, 1062-1075 (2004).
9. Lim, Y. C., Desta, Z., Flockhart, D. a & Skaar, T. C. Endoxifen (4-hydroxy-N-desmethyl-tamoxifen) has anti-estrogenic effects in breast cancer cells with potency similar to 4-hydroxy-tamoxifen. *Cancer Chemother. Pharmacol.* 55, 471-8 (2005).
10. Johnson, M. D. et al. Pharmacological characterization of 4-hydroxy- N -desmethyl tamoxifen, a novel active metabolite of tamoxifen. *Breast Cancer Res. Treat.* 85, 151-159 (2004).



11. Thomas, C. & Gustafsson, J.-Å. The different roles of ER subtypes in cancer biology and therapy. *Nat. Rev. Cancer* 11, 597–608 (2011).
12. Phan, M. & Venitz, J. Summary Minutes of the Advisory Committee Pharmaceutical Science clinical Pharmacology Subcommittee. (2006) at <<http://www.fda.gov/ohrms/dockets/ac/06/minutes/2006-4248m1.pdf>>
13. Beelen, K. et al. CYP2C19\*2 predicts substantial tamoxifen benefit in postmenopausal breast cancer patients randomized between adjuvant tamoxifen and no systemic treatment. *Breast Cancer Res. Treat.* 139, 649–55 (2013).
14. Borges, S. et al. Quantitative effect of CYP2D6 genotype and inhibitors on tamoxifen metabolism: implication for optimization of breast cancer treatment. *Clin. Pharmacol. Ther.* 80, 61–74 (2006).
15. Chamnanphon, M. et al. Association of CYP2D6 and CYP2C19 polymorphisms and disease-free survival of Thai post-menopausal breast cancer patients who received adjuvant tamoxifen. *Pharmgenomics. Pers. Med.* 6, 37–48 (2013).
16. Fernández-Santander, A. et al. Relationship between genotypes Sult1a2 and Cyp2d6 and tamoxifen metabolism in breast cancer patients. *PLoS One* 8, e70183 (2013).
17. Goetz, M. P. et al. Pharmacogenetics of tamoxifen biotransformation is associated with clinical outcomes of efficacy and hot flashes. *J. Clin. Oncol.* 23, 9312–8 (2005).
18. Goetz, M. P. et al. CYP2D6 metabolism and patient outcome in the Austrian Breast and Colorectal Cancer Study Group Trial (ABCSCG) 8. *Clin. cancer Res.* 19, 500–507 (2013).
19. Jin, Y. et al. CYP2D6 genotype, antidepressant use, and tamoxifen metabolism during adjuvant breast cancer treatment. *J. Natl. Cancer Inst.* 97, 30–9 (2005).
20. Kiyotani, K. et al. Impact of CYP2D6\*10 on recurrence-free survival in breast cancer patients receiving adjuvant tamoxifen therapy. *Cancer Sci.* 99, 995–9 (2008).
21. Kiyotani, K. et al. Significant effect of polymorphisms in CYP2D6 and ABCC2 on clinical outcomes of adjuvant tamoxifen therapy for breast cancer patients. *J. Clin. Oncol.* 28, 1287–93 (2010).
22. Lash, T. L. et al. CYP2D6 inhibition and breast cancer recurrence in a population-based study in Denmark. *J. Natl. Cancer Inst.* 103, 489–500 (2011).

23. Lim, J. S. L. et al. Impact of CYP2D6, CYP3A5, CYP2C9 and CYP2C19 polymorphisms on tamoxifen pharmacokinetics in Asian breast cancer patients. *Br. J. Clin. Pharmacol.* 71, 737-50 (2011).
24. Madlensky, L. et al. Tamoxifen metabolite concentrations, CYP2D6 genotype, and breast cancer outcomes. *Clin. Pharmacol. Ther.* 89, 718-25 (2011).
25. Moyer, A. M. et al. SULT1A1, CYP2C19 and disease-free survival in early breast cancer patients receiving tamoxifen. *Pharmacogenomics* 12, 1535-1543 (2011).
26. Mürdter, T. E. et al. Activity levels of tamoxifen metabolites at the estrogen receptor and the impact of genetic polymorphisms of phase I and II enzymes on their concentration levels in plasma. *Clin. Pharmacol. Ther.* 89, 708-17 (2011).
27. Mwinyi, J. et al. Impact of variable CYP genotypes on breast cancer relapse in patients undergoing adjuvant tamoxifen therapy. *Cancer Chemother. Pharmacol.* 73, 1181-8 (2014).
28. Nowell, S. a et al. Association of genetic variation in tamoxifen-metabolizing enzymes with overall survival and recurrence of disease in breast cancer patients. *Breast Cancer Res. Treat.* 91, 249-58 (2005).
29. Okishiro, M. et al. Genetic polymorphisms of CYP2D6 10 and CYP2C19 2, 3 are not associated with prognosis, endometrial thickness, or bone mineral density in Japanese breast cancer patients treated with adjuvant tamoxifen. *Cancer* 115, 952-61 (2009).
30. Rae, J. M. et al. CYP2D6 and UGT2B7 genotype and risk of recurrence in tamoxifen-treated breast cancer patients. *J. Natl. Cancer Inst.* 104, 452-60 (2012).
31. Regan, M. M. et al. CYP2D6 genotype and tamoxifen response in postmenopausal women with endocrine-responsive breast cancer: the breast international group 1-98 trial. *J. Natl. Cancer Inst.* 104, 441-51 (2012).
32. Saladores, P. et al. Tamoxifen metabolism predicts drug concentrations and outcome in premenopausal patients with early breast cancer. *Pharmacogenomics J.* 15, 84-94 (2015).
33. Schroth, W. et al. Breast cancer treatment outcome with adjuvant tamoxifen relative to patient CYP2D6 and CYP2C19 genotypes. *J. Clin. Oncol.* 25, 5187-93 (2007).
34. Schroth, W. et al. Association between CYP2D6 polymorphisms and outcomes among women with early stage breast cancer treated with tamoxifen. *JAMA* 302, 1429-1436 (2009).

35. Sensorn, I. et al. Association of CYP3A4/5, ABCB1 and ABCC2 polymorphisms and clinical outcomes of Thai breast cancer patients treated with tamoxifen. *Pharmacogenomics. Pers. Med.* 6, 93-8 (2013).
36. Teft, W. a et al. CYP3A4 and seasonal variation in vitamin D status in addition to CYP2D6 contribute to therapeutic endoxifen level during tamoxifen therapy. *Breast Cancer Res. Treat.* 139, 95-105 (2013).
37. Tucker, A. N. et al. Polymorphisms in cytochrome P4503A5 (CYP3A5) may be associated with race and tumor characteristics, but not metabolism and side effects of tamoxifen in breast cancer patients. *Cancer Lett.* 217, 61-72 (2005).
38. Wegman, P. et al. Genotype of metabolic enzymes and the benefit of tamoxifen in postmenopausal breast cancer patients. *Breast Cancer Res.* 7, R284-90 (2005).
39. Wegman, P. et al. Genetic variants of CYP3A5, CYP2D6, SULT1A1, UGT2B15 and tamoxifen response in postmenopausal patients with breast cancer. *Breast Cancer Res.* 9, R7 (2007).
40. Xu, Y. et al. Association between CYP2D6\*10 genotype and survival of breast cancer patients receiving tamoxifen treatment. *Ann. Oncol.* 19, 1423-9 (2008).
41. Zafra-Ceres, M. et al. Influence of CYP2D6 polymorphisms on serum levels of tamoxifen metabolites in Spanish women with breast cancer. *Int. J. Med. Sci.* 10, 932-7 (2013).
42. Gjerde, J. et al. Effects of CYP2D6 and SULT1A1 genotypes including SULT1A1 gene copy number on tamoxifen metabolism. *Ann. Oncol.* 19, 56-61 (2008).
43. Toyama, T. et al. No association between CYP2D6\*10 genotype and survival of node-negative Japanese breast cancer patients receiving adjuvant tamoxifen treatment. *Jpn. J. Clin. Oncol.* 39, 651-6 (2009).
44. Stingl, J. C. et al. Impact of CYP2D6\*4 genotype on progression free survival in tamoxifen breast cancer treatment. *Curr. Med. Res. Opin.* 26, 2535-42 (2010).
45. Abraham, J. E. et al. CYP2D6 gene variants: association with breast cancer specific survival in a cohort of breast cancer patients from the United Kingdom treated with adjuvant tamoxifen. *Breast Cancer Res.* 12, (2010).
46. Park, I. H. et al. Lack of any association between functionally significant CYP2D6 polymorphisms and clinical outcomes in early breast cancer patients receiving adjuvant tamoxifen treatment. *Breast Cancer Res. Treat.* 131, 455-61 (2012).

47. Park, H. S. et al. Association between genetic polymorphisms of CYP2D6 and outcomes in breast cancer patients with tamoxifen treatment. *J. Korean Med. Sci.* 26, 1007–13 (2011).
48. Barginear, M. F. et al. Increasing tamoxifen dose in breast cancer patients based on CYP2D6 genotypes and endoxifen levels: effect on active metabolite isomers and the antiestrogenic activity score. *Clin. Pharmacol. Ther.* 90, 605–11 (2011).
49. Beelen, K., Zwart, W. & Linn, S. C. Can predictive biomarkers in breast cancer guide adjuvant endocrine therapy? *Nat. Rev. Clin. Oncol.* 9, 529–41 (2012).
50. The Human Cytochrome P450 (CYP) allele nomenclature, The Human Cytochrome P450 (CYP) Allele Nomenclature Database. at <<http://www.cypalleles.ki.se/cyp2d6.htm>>
51. Hudis, C. a et al. Proposal for standardized definitions for efficacy end points in adjuvant breast cancer trials: the STEEP system. *J. Clin. Oncol.* 25, 2127–32 (2007).
52. Collier, J. K. et al. The influence of CYP2B6 , CYP2C9 and CYP2D6 genotypes on the formation of the potent antioestrogen Z-4-hydroxy-tamoxifen in human liver. *Br. J. Clin. Pharmacol.* 54, 157–167 (2002).
53. Province, M. a et al. CYP2D6 genotype and adjuvant tamoxifen: meta-analysis of heterogeneous study populations. *Clin. Pharmacol. Ther.* 95, 216–27 (2014).
54. Berry, D. CYP2D6 genotyping and the use of tamoxifen in breast cancer. *J. Natl. Cancer Inst.* 105, 1267–9 (2013).
55. Berry, D. a CYP2D6 genotype and adjuvant tamoxifen. *Clin. Pharmacol. Ther.* 96, 138–40 (2014).
56. Lash, T. L., Lien, E. a, Sørensen, H. T. & Hamilton-Dutoit, S. Genotype-guided tamoxifen therapy: time to pause for reflection? *Lancet. Oncol.* 10, 825–33 (2009).
57. Blackburn, H. L., Ellsworth, D. L., Shriver, C. D. & Ellsworth, R. E. Role of cytochrome P450 genes in breast cancer etiology and treatment: effects on estrogen biosynthesis, metabolism, and response to endocrine therapy. *Cancer Causes Control* 26(3):319–32 (2015).
58. Tsuchiya, Y., Nakajima, M. & Yokoi, T. Cytochrome P450-mediated metabolism of estrogens and its regulation in human. *Cancer Lett.* 227, 115–24 (2005).

59. Gjerde, J. et al. Associations between tamoxifen , estrogens , and FSH serum levels during steady state tamoxifen treatment of postmenopausal women with breast cancer. *BMC Cancer* 10, 313 (2010).
60. Jager, N. G. L., Rosing, H., Linn, S. C., Schellens, J. H. M. & Beijnen, J. H. Importance of highly selective LC-MS/MS analysis for the accurate quantification of tamoxifen and its metabolites: focus on endoxifen and 4-hydroxytamoxifen. *Breast Cancer Res. Treat.* 133, 793–8 (2012).
61. Binkhorst, L. et al. Unjustified prescribing of CYP2D6 inhibiting SSRIs in women treated with tamoxifen. *Breast Cancer Res. Treat.* 139, 923–9 (2013).
62. Goetz, M. P. et al. Loss of Heterozygosity at the CYP2D6 Locus in Breast Cancer: Implications for Germline Pharmacogenetic Studies. *J. Natl. Cancer Inst.* 107, 1–8 (2014).
63. Schroth, W. et al. CYP2D6 polymorphisms as predictors of outcome in breast cancer patients treated with tamoxifen: expanded polymorphism coverage improves risk stratification. *Clin. Cancer Res.* 16, 4468–77 (2010).
64. Ratain, M. J., Nakamura, Y. & Cox, N. J. CYP2D6 Genotype and Tamoxifen Activity: Understanding interstudy Variability in Methodological Quality. *Clin. Pharmacol. Ther.* 94, 185–187 (2014).
65. Heine, R. Ter et al. Population pharmacokinetic modelling to assess the impact of CYP2D6 and CYP3A metabolic phenotypes on the pharmacokinetics of tamoxifen and endoxifen. *Br. J. Clin. Pharmacol.* 78, 572–86 (2014).
66. Jager, N. L., Rosing, H., Schellens, J., Linn, S. & Beijnen, J. Tamoxifen dose and serum concentrations of tamoxifen and six of its metabolites in routine clinical outpatient care. *Breast Cancer Res.* 143, 447–483 (2014).
67. Kiyotani, K. et al. Dose-adjustment study of tamoxifen based on CYP2D6 genotypes in Japanese breast cancer patients. *Breast Cancer Res. Treat.* 131, 137–45 (2012).
68. Irvin, W. J. et al. Genotype-guided tamoxifen dosing increases active metabolite exposure in women with reduced CYP2D6 metabolism: a multicenter study. *J. Clin. Oncol.* 29, 3232–9 (2011).
69. Bratherton, D. et al. A comparison of two doses of tamoxifen (Novaldex) in postmenopausal women with advanced breast cancer: 10 mg bd versus 20 mg bd. *Br. J. Cancer* 50, 199–205 (1984).

70. Sismondi, P., Biglia, N., Volpi, E. & Gai, M. Tamoxifen and Endometrial Cancer. *Ann New York Acad Sci* 734, 310-321 (1994).







## CHAPTER 1.2

### An Antiestrogenic Activity Score for tamoxifen and its metabolites is associated with breast cancer outcome

*Breast Cancer Res Treat.* 2017 Feb;161(3):567-574

A.H.M. de Vries Schultink

X. Alexi

E. van Werkhoven

L. Madlensky

L. Natarajan

S.W. Flatt

W. Zwart

S.C. Linn

B.A. Parker

A.H.B Wu

J.P. Pierce

A.D.R. Huitema

J.H. Beijnen

## ABSTRACT

### Purpose

Endoxifen concentrations have been associated with breast cancer recurrence in tamoxifen-treated patients. However, tamoxifen itself and other metabolites also show antiestrogenic anti-tumor activity. Therefore, the aim of this study was to develop a comprehensive Antiestrogenic Activity Score (AAS), which accounts for concentration and antiestrogenic activity of tamoxifen and three metabolites. An association between the AAS and recurrence-free survival was investigated and compared to a previously published threshold for endoxifen concentrations of 5.97 ng/mL.

### Patients and methods

The antiestrogenic activities of tamoxifen, (Z)-endoxifen, (Z)-4-hydroxytamoxifen and *N*-desmethyltamoxifen were determined in a cell proliferation assay. The AAS was determined by calculating the sum of each metabolite concentration multiplied by an  $IC_{50}$  ratio, relative to tamoxifen. The AAS was calculated for 1370 patients with estrogen receptor alpha (ER $\alpha$ )-positive breast cancer. An association between AAS and recurrence was investigated using Cox-regression and compared with the 5.97 ng/mL endoxifen threshold using concordance indices.

### Results

An AAS threshold of 1798 was associated with recurrence-free survival, hazard ratio (HR) 0.67 (95% confidence interval (CI) 0.47-0.96), bias corrected after bootstrap HR 0.69 (95%CI: 0.48-0.99). The concordance indices for AAS and endoxifen did not significantly differ, however using the AAS threshold instead of endoxifen led to different dose recommendations for 5.2% of the patients.

## **Conclusions**

Endoxifen concentrations can serve as a proxy for the antiestrogenic effect of tamoxifen and metabolites. However, for the aggregate effect of tamoxifen and three metabolites, defined by an integrative algorithm, a trend towards improving treatment is seen and moreover, is significantly associated with breast cancer recurrence.

## INTRODUCTION

Five years of adjuvant treatment with the antiestrogenic drug tamoxifen lowers estrogen receptor alpha (ER $\alpha$ )-positive breast cancer recurrence and mortality rates.<sup>1</sup> Results from the Adjuvant Tamoxifen, Longer Against Shorter (ATLAS) trial and the Adjuvant Tamoxifen Treatment offers-more (aTTom) trial indicate that further decrease of recurrence and mortality rates can be achieved for a subset of patients by prolongation of tamoxifen treatment to up to 10 years.<sup>2,3</sup> In the postmenopausal setting, aromatase inhibitors lower recurrence if given for 5 years or in sequence for 2-3 years, before or after tamoxifen.<sup>4</sup> In premenopausal woman, aromatase inhibitors alone do not work.<sup>5</sup> The combination of aromatase inhibition and ovarian suppression (either ablation or pharmacological suppression) has shown to improve disease-free survival compared to tamoxifen treatment.<sup>6,7</sup> However, ovarian suppression can cause substantial side effects and the combination of an aromatase inhibitor and ovarian ablation did not show a difference in overall survival.<sup>6</sup> Therefore, tamoxifen remains an important treatment option. Despite tamoxifen's effectiveness in reducing recurrence and mortality rates, resistance to tamoxifen often occurs and remains a major clinical challenge.<sup>8</sup> Multiple studies have investigated variability in response to tamoxifen by focusing on patient-related factors to tailor treatment, such as cytochrome P450 (CYP) genotypes and serum concentrations of metabolites.<sup>9-14</sup> Tamoxifen is bioactivated by CYP enzymes, such as CYP2D6 and CYP3A4/5 (Fig 1).<sup>15</sup> CYP2D6 has most extensively been investigated, since it is responsible for bioactivation of tamoxifen's most important metabolite, endoxifen.<sup>15</sup> Both the CYP2D6 genotype and endoxifen concentrations have been proposed as patient-related factors correlated with breast cancer outcome.<sup>13,14,16</sup> However, publications that correlate CYP2D6 genotype with breast cancer outcome have reported conflicting results.<sup>16</sup> Even though a clear association between CYP2D6 genotype and endoxifen concentration is reported, variability in plasma concentration of endoxifen could only partially be attributed to CYP2D6 polymorphisms.<sup>13,14,17-19</sup> Therefore, Therapeutic Drug Monitoring (TDM) of endoxifen seems the best way forward to tailor tamoxifen treatment, ensuring the true phenotype of patients.<sup>16,20</sup>

A threshold of 5.97 ng/mL endoxifen has been identified previously and could be applied to tailor tamoxifen treatment, recommending an increase in tamoxifen dose if endoxifen concentrations are below 5.97 ng/mL.<sup>13</sup> The results of that study indicated that patients with an endoxifen concentration above 5.97 ng/mL had 26% lower risk of developing an invasive breast cancer recurrence or new primary breast cancer compared to patients with a lower endoxifen concentration. However, TDM of endoxifen assumes that the antiestrogenic effect of tamoxifen is attributed solely to endoxifen, ignoring the possible contribution of other metabolites and of tamoxifen itself. Tamoxifen and metabolites have varying antiestrogenic activity towards the ER $\alpha$  and occur in different concentrations in patients, each potentially contributing to a different extent to the total antiestrogenic effect. The *in vitro* inhibitory potential of tamoxifen and many of its metabolites was previously evaluated, in ER $\alpha$  binding competition assays, as well as gene transcription and breast cancer cell growth assays.<sup>17,21,22</sup> Endoxifen and 4-hydroxytamoxifen are reported to be the most potent metabolites, with both exhibiting IC<sub>50</sub> values in the low nanomolar range, while tamoxifen and *N*-desmethyltamoxifen are equally less potent with IC<sub>50</sub> values in the micromolar range.<sup>17,21,22</sup> Previous studies reporting tamoxifen and metabolite concentrations indicate that endoxifen concentrations exceed 4-hydroxytamoxifen concentrations in human serum by approximately 6 fold.<sup>23-27</sup> Tamoxifen and *N*-desmethyltamoxifen are less potent than endoxifen, but have around 10 and 14 fold higher concentrations, respectively.<sup>23-27</sup> Therefore, it is plausible that the total antiestrogenic effect of tamoxifen depends on a cumulative, intrinsic effect of tamoxifen and active metabolites and their relative concentrations in blood.

To our knowledge, an aggregate effect of tamoxifen together with its active metabolites on breast cancer outcome has never been investigated to date. The aim of this study was, therefore, to investigate if an aggregate Antiestrogenic Activity Score (AAS), which takes into account both concentration and antiestrogenic activity of tamoxifen and multiple active tamoxifen metabolites, is associated with breast cancer outcome.

To have a more accurate comparison, the relative activities of tamoxifen, N-desmethyltamoxifen, (Z)-4-hydroxytamoxifen and (Z)-endoxifen were assessed *in vitro*, using the same experimental setup.

The calculated relative activities were then used to determine the AAS and tested for correlation with outcome.

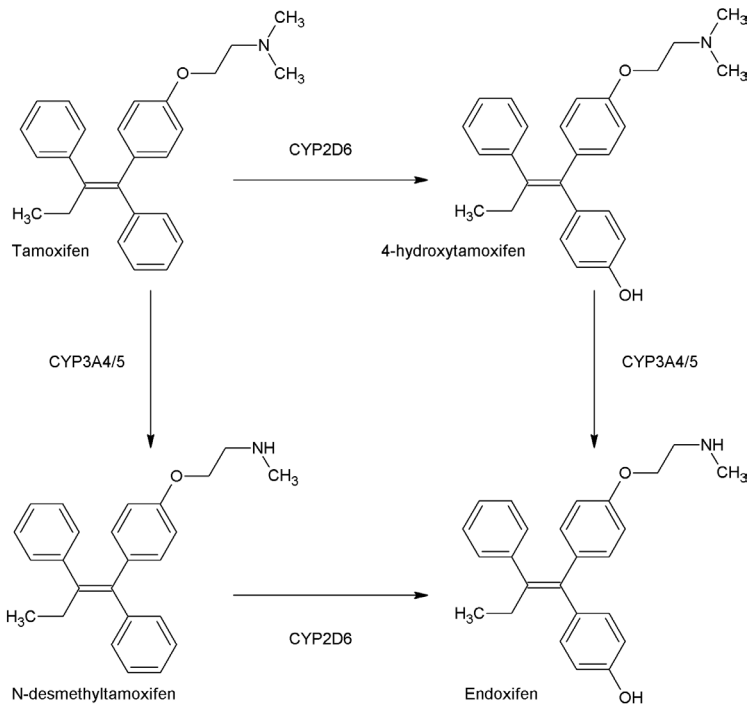


**Figure 1** Part of the biotransformation of tamoxifen<sup>15</sup>

## METHODS

### Determination of *in vitro* relative antiestrogenic activity of tamoxifen and three metabolites

The antiestrogenic activities of tamoxifen, *N*-desmethyltamoxifen, (Z)-4-hydroxytamoxifen and (Z)-endoxifen were determined using cell proliferation experiments. MCF-7 breast adenocarcinoma cells were regularly maintained in phenol-red free DMEM supplemented with l-glutamine and 10% fetal bovine serum. At 24 h prior to the experiment, cells were plated in clear bottom 384 well plates at a density of 600 cells per well. The cells were allowed to adhere for 24 h before an equal volume of two times the final concentration of the appropriate tamoxifen metabolite was added. Following compound addition, cell proliferation in the individual wells was monitored for 14 days using cell imaging for confluency assessment (IncuCyte®, Essen Bioscience).

For each biological replicate a metabolite serial dilution was carried out in DMSO, leading to a final range of tamoxifen (and metabolite) concentrations between  $10^{-6}$  M to  $10^{-11}$  M ( $10^{-6}$  M,  $10^{-7}$  M,  $10^{-8}$  M,  $10^{-9}$  M,  $10^{-10}$  M and  $10^{-11}$  M). For the control wells an equivalent dilution of DMSO was applied (1:1000). The percentage growth inhibition versus metabolite concentration was plotted, sigmoidal dose-response curves were fitted and the  $IC_{50}$  values were calculated using SigmaPlot (Systat Software, San Jose, CA). Calculation of the  $IC_{50}$  ratio was done for three independent biological replicates and the average value was used for the AAS calculation. The AAS calculation was based on the antiestrogenic activity ratios relative to tamoxifen.

### Patients

The analysis conducted in this study was based upon data from 1370 patients with ER $\alpha$ -positive breast cancer who were selected from the Women's Healthy Eating and Living (WHEL) study.<sup>28</sup> This data set was previously analyzed by Madlensky et al.<sup>13</sup> At study entry, the participants had been diagnosed with breast cancer <4 years earlier and had completed primary therapy without recurrence or development of a second primary breast cancer at onset of the study. A blood sample was taken from each patient at study entry. Data included quantifications

of tamoxifen, N-desmethyltamoxifen, 4-hydroxytamoxifen and endoxifen serum concentrations and recurrence-free survival time. To ensure steady-state blood concentrations, the patients included in the analysis had been taking tamoxifen for at least 4 months before the baseline survey. Recurrence-free survival was defined as time from diagnosis of the original breast cancer to recurrence (including local and distant recurrences, metastatic disease or new invasive primary breast cancer). The data are more extensively described elsewhere.<sup>13</sup>

### Calculation of AAS

We incorporated concentrations of tamoxifen and metabolites, corrected for antiestrogenic activity, into an algorithm.  $IC_{50}$  ratios for each metabolite ( $ICR_{metabolite}$ ) were calculated by dividing the  $IC_{50}$  value of tamoxifen by the  $IC_{50}$  values of each metabolite using the following equation:

$$ICR_{metabolite} = \frac{IC_{50} tamoxifen}{IC_{50} metabolite} \quad (1)$$

For example the  $ICR_{endoxifen}$  is calculated by dividing the  $IC_{50}$  of tamoxifen by the  $IC_{50}$  of endoxifen. For each patient, the Antiestrogenic Activity Score (AAS) was subsequently calculated as follows:

$$AAS = 1 \cdot [tam] + ICR_{NDMtam} \cdot [NDMtam] + ICR_{4Ohtam} \cdot [4Ohtam] + ICR_{endox} \cdot [endox] \quad (2)$$

where [tam], [NDMtam], [4Ohtam] and [endox] represent tamoxifen, N-desmethyltamoxifen, (Z)-4-hydroxytamoxifen and endoxifen concentrations, respectively. Concentrations were reported in ng/mL, however converted to nmol/L (nM) for calculating the AAS, since an addition component is used in the algorithm.  $ICR_{NDMtam}$ ,  $ICR_{4Ohtam}$  and  $ICR_{endox}$  represent the calculated  $IC_{50}$  ratios, respectively. Tamoxifen and metabolite concentrations were measured in serum for each patient. The AAS was defined as the amount of tamoxifen antiestrogenic



activity equivalents in nM, but was further treated as a dimensionless score. Development of this algorithm was based on a previously described comparable algorithm.<sup>29</sup>

### Statistical analysis

Patients in this analysis were selected based on the criterion that they had been taking tamoxifen for at least 4 months before the baseline survey. Time zero for an individual patient was defined as the date of the first tamoxifen administration. Patients who died or were lost to follow up before completing 4 months of tamoxifen were not included in this analysis. The data were therefore left truncated and were handled as such in Cox-regression analysis, to assess the association between the AAS and recurrence-free survival. The AAS was first entered as a continuous variable and then as dichotomous, where (since a martingale residual plot did not show any particular pattern) the threshold was determined by dichotomizing potential optimal cutoff points and chosen such that the partial likelihood was maximal. Additionally, a bootstrap with replacement was performed (n = 1000) to validate the hazard ratio (HR) using the threshold obtained from the original dataset. The concordance index was calculated for both AAS and endoxifen. Data handling and statistical analyses were conducted using R (v.3.0.1).<sup>30</sup>

## RESULTS

### Antiestrogenic activity of tamoxifen and metabolites

The results from the *in vitro* experiments are depicted in Table 1 and Fig 2. To determine the effects of tamoxifen and three of its metabolites ((Z)-4-hydroxytamoxifen, (Z)-endoxifen and N-desmethyltamoxifen) on general ER $\alpha$  activity without limiting analysis to single reporter genes, proliferation of the ER $\alpha$ -driven breast cancer cell line MCF-7 was used as a readout. As expected, (Z)-4-hydroxytamoxifen and (Z)-endoxifen were most potent at inhibiting MCF-7 cell proliferation. Tamoxifen and N-desmethyltamoxifen were far less potent. The IC<sub>50</sub> ratios for each of the tamoxifen metabolites were calculated for each experiment and averaged, resulting in 0.38, 21.8 and 74.4 for N-desmethyltamoxifen, (Z)-4-

hydroxytamoxifen and (Z)-endoxifen, respectively. The  $IC_{50}$  ratio for tamoxifen was 1 by definition. The  $IC_{50}$  ratios were entered into Eq. (2) resulting in the following algorithm for AAS:

$$AAS = 1 \cdot [tam] + 0.38 \cdot [NDMtam] + 21.8 \cdot [4Ohtam] + 74.4 \cdot [endox] \quad (3)$$

Table 1 Results of in vitro growth experiments,  $IC_{50}$  values, calculated  $IC_{50}$  ratios and average

	EXPERIMENT 1		EXPERIMENT 2		EXPERIMENT 3		AVERAGE
	$IC_{50}$ (nM)	$IC_{50}$ ratio	$IC_{50}$ (nM)	$IC_{50}$ ratio	$IC_{50}$ (nM)	$IC_{50}$ ratio	
<b>Tamoxifen</b>	106	1	88	1	188	1	1
<b>N-desmethyl-tamoxifen</b>	189	0.56	573	0.15	430	0.44	0.38
<b>(Z)-4-hydroxytamoxifen</b>	18	5.89	7	12.6	4	47	21.8
<b>(Z)-Endoxifen</b>	8	13.3	4	22	1	188	74.4

$IC_{50}$  = half maximal inhibitory concentration

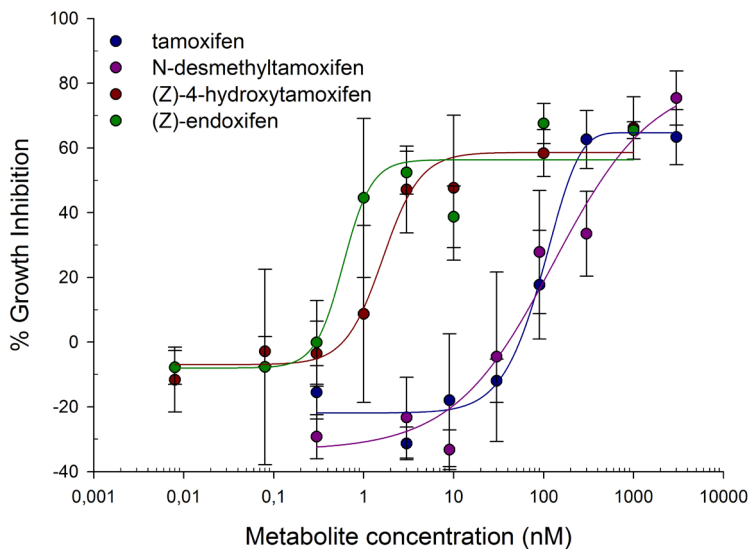


**Figure 2** Dose-response curves for tamoxifen, N-desmethyltamoxifen, (Z)-4-hydroxytamoxifen, and (Z)-endoxifen.

### Implementation of the AAS score and association with outcome

The 1370 patients from the Madlensky analysis were included in the current study.<sup>13</sup> Boxplots for tamoxifen and metabolite concentrations are included in the Supplementary files (S1). Tamoxifen concentrations were around 10 times higher than endoxifen with median values of 129 ng/mL [interquartile range (IQR): 74.8] and 12.9 ng/mL [IQR: 11.9], respectively. Endoxifen concentrations were 6.7 fold higher than 4-hydroxytamoxifen with median 1.9 ng/mL [IQR: 1.2] for 4-hydroxytamoxifen. *N*-desmethyltamoxifen concentrations exceeded tamoxifen concentrations by 1.9 fold and endoxifen concentrations by approximately 18 fold, with median 240 ng/mL [IQR: 121] for *N*-desmethyltamoxifen. These findings were in line with concentrations reported by previous publications.<sup>23-27</sup> As expected from the metabolic pathway of tamoxifen (Fig 1), correlations between tamoxifen concentrations and concentrations of its primary metabolites 4-hydroxytamoxifen and *N*-desmethyltamoxifen were seen, with correlation coefficients of 0.63 and 0.83 respectively. However, a weaker correlation between tamoxifen and endoxifen, a secondary metabolite of tamoxifen, was found (correlation coefficient 0.44). In addition, a stronger correlation between 4-hydroxytamoxifen and endoxifen concentrations was found, with a correlation coefficient of 0.86. A figure showing the correlations between tamoxifen and the three different metabolites is included in the Supplementary files (S1). Fig 3 shows the relative contribution of each compound to the AAS. The endoxifen concentration contributed to the largest extent to the AAS, followed by tamoxifen, *N*-desmethyltamoxifen and lastly 4-hydroxytamoxifen.

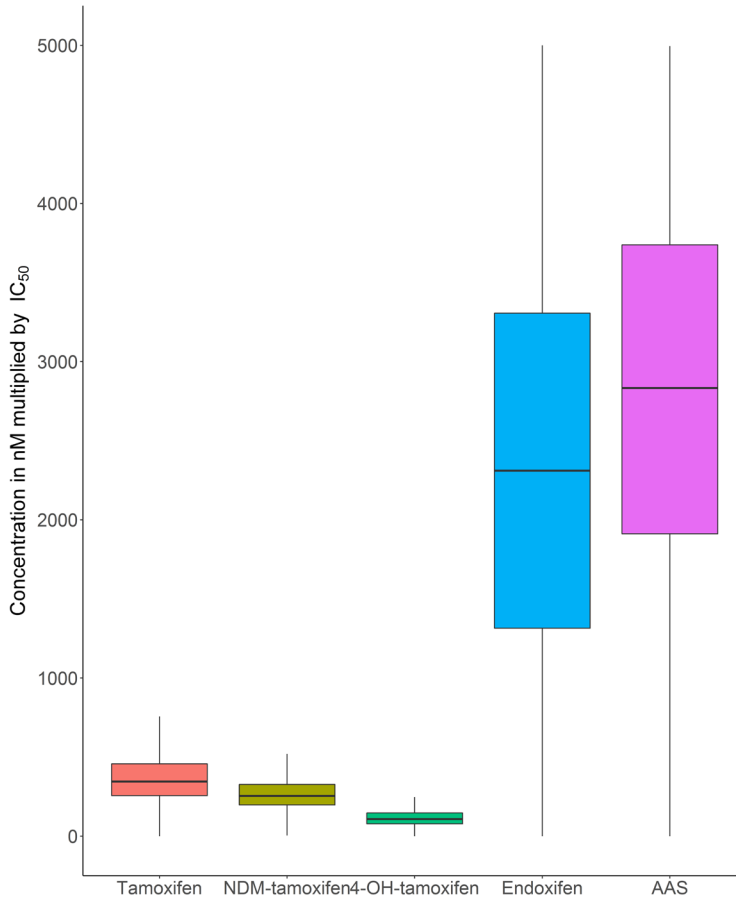


**Figure 3** Boxplots for the concentration of each metabolite multiplied by its  $IC_{50}$  ratio representing the relative contribution to the AAS. Values greater than 1.5 times the upper value of the interquartile range are considered as outliers and removed from the plot.

Menopausal status and breast cancer stage and grade were significantly associated with recurrence-free survival and were included in the Cox model as covariates. Out of 1370 patients, 178 patients experienced a recurrence, the median follow up time was 7.3 years. No association between the AAS as a continuous variable and recurrence-free survival was found, HR 1.00 (95% confidence interval (CI) 0.99-1.00). The partial likelihood method identified a relevant threshold of 1798 for the AAS. In the Cox model, patients with an  $AAS \geq 1798$  had 33% lower risk at developing a secondary breast cancer event, HR of 0.67 (95%CI 0.47-0.96).

The Kaplan-Meier curves for patients with  $AAS \geq 1798$  and  $AAS < 1798$  are depicted in Fig 4. After bootstrap resampling with replacement this result remained significant, HR 0.69 (95%CI 0.48-0.99). A table containing the type of recurrences per AAS group is added to the Supplementary files (S2).

The *in vitro* cell proliferation experiments showed some variability. Therefore, a sensitivity analysis was conducted. For 4-hydroxytamoxifen, N-desmethyltamoxifen and endoxifen the  $IC_{50}$  ratios were multiplied by 1, 1.5 and 0.5, while for tamoxifen the  $IC_{50}$  ratio remained 1. Combining the multiplied  $IC_{50}$  ratios gave 26 different integrative algorithms to calculate the AAS, in addition to the algorithm defined in Eq. (3). For all these 26 algorithms the AAS calculation, including threshold finding and HR calculation, was performed. HRs were compared to the above reported HR based on the calculation of AAS with Eq. (3). All 26 HRs were significant, ranging between 0.60 and 0.69 indicating that the findings of this study were robust.

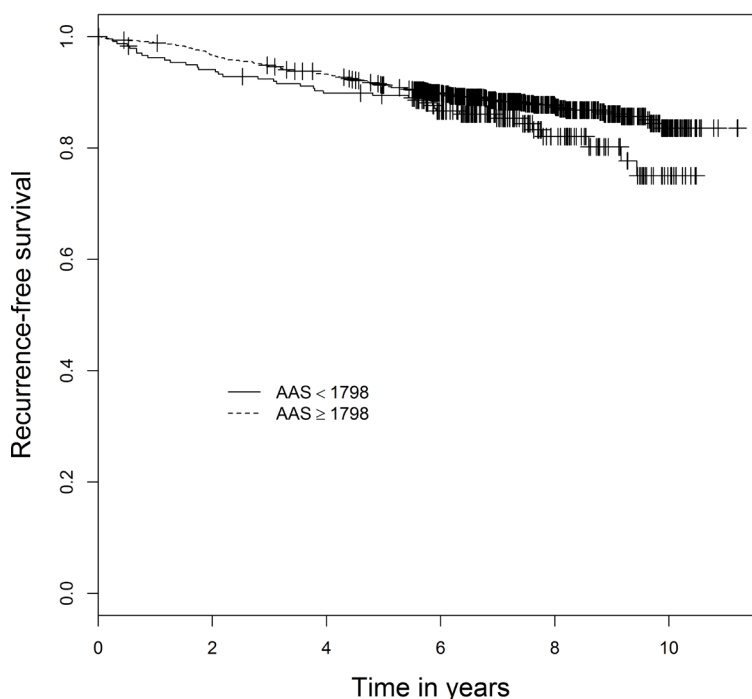


**Figure 4** Kaplan-Meier curves for AAS. Dotted line: patients with  $AAS \geq 1798$ , solid line: patients with  $AAS < 1798$ ; p-value = 0.031; AAS Antiestrogenic Activity Score; + = censored

### AAS score versus endoxifen

The AAS was compared to the endoxifen threshold in an additional analysis (Table 2). Of the 1370 patients included in the analysis, 1298 patients would be classified as above and below the threshold, either using the AAS or the endoxifen concentration threshold. Of the remaining 72 patients, 48 were identified with an AAS value above 1798, but would have been identified with an endoxifen concentration below 5.97 ng/mL (14.5% experienced recurrence). In addition, the remaining 24 patients were identified with an AAS below 1798, but would have been identified with an endoxifen concentration above 5.97 ng/mL (16.7% experienced recurrence). The concordance indices for AAS and endoxifen concentrations were similar, both with a value rounded to 0.71.

**Table 2** Threshold discriminatory value: comparison between endoxifen threshold and AAS threshold

	AMOUNT OF PATIENTS (% OF 1370)	
	Endoxifen $\geq$ 5.97 ng/mL	Endoxifen $<$ 5.97 ng/mL
AAS $\geq$ 1798	1083 (79.1)	48 (3.5)
AAS $<$ 1798	24 (1.7)	215 (15.7)

AAS = Antiestrogenic Activity Score

## DISCUSSION

In this study a novel measure for antiestrogenic efficacy for tamoxifen treatment was developed, showing that an integrative algorithm taking into consideration tamoxifen together with three active metabolites is associated with breast cancer outcome. The corrected HR of 0.69 (95%CI: 0.49-0.99) implies that patients with an AAS  $\geq$  1798 are at 31% lower risk of developing a secondary breast cancer event, as compared to patients with an AAS  $<$  1798. The data used for this analysis have been reported previously by Madlensky et al., who identified a threshold for endoxifen concentrations of 5.97 ng/mL, HR = 0.70 (95%CI 0.52-0.94), bias corrected HR = 0.74 (95%CI 0.55-1.00)<sup>13</sup>. The corrected HR of 0.74 implies that patients with endoxifen concentrations above 5.97 ng/mL have 26% lower risk at developing a secondary breast cancer event. After bootstrap correction the HR for the AAS threshold remained significant (this report), whereas the endoxifen threshold did

not.<sup>13</sup> However, this difference might be the result of different bootstrap methods. The AAS threshold resulted in a lower HR, but the concordance indices for AAS and endoxifen were both 0.71. This suggests that AAS and endoxifen concentrations alone have similar discriminating ability.

However, the cumulative effect of metabolites can theoretically be explained by comparing risk groups, identified by either the AAS or the endoxifen concentration threshold. In the 48 patients with an AAS above the threshold and an endoxifen concentration below the threshold, the low endoxifen concentration is compensated by the antiestrogenic effect of *N*-desmethyltamoxifen, 4-hydroxytamoxifen and tamoxifen. In the 24 patients with an AAS below the threshold and an endoxifen concentration above the threshold, the antiestrogenic activity according to the AAS score is insufficient, regardless of an endoxifen concentration above 5.97 ng/mL. This suggests that endoxifen antiestrogenic activity can, to some extent, be mutually compensated by tamoxifen and different metabolites.

An additional finding was the low contribution of 4-hydroxytamoxifen to the AAS. The IC<sub>50</sub> ratio for 4-hydroxytamoxifen was almost 22 and 58 times higher than the IC<sub>50</sub> ratios for tamoxifen and *N*-desmethyltamoxifen, respectively. However, the AAS demonstrates that this high antiestrogenic activity is compensated by the low concentrations of 4-hydroxytamoxifen. Therefore, it can be concluded that 4-hydroxytamoxifen is far less important than previously expected.

Interpretation of our results should take into account several limitations. The antiestrogenic activities of tamoxifen and metabolites can be different when investigated in different cell lines, or in the presence of estrogen concentrations<sup>31,32</sup>. However, the *in vitro* experiments were conducted to obtain the relative antiestrogenic activities of tamoxifen and three metabolites. Therefore, the ratios implemented in the AAS are not expected to be different in other cell lines or in presence of estrogen. Second, estrogen concentrations can be associated with breast cancer outcome<sup>7</sup>. Estrogen concentrations were not included in the analysis, since these measurements were not available for a substantial part of the cohort. However, menopausal status was significantly associated with recurrence-free survival and included in the Cox regression. Thirdly, the analysis described is a

post hoc analysis of the Madlensky study, based on a subset of patients included in the WHEL study. Thus, this study was not primarily designed to investigate the effect of tamoxifen and metabolite concentrations on breast cancer outcome. However, the data consisted of 1370 patients with ER $\alpha$ -positive breast cancer of whom breast cancer endpoints and metabolite concentrations were available, therefore, the data are suitable for the current analysis. Additionally, the study is limited because patients in the WHEL study were enrolled up to 4 years after diagnosis, therefore, patients who experienced recurrence soon after diagnosis are not taken into account in our analyses. The AAS does not take into account potential other metabolites that could contribute to the total antiestrogenic effect of tamoxifen. However, the major metabolites of tamoxifen are included, with endoxifen and 4-hydroxytamoxifen as the most potent metabolites and N-desmethyltamoxifen as the most abundant metabolite. Additionally, the *in vitro* experiments showed variability in IC<sub>50</sub> values. This variability was addressed by conducting a sensitivity analysis, which showed robust results. In addition, a selective bioanalytical method is pivotal to quantify tamoxifen and metabolite concentrations and to avoid overestimation of concentrations. Therefore, the absolute value of the AAS could deviate when using bioanalytical assays that lack high selectivity.<sup>33</sup> Lastly, the threshold was chosen such that the partial likelihood of the Cox model was maximal. A different threshold may be found by weighing a desired increase in recurrence-free survival time against the side effects of increasing the dose of tamoxifen.

In summary, this is the first analysis to demonstrate an aggregate effect of tamoxifen and three active metabolites on breast cancer outcome. Clinical decisions regarding dose adjustments based on either the AAS threshold or the endoxifen concentration threshold would be the same for 94.8% of patients. This implies, once again, that endoxifen is the most important metabolite. The results of this analysis demonstrate that endoxifen can serve as a proxy for the antiestrogenic effect of tamoxifen and three metabolites and that the AAS does not provide additional information, since the contribution of endoxifen is major and concordance indices are comparable for endoxifen and the AAS. However, for the AAS a trend towards improving treatment by measuring tamoxifen and three metabolites in comparison to measuring endoxifen, is seen. Moreover, a threshold for the tamoxifen metabolite profile is identified at an AAS of 1798



with a corresponding HR of 0.67 (95%CI 0.47-0.96). In future prospective cohort studies, it would be evident to measure tamoxifen and metabolites in addition to endoxifen, in order to further elucidate this effect.

## REFERENCES

1. The Early Breast Cancer Trialists' Collaborative Group. Effects of chemotherapy and hormonal therapy for early breast cancer on recurrence and 15-year survival: an overview of the randomised trials. *Lancet* 365, 1687–717 (2005).
2. Davies, C. et al. Long-term effects of continuing adjuvant tamoxifen to 10 years versus stopping at 5 years after diagnosis of oestrogen receptor-positive breast cancer: ATLAS, a randomised trial. *Lancet* 381, 805–816 (2013).
3. Gray, R., Rea, D. & Handley, K. ATTom: Long-term effects of continuing adjuvant tamoxifen to 10 years versus stopping at 5 years in 6,953 women with early breast cancer. *J Clin Oncol* 31: suppl., (2013).
4. Regan, M. M. et al. Assessment of letrozole and tamoxifen alone and in sequence for postmenopausal women with steroid hormone receptor-positive breast cancer: the BIG 1-98 randomised clinical trial at 8.1 years median follow-up. *Lancet Oncol.* 12, 1101–8 (2011).
5. Winer, E. P. et al. American Society of Clinical Oncology technology assessment on the use of aromatase inhibitors as adjuvant therapy for postmenopausal women with hormone receptor-positive breast cancer: status report 2004. *J. Clin. Oncol.* 23, 619–29 (2005).
6. Pagani, O. et al. Adjuvant Exemestane with Ovarian Suppression in Premenopausal Breast Cancer. *N. Engl. J. Med.* 371, 107–118 (2014).
7. Francis, P. A. et al. Adjuvant ovarian suppression in premenopausal breast cancer. *N. Engl. J. Med.* 372, 436–46 (2015).
8. The Early Breast Cancer Trialists' Collaborative Group. Relevance of breast cancer hormone receptors and other factors to the efficacy of adjuvant tamoxifen: patient-level meta-analysis of randomised trials. *Lancet* 378, 771–784 (2011).
9. Goetz, M. P. et al. CYP2D6 metabolism and patient outcome in the Austrian Breast and Colorectal Cancer Study Group Trial (ABCSG) 8. *Clin. cancer Res.* 19, 500–507 (2013).
10. Schroth, W. et al. Association between CYP2D6 polymorphisms and outcomes among women with early stage breast cancer treated with tamoxifen. *JAMA* 302, 1429–1436 (2009).
11. Rae, J. M. et al. CYP2D6 and UGT2B7 genotype and risk of recurrence in tamoxifen-treated breast cancer patients. *J. Natl. Cancer Inst.* 104, 452–60 (2012).

12. Regan, M. M. et al. CYP2D6 genotype and tamoxifen response in postmenopausal women with endocrine-responsive breast cancer: the breast international group 1-98 trial. *J. Natl. Cancer Inst.* 104, 441-51 (2012).
13. Madlensky, L. et al. Tamoxifen metabolite concentrations, CYP2D6 genotype, and breast cancer outcomes. *Clin. Pharmacol. Ther.* 89, 718-25 (2011).
14. Saladores, P. et al. Tamoxifen metabolism predicts drug concentrations and outcome in premenopausal patients with early breast cancer. *Pharmacogenomics J.* 15, 84-94 (2015).
15. Desta, Z., Ward, B. A., Soukhova, N. V & Flockhart, D. A. Comprehensive Evaluation of Tamoxifen Sequential Biotransformation by the Human Cytochrome P450 System in Vitro : Prominent Roles for CYP3A and CYP2D6. *J. Pharmacol. Exp. Ther.* 310, 1062-1075 (2004).
16. Vries Schultink, A. H. M. de, Zwart, W., Linn, S. C., Beijnen, J. H. & Huitema, A. D. R. Effects of Pharmacogenetics on the Pharmacokinetics and Pharmacodynamics of Tamoxifen. *Clin. Pharmacokinet.* 54, 797-810 (2015).
17. Mürdter, T. E. et al. Activity levels of tamoxifen metabolites at the estrogen receptor and the impact of genetic polymorphisms of phase I and II enzymes on their concentration levels in plasma. *Clin. Pharmacol. Ther.* 89, 708-17 (2011).
18. Teft, W. a et al. CYP3A4 and seasonal variation in vitamin D status in addition to CYP2D6 contribute to therapeutic endoxifen level during tamoxifen therapy. *Breast Cancer Res. Treat.* 139, 95-105 (2013).
19. Wu, A. H. B. et al. Estimation of tamoxifen metabolite concentrations in the blood of breast cancer patients through CYP2D6 genotype activity score. *Breast Cancer Res. Treat.* 133, 677-83 (2012).
20. Jager, N. G. L., Linn, S. C., Schellens, J. H. M. & Beijnen, J. H. Tailored Tamoxifen Treatment for Breast Cancer Patients: A Perspective. *Clin. Breast Cancer* 15, 1-4 (2015).
21. Lim, Y. C., Desta, Z., Flockhart, D. a & Skaar, T. C. Endoxifen (4-hydroxy-N-desmethyl-tamoxifen) has anti-estrogenic effects in breast cancer cells with potency similar to 4-hydroxy-tamoxifen. *Cancer Chemother. Pharmacol.* 55, 471-8 (2005).
22. Coezy, E., Borgna, J. & Rochefort, H. Tamoxifen and Metabolites in MCF7 Cells : Correlation between Binding to Estrogen Receptor and Inhibition of Cell Growth Tamoxifen and Metabolites in MCF7 Cells : Correlation between Binding. *Cancer Res.* 41, 317-323 (1982).

23. Johnson, M. D. et al. Pharmacological characterization of 4-hydroxy- N -desmethyl tamoxifen , a novel active metabolite of tamoxifen. *Breast Cancer Res. Treat.* 85, 151-159 (2004).
24. Jin, Y. et al. CYP2D6 genotype, antidepressant use, and tamoxifen metabolism during adjuvant breast cancer treatment. *J. Natl. Cancer Inst.* 97, 30-9 (2005).
25. Lim, H.-S. et al. Clinical implications of CYP2D6 genotypes predictive of tamoxifen pharmacokinetics in metastatic breast cancer. *J. Clin. Oncol.* 25, 3837-45 (2007).
26. Stearns, V. et al. Active Tamoxifen Metabolite Plasma Concentrations After Coadministration of Tamoxifen and the Selective Serotonin Reuptake Inhibitor Paroxetine. *J. Natl. Cancer Inst.* 95, 1758-1764 (2003).
27. Teunissen, S. F. et al. Development and validation of a quantitative assay for the determination of tamoxifen and its five main phase I metabolites in human serum using liquid chromatography coupled with tandem mass spectrometry. *J. Chromatogr. B Anal. Technol. Biomed. Life Sci.* 879, 1677-1685 (2011).
28. Pierce, J. P. et al. Influence of a diet very high in vegetables, fruit, and fiber and low in fat on prognosis following treatment for breast cancer: the Women's Healthy Eating and Living (WHEL) randomized trial. *JAMA* 298, 289-98 (2007).
29. Barginear, M. F. et al. Increasing tamoxifen dose in breast cancer patients based on CYP2D6 genotypes and endoxifen levels: effect on active metabolite isomers and the antiestrogenic activity score. *Clin. Pharmacol. Ther.* 90, 605-11 (2011).
30. R Core Team, 2018 R: A language and Environment for Statistical Computing. R Foundation for statistical computing, Vienna, Austria. at <<https://www.r-project.org/>>
31. Maximov, P. Y. et al. Simulation with cells in vitro of tamoxifen treatment in premenopausal breast cancer patients with different CYP2D6 genotypes. *Br. J. Pharmacol.* (2014).
32. Maximov, P. Y. et al. Pharmacological Relevance of Endoxifen in a Laboratory Simulation of Breast Cancer in Postmenopausal Patients. *J. Natl. Cancer Inst.* 106, 1-10 (2014).
33. Jager, N. G. L., Rosing, H., Linn, S. C., Schellens, J. H. M. & Beijnen, J. H. Importance of highly selective LC-MS/MS analysis for the accurate quantification of tamoxifen and its metabolites: focus on endoxifen and 4-hydroxytamoxifen. *Breast Cancer Res. Treat.* 133, 793-8 (2012).





## CHAPTER 1.3

### Therapeutic Drug Monitoring of endoxifen as an alternative for CYP2D6 genotyping in individualizing tamoxifen therapy

*Breast. 2018 Aug; 42:38-40 [Epub ahead of print]*

A.H.M. de Vries Schultink  
A.D.R. Huitema  
J.H. Beijnen

## **ABSTRACT**

Different strategies have been proposed to individualize tamoxifen treatment in order to improve recurrence-free survival in estrogen receptor (ER)-positive breast cancer. To date, the debate remains on which strategy should be used. The objective of this viewpoint is to highlight Therapeutic Drug Monitoring (TDM) of endoxifen, the active tamoxifen metabolite, as the preferred methodology compared to *CYP2D6* genotyping for individualizing tamoxifen therapy for ER-positive breast cancer patients treated in the adjuvant setting.



## INTRODUCTION

Individualization of tamoxifen treatment to improve recurrence-free survival in estrogen receptor (ER)-positive breast cancer patients has been investigated for years. The use of genotyping of metabolizing enzymes (mainly CYP2D6) to predict exposure to endoxifen, the most important active metabolite of tamoxifen, has widely been advocated. The underlying assumption of genotyping is, that it predicts endoxifen concentrations and that the exposure to endoxifen is related to breast cancer treatment outcome. However, the individual genotype is just one of many factors that explains variability in endoxifen exposure. Therefore, we propose to measure endoxifen concentrations for therapy individualization instead of genotyping.

## CYP2D6 GENOTYPING

The association between the CYP2D6 genotype and breast cancer outcome has extensively been researched resulting in conflicting results. In order to find a conclusive answer, results of multiple studies have been analyzed in a meta-analysis<sup>1</sup>, which demonstrated no association between CYP2D6 genotype and breast cancer outcome. However, a further analysis of this meta-analysis demonstrated that the CYP2D6 genotype is associated with disease-free survival in a subset of patients who received tamoxifen as adjuvant therapy at a dose of 20 mg/day for 5 years. This analysis, in turn, has been criticized because it excluded the ABCSG8, ATAC and BIG1-98 trials, three large prospective clinical studies, and lacked *a-priori* specified criteria for the sub analysis.<sup>2</sup> Thus, to date, no conclusive answer on the predictive value of the CYP2D6 genotype in tamoxifen treatment for breast cancer outcome exists. Nevertheless, genotyping has been proposed as a strategy to individualize tamoxifen therapy. Recently, a guideline by the Clinical Pharmacogenetics Implementation Consortium (CPIC) has been published that provides therapeutic recommendations based on the CYP2D6 genotype for ER-positive breast cancer patients who are indicated to receive adjuvant tamoxifen for 5 years.<sup>3</sup> In this guideline, the CYP2D6 genotype is classified into five different metabolizer phenotypes with activity scores (AS; in brackets) namely CYP2D6-ultrarapid (>2.0), -normal (1.5 and 2.0), -normal or

intermediate (1.0), -intermediate (0.5) and -poor metabolizers (0). The AS are supposed to reflect systemic exposure to endoxifen and with that the expected clinical endpoints of recurrence and event-free survival. Patients with an AS >1.5 are expected to reach therapeutic endoxifen concentrations and start with 20 mg tamoxifen daily. Alternative hormonal therapy is advised for all patients with an AS of 1.0 or lower. Tamoxifen dose should only be increased to 40 mg if AS is 1.0 or lower and if aromatase inhibitor use is contraindicated, according to the drafters of the guideline.<sup>3</sup>

## **THERAPEUTIC DRUG MONITORING OF ENDOXIFEN CONCENTRATIONS**

The predictive value of endoxifen plasma concentrations has been substantiated by a large retrospective analysis. An endoxifen threshold concentration of 5.97 ng/mL was identified and demonstrated that patients above this target had a 26% lower risk of getting recurrent disease.<sup>4</sup> A similar threshold has been identified by Saladores et al.<sup>5</sup> Contrary to these aforementioned findings, a recent prospective study showed no significant relation between endoxifen concentrations and objective response rate, progression free survival or clinical benefit.<sup>6</sup> Of note, the patients in this trial were treated in a neo-adjuvant- and metastatic setting and can therefore not be compared to adjuvantly treated patient cohorts. In addition, a threshold of endoxifen concentrations was not evaluated.

Based on the findings of Madlensky et al.<sup>4</sup>, Therapeutic Drug Monitoring (TDM) of endoxifen has been implemented in certain hospitals to improve treatment outcomes. Patients treated in our hospitals indicated to receive tamoxifen in the adjuvant setting initiate treatment with 20 mg tamoxifen daily. After every three months, when endoxifen concentrations are at steady state, a blood sample is drawn and analyzed. Patients continue with 20 mg tamoxifen daily when the endoxifen concentration is above 6 ng/mL. If the concentration is below 6 ng/mL, a dose increment to 40 mg tamoxifen daily is prescribed and re-evaluated after three months. In case this threshold level of endoxifen is not reached with the proposed dose increment, physicians consider a switch to alternative hormonal therapy, like aromatase inhibitors. Aromatase inhibition in postmenopausal

women with ER-positive early breast cancer has demonstrated to be superior to tamoxifen treatment. Besides, the combination of aromatase inhibition and ovarian suppression (pharmacologically or by ablation) has shown to improve disease-free survival compared to tamoxifen treatment in premenopausal women.<sup>7,8</sup> Therefore, a proposed switch to these therapies in case of sub endoxifen concentrations has clinical validation. However, ovarian suppression can cause substantial side effects and the combination of an aromatase inhibitor and ovarian ablation did not show a difference in overall survival compared to tamoxifen for premenopausal women.<sup>8</sup> Additionally, it is well known that some patients tolerate tamoxifen better than aromatase inhibitors and vice versa. As a consequence, not all patients are able to switch to aromatase inhibitors, making correct identification of patients at risk even more pivotal.

The question now can be raised whether it may be better to measure endoxifen levels rather than performing *CYP2D6* genotyping in patients treated with adjuvant tamoxifen.

## **ADVANTAGES OF THERAPEUTIC DRUG MONITORING OF ENDOXIFEN**

As previously described, studies that have linked *CYP2D6* genotype with clinical outcome yielded conflicting results and have been heavily criticized.<sup>2</sup> Not all *CYP2D6* poor and intermediate metabolizers have defined suboptimal levels of endoxifen and not all extensive or ultra-rapid metabolizers reach therapeutic concentrations of endoxifen.<sup>4,9</sup> In other words, *CYP2D6* genotyping does not fully explain variability in endoxifen concentrations: only 34-52% of the variability in endoxifen concentrations is explained by the *CYP2D6* genotype.<sup>10</sup> The residual, unexplained variability is thus high and may be attributed to a long list of other non-*CYP2D6* genotype dependent factors including co-medication, organ function, life style, other genetic factors (e.g. drug transporters), patient characteristics (age, gender, body size), adherence and those factors that are still unknown and may all vary over time. Periodic measurement of endoxifen concentrations has many advantages and can be regarded as a better defined outcome measure of all these effects than the static *CYP2D6* genotype alone. TDM will identify patients with low endoxifen levels that otherwise go unnoticed by genotyping, e.g. non-

adherence and unrecognized concomitant use of CYP2D6 inhibitors. The latter, undetected by genotyping, may even turn an ultra rapid metabolizer into a poor metabolizer with all clinical consequences which may also be the case for patients carrying rare genomic variants, that are not included in the genotype test. Other limitations of genetic testing are the inadequacy to detect de novo variants and that uncertainty exists on which single nucleotide polymorphisms need to be evaluated. In addition, the translation from genotype to phenotype has not been standardized. Measurement of endoxifen concentrations overcomes these challenges.

Feasibility of TDM of endoxifen has been demonstrated by the TADE study, where a dose increment was applied in patients with sub optimal concentrations of endoxifen, leading to therapeutic concentrations in most patients.<sup>11</sup> TDM can also evaluate the effect of tamoxifen dose increments on the endoxifen concentration. It has been demonstrated that endoxifen serves as a *proxy* for the anti-estrogen effect of tamoxifen and metabolites<sup>12</sup>, therefore only the endoxifen concentration is required for TDM.

It can be argued that dose adjustments based on TDM of endoxifen can only be applied after approximately three months of treatment, when endoxifen concentrations are at steady state. However, this short timeframe of potential sub optimal dosing is not expected to be clinically relevant, since tamoxifen treatment is indicated to reduce recurrence and mortality rates after years of treatment. Another obstacle for implementation faced by TDM of endoxifen is lack of bioanalytical method selectivity, which can result in misinterpreting plasma concentrations. However, an established selective bioanalytical method for the quantification of endoxifen is easy to implement and available.<sup>13</sup>

## CONCLUSION AND PERSPECTIVE

In conclusion, we believe, that TDM of endoxifen allows for better identification of patients with low endoxifen concentrations compared to the *CYP2D6* genotype or related activity score. Eventually, patients could start on an individualized dose based on genotyping results until steady state is reached and TDM can be performed. Subsequently, patients with an indication for adjuvant treatment with 20 mg tamoxifen daily for 5 years but low endoxifen concentrations should get a dose increment to 40 mg daily. If sub therapeutic concentrations remain, patients can switch to treatment with aromatase inhibition or aromatase inhibition with ovarian suppression.

We do recognize that both TDM of endoxifen and *CYP2D6* genotyping, lack prospective validation and that the irrefutable proof for a target level has not been provided for adjuvant tamoxifen ER-positive breast cancer treatment. Randomized, prospective TDM trials should fill this gap and provide proof for therapy adjustments based on endoxifen concentration and/or *CYP2D6* genotypes. Such studies, however, require an extremely large sample size and a lengthy follow up. Therefore, prospective validation is not likely to be established on short-term. Even if such a study would be initiated now, debates about tamoxifen therapy improvement remain important, since the question remains: how do we treat our patients best in the meantime?

## REFERENCES

1. Province, M. a et al. *CYP2D6 genotype and adjuvant tamoxifen: meta-analysis of heterogeneous study populations. Clin. Pharmacol. Ther.* 95, 216-27 (2014).
2. Berry, D. a *CYP2D6 genotype and adjuvant tamoxifen. Clin. Pharmacol. Ther.* 96, 138-40 (2014).
3. Goetz, M. P. et al. *Clinical Pharmacogenetics Implementation Consortium (CPIC) Guideline for CYP2D6 and Tamoxifen Therapy. Clin. Pharmacol. Ther.* 103, 770-7 (2018).
4. Madlensky, L. et al. *Tamoxifen metabolite concentrations, CYP2D6 genotype, and breast cancer outcomes. Clin. Pharmacol. Ther.* 89, 718-25 (2011).
5. Saladores, P. et al. *Tamoxifen metabolism predicts drug concentrations and outcome in premenopausal patients with early breast cancer. Pharmacogenomics J.* 15, 84-94 (2015).
6. Neven, P. et al. *Tamoxifen metabolism and efficacy in breast cancer - a prospective multicentre trial. Clin. Cancer Res.* 24, 2312-2319 (2018).
7. Breast, E., Trialists, C. & Group, C. *Aromatase inhibitors versus tamoxifen in early breast cancer: patient-level meta-analysis of the randomised trials. Lancet* 386, 1341-1352 (2015).
8. Pagani, O. et al. *Adjuvant Exemestane with Ovarian Suppression in Premenopausal Breast Cancer. N. Engl. J. Med.* 371, 107-118 (2014).
9. Mürdter, T. E. et al. *Activity levels of tamoxifen metabolites at the estrogen receptor and the impact of genetic polymorphisms of phase I and II enzymes on their concentration levels in plasma. Clin. Pharmacol. Ther.* 89, 708-17 (2011).
10. Schroth, W. et al. *Improved prediction of endoxifen metabolism by cyp2d6 genotype in breast cancer patients treated with tamoxifen. Front. Pharmacol.* 8, 1-9 (2017).
11. Fox, P. et al. *Dose escalation of tamoxifen in patients with low endoxifen level: Evidence for therapeutic drug monitoring - The TADE study. Clin. Cancer Res.* 22, 3164-3171 (2016).
12. Vries Schultink, A. H. M. et al. *An Antiestrogenic Activity Score for tamoxifen and its metabolites is associated with breast cancer outcome. Breast Cancer Res. Treat.* 161, 567-574 (2017).

13. Krou, S. de, Rosing, H., Nuijen, B., Schellens, J. H. M. & Beijnen, J. H. Fast and Adequate Liquid Chromatography-Tandem Mass Spectrometric Determination of Z-endoxifen Serum Levels for Therapeutic Drug Monitoring. *Ther. Drug Monit.* 39, 132-137 (2017).





## CHAPTER 1.4

### Prospective evaluation of Therapeutic Drug Monitoring of endoxifen: feasibility of observational and randomized trials

*To be submitted*

A.H.M. de Vries Schultink  
T.P.C. Dorlo  
L. Madlensky  
J.P. Pierce  
J.H. Beijnen  
A.D.R. Huitema

## ABSTRACT

Therapeutic Drug Monitoring (TDM) of endoxifen as a strategy to improve survival in patients with estrogen receptor (ER)-positive breast cancer using adjuvant tamoxifen is controversial, because the exposure-response relationship has not definitively been established and, additionally, the benefits of TDM have not been shown prospectively. Appropriately designed prospective clinical trials will be necessary to eventually demonstrate the potential benefits of TDM. We explored whether such trials are feasible and which design would be needed. A parametric time-to-event model was developed and different trial designs were simulated aiming (1) to demonstrate an exposure-response relationship between endoxifen concentrations and breast cancer recurrence and (2) to study the benefits of TDM over conventional dosing. To demonstrate the exposure-response relationship, at least 1500 patients and a follow-up of 15 years are needed assuming a 29% reduction in the hazard of recurrence for patients with an endoxifen concentration  $>5.97$  ng/ml compared to patients with lower endoxifen concentrations. The most feasible approach to validate TDM of endoxifen is randomizing patients with low endoxifen concentrations to continuation of 20 mg/day or a dose increment to 40 mg/day (1:1). For this design a total of 3200 patients with low endoxifen concentrations and 15 years follow up are needed. The simulations in this study demonstrate that prospective validation of TDM of endoxifen could be feasible, though it would require a larger sample size and longer follow up time than previously conducted trials have reported so far.

## INTRODUCTION

Tamoxifen is an anti-estrogenic drug that has been used to treat estrogen receptor (ER)-positive breast cancer for decades. Five years of adjuvant treatment with tamoxifen lowers ER-positive breast cancer recurrence and mortality rates.<sup>1</sup> Despite the proven efficacy of tamoxifen, 25 to 30% of patients experience recurrence within 10 years.<sup>1</sup> Variability in response has been attributed to variability in pharmacokinetics, more specifically to variability in endoxifen concentrations, the most important active metabolite of tamoxifen.

Both endoxifen concentrations and the *CYP2D6* genotype, a gene encoding the enzyme CYP2D6, predominantly responsible for bio-activation of tamoxifen into endoxifen, have been proposed as predictive markers for recurrence. Therapeutic Drug Monitoring (TDM) of endoxifen seems the best way forward to tailor tamoxifen treatment, since variability in concentration of endoxifen can only partially be attributed to the *CYP2D6* genotype.<sup>2-5</sup> An endoxifen concentration >5.97 ng/ml has been associated with 26% lower risk of breast cancer recurrence (hazard ratio (HR) 0.74 (95% confidence interval (CI) 0.55-1.00) as reported by a retrospective analysis<sup>5</sup>. This target can be applied to tailor tamoxifen treatment, recommending an increase in tamoxifen dose from 20 mg to 40 mg daily if endoxifen concentrations are below this PK target. However, TDM of endoxifen is currently not common clinical practice. Arguments for not applying TDM of endoxifen is the lack of prospective validation of the exposure-response relationship and the lack of prospective validation of applying TDM to improve breast cancer recurrence rates. Prospective validation of the exposure-response relationship is aimed at by two recently published prospective observational trials, both of which did not find a relationship between endoxifen concentrations and breast cancer recurrence. A prospective multicenter trial by Neven et al., did not find a relation between endoxifen concentrations and objective response rate or progression free survival (PFS) in 247 postmenopausal ER-positive breast cancer patients treated with tamoxifen 20 mg daily in the neoadjuvant or metastatic setting.<sup>6</sup> The median follow-up time for PFS was 32.5 months. However, it is difficult to extrapolate these findings to early breast cancer and adjuvant treatment where recurrences tend to occur much later after initiating treatment with tamoxifen.

The CYPTAM trial is another prospective observational trial including 667 patients with early ER-positive breast cancer.<sup>7</sup> No relation between endoxifen concentrations (continuous, categorical or at a PK target of 5.97 ng/mL) and relapse-free survival was found. The average follow up time for this trial was 6.4 years (range 0.10 to 9.30 years).

Recurrence under tamoxifen occurs in around 25 to 30% of patients treated in the adjuvant setting and can take place years after initiating treatment.<sup>1</sup> This relatively low incidence of events and long time-to-event, indicates that a long follow up time and a large sample size is warranted to have sufficient power to detect a difference in events between patients with high and low endoxifen concentrations. Such a long follow up time is additionally complicated by dropout, switch to alternative therapies (censoring) and adherence. All these factors contribute to an inherent decrease in power of observational or randomized trials. Time-to-event modelling provides a way to quantify the changes in hazard over time by estimating a parametric model which allows simulation of different trial scenarios. In this analysis, a time-to-event model was developed and different trial designs were simulated aiming to (1) demonstrate an exposure-response relationship between endoxifen concentrations and breast cancer recurrence and (2) to study the benefits of TDM over conventional dosing, by conducting clinical trial simulations. This analysis was based on TDM data from clinical practice and time-to-event data from a previous published analysis.

## METHODS

### Data

Endoxifen concentrations from breast cancer patients treated with tamoxifen in the adjuvant setting and for whom TDM of endoxifen was applied in the Netherlands Cancer Institute, were available. Blood samples were drawn at least 3 months after start of treatment with 20 mg tamoxifen daily, to ensure steady state concentration of endoxifen. Endoxifen concentrations were determined using a selective liquid chromatography-tandem mass spectrometry (LC-MS/MS) method.<sup>8</sup> If the dose was increased based on a low endoxifen concentration (<5.97 ng/mL) a second sample was drawn at least 3 months after dose adaptation.

A parametric time-to-event model was developed based upon recurrence-free survival data from patients selected from the Women's Healthy Eating and Living (WHEL) study.<sup>9</sup> This dataset has been used in a previous analysis.<sup>5</sup> The dataset contained 1370 patients with ER-positive breast cancer indicated to use tamoxifen 20 mg/day for 5 years and whom were followed for an average time of 7.3 years after inclusion and an average of 9.1 years after diagnosis. Information on tumor status, tumor grade and menopausal status was available in addition to one endoxifen concentration. The data have extensively been described elsewhere.<sup>5</sup>

## **Software**

Time-to-event modeling and simulation analyses were performed in NONMEM (version 7.3.0, ICON Development Solutions, Ellicott City, MD, USA) and Perl-speaks-NONMEM (version 4.4.8).<sup>10,11</sup> Laplacian estimation method was used for parameter estimation. Data handling, graphical evaluation and power calculations were performed using R (version 3.3.1).<sup>12</sup>

## **Parametric time-to-event model development**

A parametric time-to-event model was developed to be able to perform Monte Carlo simulations, which is not possible with the previously published Cox proportional hazards model.

Different time-to-event models were evaluated, including Gompertz, Weibull and exponential distribution hazard functions.<sup>13</sup> Tumor grade, tumor stage, menopausal status and endoxifen concentrations were evaluated as predictors of recurrence-free survival. Endoxifen concentrations were classified as above or below the PK target of 5.97 ng/mL. Model evaluation was performed using visual predictive checks, evaluation of objective function value change (dOFV) and evaluation of the plausibility of the parameter estimates.

## **Trial simulations**

Firstly, simulations were conducted to evaluate the optimal design of a prospective observational trial to evaluate the exposure-response relationship between endoxifen concentrations and breast cancer recurrence. Secondly,

simulations were conducted to evaluate the optimal design of a randomized controlled trial (RCT), to determine the benefits of endoxifen TDM to improve breast cancer outcome. Eligibility and intervention for each design was described as follows (Figure 1):

**Observational design:** Patients with early ER-positive breast cancer that initiate treatment with tamoxifen with 20 mg/day were included. No TDM was applied and only follow up was performed.

Breast cancer recurrence was compared between patients with an endoxifen concentrations below the PK target to patients with endoxifen concentrations above the PK target. Different PK target levels were evaluated: 5.97 ng/mL, 4 ng/mL and 8 ng/mL.

**RCT design 1:** Patients with early ER-positive breast cancer that initiate treatment with tamoxifen with 20 mg/day were included and randomized (1:1) to either the control arm or the intervention arm. In the control arm, no TDM was applied and only follow up was performed. In the intervention arm, TDM was applied after three months. Patients with endoxifen concentrations  $\leq 5.97$  received a dose increment to 40 mg/day. Follow-up was performed until recurrence or up to 15 years.

**RCT design 2:** Patients with early ER-positive breast cancer that initiate treatment with tamoxifen with 20 mg/day were eligible for inclusion. After three months endoxifen concentrations were determined in all patients. Patients with endoxifen concentrations  $\leq 5.97$  were randomized (1:1) to either the control arm or the intervention arm. Patients in the control arm continued with tamoxifen 20 mg/day, the intervention arm received tamoxifen 40 mg/day. Follow-up of randomized patients was performed until recurrence or up to 15 years.

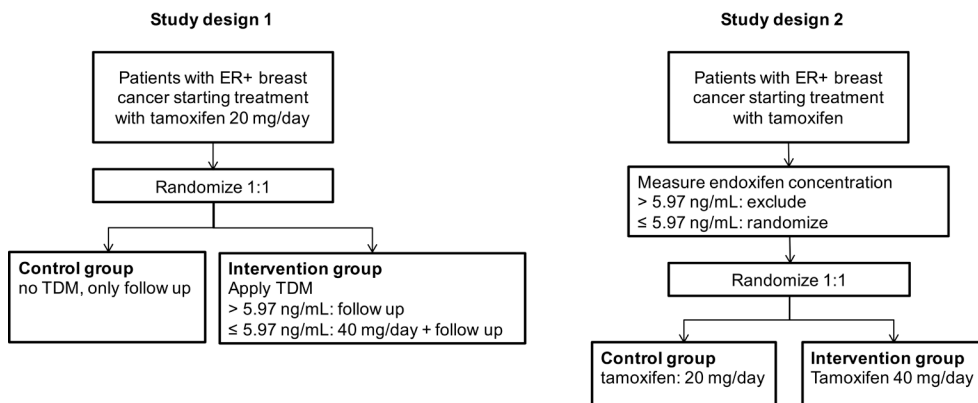


**Figure 1** Randomized controlled trial designs to determine feasibility of therapeutic drug monitoring of endoxifen for estrogen receptor positive breast cancer. ER + = estrogen receptor-positive, TDM = Therapeutic Drug Monitoring.

Proportions of tumor grade, stage and menopausal status imputed in the simulation dataset, were comparable to reported by the Madlensky trial.<sup>5</sup> Tumor grade and stage were sampled from the Madlensky trial data as pairs. Different proportions of patients above and below the PK target were sampled for the observational design and for the control arm versus the intervention arm in the RCTs, based on proportions evaluated in the clinical TDM data. Each design was simulated with varying number of patients, with  $n$  ranging from 500 to 3000 patients for the observational design, 1000 to 25,000 patients per arm for RCT design 1 and 100 to 2300 patients per arm for RCT design.<sup>2</sup> Each study was simulated 1000 times and for each trial the hazard ratio between the intervention and the control arm was determined using a Cox proportional hazards model. This model was also corrected for tumor grade, stage and menopausal status. The power was determined by the percentage of trials with a significant difference in recurrence-free survival between the control and the intervention arm, with  $p < 0.05$ .

For the observational design, power was determined by the fraction of trials with a significant difference in recurrence-free survival between patients below and above the PK target value. Time to recurrence was simulated up to 15 years, to determine the most feasible design. Subsequently, a sensitivity analysis was performed to investigate the effect of shorter follow up times. In addition, the uncertainty in the effect of the PK target on the hazard was evaluated by assuming a factor 2 increase or decrease of this effect on the hazard.

## RESULTS

### Pharmacokinetics

Proportions of patients with endoxifen concentrations below and under the PK target were imputed in the simulation datasets based on proportions observed in the clinical TDM data. In total, 976 samples of 713 patients were available, of which 658 patients had a first sample taken during treatment with 20 mg tamoxifen daily. In this group, 213 patients (32.4%) did not reach the target concentration of 5.97 ng/ml, 113 had a concentration below 4 ng/mL (17.2%) and 313 had a concentration below 8 ng/mL (47.6%).

Of 213 patients with concentrations below 5.97 ng/ml, 117 patients received a dose increment to 30 or 40 mg depending on the measured endoxifen concentration, of which 89 patients (76.1%) reached the target at the second sample. In total, in the TDM group, 92.2% of patients reached the PK target of 5.97 ng/ml compared to 67.6% if no TDM is applied.

Proportions of patients below and under the PK target of 5.97 ng/ml were imputed in the simulation datasets for the RCT designs as follows. The control arm of RCT design 1 had 32.4% of patients below and 67.6% of patients above the target concentration. The intervention arm had 92.2% of patients above and 7.8% of patients below the target concentrations. The control arm of RCT design 2 had 100% of patients below the target concentrations and the intervention arm 23.9% (corresponding to the fraction of patients not reaching the target after TDM guided dose increase) below the target concentration.



## Parametric time-to-event model development

The baseline hazard was best described by a Weibull distribution model where the hazard increased over time (Table 1). A higher tumor grade or stage was associated with an increased risk of recurrence. Tumor stage IIB and IIIC had a similar effect on the hazard and were, therefore, imputed in the model as a single group. Patients for whom tumor grade data was missing (9.4%), were assumed to have a tumor grade 1. In addition, postmenopausal patients had a decreased risk of recurrence compared to premenopausal patients. Having an endoxifen steady-state concentration above 5.97 ng/mL resulted in a decreased hazard of recurrence compared with patients not attaining this PK target, though not significantly in the parametric time-to-event model in contrast to the Cox proportional hazards model previously published (dOFV -3.64). The Weibull model was described as follows:

$$h(t) = \lambda \cdot t^{\alpha-1} \cdot e^{\beta_1 \cdot \text{cov}_1 + \beta_2 \cdot \text{cov}_2 + \beta_n \cdot \text{cov}_n}$$

Where  $\lambda$  is the hazard coefficient,  $\alpha$  the shape parameter,  $\beta_n$  the covariate effects and  $\text{cov}_n$  the binary covariate (either 1 or 0). Visual predictive checks, stratified on endoxifen concentrations below and above a PK target of 5.97 ng/mL are depicted in Figure 2. Visual predictive checks stratified on other covariates are depicted in Supplementary files 1 (Figure S1.1-Figure S1.3). Censoring or dropout occurred randomly in 94% of the cases between 6 and 15 years after diagnosis. This random dropout was taken into account in all of the subsequent simulations.

**Table 1** Parameter estimates Weibull model for recurrence-free survival.

PARAMETER	ESTIMATE	RSE (%)	COVARIATE EFFECT
Hazard coefficient ( $\lambda$ ) (/year)	0.0345	21	-
Shape ( $\alpha$ )	1.68	6	-
Stage IIB & IIIA	1.01	16	2.75
Stage IIIC	2.06	12	7.85
Grade 2	0.438	46	1.55
Grade 3	0.718	30	2.05
Postmenopausal status	-0.810	32	0.44
Endoxifen $\geq 5.97$ ng/mL	-0.348	51	0.71

RSE = relative standard error derived from the NONMEM omega matrix. Covariate effect on hazard is calculated as follows:  $\exp(\text{estimate})$ . For example, postmenopausal patients have 0.44 times decreased hazard of experiencing breast cancer recurrence compared to premenopausal patients.

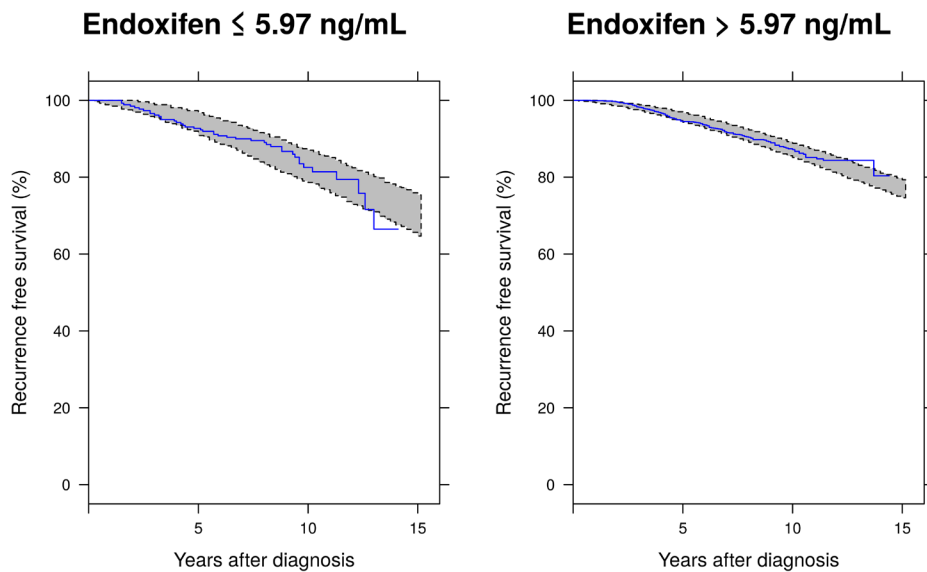


**Figure 2** Kaplan-Meier plots for recurrence-free survival data stratified by above and below the endoxifen PK target value of 5.97 ng/mL (solid lines) and 95% prediction intervals (shaded area), based on 500 simulations.

### **Trial simulations**

Results of the clinical trial simulation of the observational study are shown in Figure 3. These simulations demonstrated that 1500 patients and an intended follow up time of 15 years are needed to demonstrate that patients with endoxifen steady-state concentrations above a PK target of 5.97 ng/ml have a 29% reduction in the hazard of recurrence compared to patients not achieving this PK target (HR 0.71, power of 80% and significance level  $p < 0.05$ ). The number of required participants to identify the exposure-response relationship would be 2200 and 3000 patients, for 10 and 8 years follow up, respectively. The estimated PK target effect was a 29% reduction in hazard of recurrence for patients with endoxifen concentrations above the PK target in accordance with the published estimate. However, if this effect is actually twice as large, indicating a decreased hazard of 50% for patients above the PK target (HR 0.50), approximately 750 patients and at least 8 years of intended follow up are needed. In case the PK target effect is actually 2-fold lower, indicating a decreased hazard of 16% for patients above the PK target (HR 0.84), approximately 6000 patients or more are needed to find this difference in hazard (Figure 3).

Sensitivity analysis of the PK target using a PK target value of 4 ng/mL, demonstrated that 2300 patients and an intended follow-up time of 15 years are needed to find a similar effect (HR 0.71), while a PK target of 8 ng/mL endoxifen demonstrated that 1400 patients and 15 years of follow up are needed to find a similar effect (HR 0.71). More detailed results are reported in the Supplementary files 1 (Figure S1.4 and Figure S1.5).

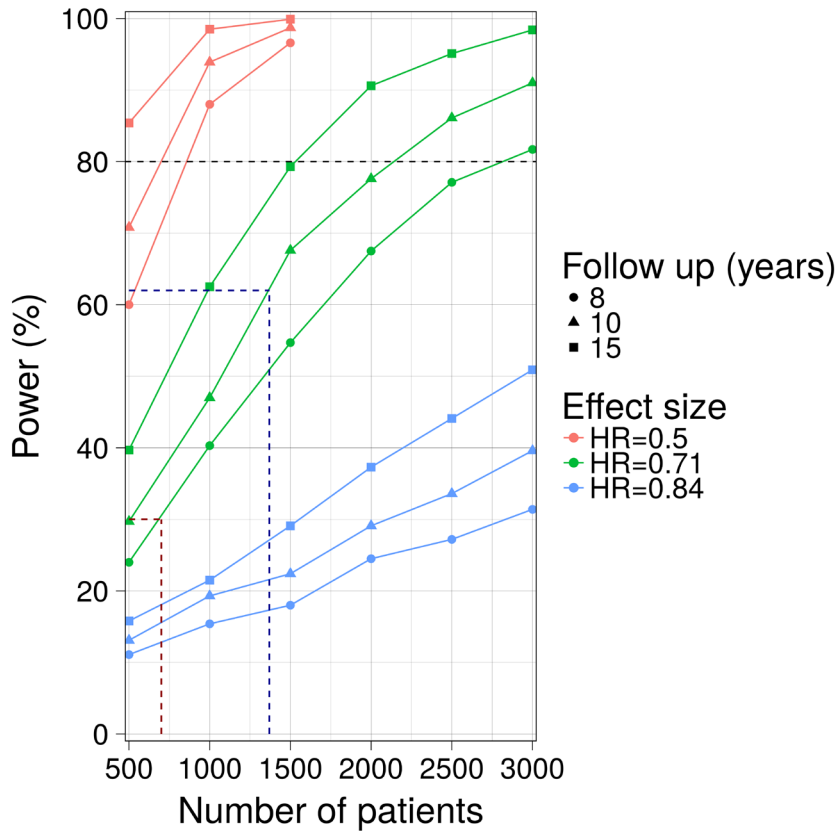


**Figure 3** Power calculation for observational designs with follow up times of 8, 10 and 15 years and effect size differences between patients below and above a PK target of 5.97 with corresponding assumed hazard ratios (HR) of 0.71, 0.50 and 0.84. The dotted red line is the estimated power of the CYPTAM study ( $n=700$ )<sup>7</sup> and the dotted darkblue line is the estimated power of the Madlensky trial ( $n=1370$ ).<sup>5</sup>

In order to prospectively validate application of endoxifen TDM to improve breast cancer outcome (assuming the previously estimated HR of 0.71), using a design 2 study demonstrated to be more feasible than a design 1 study (Figure 4). Design 1 needs 25,000 patients per study-arm to reach a power of 79.8% ( $n=50,000$  patients in total). Design 2 needs 1600 patients per arm to demonstrate the same effect (power of 82.9%). For design 2, three-fold more patients are needed to identify the 32.5% of patients with low endoxifen concentrations.

A design with 1600 patients per arm (n=3200) would therefore need screening of approximately 9600 patients. Additionally, a 1:2 design was evaluated for design 2 (Supplementary files 1, Figure S1.6). In total 3450 patients (1150 in the control arm and 2300 in the intervention arm) are needed to detect a significant difference between the control and the intervention arm with a power of 80%. In total, 10,350 patients need to be screened to identify 3450 patients with low endoxifen concentrations. A sensitivity analysis was performed for design 2 with a randomization ratio of 1:1, with 1600 patients per arm to evaluate the impact of a decrease in follow-up time and a difference in PK target effect on the power of this trial. Decreasing the follow up time to 10 years decreases the power to 63.9%, for 8 and 5 years the power decreases to 53.3% and 31.4%, respectively. In case the PK target effect is 2-fold higher or 2-fold lower, the power increases to almost a 100% or decreases to 33.1%, respectively. (Figure 5)

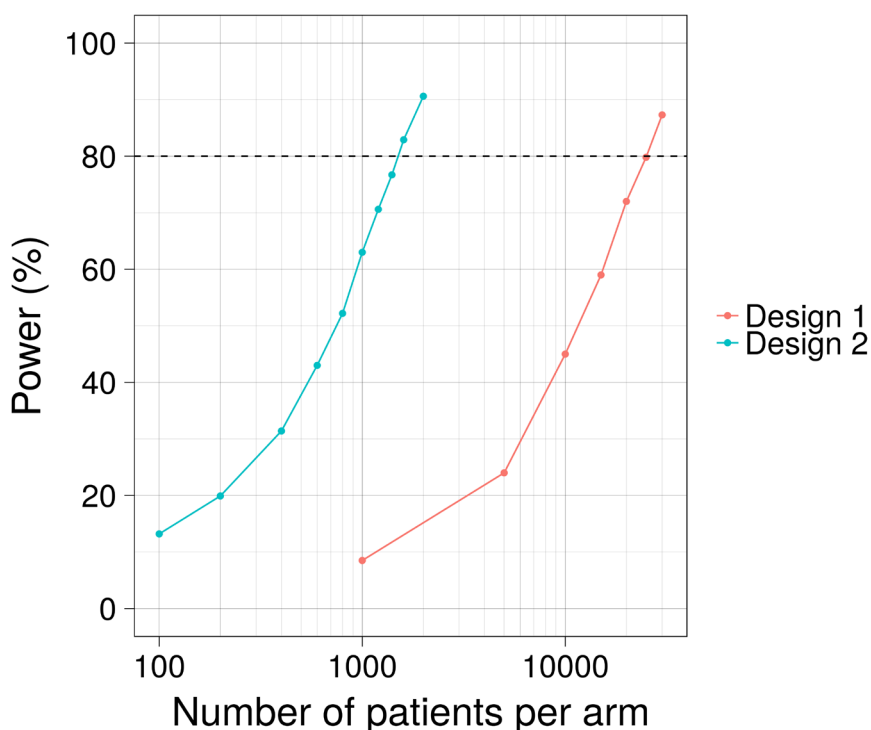


**Figure 4** Power calculations for RCT design 1 and 2 for varying numbers of patients per study-arm. Simulations were performed with an intended follow up of 15 years and random dropout. Number of patients per arm is depicted on a log-transformed axis.

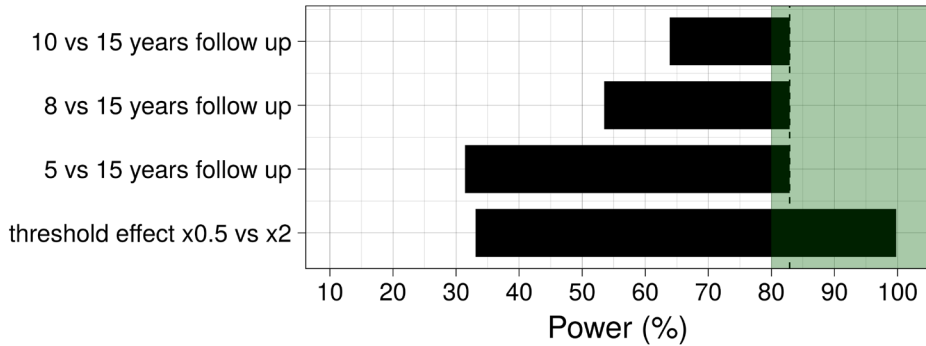


**Figure 5** Sensitivity analysis for design 2 with 1600 patients per arm. Dotted line is the power for 15 year follow up with random dropout and a difference in hazard of 0.71 for patients with an endoxifen concentration  $< 5.97$  (82.9%), green area is power  $\geq 80\%$ .

## DISCUSSION

The clinical trial simulations in this study demonstrated that a large sample size and long follow up time are needed to demonstrate an exposure-response relationship between endoxifen concentrations and breast cancer recurrence and to evaluate endoxifen TDM to improve breast cancer outcome. If an exposure-response relationship with a PK target value of 5.97 ng/ml and a difference in hazard of 29% (HR 0.71) exists, 1500 patients and an intended follow up of 15 years are needed to find this effect in an observational design with a power of approximately 80%. As this assumed PK target may be debatable, we performed a sensitivity analysis using PK target values of 4 ng/mL and 8 ng/mL. If the PK target values would be actually 8 ng/mL, less patients are needed to find an exposure-response relationship. However, TDM of endoxifen will become less effective, given that the currently used dose increment to 40 mg will not be sufficient for most patients to attain a target concentration of 8 ng/mL. If the PK target value is actually 4 ng/mL more patients are needed to find a difference an exposure-response relationship. However, applying TDM becomes more feasible, since a dose increment to 40 mg will lead to higher percentage of patients attaining a target concentration of 4 ng/mL.

The most feasible RCT design to determine the effect of TDM on breast cancer outcome is a design where only patients with low endoxifen concentrations are randomized (design 2), and where patients are randomized 1:1. In total, 9600 patients are needed to identify 3200 patients with low endoxifen concentrations, to determine if TDM of endoxifen improves breast cancer outcome with a power of 82.9% and an assumed reduction in hazard of recurrence of 29% (HR 0.71). In design 1, there is a risk that patients in the control arm find alternative ways to determine their endoxifen concentrations, since their dose is not increased. Similarly, in design 2 patients in the control arm know that their endoxifen concentration is considered below target and may seek alternative ways to increase the dose. Both effects may potentially lead to bias which may be circumvented by a placebo-controlled blind design.

The feasibility of a clinical trial is determined by various factors such as willingness of patients to participate or to be randomized, willingness of clinicians to recruit participants, costs, follow up time and number of eligible patients. In this analysis degree of feasibility was narrowed down to number of patients and follow up time. Including 1500 patients in an observational trial with an intended follow up time of 15 years is likely to be feasible, since a previous study managed to include 1370 patients with a follow up time from diagnosis of 10 years.<sup>5</sup> In addition, 11 hospitals from the Netherlands and Belgium participated in the prospective CYPTAM study, including almost 700 patients.<sup>7</sup> Therefore, in terms of inclusion, a multicenter observational trial is likely to be feasible, if an estimated 20 hospitals would participate. Moreover, in 2018, 170.000 new cases of breast cancer were reported for Western Europe alone, of whom approximately 80% has hormone receptor positive breast cancer. An international multicenter randomized controlled trial including 9600 patients, of whom 3200 are randomized, could, therefore, also potentially be feasible in terms of inclusion.

Up to date, none of the proposed prospective clinical trials have been performed. Based on our simulations, the Madlensky trial had the highest probability of determining an effect compared to other prospective or retrospective trials<sup>6,7</sup>, with a power of approximately 62% to detect an exposure-response relationship.

The results of this trial have not led to a collective implementation of TDM of endoxifen because of its retrospective design. However, patients were included and followed in a large randomized controlled trial, where data was collected prospectively.<sup>9</sup> This trial could therefore be seen as a sub analysis of a prospective study, which is marginally different from a prospective observational trial. The CYPTAM trial included little over half the patients the Madlensky trial included, with a shorter follow up time.<sup>7</sup> Based on the simulations presented in this trial, it had an estimated power of approximately 30% to detect a significant exposure-response relationship if it exists, assuming a follow-up of 15 years, which had not yet been reached in this trial. A conclusive answer on whether TDM of endoxifen is indicated for patients with early ER-positive breast cancer is therefore not yet available.

The simulations performed in this study should be interpreted in the light of some limitations. The estimated relative standard error of the PK target effect on the hazard was 51%, indicating a high uncertainty in this effect. Therefore, a sensitivity analysis was performed to demonstrate the impact of different effect sizes on the power and sample size of the different designs.

The covariate effect of a PK target above and under the 5.97 ng/mL was imputed as a fixed covariate in the model. As tamoxifen improves 5, 10 and 15 year recurrence rates, early recurrences are not expected to be relevantly attributable to lower endoxifen concentrations in the first three months of treatment prior to steady-state. The potential risk of recurrence before patients reached steady-state concentrations was therefore not considered in the model.

A Cox proportional hazards model was used to determine the power of each trial design, instead of using a parametric model to evaluate how many patients are needed to find a significant covariate effect in the time-to-event model. A Cox regression analysis calculates the relative difference in hazard between two groups, assuming a constant hazard over time. Using a Weibull distribution, the hazard can change over time. However, a Cox proportional hazard model is often used to analyze survival data in clinical trials.



Therefore, using a Cox model to evaluate study outcome of the simulated trials instead of parametric time-to-event models was considered a better reflection of the current practice of analyzing clinical trials.

Adherence has been described as a major issue using endocrine treatment for a long period of time and non-adherence has been described to increase the hazard of experiencing breast cancer recurrence.<sup>14</sup> Data on adherence was not available in the dataset available, thwarting evaluation of adherence on study outcome in a sensitivity analysis. However, the model was developed based on data from a previously conducted clinical trial. Therefore, it was expected that patients in this trial are similarly adherent to patients in another observational or randomized trial, which makes results of our simulation reasonably realistic.

Adjuvant endocrine therapy for postmenopausal patients with ER-positive breast cancer consists of sequential treatment with 2 or 3 years tamoxifen followed by 3 or 2 years treatment with an aromatase inhibitor (or vice versa).<sup>15</sup> This switch to aromatase inhibition is not considered in the trial simulations, since the model was developed based on patients receiving tamoxifen for 5 years. Censoring patients at the time of switching to aromatase inhibition would impact follow up time and, therefore, cause a drastic decrease in power. Therefore, if one of the proposed trials is initiated, patients switching to aromatase inhibition, should be followed up and not censored. Subsequently, a switch to aromatase inhibition should be accounted for in the Cox proportional hazards model.

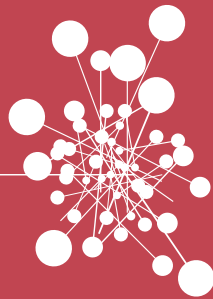
Currently, no prospective or retrospective trial with sufficient power and follow up has been performed to detect the proposed exposure-response relationship between endoxifen and breast cancer recurrence. Therefore, a conclusive answer on whether TDM of endoxifen is indicated for patients with early ER-positive breast cancer is not available. Our clinical trial simulations indicate that an observational or randomized trial where only the patients with low endoxifen steady-state plasma concentration are randomized could both be feasible, though would require a multicenter trial and international collaboration. If such a trial would be initiated, follow-up times of 10 to 15 years are necessary.

## REFERENCES

1. Davies, C., Godwin, J. & Gray, R. Relevance of breast cancer hormone receptors and other factors to the efficacy of adjuvant tamoxifen: patient-level meta-analysis of randomised trials. *Lancet* 771-784 (2011).
2. Mürdter, T. E. et al. Activity levels of tamoxifen metabolites at the estrogen receptor and the impact of genetic polymorphisms of phase I and II enzymes on their concentration levels in plasma. *Clin. Pharmacol. Ther.* 89, 708-17 (2011).
3. Saladores, P. et al. Tamoxifen metabolism predicts drug concentrations and outcome in premenopausal patients with early breast cancer. *Pharmacogenomics J.* 15, 84-94 (2015).
4. Teft, W. a et al. CYP3A4 and seasonal variation in vitamin D status in addition to CYP2D6 contribute to therapeutic endoxifen level during tamoxifen therapy. *Breast Cancer Res. Treat.* 139, 95-105 (2013).
5. Madlensky, L. et al. Tamoxifen metabolite concentrations, CYP2D6 genotype, and breast cancer outcomes. *Clin. Pharmacol. Ther.* 89, 718-25 (2011).
6. Neven, P. et al. Tamoxifen metabolism and efficacy in breast cancer - a prospective multicentre trial. *Clin. Cancer Res.* 24, 2312-2319 (2018).
7. Sanchez-Spitman, A. et al. Tamoxifen Pharmacogenetics and Metabolism: Results From the Prospective CYPTAM Study. *J. Clin. Oncol.* (2019). doi:10.1200/JCO.18.00307
8. Jager, N. G. L., Rosing, H., Linn, S. C., Schellens, J. H. M. & Beijnen, J. H. Importance of highly selective LC-MS/MS analysis for the accurate quantification of tamoxifen and its metabolites: focus on endoxifen and 4-hydroxytamoxifen. *Breast Cancer Res. Treat.* 133, 793-8 (2012).
9. Pierce, J. P. et al. Influence of a diet very high in vegetables, fruit, and fiber and low in fat on prognosis following treatment for breast cancer: the Women's Healthy Eating and Living (WHEL) randomized trial. *JAMA* 298, 289-98 (2007).
10. Beal, S., Sheiner, L., Boeckmann, A. & Bauer, R. NONMEM 7.3.0 Users Guides. (1989-2013). ICON Development Solutions, Hanover, MD.
11. Lindbom, L., Ribbing, J. & Jonsson, E. N. Perl-speaks-NONMEM (PsN) - A Perl module for NONMEM related programming. *Comput. Methods Programs Biomed.* 75, 85-94 (2004).

12. R Core Team, 2018 *R: A language and Environment for Statistical Computing*. R Foundation for statistical computing, Vienna, Austria. at <<https://www.r-project.org/>>
13. Holford, N. A Time to Event Tutorial for Pharmacometricians. *CPT pharmacometrics Syst. Pharmacol.* 2, 1-8 (2013).
14. Chirgwin, J. H. et al. Treatment Adherence and Its Impact on Disease-Free Survival in the Breast International Group 1-98 Trial of Tamoxifen and Letrozole , Alone and in Sequence. *J. Clin. Oncol.* 34, 2452-2459 (2016).
15. Early Breast Cancer Trialists' Collaborative Group. Aromatase inhibitors versus tamoxifen in early breast cancer: patient-level meta-analysis of the randomised trials. *Lancet* 386, 1341-1352 (2015).





# CHAPTER 2

PHARMACOKINETICS AND  
PHARMACODYNAMICS: MCLA-128



## CHAPTER 2.1

Translational PK-PD modeling analysis  
of MCLA-128, a HER2/HER3  
bispecific monoclonal antibody,  
to predict clinical efficacious exposure and dose

*Invest New Drugs 2018 Dec;36(6):1006-1015*

A.H.M. de Vries Schultink  
R.P. Doornbos  
A.B.H. Bakker  
K. Bol  
M. Throsby  
C. Geuijen  
D. Maussang  
J.H.M. Schellens  
J.H. Beijnen  
A.D.R. Huitema

## ABSTRACT

### Introduction

MCLA-128 is a bispecific monoclonal antibody targeting the HER2 and HER3 receptors. Pharmacokinetics (PK) and pharmacodynamics (PD) of MCLA-128 have been evaluated in preclinical studies in cynomolgus monkeys and mice. The aim of this study was to characterize the PK and PD of MCLA-128 and to predict a safe starting dose and efficacious clinical dose for the First-In-Human study.

### Methods

A PK-PD model was developed based on PK data from cynomolgus monkeys and tumor growth data from a mouse JIMT-1 xenograft model. Allometric scaling was used to scale PK parameters between species. Simulations were performed to predict the safe and efficacious clinical dose, based on AUCs, receptor occupancies and PK-PD model simulations.

### Results

MCLA-128 PK in cynomolgus monkeys was described by a two-compartment model with parallel linear and nonlinear clearance. The xenograft tumor growth model consisted of a tumor compartment with a zero-order growth rate and a first-order dying rate, both affected by MCLA-128. Human doses of 10 to 480 mg q3wk were predicted to show a safety margin of >10-fold compared to the cynomolgus monkey AUC at the no-observed-adverse-effect-level (NOAEL). Doses of  $\geq 360$  mg resulted in predicted receptor occupancies above 99% ( $C_{max}$  and  $C_{ave}$ ). These doses showed anti-tumor efficacy in the PK-PD model.

### Conclusions

This analysis predicts that a flat dose of 10 to 480 mg q3wk is suitable as starting dose for a First-in-Human study with MCLA-128. Flat doses  $\geq 360$  mg q3wk are expected to be efficacious in human, based on receptor occupancies and PK-PD model simulations.



## INTRODUCTION

MCLA-128 is a full length humanized IgG1 bispecific monoclonal antibody (mAb) with enhanced antibody-dependent cell mediated cytotoxicity (ADCC) targeting the HER2 and HER3 receptor tyrosine kinases. MCLA-128 is developed to overcome HER3-mediated resistance to EGFR and HER2-targeted therapies. Current HER2-targeted therapies are approved for HER2-amplified breast and gastric cancers, either as single agents or in combination with other anti-cancer drugs.<sup>1,2</sup> However, a proportion of patients treated with these therapies show primary or acquired resistance.<sup>3,4</sup> A major resistance mechanism is mediated via HER3 activation. Its ligand heregulin drives dimerization of HER3 with HER2, resulting in potent activation of the PI3K/AKT pathway with subsequent enhanced growth and survival of HER2-amplified tumors. Heregulin stimulation was shown to mediate resistance to trastuzumab and lapatinib therapy.<sup>5-7</sup> Alternatively, HER3 upregulation in HER2-amplified tumors can also result in ligand-independent dimerization of HER3 with HER2 and enhanced cell survival (7). The simultaneous targeting of HER2 and HER3 by MCLA-128 could overcome this resistance. MCLA-128 is expected to directly inhibit tumor growth by blocking HER2:HER3 signaling and, through the ADCC mechanism, eliminate tumor cells via recruitment of natural killer effector cells to tumor cells coated with MCLA-128.

In vitro results show that MCLA-128 inhibits proliferation of HER2 over-expressing and HER2-low cells stimulated with heregulin. MCLA-128 shows significantly higher potency than lapatinib, trastuzumab alone or to the combination of trastuzumab and pertuzumab.<sup>8</sup>

Preclinical in vivo research was conducted in cynomolgus monkeys and in tumor xenograft models in mice to understand the preclinical pharmacokinetics (PK) and pharmacodynamics (PD) of MCLA-128. The aim of this study was to develop a preclinical PK-PD model for MCLA-128 based on (i) PK characteristics of MCLA-128 in cynomolgus monkeys and (ii) the effect of MCLA-128 on tumor growth in mouse xenograft models.

The preclinical PK model was used to predict the safe starting dose in humans, to support selection of the First-In-Human dose for the Phase I dose-finding trial, and to identify the clinical doses that reach a sufficient percentage of receptor occupancy. In addition, the full preclinical PK-PD model was used to evaluate the anti-tumor activity of the proposed clinical doses.

## **MATERIAL AND METHODS**

### **Generation of MCLA-128**

MCLA-128 was engineered using proprietary CH3 technology, and is composed of two identical common light chains and two different heavy chains (anti-HER2 and anti-HER3). ADCC-enhancement was achieved by low fucose glycoengineering using the GlymaxX® technology.<sup>8</sup>

### **Data (1) PK of MCLA-128 in cynomolgus monkeys**

PK data from 28 cynomolgus monkeys was combined from a single dose toxicity study and the first week of a repeated dose toxicity study. In the single dose toxicity study, 14 blood samples per animal were drawn and sampling times ranged from 0 to 1007 hours. Each dosing regimen of 10 mg/kg, 30 mg/kg and 100 mg/kg was administered intravenously to one female and one male animal (total n=6). In the repeated dose toxicity study, 22 animals received a weekly dose of MCLA-128 for five weeks; only data from the first week was included in the analysis. A dosing regimen of 10 mg/kg (n=6), 30 mg/kg (n=6) and 100 mg/kg (n=10) was administered with equal distribution between female and male animals. Ten samples per animal were drawn and sampling times ranged from 0 to 168 hours. MCLA-128 was quantified in serum using a validated electrochemiluminescence immunoassay (lower limit of quantification (LLOQ): 78 ng/mL). The experiments in cynomolgus monkeys were conducted at Charles River Laboratories Edinburg (preclinical services). All procedures were performed in accordance with the UK Animals (Scientific Procedures) Act, 1986, approved by institutional ethical review committees and conducted under the authority of the Project License.

## **Data (2): Antitumor efficacy in xenograft models.**

MCLA-128 antitumor activity was evaluated in a human breast carcinoma model using the JIMT-1 cell line. In this experiment, 8 to 12 weeks old female CB.<sup>17</sup> SCID mice were injected subcutaneously in the right flank with  $5 \cdot 10^6$  JIMT-1 tumor cells. Treatment started 8 days after tumor cell implantation, with tumor volumes ranging from 108 to 172 mm<sup>3</sup>. Animals (n=10 per group) received weekly intraperitoneal (i.p) injections of either PBS, MCLA-128 at 2.5 mg/kg or MCLA-128 at 25 mg/kg for four weeks (4 doses in total). Mice were euthanized on day 68 or when tumor size reached 800 mm<sup>3</sup>. Tumors from mice were extracted 24 hours after the last dose. Tumor size was determined with a caliper twice weekly and tumor volume was calculated using the following equation: tumor volume (mm<sup>3</sup>) = (width<sup>2</sup> · length) · 0.5. Efficacy data were used to develop the PD model.

Mouse xenograft studies were performed by Charles River Discovery Services North Carolina, USA and the experimental protocol was approved by the site's Institutional Animal Care and Use Committee. The facility is accredited by the Association for Assessment and Accreditation of Laboratory Animal Care International (AAALAC).

## **PK modeling**

The structural PK characteristics of monoclonal antibodies (mAbs) are usually described by a two-compartment model with either linear, nonlinear or parallel linear and nonlinear clearances.<sup>9</sup> Antibodies follow primarily linear clearance through cellular uptake followed by lysosomal degradation, mediated by the neonatal Fc receptor (FcRn). In addition, the Fab region of the antibody can bind to the target receptor, leading to a saturable clearance pathway, known as target mediated drug disposition (TMDD).<sup>10,11</sup> The starting point for model development in the current analysis was a two-compartment model for which different combinations of linear and nonlinear clearance were evaluated. The PK model was directly scaled to a 70 kg human using allometric scaling.

### Tumor growth modeling

Non-perturbed tumor growth models were evaluated in the untreated mice. Different growth models were evaluated, such as Gompertz growth, zero-order growth (linear) and first-order (exponential) growth.<sup>12</sup>

PK sampling was not performed in the xenograft study. Therefore, the previously established PK model developed based on cynomolgus monkey data was allometrically scaled to a 0.02 kg mouse to predict concentration-time profiles and assess their relation to tumor growth in the treated animals.<sup>13,14</sup>

The MCLA-128 anti-tumor effect was modeled to impact either the tumor growth rate ( $K_g$ ), the tumor dying rate ( $K_d$ ) or both. Different models to describe these effects were evaluated, such as direct effect models, indirect response models and use of transit and effect compartments, to establish the correct delay in effect, seen in the individual plots describing tumor volume over time. The drug effect was modeled as either a linear effect or an  $E_{max}$  model. Additionally, a tumor growth rate increase over time was considered.

### Statistical model development

Inclusion of inter individual variability was considered for all structural model parameters as follows:

$$P_i = P_{pop} \cdot \exp(\eta_i)$$

Where  $P_i$  is the individual parameter estimate for individual  $i$ , and  $P_{pop}$  is the typical population parameter estimate, and where  $\eta_i$  was assumed to be distributed normally distributed with mean 0 and variance  $\omega^2$ . Residual unexplained variability was described as a proportional and additive error model for the PK model:

$$C_{obs,ij} = C_{pred,ij} \cdot (1 + \varepsilon_{p,ij}) + \varepsilon_{a,ij}$$

For the PD part of the model residual variability was described by a proportional error model:

$$C_{obs,ij} = C_{pred,ij} \cdot (1 + \varepsilon_{p,ij})$$

Where  $C_{obs,ij}$  represents the observed concentration for individual  $i$  and observation  $j$ ,  $C_{pred,ij}$  represents the individual predicted concentration,  $\varepsilon_{p,ij}$  the proportional error and  $\varepsilon_{a,ij}$  the additive error, both distributed following  $N(0, \sigma^2)$ .

For PK data, the first data point below the LLOQ (78 ng/mL) was fixed to LLOQ/2 and a fixed additive error component of LLOQ/2 was included in the model to account for uncertainty in these observations.<sup>15</sup>

### Model evaluation

Models were evaluated based on general goodness-of-fit (GOF) plots, plausibility, stability and precision of parameter estimates and change in objection function value (OFV) where a  $p < 0.01$  was considered significant, meaning that a OFV drop of  $> 6.63$  (degree of freedom = 1) was considered as a significant improvement.

### Software

Data management, graphical evaluation and simulations were performed using R (version 3.0.1).<sup>16</sup> Nonlinear mixed effects modeling was performed using NONMEM (version 7.3.0, ICON Development Solutions, Ellicott City, MD, USA) and Perl-speaks-NONMEM (version 4.4.8).<sup>17,18</sup> Piraña (version 2.9.2) was used as graphical user interface.<sup>19</sup> All models were estimated using First Order Conditional Estimation method with  $\eta$ - $\varepsilon$  interaction (FOCE-I).

### Determination of the safe starting dose and clinical efficacious dose

A safe starting dose for the First-In-Human study of MCLA-128 was identified by calculation of safety margins based on the simulated exposure in humans at different dose levels. Subsequently, a clinical target exposure and dose was determined by calculation of receptor occupancies for different dose levels, based on the simulated exposures in human and the estimated  $K_m$  value. Doses with a receptor occupancy above 99%, based on the maximum and average MCLA-128 concentration in the first cycle, were expected to have a clinical effect. In addition, a simulation with the tumor growth model was performed in mice, to evaluate the potential human anti-tumor efficacy of the proposed clinical dose regimens.

First, the safety margins were calculated for different simulated dose levels. The safety margins were based on the no-observed-adverse-effect-level (NOAEL) of MCLA-128 in monkeys included in the multiple dose toxicity study, which was determined at 100 mg/kg. The mean  $AUC_{0-inf}$  of 193 g·hr/L was calculated using the PK data of the monkeys included in the single dose toxicity study that received 100 mg/kg, to assure that the exposure to MCLA-128 was not compromised by possible generation of anti-drug antibodies. The safety margin was calculated by dividing the 193 g·hr/L  $AUC_{0-inf}$  by the predicted model-based  $AUC_{0-inf}$ . The AUCs were computed using a non-compartmental analysis of both the observed and simulated data. Second, the receptor occupancies based on the maximal, trough and average concentrations ( $C_{max}$ ,  $C_{trough}$  and  $C_{ave}$ , respectively) were calculated, using the same simulated exposure data as used for obtaining the safety margins. The receptor occupancies were calculated based on the estimated  $K_m$  value, using the following equation:

$$\%RO = 100 \cdot \frac{C_{max\ or\ trough\ or\ average}}{K_m + C_{max\ or\ trough\ or\ average}}$$

Lastly, to evaluate the potential human anti-tumor efficacy the proposed clinical dose regimens for MCLA-128 were evaluated with the preclinical PK-PD model in mice.

Tumor stasis at day 21 was evaluated after applying a regimen of a weekly dose for three weeks. The dose input was chosen so that the total exposure (AUC) of the three doses, mimicked the exposure of proposed clinical doses administered once in a 21-day cycle.

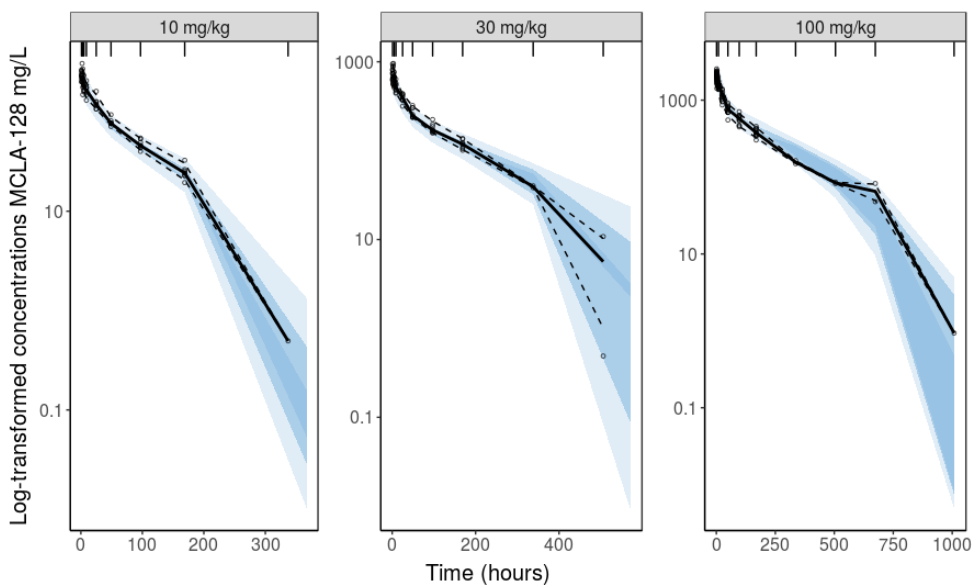


**Figure 1** Visual Predictive Checks (VPCs) for PK data from cynomolgus monkeys stratified on dose group (10 mg/kg, 30 mg/kg, 100 mg/kg). The solid line represents the median, the dashed line represents the 95% prediction interval of the observed MCLA-128 observations. The shaded areas show the 95% confidence interval around the prediction interval (n=500).

**Table 1 Allometrically scaled PK parameters describing MCLA-128 concentration-time data in cynomolgus monkeys and mice. Parameters estimated for a 70 kg human and scaled to 0.02 kg mice.**

	UNITS	ESTIMATES	RSE (%)	SHRINKAGE (%)	SCALED PARAMETERS MICE
<b>Parameter</b>					
CL	L/h	0.0125	9.4	-	2.75·10 <sup>-5</sup>
V <sub>1</sub>	L	3.17	2.9	-	9.06·10 <sup>-4</sup>
Q	L/h	0.0313	6.5	-	6.88·10 <sup>-5</sup>
V <sub>2</sub>	L	3.51	14.7	-	1.00·10 <sup>-3</sup>
V <sub>max</sub>	mg/h	0.500	10.3	-	1.10·10 <sup>-3</sup>
K <sub>m</sub>	mg/L	0.219	Fixed	-	0.219
<b>Between-subject variability (%)</b>					
CL	CV	13.2		12.6	-
V <sub>1</sub>	CV	14.6		3.8	-
<b>Residual variability</b>					
Prop	SD	0.108	1	10.6	-
Add	SD	0.039	Fixed		-

*CL<sub>L</sub> = linear clearance, V<sub>1</sub> = volume of distribution in the central compartment, Q = distributional clearance, V<sub>2</sub> = volume of distribution in the peripheral compartment, V<sub>max</sub> = maximum velocity, when all drug-targets are saturated, K<sub>m</sub> = concentration at which half the drug-targets are occupied, Prop = proportional error, Add = additive error, CV = coefficient of variation, SD = standard deviation.*

## RESULTS

### PK model

A two-compartment model with parallel linear and nonlinear clearances from the central compartment described the data best. The nonlinear clearance was described using Michaelis-Menten kinetics. The final model structure was defined by the following differential equations:

$$\frac{d(A_1)}{d(t)} = -\frac{CL}{V_1} \cdot A_1 - \frac{V_{max} \cdot C_1}{K_m + C_1} - \frac{Q}{V_1} \cdot A_1 + \frac{Q}{V_2} \cdot A_2 \quad (1)$$

$$\frac{d(A_2)}{d(t)} = \frac{Q}{V_1} \cdot A_1 - \frac{Q}{V_2} \cdot A_2 \quad (2)$$



Where CL represents the linear clearance, Q the intercompartmental clearance,  $V_1$  the volume of distribution in the central compartment and  $V_2$  the volume of distribution in the effect compartment,  $A_1$  the amount of drug in the central compartment,  $V_{max}$  the maximum elimination rate,  $C_1$  the drug concentration in the central compartment,  $K_m$  the drug concentration at which half the drug-targets are occupied and  $A_2$  the amount in the peripheral compartment. Scaling of the model to a 70 kg human or 0.02 kg mouse was performed using the following equations, respectively:

$$P_{monkey\_pop} = \theta_{human\_pop} \cdot \frac{WT}{70}^{factor}$$

$$P_{mouse\_pop} = \theta_{human\_pop} \cdot \frac{0.02}{70}^{factor}$$

On CL, Q, and  $V_{max}$  a factor of 0.75 was used and on  $V_1$  and  $V_2$  a factor of 1 was used. MCLA-128 is fully cross-reactive with cynomolgus monkey HER2 and HER3 receptors and mice were implanted with human HER2 and HER3 expressing tumors. Therefore,  $K_m$  was not scaled and fixed to the parameter estimate in cynomolgus monkeys (0.219 mg/L) for both human and mice.<sup>20,21</sup> Parameter estimates for a 70 kg human and the calculated scaled parameters for a 0.02 kg mouse are depicted in Table 1. The visual predictive checks (VPCs) demonstrate that the model accurately describes the observed PK data in cynomolgus monkeys for each dose-group (Figure 1).

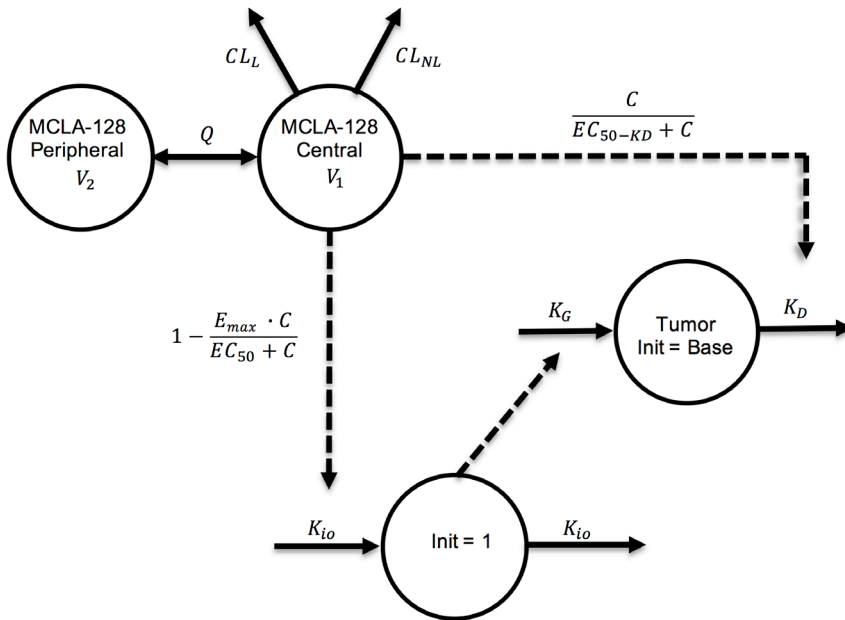


**Figure 2** Schematic structure of the PK-PD model in mice.  $CL_L$  linear clearance,  $CL_{NL}$  nonlinear clearance,  $V_1$  volume of distribution central compartment,  $V_2$  volume of distribution peripheral compartment.  $K_G$  zero-order tumor growth rate,  $K_D$  tumor dying rate,  $K_{io}$  production and loss of drug effect on  $K_G$ ,  $E_{max}$  maximum effect of MCLA-128 on  $K_{io}$  (fixed to 1).  $EC_{50}$  MCLA-128 concentration with 50% of maximum effect on  $K_{io}$ ,  $EC_{50-KD}$  concentration MCLA-128 with 50% of maximum effect on  $K_D$ . Dotted lines drug effects.

### PK-PD model

The preclinical PK-PD model was based on the scaled PK model from cynomolgus monkeys to mice and the xenograft experiments conducted in mice. First, the non-perturbed tumor growth in the vehicle-treated mice was modelled. This was best described by a zero-order growth rate ( $K_G$ ). The MCLA-128 anti-tumor effect in this experiment was modeled to target the proliferation and dying rate ( $K_G$  and  $K_D$ ) of the tumor. The effect on  $K_G$  was described by an indirect response model, where the in-rate ( $K_{io}$ ) in the indirect effect compartment was affected by the predicted MCLA-128 concentration using an inhibitive  $E_{max}$  equation.

The effect of the predicted MCLA-128 concentrations on  $K_D$  was modeled directly with an  $E_{max}$  model. An indirect response model and effect compartment model were evaluated to investigate a delay of the effect on  $K_D$ , but this could not be identified. Addition of an increasing tumor growth rate over time (modelled by inclusion of the  $\lambda$  term) led to a significant increase of model fit and was implemented in the final model. The structural model is depicted in Figure 2 and the estimated PD model parameters are depicted in Table 2. Goodness of fit plots and a plot demonstrating observed tumor volume versus predicted population mean, demonstrated adequate fit of the model (Figure 3 and 4).

**Table 2 Population parameter estimates for the preclinical PK/PD model<sup>a</sup>: the effect of MCLA-128 on tumor growth in JIMT-1 xenograft models.**

PARAMETER	UNITS	PARAMETER ESTIMATES	RSE (%)	SHRINK-AGE (%)
<i>Population PD parameters in mice</i>				
Tumor baseline value (Base)	mm <sup>3</sup>	177	6.7	-
Zero order tumor growth rate ( $K_G$ )	hr <sup>-1</sup>	0.338	22.2	-
First order tumor dying rate ( $K_D$ )	mm <sup>3</sup> /hr	0.004	15.9	-
Production and loss of drug effect on $K_G$ ( $K_{iG}$ )	hr <sup>-1</sup>	0.143	18.3	-
MCLA-128 concentration with 50% of maximum effect on $K_{iG}$ ( $EC_{50}$ )	mg/L	2.60	47.7	-
MCLA-128 concentration with 50% of maximum effect on $K_D$ ( $EC_{50_{KD}}$ )	μg/L	0.0102	25.1	-
Progression factor	week <sup>-1</sup>	0.172	23	-
<i>Between-subject variability (%)</i>				
Baseline	CV	20.6		16.8
$K_G$	CV	55.1		1.10
$K_D$	CV	35.5		24.8
<i>Residual variability</i>				
Proportional residual error tumor compartment	CV	25.6	7.4	5.9

<sup>a</sup>Population PK parameters were scaled to mice to drive the tumor growth model, parameters reported in Table 1. RSE = relative standard error, CV = coefficient of variation, SD = standard deviation

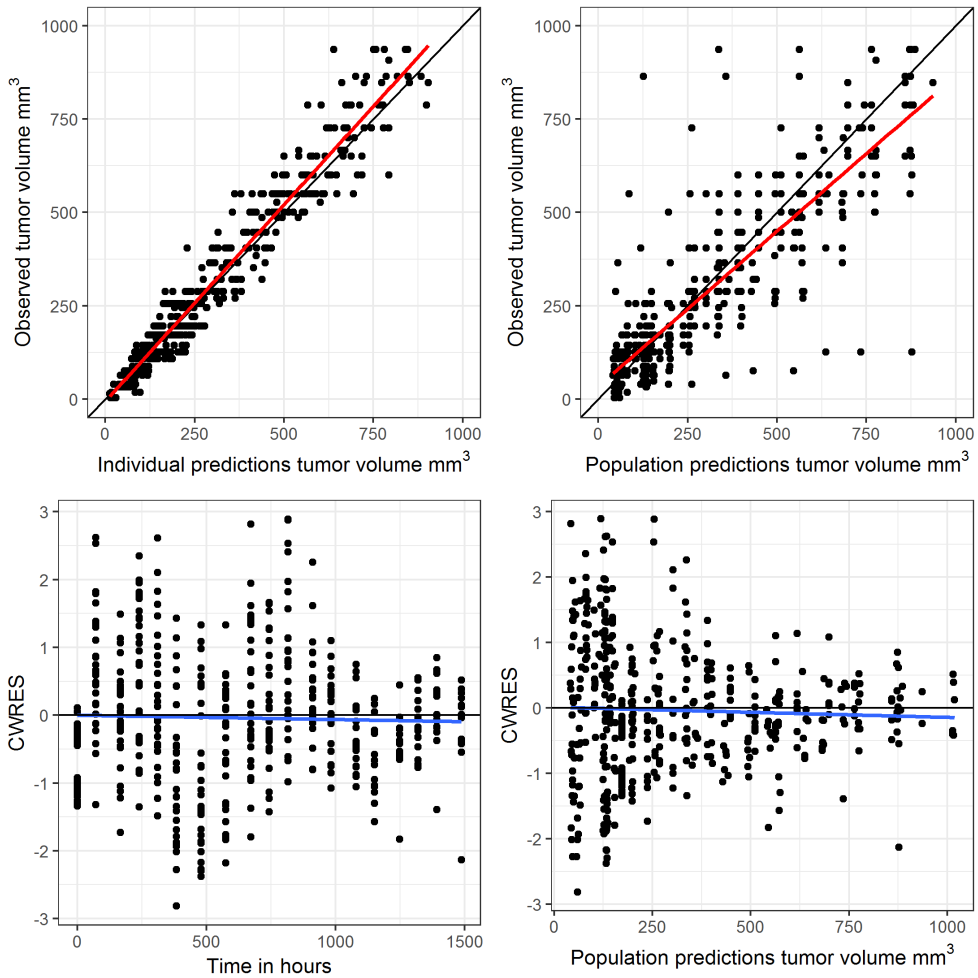


**Figure 3** Goodness of fit plots tumor growth model, CWRES = conditional weighted residuals.

### Safe starting dose and clinical efficacious dose

The safety margins and percentages receptor occupancies at predicted maximum, trough and average concentrations were calculated for the anticipated clinical doses. Results are depicted in Table 3. Clinical doses ranging from 10 to 480 mg

flat dose MCLA-128 showed a safety margin > 10-fold and doses  $\geq 360$  mg had an expected receptor occupancy higher than 99% for both  $C_{max}$  and  $C_{ave}$ . In addition, a sensitivity analysis for the  $K_m$  was conducted for  $K_m$  values ranging from 0.0219 mg/L to 2.19 mg/L, since this parameter showed a high relative standard error (RSE) of 74% value in the monkey estimation. The sensitivity analysis showed permanent adequate receptor occupancies for varying  $K_m$  values and values of higher than 99% for doses starting from 160 mg ( $K_m$  of 0.0219 mg/L) and 750 mg ( $K_m$  of 2.19 mg/L). Subsequently, the tumor volumes over time in 0.02 kg mice were simulated with the established preclinical PK-PD model for dose levels of 9.5 mg/kg, 20 mg/kg and 24 mg/kg given once every week (q1wk) for 3 weeks (Figure 5). These dose levels had AUCs corresponding to the 360 mg, 750 mg and 900 mg flat dose of MCLA-128 given q3wk in the First-In-Human study, and demonstrated profound tumor stasis at day 21.

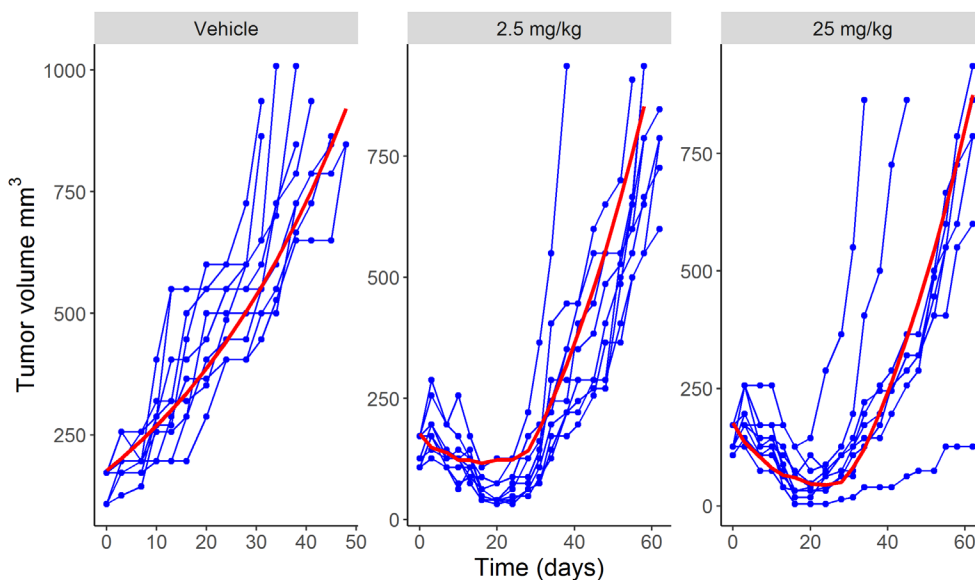


**Figure 4** Individual tumor volume over time curves for each dose group (vehicle, 2.5 mg/kg and 25 mg/kg). Blue dots and lines observed tumor volumes, red line = population prediction.

**Table 3 Simulation results of MCLA-128 exposure (AUC) and predicted receptor occupancy (RO) for different flat doses of MCLA-128 administered to humans once every 3 weeks.**

FLAT DOSE (MG)	AUC (g·hr/L)	SAFETY Margin	C <sub>MAX</sub> %RO	C <sub>AVE</sub> %RO	C <sub>TROUGH</sub> %RO
10	0.031	6226	93.5	22.6	0.021
20	0.10	1930	96.6	48.8	0.074
40	0.33	585	98.3	75.1	0.253
80	1.00	193	99.1	90.2	0.874
160	2.97	65	99.6	96.4	3.29
240	5.57	35	99.7	98.1	8.12
360	10.4	19	99.8	99.0	23.8
480	16.0	12	99.9	99.3	75.7
600	22.4	9	99.9	99.5	96.5
750	31.4	6	99.9	99.6	98.4
900	41.1	5	99.9	99.7	99.0
1000	47.9	4	99.9	99.7	99.2
1200	62.0	3	99.9	99.8	99.3

$C_{max}$  = maximum concentration,  $C_{ave}$  = average concentration, RO = receptor occupancy,  $RO = 100 \cdot C_{max}$  or  $C_{trough}$  or  $C_{average} / (K_m + C_{max}$  or  $C_{trough}$  or  $C_{average})$

## DISCUSSION

In this analysis, the preclinical PK characteristics of MCLA-128 were quantified in cynomolgus monkeys and subsequently predicted for humans. The PK profiles were well described by a two-compartment model with parallel linear and nonlinear clearance pathways. Predicted parameters were in accordance with previously published PK characteristics of different therapeutic mAbs in human, with a median (range) of  $V_1$  and  $V_2$  of 3.1 L (2.4-5.5) and 2.8 L (1.3-6.8), respectively, and for linear clearance ( $CL_L$ ) 0.013 L/h (0.003-0.223).<sup>9</sup> Estimates for  $V_{max}$  and  $K_m$  varied widely among the different IgG mAbs, but the Michaelis Menten estimates for MCLA-128 were within this wide range.<sup>9</sup> Cynomolgus monkeys are considered to be the most relevant species to predict PK of monoclonal antibodies in human.<sup>22</sup> In addition, healthy cynomolgus monkeys express HER2 and HER3 receptors with binding epitopes for MCLA-128 that are conserved between human and cynomolgus monkeys. This is a requirement to determine the nonlinear (target mediated) clearance pathway.

Moreover, the design of MCLA-128 using the CH3 engineering and the low fucose glycoengineering technologies did not alter the IgG PK characteristics of the compound, since PK parameters were in the range of previously published parameters of other therapeutic IgG mAbs.

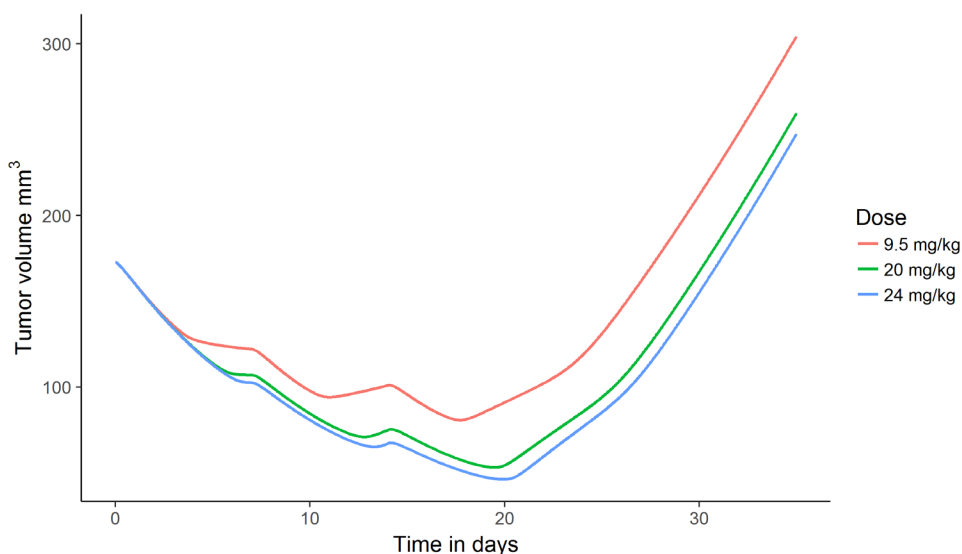


**Figure 5** Simulation of tumor growth in mice, with administered doses of 9.5, 20 and 24 mg/kg q1wk for three weeks, corresponding with AUCs after 360, 750 and 900 mg flat dose of MCLA-128 given q3wk to humans.

Subsequently, the established PK model was used to predict safety in humans. Dose levels of 10 to 480 mg flat dose of MCLA-128 given q3wk have predicted AUCs that are at least 10-fold lower than the NOAEL corresponding AUC in monkeys. Doses of 10 to 480 mg were, therefore, considered suitable as a First-In-Human starting dose. However, following the CHMP guideline on identifying and mitigating risk for such studies<sup>23</sup>, other non-clinical safety pharmacology and toxicology data should also be taken into account to determine the optimal starting dose for the Phase I dose-escalation trial, including the identification of the factors of risk.

Concerns may be derived from particular knowledge or lack thereof regarding the mode of action, the nature of the target, and/or the relevance of animal models. Obtaining the exposures in humans using a PK modeling and simulation approach is preferred over traditional calculation of the human equivalent dose, since (non-linear) pharmacokinetic characteristics are taken into account.<sup>24,25</sup> In addition, antibodies are suitable compounds for this approach, since no metabolites are formed and no enzymatic metabolism is present, which might trouble the prediction of exposure from animal to human.<sup>9,22</sup>

The PK model was then used to determine the pharmacological active doses based on receptor occupancies. Doses  $\geq 360$  mg flat dose of MCLA-128 given q3wk are expected to reach a receptor occupancy superior to 99% at  $C_{\max}$  and  $C_{\text{avg}}$ , and at  $C_{\text{trough}}$  of 24%. However, the receptor occupancies are calculated using the model estimated  $K_m$  value based on healthy cynomolgus monkeys. These cynomolgus monkeys did not bear HER2/HER3 expressing tumors, but only endogenously expressed HER3 and HER2 epitopes. It is expected that tumor-bearing patients demonstrate higher expression of HER2 and HER3 receptors. Therefore, the clinical model estimate for the  $V_{\max}$  and  $K_m$  could be different. The sensitivity analysis demonstrated that for a 10-fold increase in the  $K_m$  value, a 750 mg flat dose MCLA-128 would attain a receptor occupancy of 99% at  $C_{\max}$ . In addition, for trastuzumab, a  $K_m$  value of 3.7 mg/L has been identified in patients with HER2-amplified advanced gastric or gastroesophageal junction cancer.<sup>26</sup> This  $K_m$  is in the same order of magnitude as the  $K_m$  of MCLA-128 used in the sensitivity analysis (2.19 mg/L). Moreover, in breast cancer, only linear PK models for trastuzumab have been identified potentially indicating that all target is saturated and, that the target mediated clearance of trastuzumab is of minor importance in breast cancer at therapeutic dose levels.<sup>27</sup>

Finally, the proposed effective doses in human were evaluated using the preclinical PK-PD model. The final tumor growth (PD) model included an effect on the tumor growth rate and on the tumor dying rate. The low  $EC_{50}$  value for the effect on  $K_d$  ( $EC_{50_{KD}}$ ) suggests that the anti-tumor activity is present during almost the complete time course between administrations in mice for doses of 2.5 mg/kg and higher.



The JIMT-1 cell line has higher HER2 expression than HER3 expression and is reported to overexpress the HER3 ligand heregulin.<sup>28,29</sup> The JIMT-1 cell line is resistant to HER2 targeted therapies and partially dependent on autologous heregulin for growth which can be effectively blocked in vitro by MCLA-128.<sup>28</sup> The JIMT-1 cell line was therefore considered suitable for determining the direct effect of MCLA-128 on tumor growth in a xenograft setting. However, this approach may underpredict the true anti-tumor efficacy of MCLA-128 due to the inherent limitations of the xenograft models: immunodeficient mice were used in the JIMT-1 xenograft model and therefore the ADCC-related mechanism of action could not be evaluated. As a result, the low  $EC_{50\_KD}$  is expected to represent the natural dying rate of the tumor resulting from a decrease in tumor growth rate. On the other hand, the exposure of MCLA-128 in mice was predicted using an allometrically scaled PK model, the true exposure in mice is expected to be higher, since humanized mAbs have a high affinity for mouse and rat FcRn, resulting in a decrease in linear clearance, subsequently resulting in higher concentrations.<sup>30</sup> Therefore, it is expected that the  $EC_{50}$  parameters for anti-tumor activity are higher than estimated in the preclinical PK/PD model. It is unclear how these two findings are balanced, hence how they affect the preclinical predictions of tumor growth. However, we expect that the true anti-tumor efficacy is stronger than simulated, since lack of the ADCC effect is expected to have a stronger impact on predictions than an increase in the  $EC_{50}$  parameter. Nevertheless, MCLA-128 demonstrated a profound anti-tumor activity in mice.

Receptor occupancies based on  $C_{max}$  and  $C_{ave}$  were expected to be >99% starting as of 360 mg MCLA-128 given q3wk and receptor occupancies based on  $C_{trough}$  at the end of a 3-week dosing interval were >99% as of 900 mg (Table 3). Since the anti-tumor effects of MCLA-128 are mediated via receptor binding, it is expected that a further increase in dose will not lead to a significant increase in effect, for doses reaching receptor occupancies >99%. Likewise, both drug effects in the PK-PD model were described by an  $E_{max}$  model, confirming an asymptotic approach of the maximum effect. However, the tumor growth model was not able to capture a plateau in effect starting from approximately 360 mg or 900 mg q3wk, because data about receptor and receptor-drug complex concentrations was lacking.

In general, in this analysis all available relevant PK and PD data before start of the First-in-Human trial were combined in a comprehensive modeling framework to fully evaluate the safe starting dose and predicted efficacious dose range. This framework can be applied similarly for the evaluation of other monoclonal antibodies.

## **CONCLUSION**

A preclinical predictive PK-PD model describing the relation between MCLA-128 exposure and tumor volume over time was developed and demonstrated the anti-tumor efficacy of MCLA-128. The calculation of the safety margins demonstrated that flat doses of 10 to 480 mg MCLA-128 given q3wk are expected to be safe as starting dose for a First-In-Human study with MCLA-128 based on the NOAEL exposure in cynomolgus monkeys. However, other non-clinical safety pharmacology and toxicology data should also be taken into consideration to determine the optimal starting dose for the Phase I dose escalation trial, including the identification of the factors of risk. The simulations and the estimations of receptor occupancy for different dose levels showed that flat doses  $\geq 360$  mg of MCLA-128 given q3wk are likely to be efficacious in human.

## REFERENCES

1. Arteaga, C. et al. Treatment of HER2-positive breast cancer: current status and future perspectives. *Nat. Rev. Clin. Oncol.* 9, 16-32 (2011).
2. Baselga, J., Cortes, J., Kim, S., Im, S. & Hegg, R. Pertuzumab plus Trastuzumab plus Docetaxel for Metastatic Breast Cancer. *N. Engl. J. Med.* 366, 109-119 (2012).
3. Pohlmann, P. R., Mayer, I. a & Mernaugh, R. Resistance to Trastuzumab in Breast Cancer Resistance to Trastuzumab in Breast Cancer. *Clin. Cancer Res.* 15, 7479-7491 (2009).
4. Wong, A. L. a. & Lee, S.-C. Mechanisms of Resistance to Trastuzumab and Novel Therapeutic Strategies in HER2-Positive Breast Cancer. *Int. J. Breast Cancer* 2012, 1-13 (2012).
5. Wilson, T. R. et al. Widespread potential for growth-factor-driven resistance to anticancer kinase inhibitors. *Nature* 487, 505-509 (2012).
6. Sergina, N. V et al. Escape from HER-family tyrosine kinase inhibitor therapy by the kinase-inactive HER3. *Nature* 445, 437-441 (2007).
7. Garrett, J. T. et al. Transcriptional and posttranslational up-regulation of HER3 (ErbB3) compensates for inhibition of the HER2 tyrosine kinase. *Proc. Natl. Acad. Sci. U. S. A.* 108, 5021-6 (2011).
8. Geuijen, C., Rovers, E., Nijhuis, R. & Visser, T. Preclinical activity of MCLA-128, an ADCC enhanced bispecific IgG1 antibody targeting the HER2:HER3 heterodimer. *J. Clin. Oncol.* 32, (suppl; abstr 560) (2014).
9. Dirks, N. L. & Meibohm, B. Population pharmacokinetics of therapeutic monoclonal antibodies. *Clin. Pharmacokinet.* 49, 633-59 (2010).
10. Dostalek, M., Gardner, I., Gurbaxani, B. M., Rose, R. H. & Chetty, M. Pharmacokinetics, pharmacodynamics and physiologically-based pharmacokinetic modelling of monoclonal antibodies. *Clin. Pharmacokinet.* 52, (2013).
11. Gibiansky, L. & Gibiansky, E. Target-mediated drug disposition model: relationships with indirect response models and application to population PK-PD analysis. *J. Pharmacokinet. Pharmacodyn.* 36, 341-51 (2009).
12. Ribba, B. et al. A review of mixed-effects models of tumor growth and effects of anticancer drug treatment used in population analysis. *CPT pharmacometrics Syst. Pharmacol.* 3, e113 (2014).

13. Mordenti, J. Man versus beast: Pharmacokinetic scaling in mammals. *J. Pharm. Sci.* 75, 1028-1040 (1986).
14. Mordenti, J., Chen, S. A., Moore, J. A., Ferraiolo, B. L. & Green, J. D. Interspecies scaling of clearance and volume of distribution data for five therapeutic proteins. *Pharm. Res.* 8, 1351-1359 (1991).
15. Beal, S. L. Ways to fit a PK model with some data below the quantification limit. *J. Pharmacokinet. Pharmacodyn.* 28, 481-504 (2001).
16. R Core Team, 2018 *R: A language and Environment for Statistical Computing*. R Foundation for statistical computing, Vienna, Austria. at <<https://www.r-project.org/>>
17. Beal, S., Sheiner, L., Boeckmann, A. & Bauer, R. NONMEM 7.3.0 Users Guides. (1989-2013). ICON Development Solutions, Hanover, MD.
18. Lindbom, L., Ribbing, J. & Jonsson, E. N. Perl-speaks-NONMEM (PsN) - A Perl module for NONMEM related programming. *Comput. Methods Programs Biomed.* 75, 85-94 (2004).
19. Keizer, R. J., Karlsson, M. O. & Hooker, A. Modeling and Simulation Workbench for NONMEM: Tutorial on Pirana, PsN, and Xpose. *CPT pharmacometrics Syst. Pharmacol.* 2, e50 (2013).
20. Singh, A. P. et al. Quantitative Prediction of Human Pharmacokinetics for mAbs Exhibiting Target-Mediated Disposition. *AAPS J.* 17, 389-399 (2015).
21. Dong, J. Q. et al. Quantitative prediction of human pharmacokinetics for monoclonal antibodies: retrospective analysis of monkey as a single species for first-in-human prediction. *Clin. Pharmacokinet.* 50, 131-42 (2011).
22. Deng, R. et al. Projecting human pharmacokinetics of therapeutic antibodies from nonclinical data: What have we learned? *MAbs* 3, 61-66 (2011).
23. Committee for medicinal products for human use, E. Guideline on Strategies to Identify and Mitigate Risks for First-In-Human Clinical Trials with Investigational Medicinal Products (2007) at <[http://www.ema.europa.eu/docs/en\\_GB/document\\_library/Scientific\\_guideline/2009/09/WC500002988.pdf](http://www.ema.europa.eu/docs/en_GB/document_library/Scientific_guideline/2009/09/WC500002988.pdf)>
24. Mahmood, I., Green, M. D. & Fisher, J. E. Selection of the first-time dose in humans: Comparison of different approaches based on interspecies scaling of clearance. *J. Clin. Pharmacol.* 43, 692 (2003).
25. Reigner, B. G. & Blesch, K. Estimating the starting dose for entry into humans: Principles and practice. *Eur. J. Clin. Pharmacol.* 57, 835-845 (2002).

26. Cosson, V. F., Ng, V. W., Lehle, M. & Lum, B. L. Population pharmacokinetics and exposure-response analyses of trastuzumab in patients with advanced gastric or gastroesophageal junction cancer. *Cancer Chemother. Pharmacol.* 73, 737-47 (2014).
27. Bruno, R. et al. Population pharmacokinetics of trastuzumab in patients with HER2+ metastatic breast cancer. *Cancer Chemother. Pharmacol.* 56, 361-9 (2005).
28. Tanner, M. et al. Characterization of a novel cell line established from a patient with Herceptin-resistant breast cancer. *3*, 1585-1592 (2004).
29. Köninki, K. et al. Multiple molecular mechanisms underlying trastuzumab and lapatinib resistance in JIMT-1 breast cancer cells. *Cancer Lett.* 294, 211-219 (2010).
30. Ober, R. J. Differences in promiscuity for antibody-FcRn interactions across species: implications for therapeutic antibodies. *Int. Immunol.* 13, 1551-1559 (2001).



## CHAPTER 2.2

Population pharmacokinetics of MCLA-128,  
a HER2/HER3 bispecific  
monoclonal antibody,  
in patients with solid tumors

*Submitted*

A.H.M. de Vries Schultink  
K. Bol  
R.P. Doornbos  
E. Wasserman  
T.P.C. Dorlo  
J.H.M. Schellens  
J.H. Beijnen  
A.D.R. Huitema

## ABSTRACT

### Introduction

MCLA-128 is a bispecific monoclonal antibody targeting the HER2 and HER3 receptor and is in development to overcome HER3 mediated resistance to anti-HER2 therapies. The aims of this analysis were to characterize the population pharmacokinetics (PK) of MCLA-128 in patients with various solid tumors included in a phase I/II trial, to evaluate patient-related factors that affect the disposition of MCLA-128 and assess whether fixed dosing is appropriate.

### Methods

MCLA-128 concentration data following intravenous administration were collected in a phase I/II clinical trial. PK data were analyzed using nonlinear mixed-effects modeling. Different compartmental models were evaluated. Various body size parameters including body weight, body surface area and fat-free mass (FFM) were evaluated as covariates in addition to age, sex and tumor type.

### Results

In total, 1115 serum concentration measurements were available from 116 patients. PK of MCLA-128 was best described by a two-compartment model with linear and nonlinear (Michaelis-Menten) clearance. FFM significantly affected the linear clearance and volume of distribution of the central compartment of MCLA-128, explaining 8.4% and 5.6% of inter-individual variability, respectively. No other significant covariate relationships were found. Simulations demonstrated that dosing based on body size parameters resulted in similar  $AUC_{0-\tau}$ , maximum and trough concentrations of MCLA-128, compared to fixed dosing.

### Conclusions

This analysis demonstrated that the PK of MCLA-128 exhibits similar disposition characteristics as other therapeutic monoclonal antibodies and that a fixed dose of MCLA-128 in patients with various solid tumors would be appropriate.



## INTRODUCTION

MCLA-128 is a full-length humanized IgG1 bispecific monoclonal antibody with enhanced antibody-dependent cell-mediated cytotoxicity (ADCC). It targets the HER2 and HER3 transmembrane receptor tyrosine kinases. The mechanism of action is expected to rely on direct inhibition of tumor growth by blocking HER2:HER3 signaling and, via ADCC leading to elimination of tumor cells via recruitment of immune effector cells to tumor cells that have bound MCLA-128<sup>1</sup>. MCLA-128 is developed to overcome HER3-mediated resistance to epidermal growth factor receptor (EGFR) and HER2-targeted therapies in patients with HER2 overexpressing or amplified tumors. Current HER2-targeted therapies are approved for HER2-amplified breast and gastric cancers, either as single agent or in combination with other anticancer drugs.<sup>2,3</sup> A proportion of patients treated with these therapies, however, show primary or acquired resistance.<sup>4,5</sup> Resistance is often mediated by HER3 activation, either by upregulation of HER3 receptors in HER2-amplified tumors, or directly by the HER3 ligand, heregulin. Upregulation of HER3 in HER2-amplified tumors can result in ligand-independent dimerization of HER3 with HER2 and enhanced cell survival.<sup>6</sup> Alternatively, heregulin, drives dimerization of HER3 with HER2, resulting in potent activation of the PI3K/AKT pathway leading to enhanced growth and survival of HER2-amplified tumors. Heregulin stimulation was shown to mediate resistance to trastuzumab and lapatinib therapy.<sup>6-8</sup> The targeting of HER2 and HER3 by MCLA-128 could overcome this resistance. *In vitro* results have shown that MCLA-128 inhibits proliferation of HER2 over-expressing and HER2-low cells stimulated with heregulin. It also shows significantly higher potency than lapatinib, trastuzumab alone or to the combination of trastuzumab and pertuzumab.<sup>1</sup> *In vivo* MCLA-128 demonstrates potent anti-tumor activity in relevant xenograft models.<sup>9</sup> Previously, PK of MCLA-128 in cynomolgus monkeys was described by a two-compartment model with linear and non-linear clearance from the central compartment.<sup>9</sup>

The objectives of this analysis are to characterize the population pharmacokinetics (PK) of MCLA-128 in patients with various solid tumors included in a phase I/II trial, identify patient-related factors that potentially influence the disposition of

MCLA-128 and to evaluate whether fixed dosing of MCLA-128 would be appropriate. In addition, the appropriateness of animal-to-human PK scaling was evaluated for MCLA-128.

## MATERIAL AND METHODS

### Generation of MCLA-128

MCLA-128 was engineered using proprietary CH3 technology, and is composed of two identical common light chains and two different heavy chains (anti-HER2 and anti-HER3). ADCC-enhancement was achieved by low fucose glycoengineering using the GlymaxX® technology.<sup>1</sup>

### Data

This analysis was performed on data from patients in a phase I/II clinical trial (NCT02912949) of MCLA-128. The protocol was approved by the Ethics Committees of all participating centers and all patients provided written informed consent before study entry. Data was pooled from the dose-escalation and dose-expansion cohorts. Patients in the dose-escalation cohorts were treated with flat doses ranging between 40 mg and 900 mg MCLA-128, administered q3wk and patients in the dose-expansion cohort were treated with a flat dose of 750 mg MCLA-128, administered every 3 weeks. MCLA-128 was administered i.v. as a 1-hour (dose levels  $\leq$  360 mg) or 2-hour infusion (dose levels  $>$  360 mg). Patients with advanced solid tumors were included in the dose-escalation cohorts. Patients with selected advanced solid tumors (gastric, breast, endometrium esophagus-gastric junction, colon and non-small-cell lung carcinoma (NSCLC)) expressing HER2 or HER3 receptors, were included in the dose-expansion cohort.

For the assessment of MCLA-128 PK, samples were collected on day 1 of cycle 1 at pre-dose, end of infusion (EOI) and 1, 2, 4, 8 and 24 hours after EOI, any time on day 3 or 4, 8 and 15, and on day 1 of cycle 2, 3 and 4 at pre-dose and end of infusion. Samples were shipped frozen on dry ice and stored at  $-80^{\circ}\text{C}$  until analysis. MCLA-128 was quantified in serum using a validated electrochemiluminescence immunoassay, with a lower limit of quantification (LLOQ) of 0.05 mg/L.

## Population PK analysis

### *Structural model*

Nonlinear mixed-effects modeling was used for the population PK analysis. The preclinical modeling analysis in cynomolgus monkeys identified a two-compartment model with linear and nonlinear (Michaelis-Menten) clearance from the central compartment to describe PK data of MCLA-128 best.<sup>9</sup> Such model structures have been well established for the pharmacokinetics of other monoclonal antibodies as well.<sup>10</sup> Therefore, a two-compartment model was used as a starting point for the structural model building of the population PK analysis and the following parameters were estimated: linear clearance (CL), intercompartmental clearance (Q), volumes of distribution of the central and peripheral compartment ( $V_1$  and  $V_2$ , respectively), the maximum elimination rate of the nonlinear clearance ( $V_{max}$ ) and the Michaelis-Menten constant ( $K_m$ ). One- and two-compartment models with only linear clearance were also evaluated.

### *Statistical model*

Inter-individual variability (IIV) was evaluated for each of the PK parameters using an exponential model:

$$P_i = P_{pop} \cdot \exp(\eta_i)$$

Where  $P_i$  is the individual parameter estimate for individual  $i$ ,  $P_{pop}$  the population parameter and  $\eta_i$  the individual value of IIV for subject  $i$ , with  $\eta$  following a normal distribution  $N(0, \omega^2)$ . Off-diagonal elements of the variance-covariance matrix were evaluated to identify covariances between the individual random effects. Subsequently, correlations between the random effects were derived from the covariances. To account for the difference between observed MCLA-128 concentrations and model-predicted concentrations, a proportional and combined proportional and additive residual error model were. Data points below the LLOQ were imputed as LLOQ/2 (0.025 mg/L) and additive residual variability was fixed to this value.<sup>11</sup>

### Covariate analysis

Continuous (age, height, body weight, body surface area (BSA) and fat-free mass (FFM) at baseline) and categorical (tumor type and gender) covariates were evaluated for inclusion in the model. For continuous covariates, missing values were imputed by the median value. Body weight, BSA and FFM were independently tested for their effect on  $C_L$ ,  $V_1$  and  $V_{max}$ . BSA and FFM were calculated using the following equations<sup>12</sup>:

$$BSA = \sqrt{\frac{WT \cdot HT}{3600}}$$

$$BMI = \frac{WT}{\frac{HT}{100}^2}$$

$$FFM_{men} = \frac{9.27 \cdot 10^3 \cdot WT}{6.68 \cdot 10^3 + 216 \cdot BMI}$$

$$FFM_{women} = \frac{9.27 \cdot 10^3 \cdot WT}{8.87 \cdot 10^3 + 244 \cdot BMI}$$

Where WT is body weight in kilograms, HT is height in centimeters and BMI is body mass index.

Additionally, the magnitude of target expression (HER2 and/or HER3) is expected to affect the capacity of target-mediated clearance. Therefore, tumor type was evaluated as a covariate on  $V_{max}$ . Age and gender were evaluated on CL and  $V_1$ . Since body size measures are influenced by gender, gender was only evaluated with body size covariates already included in the model. Continuous covariates were implemented using the following equation:

$$P_i = P_{pop} \cdot \frac{COV}{Median(COV)}^{\theta_{cov}}$$

Where  $P_i$  is the individual parameter,  $P_{pop}$  the population parameter,  $\theta_{cov}$  is the covariate effect parameter, COV the continuous covariate value. The dichotomous covariate (gender) was implemented as follows:

$$P_i = P_{pop} \cdot (\theta_{cov})^{GENDER}$$

Where  $\theta_{cov}$  represents the fractional change in population parameter for female (1) compared to man (0). Tumor type was evaluated as categorical covariate by estimating a separate parameter for each type, for all the tumor types that affected at least 5% of patients. The selected covariates were evaluated using a forward inclusion and backward elimination method. For forward inclusion, a significance level of  $p < 0.01$  was used, corresponding to a decrease of objective function value (OFV) of  $> 6.63$ . A significance level of  $p < .005$  was set for backward elimination, corresponding to an increase of OFV of  $> 7.88$ .

#### *Model evaluations*

Models were evaluated based on general goodness-of-fit (GOF) plots, mechanistic plausibility, stability and precision of parameter estimates and change in OFV where  $p < 0.01$  was considered significant (OFV drop of  $> 6.63$ , with 1 degree of freedom). In addition, visual predictive checks (VPCs) were performed to evaluate the performance of the model. Parameter uncertainty was obtained from the default covariance step in NONMEM and from the sampling importance resampling (SIR) method.<sup>13</sup>

#### *Software*

Nonlinear mixed-effects modeling was performed using NONMEM (version 7.3.0, ICON Development Solutions, Ellicott City, MD, USA) and Perl-speaks-NONMEM (version 4.4.8).<sup>14,15</sup> All models were estimated using the First-Order Conditional Estimation method with  $\eta$ - $\epsilon$  interaction (FOCE-I). Pirana (version 2.9.2) was used as graphical user interface.<sup>16</sup> Data handling, graphical evaluation and simulations were performed using R (version 3.3.1).<sup>17</sup>

## Simulations

In order to evaluate whether flat dosing of MCLA-128 is appropriate for this patient population, simulations were performed. First, the combinations of body weight, height and gender values for the simulation dataset were randomly sampled (with replacement) from the original dataset, with even proportions of male and female subjects. The combinations of weight, height and gender values were sampled as fixed combinations, to preclude sampling of irrational weight, height and gender combinations. Subsequently, concentration-time profiles of MCLA-128 were simulated for patients receiving 750 mg flat dose, 420 mg/m<sup>2</sup> and 11 mg/kg MCLA-128 administered once every 3 weeks in an IV infusion of 2 hours, using the final model. The weight-based dosages were rounded and chosen such that the median BSA and weight in the study population (1.78 m<sup>2</sup> and 68.2 kg) corresponded to a flat-dose of 750 mg. Each simulation dataset consisted of 3000 patients (n=1000 per group). The AUC<sub>0-t</sub>, maximum concentration (C<sub>max</sub>), average concentration (C<sub>ave</sub>) and trough concentrations (C<sub>trough</sub>) on day 21 were assessed and compared between the flat, BSA-based and weight-based dosing groups. Negative simulated concentrations were fixed to 0.001 mg/L.

Additional simulations were performed to evaluate the translational and predictive performance of the previously developed preclinical PK model, that was based on data from cynomolgus monkeys and for this purpose allometrically scaled to human.<sup>9</sup> A VPC was performed using the original clinical dataset including only observations and dose records of patients that received 750 mg flat dose MCLA-128.

## RESULTS

### Data

Pharmacokinetic data was available for 116 patients. Of these 116 patients, 93 patients received a dose of 750 mg q3wk. The remaining patients received 40 mg (n=1), 80 mg (n=2), 160 mg (n=1), 240, 360, 480 mg (each n=3), 600 mg (n=7) and 900 mg (n=3) MCLA-128. In total, 1115 observations, with median [range] of 10 [1-10] observations per patient, were included in the analysis. Overall, 22 of the

1115 observations (2%) were below the LLOQ and fixed to a value of 0.025 mg/L (LLOQ/2). Patient demographics are depicted in Table 1. Height was missing for one female patient with a relative high weight and one male patient with a relative low weight, therefore the median height of the population (164 cm) was imputed.

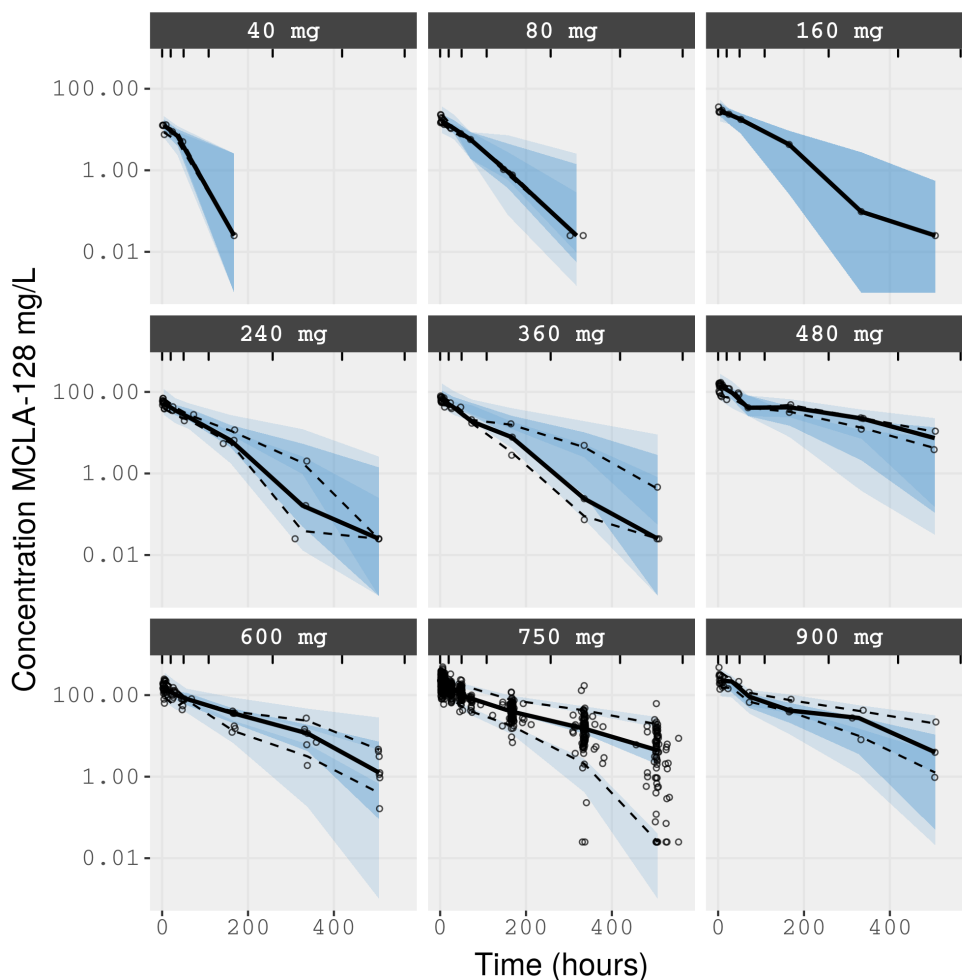


**Figure 1** Visual Predictive Check (VPC) for MCLA-128 concentrations plotted on a log-scale, stratified on dose. Open circles are observed MCLA-128 concentrations in the first cycle of patients receiving MCLA-128 every 3 weeks, the solid line represents the median of the observed data, the dashed lines represent the 5th and 95th percentiles of the observed data, the shaded areas represent the 95% confidence interval of the simulated data for the corresponding percentiles (n=500).

**Table 1 Patient demographics and characteristics of patients included in the analysis at study entry.**

N = 116	
MEDIAN [RANGE]	
Age (years)	59 [25-83]
Weight (kg)	68.2 [40.2-112]
Height (cm)	164 [147-199]
BSA (m <sup>2</sup> )	1.78 [1.30-2.33]
FFM (kg)	43.1 [28.6-72.45]
<b>Number of patients (%)</b>	
<b>Gender</b>	
Female	76 (65.5)
Male	40 (34.5)
<b>Tumor type</b>	
Breast	17 (14.7)
Colorectal	9 (7.8)
Endometrium	13 (11.2)
Gastric	25 (21.5)
Lung	8 (6.9)
Ovarian	36 (31)
Others	8 (6.9)

BSA = Body Surface Area, FFM = Fat Free Mass<sup>12</sup>

### PK model

A two-compartment model with parallel linear and nonlinear clearances from the central compartment described the data best (adding a second compartment to a one-compartment model with linear clearance decreased OFV with 4059 points and adding nonlinear clearance to a two-compartment model with linear clearance decreased the OFV with 384 points). The nonlinear clearance was described using Michaelis-Menten kinetics. The final model structure was defined by the following differential equations:



$$\frac{d(A_1)}{d(t)} = -\frac{CL}{V_1} \cdot A_1 - \frac{V_{max} \cdot C_1}{K_m + C_1} - \frac{Q}{V_1} \cdot A_1 + \frac{Q}{V_2} \cdot A_2 \quad (1)$$

$$\frac{d(A_2)}{d(t)} = \frac{Q}{V_1} \cdot A_1 - \frac{Q}{V_2} \cdot A_2 \quad (2)$$

Where CL represents the linear clearance, Q the intercompartmental clearance,  $V_1$  the volume of distribution in the central compartment and  $V_2$  the volume of distribution in the effect compartment,  $A_1$  the amount of drug in the central compartment,  $V_{max}$  the maximum elimination rate,  $C_1$  the drug concentration in the central compartment,  $K_m$  the drug concentration at which half the drug-targets are occupied and  $A_2$  the amount in the peripheral compartment. A combined proportional and additive residual error model described residual variability best. Body size parameters body weight, BSA and FFM were all, univariately, identified as significant covariates affecting CL and  $V_1$ , where FFM provided the best model fit and led to an objective function value (OFV) drop of 131. FFM explained 8.4% of IIV in CL and 5.6% of IIV in  $V_1$ . After implementation of gender-specific FFM in the model, gender had no significant additional impact on the PK parameters of MCLA-128. Observed gender differences in concentration-time curves were thus explained by the gender-specific differences in FFM (median of 58.7 kg FFM in men vs. 39.8 kg FFM in women). In addition, age and the different tumor types had no significant effect on the PK of MCLA-128. The parameter estimates of the final model are depicted in Table 2. The 95% confidence intervals of the SIR indicated that parameter estimates were precise. In addition, the VPC, stratified on the different dose-groups demonstrated good model fit across the dose range evaluated (Figure 1).

**Table 2** Model parameters and evaluation of parameter uncertainty using sampling importance resampling (SIR).

Parameter	BASE MODEL	COVARIATE MODEL	SIR RESULTS
	OFV 7575	OFV 7444	
	Estimates (RSE%) [shrinkage%]	Estimates (RSE%) [shrinkage%]	[95%CI]
CL (L/h)	0.0322 (4)	0.0303 (4)	[0.0287-0.0321]
$V_1$ (L)	3.66 (2)	3.52 (2)	[3.38-3.66]
Q (L/h)	0.0256 (10)	0.0253 (8)	[0.0212-0.0297]
$V_2$ (L)	1.69 (7)	1.65 (6)	[1.43-1.86]
$V_{max}$ (mg/h)	0.122 (11)	0.117 (15)	[0.0859-0.152]
$K_m$ (mg/L)	0.26 (31)	0.205 (26)	[0.119-0.326]
FFM on CL	-	1.20 (14)	[0.934-1.46]
FFM on $V_1$	-	0.71 (14)	[0.531-0.878]
<b>Between-subject variability</b>			
$\omega_{CL}$ (CV%)	46.9 (10) [2]	38.5 (7) [3]	[33.7-43.9]
$\omega_{V1}$ (CV%)	26.6 (6) [4]	21.0 (8) [6]	[18.2-24.1]
$\omega_{Vmax}$ (CV%)	66.9 (16) [28]	67.8 (14) [28]	[53.4-84.6]
Correlation $\omega_{CL} \sim \omega_{V1}^a$	0.70	0.54 (11)	[0.47-0.60]
<b>Residual unexplained variability</b>			
Prop.error (CV%)	18.9 (7)	18.6 (3)	[17.8-19.6]
Add error (SD mg/L)	0.025 fixed	0.025 fixed	-

OFV = Objective function value, CL = linear clearance,  $V_1$  = volume of distribution central compartment, Q = intercompartmental clearance,  $V_2$  = volume of distribution peripheral compartment,  $V_{max}$  = maximum non-linear clearance capacity,  $K_m$  = Michaelis Menten constant, concentration at which 50% of the target is occupied, FFM = fat free mass, RSE = relative standard error, CV = coefficient of variation, Prop. = proportional, add = additive, SD = standard deviation, CI = confidence interval, SIR = sampling importance resampling.

## Simulations

Simulations of the final model with flat, body weight-based and BSA-based doses demonstrated comparable values of  $AUC_{0-t}$ ,  $C_{max}$ ,  $C_{ave}$  and  $C_{trough}$  concentrations, with differences in geometric means below 5% and comparable coefficients of variation (Table 3 and Figure 2). This indicates that weight or BSA-based dosing does not lower variability in exposure between patients, compared to flat dosing of MCLA-128.

Moreover, the effect of body size parameters on CL and  $V_1$  on exposure parameters is minimal. In addition, the percentage of patients with trough concentrations below the estimated  $K_m$  value (0.205 mg/L) is similar between the different dosing strategies, around 20% (Table 3). Approximately 3% of the simulated concentrations were below zero and fixed to 0.001 mg/L.

**Table 3 Comparison of exposure variables between different dosing strategies (n=1000 / dosing group).**

	750 MG gMEAN (CV%)	420 MG/M <sup>2</sup> gMEAN (CV%)	11 MG/KG gMEAN (CV%)	% dgM FLAT VS. BSA	% dgM FLAT VS. WT
$C_{trough}$ (mg/L)	1.22 (138)	1.26 (131)	1.28 (129)	3.28	4.92
$C_{ave}$ (mg/L)	37.2 (43)	37.8 (37)	38.1 (37)	1.61	2.42
$C_{max}$ (mg/L)	222.5 (30)	225.9 (25)	228.1 (27)	1.53	2.52
$AUC_{0-t}$ (mg.hr/mL)	18.8 (43)	19.1 (37)	19.2 (37)	1.60	2.13
$\% C_{trough} < K_m^*$	21.4%	20.2%	20.6%		

\*Percentage of patients with trough concentrations below the  $K_m$  value of 0.205 mg/L, gMean = geometric mean, CV = coefficient of variation, dgM = difference in geometric mean. Flat vs. BSA = flat dosing versus BSA-based dosing, Flat vs. WT flat = dosing versus weight-based dosing.

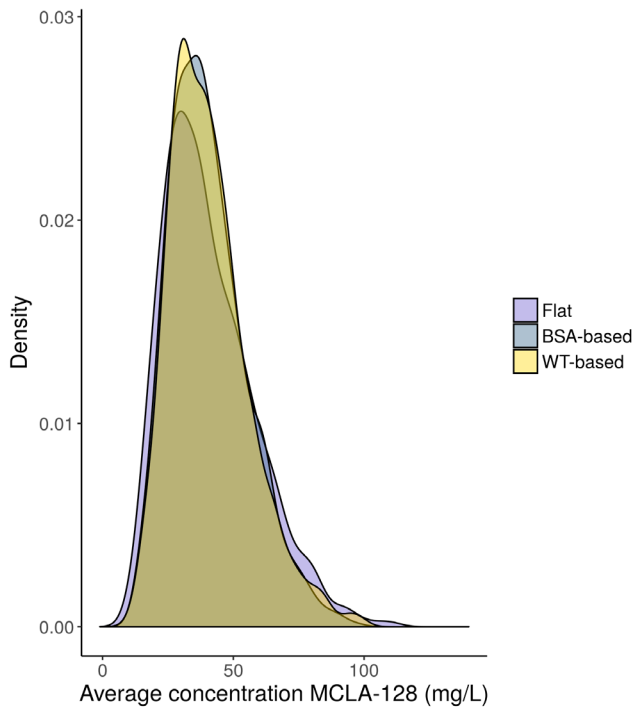


**Figure 2** Distribution of simulated MCLA-128 average concentration ( $C_{ave}$ ) for flat dosing (750 mg), BSA-based dosing (420 mg/m<sup>2</sup>) and WT-based dosing (11 mg/kg) with n=1000 per dosing strategy. BSA = body surface area, WT = body weight.

The simulations performed with the preclinical PK model, scaled from cynomolgus monkeys to human, were compared to the observed PK data in a VPC (Figure 3, left panel). Predictions based on the preclinical model were slightly higher than observed MCLA-128 concentrations, where at the lower concentrations high variability was observed, while observations appeared to be slightly overpredicted. In the clinical PK model IIV on  $V_{max}$  was included, to account for the differences in HER2 expression between patients. Including IIV on  $V_{max}$  in the preclinical model, showed a better prediction of the lower concentrations observed in patients with HER2 expressing tumors. (Figure 3, right panel).

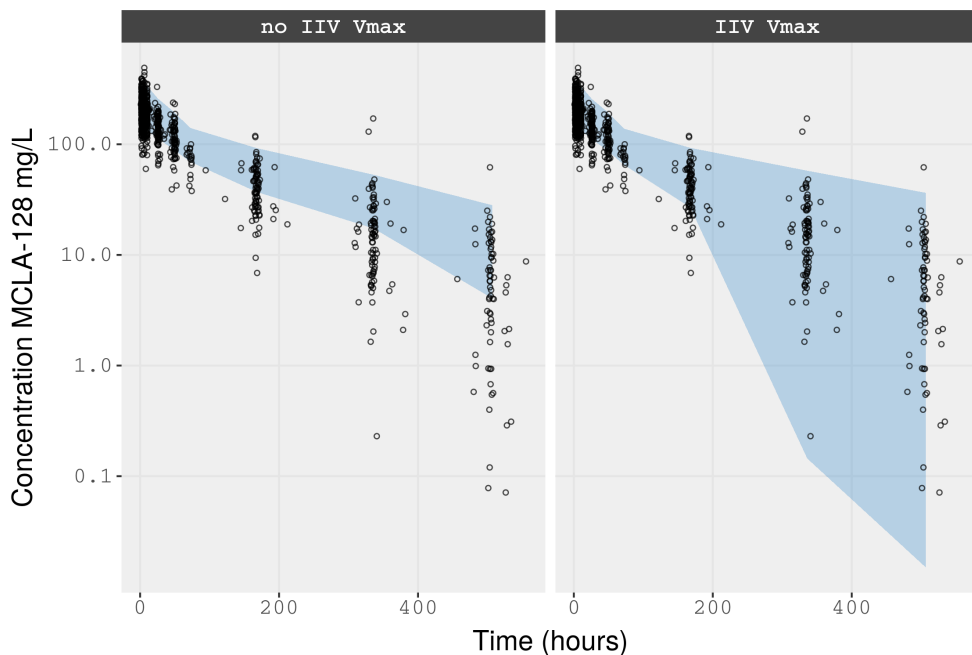


**Figure 3** Visual Predictive Check for MCLA-128 concentrations over time. Shaded blue area is the 95% prediction interval of simulated concentrations (n=1000) using the preclinical pharmacokinetic model (left panel) and the preclinical pharmacokinetic model with inter-individual variability on  $V_{max}$  (right panel), patients received a dose regimen of 750 mg MCLA-128 flat dose administered every 3 weeks; open circles are observed MCLA-128 concentrations in the first cycle of patients participating in the 750 mg cohort of the clinical trial.

## DISCUSSION

The pharmacokinetics of MCLA-128 were best described by a two-compartment model with parallel linear and nonlinear clearance from the central compartment. The estimated PK parameters of the final model were in accordance with the general pharmacokinetic characteristics of therapeutic monoclonal antibodies as previously described.<sup>10,18</sup>

The following median (range) values were reported for monoclonal antibodies: 3.1 L (2.4-5.5) and 2.8 L (1.3-6.8) for  $V_1$  and  $V_2$ , respectively, and 0.013 L/h (0.003-0.223) for CL. Estimations for  $V_{\max}$  and  $K_m$  varied widely among different monoclonal antibodies, with  $V_{\max}$  values ranging from 0.004 to 4.38 mg/h and  $K_m$  values between 0.033 and 74 mg/L.<sup>10</sup> The Michaelis-Menten estimates for MCLA-128 were within this wide range. The estimate of  $K_m$  (0.205 mg/L) is also comparable to the dissociation constants for HER2 and HER3, 0.467 mg/L and 0.292 mg/L, respectively.<sup>19</sup> These findings confirm the plausibility of the parameter estimates.

The different tumor types, gender and age were not identified to significantly impact the disposition of MCLA-128. Body size measurements (body weight, BSA and FFM) affected linear CL and  $V_1$ , where inclusion of FFM led to the best model fit. From a physiological point of view, FFM is also expected to be more closely related to the distribution and linear elimination of monoclonal antibodies than total body weight. Distribution of monoclonal antibodies is mainly limited to blood plasma and extracellular fluids, due to their size and hydrophilic character. It has been demonstrated that blood volume correlates better with FFM or lean body weight, than with total body weight, since blood volume does not proportionally increase with body weight.<sup>20</sup> Monoclonal antibodies are metabolized via proteolytic catabolism and intracellular degradation after binding to the target. Proteolytic catabolism is mediated via the FcRn receptor and is a linear process at therapeutic concentrations of monoclonal antibodies.<sup>18,21</sup> Proteolytic catabolism of IgG antibodies takes place in the skin, muscle, liver and gut tissue<sup>18</sup> and is thus expected to be more closely related to FFM than measures relying on total body weight and size. In the final model, FFM explained 8.4% and 5.6% of between-subject variability in CL and  $V_1$ , respectively, indicating rather limited clinical relevance of FFM on CL and  $V_1$ . The estimated effect of FFM on CL and  $V_1$  was relatively high, with exponents of 1.2 and 0.8, respectively. Simulations demonstrated that exposure measures ( $AUC_{0-T}$ ,  $C_{\max}$ ,  $C_{\text{ave}}$  and  $C_{\text{trough}}$ ) and variability in exposure measures were comparable between flat dosing and body-size-based dosing strategies. In addition, the proportion of patients with a  $C_{\text{trough}}$  below the  $K_m$  value was around 20% for all dosing strategies, indicating that target attainment is similar between dosing strategies. Therefore, there appears no rationale for body-size-based dosing over flat dosing of MCLA-128, which is in agreement with the findings for other therapeutic monoclonal antibodies in oncology.<sup>22</sup>

The observed concentration-time data of the patients in the clinical trial was used to evaluate the predictive value of the preclinical model.<sup>9</sup> The preclinical model slightly overpredicted the observed concentrations of MCLA-128 in patients receiving 750 mg q3wk. The preclinical model was based on data from healthy cynomolgus monkeys and was allometrically scaled to human. These healthy cynomolgus monkeys expressed endogenous HER2. Patients were included in the trial based on HER2 expression on their tumors, and are expected to have a greater nonlinear CL capacity, potentially leading to lower concentrations of MCLA-128 in human, typically seen at lower concentrations. Though the estimate of  $V_{\max}$  in the preclinical model was higher compared to the clinical model (0.500 mg/h vs 0.117 mg/h), the variability in the clinical  $V_{\max}$  was much higher. Including this variability in the preclinical model, demonstrated that the overprediction of observed MCLA-128 concentrations can be attributed to variability in target expression between patients included in the trial. To extrapolate the preclinical model, the preclinical CL, Q,  $V_{\max}$ ,  $V_1$  and  $V_2$  parameters were allometrically scaled using a fixed exponent value of 0.75 for CL, Q and  $V_{\max}$  and a value of 1 for  $V_1$  and  $V_2$ . These exponents were fixed, since the weight-range of the cynomolgus monkeys was narrow and did not allow for appropriate estimation of the exponent value, this might also have contributed to the slight discrepancy between the predicted MCLA-128 concentrations from preclinical data and the observed concentration in the clinical trial. However, this post-hoc evaluation of the preclinical model showed that very reasonable and useful estimates of human exposure can be obtained from cynomolgous monkey data to support initial dose selection for these type of monoclonal antibodies.

Data on the generation of anti-drug antibodies (ADAs) was not available at the time of analysis and, therefore, not accounted for in the analysis. However, it can be expected that excluding the formation of ADA from the model did not affect our results, since only PK data of the first treatment cycle was included in the analysis.

In conclusion, a PK model was developed that adequately described the PK characteristics of MCLA-128 over a range of doses. FFM was found to significantly affect CL and  $V_1$  and explained part of the IIV in these parameters.

However, simulations demonstrated that the impact of body size parameters on the disposition of MCLA-128 was minimal and that flat dosing of MCLA-128 is appropriate for patients with solid tumors. It contributes to the existing evidence that flat dosing is to be preferred for anticancer monoclonal antibodies.



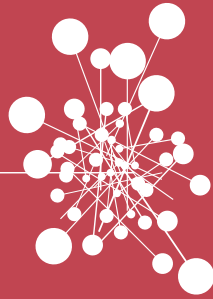
## REFERENCES

1. Geuijen, C., Rovers, E., Nijhuis, R. & Visser, T. Preclinical activity of MCLA-128, an ADCC enhanced bispecific IgG1 antibody targeting the HER2:HER3 heterodimer. *J. Clin. Oncol.* 32, (suppl; abstr 560) (2014).
2. Arteaga, C. et al. Treatment of HER2-positive breast cancer: current status and future perspectives. *Nat. Rev. Clin. Oncol.* 9, 16-32 (2011).
3. Baselga, J., Cortes, J., Kim, S., Im, S. & Hegg, R. Pertuzumab plus Trastuzumab plus Docetaxel for Metastatic Breast Cancer. *N. Engl. J. Med.* 366, 109-119 (2012).
4. Pohlmann, P. R., Mayer, I. a & Mernaugh, R. Resistance to Trastuzumab in Breast Cancer Resistance to Trastuzumab in Breast Cancer. *Clin. Cancer Res.* 15, 7479-7491 (2009).
5. Wong, A. L. a. & Lee, S.-C. Mechanisms of Resistance to Trastuzumab and Novel Therapeutic Strategies in HER2-Positive Breast Cancer. *Int. J. Breast Cancer* 2012, 1-13 (2012).
6. Sergina, N. V et al. Escape from HER-family tyrosine kinase inhibitor therapy by the kinase-inactive HER3. *Nature* 445, 437-441 (2007).
7. Wilson, T. R. et al. Widespread potential for growth-factor-driven resistance to anticancer kinase inhibitors. *Nature* 487, 505-509 (2012).
8. Garrett, J. T. et al. Transcriptional and posttranslational up-regulation of HER3 (ErbB3) compensates for inhibition of the HER2 tyrosine kinase. *Proc. Natl. Acad. Sci. U. S. A.* 108, 5021-6 (2011).
9. de Vries Schultink, A.H.M. et al. Translational PK-PD modeling analysis of MCLA-128, a HER2/HER3 bispecific monoclonal antibody, to predict clinical efficacious exposure and dose. *Invest. New Drugs* 36, 1006-1015 (2018).
10. Dirks, N. L. & Meibohm, B. Population pharmacokinetics of therapeutic monoclonal antibodies. *Clin. Pharmacokinet.* 49, 633-59 (2010).
11. Beal, S. L. Ways to fit a PK model with some data below the quantification limit. *J. Pharmacokinet. Pharmacodyn.* 28, 481-504 (2001).
12. Janmahasatian, S. et al. Quantification of Lean Bodyweight. *Clin. Pharmacokinet.* 44, 1051-1065 (2005).

13. Dosne, A. G., Bergstrand, M., Harling, K. & Karlsson, M. O. Improving the estimation of parameter uncertainty distributions in nonlinear mixed effects models using sampling importance resampling. *J. Pharmacokinet. Pharmacodyn.* 43, 583–596 (2016).
14. Beal, S., Sheiner, L., Boeckmann, A. & Bauer, R. NONMEM 7.3.0 Users Guides. (1989–2013). ICON Development Solutions, Hanover, MD.
15. Lindbom, L., Ribbing, J. & Jonsson, E. N. Perl-speaks-NONMEM (PsN) - A Perl module for NONMEM related programming. *Comput. Methods Programs Biomed.* 75, 85–94 (2004).
16. Keizer, R. J., Karlsson, M. O. & Hooker, A. Modeling and Simulation Workbench for NONMEM: Tutorial on Pirana, PsN, and Xpose. *CPT pharmacometrics Syst. Pharmacol.* 2, e50 (2013).
17. R Core Team, 2018 R: A language and Environment for Statistical Computing. R Foundation for statistical computing, Vienna, Austria. at <<https://www.r-project.org/>>
18. Keizer, R. J., Huitema, A. D. R., Schellens, J. H. M. & Beijnen, J. H. Clinical pharmacokinetics of therapeutic monoclonal antibodies. *Clin. Pharmacokinet.* 49, 493–507 (2010).
19. Geuijen, C. A. W. et al. Unbiased Combinatorial Screening Identifies a Bispecific IgG1 that Potently Inhibits HER3 Signaling via HER2-Guided Ligand Blockade. *Cancer Cell* 33, 922–935 (2018).
20. Boer, P. Estimated lean body mass as an index for normalization of body fluid volumes in humans. *Am. J. Physiol.* 247, F632–6 (1984).
21. Mould, D. & Green, B. Pharmacokinetics and Pharmacodynamics of Monoclonal Antibodies. *Biodrugs* 24, 23–39 (2010).
22. Hendriks, J. J. M. A. et al. Fixed Dosing of Monoclonal Antibodies in Oncology. *Oncologist* 22, 1212–1221 (2017).







# CHAPTER 3

PHARMACOKINETICS AND  
PHARMACODYNAMICS: TOXICITY



## CHAPTER 3.1

### Pharmacodynamic modeling of adverse effects of anti-cancer drug treatment

*Eur J Clin Pharmacol* 2016 Jun; 72(6):645-653

A.H.M. de Vries Schultink  
A.A. Suleiman  
J.H.M. Schellens  
J.H. Beijnen  
A.D.R. Huitema

## **ABSTRACT**

### **Purpose**

Adverse effects related to anti-cancer drug treatment influence patients quality of life, have an impact on the realized dosing regimen and can hamper response to treatment. Quantitative models that relate drug exposure to the dynamics of adverse effects have been developed and proved to be very instrumental to optimize dosing schedules. The aims of this review were (i) to provide a perspective of how adverse effects of anti-cancer drugs are modeled and (ii), to report several model structures of adverse effect models that describe relationships between drug concentrations and toxicities.

### **Methods**

Various quantitative pharmacodynamic models that model adverse effects of anti-cancer drug treatment were reviewed.

### **Results**

Quantitative models describing relationships between drug exposure and myelosuppression, cardiotoxicity and graded adverse effects like fatigue, hand food syndrome (HFS), rash and diarrhea have been presented for different anti-cancer agents, including their clinical applicability.

### **Conclusions**

Mathematical modeling of adverse effects proved to be a helpful tool to improve clinical management and support decision-making (especially in establishment of the optimal dosing regimen) in drug development. The reported models can be used as templates for modeling a variety of anti-cancer induced adverse effects to further optimize therapy.



## INTRODUCTION

Adverse effects are a major problem in the treatment with both cytotoxic drugs and newer targeted therapies, resulting in dose reductions, dose delays and treatment cessation. Toxicity can impair quality of life, jeopardize treatment adherence and necessitate dose reductions and dose delays, which can negatively affect response to treatment and outcome.<sup>1,2</sup> The tendency in cytotoxic anti-cancer drug treatment is to dose drugs around the maximum tolerated dose (MTD), which assumes that the highest possible dose achieves the maximum effect.<sup>3</sup> Adverse effects are, therefore, frequently observed during treatment with cytotoxic drugs. Targeted therapies are expected to have less toxicity, mainly because of two reasons: (i) these therapies are specific to a tumor-target and induce less off target toxicity, and (ii) targeted therapies might have maximum target inhibition at lower concentrations than the MTD. The latter has led to the suggestion that targeted therapies should be dosed around the optimal biological dose (where target saturation is maximal) rather than the MTD. However, definition of the optimal biological dose is hampered by the lack of validated biomarkers for efficacy, lack of information on the relation between target binding and survival measures and yet information on the highest possible dose remains of value.<sup>4</sup> As a consequence, targeted therapies are still often dosed around the MTD.<sup>2</sup>

Adverse effects related to cancer therapy are typically graded by the National Cancer Institute's Common Terminology Criteria for Adverse Events (NCI-CTC-AE). A conventional and common approach to analyze toxicity data, is to calculate the proportion of patients that experienced a certain (severe) grade of toxicity.<sup>5</sup> Subsequently, these proportions can be statistically related to dosing groups, area under the plasma concentration-time curve (AUC) or other summary variables for exposure.<sup>6</sup> However, it is essential to have information on the dynamic relation between exposure and toxicity, which provides information on when the toxicity occurs, what the severity is over time and if or when the adverse effect is reversed. For this purpose, quantitative models are becoming increasingly important. These models describe the time course of toxicities related to exposure, as will be described throughout this review.

Since modeling adverse effects is becoming increasingly important in anti-cancer drug treatment and drug development, an overview of existing modeling approaches can be helpful for future research. Therefore, the aim of this review is to give a perspective of modeling adverse effects of anti-cancer drugs and report several model structures that describe relationships between drug concentrations and toxicities, thereby focusing on the fixed effects of nonlinear mixed effects models.

## **MODELING ADVERSE EFFECTS**

### **Myelosuppression**

Myelosuppression is the leading dose limiting toxicity in treatment with cytotoxic agents. Hematological toxicity consists of low leukocyte, thrombocyte and platelet counts, potentially leading to life-threatening infections, anemia and bleeding. Neutropenia, a subtype of leucopenia, is the most common and serious hematologic toxicity observed during treatment with cytotoxic anti-cancer drugs.<sup>7</sup> Myelosuppression can necessitate dose reductions and dose delays, potentially resulting in suboptimal drug exposure. Early approaches to describe hematological toxicity aimed at finding correlations between summary variables of exposure and summary variables of myelosuppression, not taking into account the complete time course of either drug concentration or myelosuppression. Survival fraction of blood cells or percentage change in blood count were typically used as summary variables for myelosuppression, whereas average drug concentration, AUC or peak drug concentration were used to summarize exposure.<sup>8-10</sup> These models have major limitations such as poor predictive value and lack of description of the dynamics of toxicity.

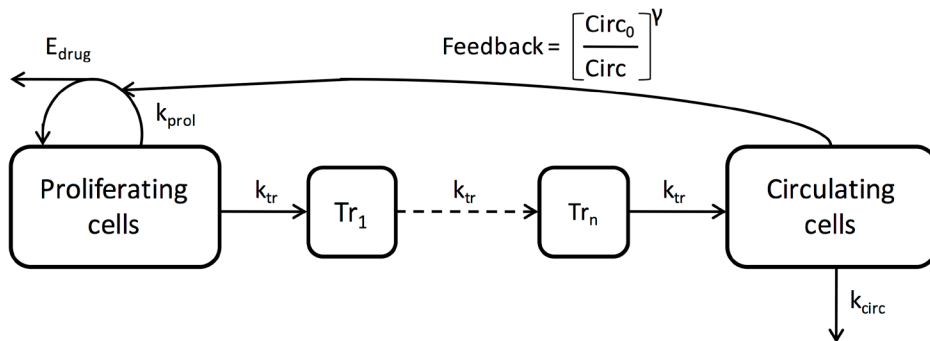


**Figure 1** General model structure for myelosuppression.  $E_{\text{drug}}$  drug effect,  $k_{\text{tr}}$  maturation rate constant,  $k_{\text{prol}}$  proliferation rate constant,  $k_{\text{circ}}$  degradation rate constant  $Tr_n$  transition compartment,  $\text{Circ}_0$  circulating cells at baseline,  $\text{Circ}$  amount of circulating cells,  $\gamma$  factor for impact of feedback.

### Empirical models

The first models describing the complete time-course of myelosuppression were empirical models. One model described the time course of leucopenia in patients treated with etoposide, and used a lag-time to account for the delay in the myelosuppressive effect, and a cubic spline function, which represented the deviation of white blood cell (WBC) count from baseline.<sup>11</sup> An  $E_{\text{max}}$  model described the decline in WBC count from baseline, which was dependent on the effective concentration of etoposide. A similar empirical model was published for paclitaxel induced leucopenia.<sup>12</sup>

### Semi-mechanistic models

Currently, a more mechanistic modeling approach is used. Mechanistic models mimic the physiological processes of haematopoiesis. Generally, this improves the predictive value of the model, since the mechanism related parameters represent actual physiological processes. Haematopoiesis is characterized by proliferation of progenitor cells in the bone marrow, followed by maturation and degradation of blood cells.<sup>13</sup> To make useful models for pharmacokinetic and pharmacodynamic (PK-PD) analysis, several simplified semi-mechanistic

models have been developed (Table 1).<sup>14-19</sup> These semi-mechanistic models are all characterized by a proliferation cell compartment or progenitor compartment containing cells that have self-renewing capacity and a compartment representing circulating cells. In order to account for the maturation process, that delays the effect of the drug, either lag-time or one to multiple transit compartments are added to the model structure. In some of the semi-mechanistic models a feedback loop is incorporated to describe the rebound of blood cells, exceeding the blood count at baseline, which occurs when drug concentrations decrease. Typically, this feedback effect is driven by the amount of circulating blood cells, which affect the rate of proliferation in the progenitor compartment. Drug effects were modeled to affect the proliferation rate or the amount of progenitor cells. Model characteristics of five published semi-mechanistic models are summarized in Table 1. A general model structure for myelosuppression is depicted in Figure 1.

The first semi-mechanistic model developed used a two compartment indirect response model to describe the time course of leucopenia in paclitaxel and etoposide treated patients<sup>14</sup>. The drug inhibited the proliferating cells only during a sensitive stage. This model is the only model that used lag time to mimicking the maturation process instead of using transit compartments.

In 2000 Friberg et al. published a semi-mechanistic model, modelling the absolute neutrophil counts (ANC) in 2'-deoxy-2'-methylidenecytidine (DMDC) treated patients.<sup>15</sup> This model contained three additional proliferating compartments and five non-mitotic compartments. The first order elimination from the first progenitor compartment was proportional to the DMDC concentration. A fraction of the effect of DMDC on the first progenitor compartment was added to the other proliferating compartments. The non-mitotic compartments were not affected by DMDC concentration. Cytotoxic anti-cancer drugs only affect proliferating cells, therefore this is a more elegant way of incorporating the maturation chain and the delay in drug effect as compared to using lag time.

Table 1 Semi mechanistic models describing blood count over time.

REFERENCE	DRUG	OBSERVED VARIABLE	PAR <sup>A</sup>	TR <sup>B</sup>	KPROL <sup>C</sup>	DRUG EFFECT	
Minami 1998	[14]	Paclitaxel	WBC	4	Lag time	Zero order	E <sub>max</sub>
Friberg 2000	[15]	DMDC	ANC	7	9	Zero order	E <sub>max</sub>
Zamboni 2001	[16]	Topotecan	ANC	4	1	Zero order	E <sub>max</sub>
Friberg 2002	[17]	Docetaxel Etoposide Paclitaxel	ANC WBC	5	3	First order	Linear
Panetta 2003	[18]	TMZ	ANC	5	2	First order	E <sub>max</sub>
Bulitta 2009	[19]	Paclitaxel Paclitaxel EL	ANC	5	1 <sup>D</sup>	Zero order	Linear

WBC = white blood cell count, ANC = absolute neutrophil count, TMZ = temozolomide

<sup>A</sup> Number of parameters estimated in pharmacodynamic model

<sup>B</sup> Number of transit compartments or if lag time is used

<sup>C</sup> Proliferation rate constant;

<sup>D</sup> Maturing pool of cells.

The most well-known semi-mechanistic model for myelosuppression by Friberg et al. published in 2002, is often referred to as the golden standard for modeling the time-course of myelosuppression.<sup>17</sup> Development was based on data from docetaxel, etoposide and paclitaxel treated patients in whom ANC and WBC was measured. The model structure is described by the following equations:

$$\frac{dProl}{dt} = k_{in} \cdot P_{cells} \cdot (1 - E_{drug}) \cdot \frac{Circ_0}{Circ}^\gamma - k_{tr} \cdot P_{cells}$$

$$\frac{dTransit1}{dt} = k_{tr} \cdot P_{cells} - k_{tr} \cdot Transit1$$

$$\frac{dTransit2}{dt} = k_{tr} \cdot Transit1 - k_{tr} \cdot Transit2$$

$$\frac{dTransit3}{dt} = k_{tr} \cdot Transit2 - k_{tr} \cdot Transit3$$

$$\frac{dCirc}{dt} = k_{tr} \cdot Transit3 - k_{circ} \cdot Circ$$

Where  $k_{in}$  represents the first-order proliferation input,  $P_{cells}$  the amount of cells in the proliferation compartment and  $E_{drug}$  the drug effect. The feedback mechanism was described by  $(Circ_0/Circ)^\gamma$ . Where  $Circ_0$  was the ANC or WBC blood count at baseline,  $Circ$  the amount of circulating blood cells and  $\gamma$  the parameter estimate to determine the impact of the feedback. Transit1-3 represent the amount of cells in the transit compartments and  $k_{tr}$  the rate constant between compartments. Degradation of circulating cells is described by the rate constant  $k_{circ}$ . The first-order proliferation input is different from previously described models, which used a zero-order rate constant of proliferation. It was assumed that the proliferation, maturation and degradation rate constants were equal. Therefore, only three system-related parameters were estimated. An analysis was conducted to evaluate the consistency of the system-related parameters, by fixing them and re-estimating the drug-related parameters. The drug-related parameter estimates were comparable. Additionally, the system-related parameter estimates were similar for different drugs, enabling interchangeability of the model between drugs. In 2003 a model with similar characteristics was published.<sup>18</sup>

The most recent model for myelosuppression is a multiple-pool lifespan model for neutropenia.<sup>19</sup> This model estimates the lifespan of cells staying in a certain stage, starting with duration of the cells in the progenitor compartment, followed by duration in the maturation compartment and lastly by duration in the circulation until degradation of the neutrophils. The model requires extensive computing with use of 17 differential equations.

In conclusion, the model published by Friberg et al. in 2002 is most frequently used and has several advantages above the other models.<sup>17</sup> This model has a clear separation between drug-related and system-related parameters, making the model applicable to different drugs. Additionally, the model only estimates few system-related parameters, allowing it to model sparse data sets. Four of the reported models in this review have been compared to the model by Friberg et al. using ANC data from patients treated with a PI3K inhibitor.<sup>20</sup>

The results of this analysis implicated that none of the models showed superior performance to the model by Friberg et al.<sup>17,20</sup> Lastly, this model has been used in multiple studies with different drugs and research aims and has also been modified and applied to describe thrombocytopenia in patients treated with cytotoxic anti-cancer drugs or targeted therapies.<sup>21-33</sup> The extensive application, the limited number of system-related parameters and the overall experience with this model, makes it the best starting point for modeling myelosuppression.

### **Cardiovascular adverse effects**

For both cytotoxic and targeted therapies cardiovascular toxicity has been reported. Anthracyclines can cause arrhythmias during or after administration and chronic cardiac toxicity, resulting in irreversible left ventricular dysfunction and congestive heart failure (CHF).<sup>34</sup> Anthracycline-induced CHF has been related to dose, where patients receiving a cumulative dose of 550 mg/m<sup>2</sup> doxorubicin were at increased risk of developing CHF.<sup>35</sup> Trastuzumab has also been associated with cardiac complications, inducing (reversible) left ventricular systolic dysfunction, which can result in CHF.<sup>36</sup> Additionally, tyrosine kinase inhibitors, targeting the vascular-endothelial growth factor receptor (VEGFR), have been associated with hypertension and cardiac arrhythmias as well as other systemic anti-cancer drugs.<sup>37-39</sup>

#### *Hypertension*

Pharmacodynamic models have been developed for lenvatinib and sunitinib induced hypertension, describing the change in blood pressure (BP) over time in relation to treatment (Table 2).<sup>40,41</sup> The relationship between lenvatinib exposure and increase of diastolic (d) and systolic (s) BP was best described by an indirect response model with two effect models for dBP and sBP. The plasma concentration of lenvatinib at the time point of BP measurement was used as input rate for the indirect effect model with a linear function.<sup>40</sup> Additionally, this model included the effect of anti-hypertensive therapy on blood pressure. A similar indirect response model is used to describe the increase of dBP in sunitinib treated patients.<sup>41</sup>

**Table 2 Pharmacodynamic models describing continuous and categorical adverse effect.**

REFERENCE	DRUG	AE <sup>A</sup>	OBSERVED VARIABLE	PAR <sup>B</sup>	DRUG EFFECT	
<b>Continuous adverse effects</b>						
van Hasselt 2011	[42]	Trastuzumab	Cardiotoxicity	LVEF	3	$E_{max}$
Keizer 2010	[40]	Lenvatinib	Hypertension	BP	3	Linear
Hansson 2013	[41]	Sunitinib	Hypertension	dBp and sBP	3	Linear
Marostica 2015	[43]	Moxifloxacin	QT prolongation	QTc	4	Linear
<b>Categorical adverse effects</b>						
Keizer 2010	[40]	Lenvatinib	Proteinuria	CTC	6	Linear
Hénin 2008	[48]	Capecitabine	HFS	CTC	10	$E_{max}$
Hansson 2013	[41]	Sunitinib	HFS and fatigue	CTC	12	$E_{max}$
Suleiman 2015	[49]	Erlotinib	Rash and diarrhea	CTC	6	Linear

HFS = hand foot syndrome, CTC NCI-CTC-AE, LVEF = left ventricular ejection fraction, BP = blood pressure, d = diastolic, s = systolic, QTc = heart rate-corrected QT interval.

<sup>A</sup>Adverse effect

<sup>B</sup>Number of model parameters estimated in structural pharmacodynamic model (fixed effects excluding drug effect parameters).

### Cardiotoxicity

Cardiotoxicity as expressed as decline in left ventricular ejection fraction (LVEF) was used to develop a pharmacodynamic with an effect compartment model to describe the decrease in LVEF over time, related to trastuzumab exposure.<sup>42</sup> Recovery of the LVEF was implemented in the model. Additionally, the model incorporated the prior cumulative anthracycline dose as a covariate and found that this dose was an important determinant for the sensitivity to LVEF decline.

The relation between exposure and increase in BP and decrease of LVEF, as reported in both papers, are empirical models.<sup>40,42</sup> It is, therefore, difficult to extrapolate these models directly between different drugs that might induce hypertension.



### QT interval prolongation

Anti-cancer drugs, such as anthracyclines and tyrosine kinase inhibitors, can prolong the QT interval, which can lead to severe cardiac arrhythmias, such as Torsade de Points.<sup>38</sup> Concentration-QT modeling can provide important information on the relation between exposure and heart rate-corrected QT interval (QTc).<sup>43,44</sup> However, these models are mainly developed for anti-arrhythmic drugs and not for anti-cancer drugs. A recent publication investigated the effect of moxifloxacin, a compound that prolongs the QT interval, by developing a PK-PD model for translational purposes.<sup>43</sup> The time course of the QT interval is described by three components: the individual heart rate correction, the circadian rhythm and the drug effect:

$$QT = QT_0 \cdot \frac{RR}{RR_{ref}}^\alpha + A \cdot \cos \frac{2\pi}{24}(t - \phi) + E_{drug}$$

Where  $QT_0$  represents the QT interval at baseline,  $RR$  is heart rate and  $RR/RR_{ref}$  is multiplied by  $QT_0$  to correct for individual heart rate.  $A$  and  $\phi$  represent the amplitude and the phase of the circadian rhythm and  $E_{drug}$  represent the drug effect. Subsequently, the probability of QT-prolongation above a critical threshold (e.g. >10 ms or >20 ms) can be derived. An effect compartment can be considered for modeling the ECG time course.<sup>45</sup> Similar model structures could be used to model QT prolongation induced by anti-cancer drugs.

### Ordered categorical adverse effects

Typically, cancer therapy related adverse effects are graded using the ordered NCI-CTC-AE scale, ranging from 0-5. This range represents, no adverse effects (0) to, mild, moderate, severe, life-threatening adverse effects and lastly death (5). Adverse effects such as vomiting, diarrhea, rash, fatigue and hand foot syndrome are solely described by this ordered categorical scale. A conventional approach to describe the relation between exposure and the occurrence of a certain grade, is by statistically comparing the incidence of grades between different dose groups. Early models for these type of adverse effects used ordered logistic regression or proportional odds models.<sup>46,47</sup> Both comparing the incidence of

adverse effects and the ordered logistic regression approach have shortcomings. In these analyses, only the most severe grade of the adverse effect observed in a patient is used. By comparing incidences, the already categorized data is dichotomized, leading to substantial loss of information and ignoring the time course of the effect. Furthermore, the dependency of the previous observed grade in predicting the probability of the occurrence of the next graded adverse effect is not taken into account. This problem can be addressed by implementing a Markov process in the model. First-order Markov models take into account the value of the preceding observation. The proportional odds model can be extended with a first order Markov model.<sup>48</sup> In this way the probability of transition between severity grades of adverse effects depends on the preceding grade. Typically, the logit transformation is used to constrain values of probabilities between 0 and 1, similar to the logistic regression approach. This approach has been used for modeling different anti-cancer induced graded adverse effects (Table 2).

HFS has been described by a proportional odds model with a Markov process to model the cumulative probabilities of getting a grade 0, 1 or  $\geq 2$  for HFS related to accumulation of capecitabine.<sup>49</sup> HFS and fatigue in sunitinib treated patients has been modeled using a first-order Markov model, that was similar to the extension of the proportional odds model.<sup>41</sup> Vascular endothelial growth factor receptor 3 (sVEGFR-3) was identified as biomarker and its relative change over time was modeled as predictor of the occurrence and severity of fatigue and HFS.

Keizer et al. used a Markov transition model to describe proteinuria in patients treated with the VEGFR-inhibitor lenvatinib.<sup>40</sup> Using a compartmental structure, each adverse event grade is represented with a compartment, which in turn is denoted with its own differential equation. The probability of experiencing a certain grade is represented by the corresponding compartment amount. The amounts in all compartments sum up to 1 at any time. At each observation, these amounts are reset to a full probability for the observed state and 0 for all other states, and hence a first-order Markov property is introduced. The rate constants for the movement of these amounts (i.e. probabilities) between compartments, which reflect the transitions between the different grades, are then estimated (Figure 2).

As Markov models potentially allow transition between all states in the model, assumptions can be made to reduce the number of parameters to be estimated. For this reason, in the analysis of Keizer et al. only the transitions between neighboring grades were estimated. The following differential equations were used:

$$\frac{dP(Gr_0)}{dt} = k_{10} \cdot P(1) - k_{01} \cdot P(0)$$

$$\frac{dP(Gr_1)}{dt} = k_{01} \cdot P(0) + k_{21} \cdot P(2) - k_{10} \cdot P(1) - k_{12} \cdot P(1)$$

$$\frac{dP(Gr_2)}{dt} = k_{12} \cdot P(1) + k_{32} \cdot P(3) - k_{21} \cdot P(2) - k_{23} \cdot P(2)$$

$$\frac{dP(Gr_3)}{dt} = k_{23} \cdot P(2) - k_{32} \cdot P(3)$$

Recently, a modeling and simulation framework for erlotinib induced rash and diarrhea in patients with NSCLC was published.<sup>50</sup> The model structure was similar to the model used by Keizer et al., which was a continuous-time Markov model.

The use of Markov processes is preferred over use of the proportional odds model for modeling ordered graded adverse effects. Markov models allow use of total longitudinal data on graded toxicities over time. Furthermore, these models take the preceding grade observed into account, which enables the precise characterization of the dynamics of toxicity. The Markov models currently published are empirical models. More mechanistic elements can easily be introduced in these models for instance using latent variables describing the underlying pharmacodynamic effects. However, this underlying mechanism is in most cases unknown. The major drawback of analyzing graded or categorical data is the fact that information is lost by using categories. In some cases, there is not a sufficient number of observations of severely graded adverse effects. Therefore, grades are sometimes merged together, leading to loss of already categorized information. However, if the clinical relevance between merged grades is not

profound, this is an acceptable approach. Though, if available the underlying observations might be better than the use of grades (e.g. blood pressure, instead of grades for hypertension).

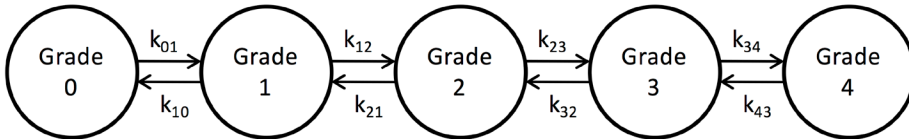


**Figure 2** General structure Markov model. Amount in compartment probability,  $k_{xx}$  rate constants between probabilities.<sup>40,50</sup>

## APPLICATION OF ADVERSE EFFECT MODELS

Developed models for adverse effects have been applied to support decision-making regarding treatment optimization and clinical development. Ideally PK-PD modeling frameworks are developed that integrate data on pharmacokinetics, adverse effects and efficacy. An example of such a framework is available for sunitinib.<sup>41</sup> This paper did not only include modeling of ANC, fatigue, blood pressure and HFS, but also investigated if adverse effects were predictive for overall survival. Hypertension and neutropenia were found predictive for overall survival, functioning as biomarkers for treatment response.

Adverse effect models can additionally support decision-making regarding dose adjustments and dose individualizations, using simulation methods. The previously described modeling and simulation framework for erlotinib-induced rash and diarrhea investigated the safety of high-dose erlotinib pulses (1600 mg/week + 50 mg/day remaining week days) proposed, compared to the standard dose (150 mg/day) and different other dosing regimens.<sup>50</sup> Based on a simulation analysis using the framework developed, severe rash was predicted to occur in 20% of patients treated with the pulsed dosing regimen, compared to 12% in patients treated with the standard dosing regimen.

In contrast with the common perception, radiotherapy was found to attenuate erlotinib-induced rash significantly, which advocates for using erlotinib and radiotherapy together. The framework also included a survival model, finding that experiencing rash at any grade was associated with improved clinical efficacy in terms of survival, albeit not significantly. Another example demonstrated that modeling can be helpful for determining individual dose adjustment of capecitabine to reduce severe grade HFS while maintaining efficacy.<sup>51</sup> The paper reports a clinical trial simulation in which the proportional odds Markov model was used on individual patient data.<sup>49</sup> Intolerable HFS (grade  $\geq 2$ ) was predicted for the next treatment cycle, based on the previous cycle for each patient. Dose adjustments were made accordingly. Individualized dose adjustments using the Markov model were compared to using standard dose adjustments and found to reduce the duration of intolerable HFS by 10 days without loss of efficacy. Both modeling frameworks are examples of how a modeling approach can support dose adjustments and dose individualizations using predictive simulation methods.

Lastly, modeling and simulation of adverse effect models can optimize treatment and support clinical trial designs. The hypertension model, discussed in this review, has been used to optimize treatment with lenvatinib.<sup>52</sup> This paper investigated four strategies to clinically manage lenvatinib induced hypertension to maximize both the number of patients on treatment and the average dose level during treatment, with use of simulations. An adverse effect-guided dose titration could potentially increase drug exposure without additional toxicity. Additionally, a design where anti-hypertensive treatment was followed by lenvatinib dose reduction proved to keep a large number of patients on treatment. This approach aimed at minimizing treatment cessation due to toxicity in order to improve response to treatment. The intervention designs were supportive of development of a phase II clinical trial design.

## DISCUSSION

This review reports several structural models for modeling adverse effects of anti-cancer drugs. Firstly, the best modeling approach depends on the type of data available and secondly, on whether or not prior knowledge of the underlying mechanism of the adverse effect is available. If the adverse effect is reported as continuous variable and prior knowledge on the mechanism behind the effect, the best approach is to develop a mechanism or semi-mechanism based model. Mechanistic models generally have a better predictive performance and potentially allow for extrapolation beyond the conditions on which the model was developed. The model by Friberg et al., published in 2002, proves to be the best starting point for modeling hematologic toxicity, with only few pharmacodynamic parameters to be estimated and the mechanistic approach makes the model interchangeable between different anti-cancer drugs.<sup>17</sup> If no prior mechanistic knowledge is available or implementation in the model is impossible, data can be modeled using generic pharmacodynamic effect models. This more empirical approach can give insight in how an adverse effect evolves over time, if data is continuous. In some cases, the underlying continuous measurement is graded using the NCI-CTC-AE scale. For example, hypertension can be graded as such, however, the underlying continuous measurement, blood pressure, is needed to grade this toxicity. Therefore, blood pressure measurement itself can be used to develop PK-PD models. In conclusion, if an underlying continuous measurement is available, this longitudinal continuous data is preferred over ordered graded data, since it is less prone to loss of information. In subsequent simulation studies, the clinically well accepted graded score can still be derived from the continuous data. Adverse effects like diarrhea, vomiting and HFS are difficult to quantify and are described by ordered categorical grades. In this case, the best approach is to model the probabilities using a proportional odds model with a Markov process. The probability of a certain grade will then depend on the previously observed grade, which is true for almost all observed effects in oncology.

Modeling and simulation methods for adverse effects are preferred over the conventional comparison of adverse effect incidences between dosing groups. Quantitative models consider the variability between patients, allowing integration of patient characteristics that might be important in predicting the safety profile. Patient characteristics can alter systemic exposure to the drug and may lead to differences in onset, severity and duration of adverse effects. Typically, physiological factors such as age, body size, gender, kidney function and liver function can alter exposure, as well as pharmacogenetic factors and administration of other drugs.<sup>53</sup> Integration of these patient characteristics can be helpful in managing individual dose adaptations. In addition, proposed models can be used to model adverse effects driven by combination therapy, which is often applied in the oncology setting.

Established PK-PD models can predict different clinical scenarios. These simulations are particularly helpful in finding the optimal relationship between exposure and safety. Ideally, a PK-PD modeling framework is developed, that integrates data on exposure, efficacy and toxicity, to assess the optimal balance between safety and efficacy.<sup>41,54</sup> Modeling tumor growth as a biomarker for efficacy can be of added value in assessing this balance.<sup>55</sup>

In conclusion, mathematical modeling of adverse effects can provide insight in how toxicities evolve over time and if or what patient related factors can impact this time course. In addition, a modeling approach includes all available data, minimizing loss of information as is typically the case using more conventional methods of analyzing toxicity data. At last, modeling and simulation frameworks have been proved to support clinical trial designs, to optimize treatment and to guide dose adjustments or dose individualizations. Therefore, modeling adverse effects proves to be a helpful tool for both improvement of clinical management and support of decisions regarding drug development.

## REFERENCES

1. Hryniuk, W. More Is Better. *J. Clin. Oncol.* 6, 1365–1367 (1988).
2. Niraula, S. et al. The Price We Pay for Progress: A Meta-Analysis of Harms of Newly Approved Anticancer Drugs. *J. Clin. Oncol.* 30, 3012–3019 (2012).
3. Tannock, I. F. et al. Methotrexate, and Fluorouracil Chemotherapy for Patients With Metastatic Breast Cancer. *J. Clin. Oncol.* 6, 1377–1387 (2012).
4. Sleijfer, S. & Wiemer, E. Dose Selection in Phase I Studies: Why We Should Always Go for the Top. *J. Clin. Oncol.* 26, 1576–1578 (2008).
5. Hainsworth, J. D. et al. Phase II Trial of Bevacizumab and Everolimus in Patients With Advanced Renal Cell Carcinoma. *J. Clin. Oncol.* 28, 2131–2136 (2010).
6. Gray, J. E. et al. A first-in-human phase I dose-escalation, pharmacokinetic, and pharmacodynamic evaluation of intravenous LY2090314, a glycogen synthase kinase 3 inhibitor, administered in combination with pemetrexed and carboplatin. *Invest. New Drugs* 3, (2015).
7. Crawford, J., Dale, D. C. & Lyman, G. H. Chemotherapy-Induced Neutropenia: Risks, Consequences, and New Directions for Its Management. *Cancer* 100, 228–237 (2004).
8. Zhou, H. et al. Population pharmacokinetics/toxicodynamics (PK/TD) relationship of SAM486A in phase I studies in patients with advanced cancers. *J. Clin. Pharmacol.* 40, 275–283 (2000).
9. Jakobsen, P. et al. A randomized study of epirubicin at four different dose levels in advanced breast cancer. Feasibility of myelotoxicity prediction through single blood-sample measurement. *Cancer Chemother. Pharmacol.* 28, 465–469 (1991).
10. Minami, H., Ando, Y., Sakai, S. & Shimokata, K. Clinical and pharmacologic analysis of hyperfractionated daily oral etoposide. *J. Clin. Oncol.* 13, 191–199 (1995).
11. Karlsson, M. O., Port, R. E., Ratain, M. J. & Sheiner, L. B. A population model for the leukopenic effect of etoposide. *Clin. Pharmacol. Ther.* 57, 325–334 (1995).
12. Karlsson, M. O., Molnar, V., Bergh, J., Freijs, A. & Larsson, R. A general model for time-dissociated pharmacokinetic-pharmacodynamic relationships exemplified by paclitaxel myelosuppression. *Clin. Pharmacol. Ther.* 63, 11–25 (1998).



13. Haurie, C., Dale, D. C. & Mackey, M. C. Cyclical neutropenia and other periodic hematological disorders: a review of mechanisms and mathematical models. *Blood* 92, 2629-2640 (1998).
14. Minami, H. et al. Indirect-response model for the time course of leukopenia with anticancer drugs. *Clin. Pharmacol. Ther.* 64, 511-521 (1998).
15. Friberg, L. E., Brindley, C. J., Karlsson, M. O. & Devlin, A. J. Models of schedule dependent haematological toxicity of 2'-deoxy-2'-methylidenecytidine (DMDC). *Eur. J. Clin. Pharmacol.* 56, 567-574 (2000).
16. Zamboni, W. C. et al. Pharmacodynamic model of topotecan-induced time course of neutropenia. *Clin. Cancer Res.* 7, 2301-2308 (2001).
17. Friberg, L. E. Model of Chemotherapy-Induced Myelosuppression With Parameter Consistency Across Drugs. *J. Clin. Oncol.* 20, 4713-4721 (2002).
18. Panetta, J. C. et al. A mechanistic mathematical model of temozolomide myelosuppression in children with high-grade gliomas. *Math. Biosci.* 186, 29-41 (2003).
19. Bulitta, J. B. et al. Multiple-pool cell lifespan models for neutropenia to assess the population pharmacodynamics of unbound paclitaxel from two formulations in cancer patients. *Cancer Chemother. Pharmacol.* 63, 1035-1048 (2009).
20. Soto, E. et al. Comparison of different semi-mechanistic models for chemotherapy-related neutropenia: Application to BI 2536 a Plk-1 inhibitor. *Cancer Chemother. Pharmacol.* 68, 1517-1527 (2011).
21. Sostelly, A. et al. Can we predict chemo-induced hematotoxicity in elderly patients treated with pegylated liposomal doxorubicin? Results of a population-based model derived from the DOGMES phase II trial of the GINECO. *J. Geriatr. Oncol.* 4, 34-45 (2013).
22. Hasselt, J. G. C. Van et al. Population pharmacokinetic-pharmacodynamic analysis for eribulin mesilate-associated neutropenia. *Br. J. Clin. Pharmacol.* 76, 412-424 (2013).
23. Joerger, M. et al. Evaluation of a pharmacology-driven dosing algorithm of 3-weekly paclitaxel using therapeutic drug monitoring: A pharmacokinetic-pharmacodynamic simulation study. *Clin. Pharmacokinet.* 51, 607-617 (2012).
24. Trocóniz, I. F. et al. Population pharmacokinetic/pharmacodynamic modeling of drug-induced adverse effects of a novel homocamptothecin analog, elomotecan (BN80927), in a Phase I dose finding study in patients with advanced solid tumors. *Cancer Chemother. Pharmacol.* 70, 239-250 (2012).

25. Hansson, E. K. & Friberg, L. E. The shape of the myelosuppression time profile is related to the probability of developing neutropenic fever in patients with docetaxel-induced grade IV neutropenia. *Cancer Chemother. Pharmacol.* 69, 881–890 (2012).
26. Kloft, C., Wallin, J., Henningsson, A., Chatelut, E. & Karlsson, M. O. Population pharmacokinetic-pharmacodynamic model for neutropenia with patient subgroup identification: Comparison across anticancer drugs. *Clin. Cancer Res.* 12, 5481–5490 (2006).
27. Friberg, L. E., Freijls, a, Sandström, M. & Karlsson, M. O. Semiphysiological model for the time course of leukocytes after varying schedules of 5-fluorouracil in rats. *J. Pharmacol. Exp. Ther.* 295, 734–740 (2000).
28. Soto, E. et al. Prediction of neutropenia-related effects of a new combination therapy with the anticancer drugs BI 2536 (a Plk1 inhibitor) and pemetrexed. *Clin. Pharmacol. Ther.* 88, 660–667 (2010).
29. Kaefer, A. et al. Mechanism-based pharmacokinetic/pharmacodynamic meta-analysis of navitoclax (ABT-263) induced thrombocytopenia. *Cancer Chemother. Pharmacol.* 74, 593–602 (2014).
30. Quartino, A. L., Karlsson, M. O., Lindman, H. & Friberg, L. E. Characterization of Endogenous G-CSF and the Inverse Correlation to Chemotherapy-Induced Neutropenia in Patients with Breast Cancer Using Population Modeling. *Pharm. Res.* 3390–3403 (2014).
31. Chalret du Rieu, Q. et al. Pharmacokinetic/Pharmacodynamic modeling of abexinostat-induced thrombocytopenia across different patient populations: application for the determination of the maximum tolerated doses in both lymphoma and solid tumour patients. *Invest. New Drugs* 32, 985–994 (2014).
32. Hayes, S. et al. Population PK/PD modeling of eltrombopag in subjects with advanced solid tumors with chemotherapy-induced thrombocytopenia. *Cancer Chemother. Pharmacol.* 71, 1507–1520 (2013).
33. Bender, B. C. et al. A population pharmacokinetic/pharmacodynamic model of thrombocytopenia characterizing the effect of trastuzumab emtansine (T-DM1) on platelet counts in patients with HER2-positive metastatic breast cancer. *Cancer Chemother. Pharmacol.* 70, 591–601 (2012).
34. SLordal, L. & Spigset, O Heart failure induced by non-cardiac drugs. *Drug Saf* 29, 567–86 (2006).
35. Lefrak, E. A., Pitha, J., Rosenheim, S. & Gottlieb, J. A. A Clinicopathologic Analysis of Adriamycin Cardiotoxicity. *Cancer* 32, 302–14 (1973).

36. Keefe, D. L. Trastuzumab-associated cardiotoxicity. *Cancer* 95, 1592-1600 (2002).
37. Chu, W. et al. Association between CYP3A4 genotype and risk of endometrial cancer following tamoxifen use. *Carcinogenesis* 28, 2139-42 (2007).
38. Suter, T. M. & Ewer, M. S. Cancer drugs and the heart: Importance and management. *Eur. Heart J.* 34, 1102-1111 (2013).
39. Senkus, E. & Jassem, J. Cardiovascular effects of systemic cancer treatment. *Cancer Treat. Rev.* 37, 300-311 (2011).
40. Keizer, R. J. et al. A model of hypertension and proteinuria in cancer patients treated with the anti-angiogenic drug E7080. *J. Pharmacokinet. Pharmacodyn.* 37, 347-363 (2010).
41. Hansson, E. K. et al. PKPD Modeling of Predictors for Adverse Effects and Overall Survival in Sunitinib-Treated Patients With GIST. *CPT pharmacometrics Syst. Pharmacol.* 2, e85 (2013).
42. Hasselt, J. G. C. van, Boekhout, A. H., Beijnen, J. H., Schellens, J. H. M. & Huitema, A. D. R. Population pharmacokinetic-pharmacodynamic analysis of trastuzumab-associated cardiotoxicity. *Clin. Pharmacol. Ther.* 90, 126-132 (2011).
43. Marostica, E. & Ammel, K. Van Modelling of drug-induced QT-interval prolongation : estimation approaches and translational opportunities. *J. Pharmacokinet. Pharmacodyn.* 42, 659-679 (2015).
44. Piotrovsky, V. Pharmacokinetic-pharmacodynamic modeling in the data analysis and interpretation of drug-induced QT/QTc prolongation. *AAPS J.* 7, E609-E624 (2005).
45. Holford, N., Coates, P., Guentert, T., Riegelman, S. & Sheiner, L. The effect of quinidine and its metabolites on the electrocardiogram and systolic time intervals: concentration effect relationships. *Br. J. Clin. Pharmacol.* 11, 187-195 (1981).
46. Mould, D. et al. A population pharmacokinetic-pharmacodynamic and logistic regression analysis of lotrafiban in patients. *Clin. Pharmacol. Ther.* 69, 210-222 (2001).
47. Xie, R., Mathijssen, R. H. J., Sparreboom, A., Verweij, J. & Karlsson, M. O. Clinical pharmacokinetics of irinotecan and its metabolites in relation with diarrhea. *Clin. Pharmacol. Ther.* 72, 265-275 (2002).
48. Zingmark, P. H., Kågedal, M. & Karlsson, M. O. Modelling a spontaneously reported side effect by use of a Markov mixed-effects model. *J. Pharmacokinet. Pharmacodyn.* 32, 261-281 (2005).

49. Hénin, E. et al. A dynamic model of hand-and-foot syndrome in patients receiving capecitabine. *Clin. Pharmacol. Ther.* 85, 418–425 (2009).
50. Suleiman, A. A. et al. A Modeling and Simulation Framework for Adverse Events in Erlotinib-Treated Non-Small-Cell Lung Cancer Patients. *AAPS J.* 17, 1483–91 (2015).
51. Paule, I. et al. Dose adaptation of capecitabine based on individual prediction of limiting toxicity grade: Evaluation by clinical trial simulation. *Cancer Chemother. Pharmacol.* 69, 447–455 (2012).
52. Keizer, R. J. et al. Model-based treatment optimization of a novel VEGFR inhibitor. *Br. J. Clin. Pharmacol.* 74, 315–326 (2012).
53. Mathijssen, R. H. J., Sparreboom, A. & Verweij, J. Determining the optimal dose in the development of anticancer agents. *Nat. Rev. Clin. Oncol.* 11, 272–81 (2014).
54. Graham, G., Gupta, S. & Aarons, L. Determination of an optimal dosage regimen using a Bayesian decision analysis of efficacy and adverse effect data. *J. Pharmacokinet. Pharmacodyn.* 29, 67–88 (2002).
55. Ribba, B. et al. A review of mixed-effects models of tumor growth and effects of anticancer drug treatment used in population analysis. *CPT pharmacometrics Syst. Pharmacol.* 3, e113 (2014).





## CHAPTER 3.2

# Pharmacodynamic modeling of cardiac biomarkers in breast cancer patients treated with anthracycline and trastuzumab regimens

*J Pharmacokinet Pharmacodyn.* 2018 Jun;45(3):431-442

A.H.M. de Vries Schultink  
A.H. Boekhout  
J.A. Gietema  
A.M. Burylo  
T.P.C. Dorlo  
J.G.C. van Hasselt  
J.H.M. Schellens  
A.D.R. Huitema

## ABSTRACT

### Objectives

Trastuzumab is associated with cardiotoxicity, manifesting as a decrease of the left-ventricular ejection fraction (LVEF). Administration of anthracyclines prior to trastuzumab increases risk of cardiotoxicity. High-sensitive troponin T and N-terminal-pro-brain natriuretic peptide (NT-proBNP) are molecular markers that may allow earlier detection of drug-induced cardiotoxicity. In this analysis we aimed to quantify the kinetics and exposure-response relationships of LVEF, troponin T and NT-proBNP measurements, in patients receiving anthracycline and trastuzumab.

### Methods

Repeated measurements of LVEF, troponin T and NT-proBNP and dosing records of anthracyclines and trastuzumab were available from a previously published clinical trial. This trial included 206 evaluable patients with early breast cancer. Exposure to anthracycline and trastuzumab was simulated based on available dosing records and by using a kinetic-pharmacodynamic (K-PD) and a fixed pharmacokinetic (PK) model from literature, respectively.

### Results

The change from baseline troponin T was described with a direct effect model, affected by simulated anthracycline concentrations, representing myocyte damage. The relationship between trastuzumab and LVEF was described by an indirect effect compartment model. The  $EC_{50}$  for LVEF decline was significantly affected by the maximum troponin T concentration after anthracycline treatment, explaining 15.1% of inter-individual variability. In this cohort, NT-proBNP changes could not be demonstrated to be related to anthracycline or trastuzumab treatment.



## **Conclusions**

Pharmacodynamic models for troponin T and LVEF were successfully developed, identifying maximum troponin T concentration after anthracycline treatment as a significant determinant for trastuzumab-induced LVEF decline. These models can help identify patients at risk of drug-induced cardiotoxicity and optimize cardiac monitoring strategies.

## INTRODUCTION

Trastuzumab is a monoclonal antibody that targets the human epidermal growth factor receptor 2 (HER2) and is used to treat HER2-positive metastatic and early breast cancer and metastatic gastric cancer.<sup>1-3</sup> Despite improvement in overall and progression free survival, application of the drug is hampered by cardiac adverse effects, leading to dose reductions, dose-delays and treatment interruption or withdrawal with an increased recurrence risk as a consequence.<sup>4</sup> Trastuzumab-induced cardiotoxicity is manifested as an asymptomatic decrease of the left-ventricular ejection fraction (LVEF) and development of congestive heart failure.<sup>5</sup> The mechanism behind this cardio-toxic effect is not completely elucidated, though it has been demonstrated that trastuzumab causes structural and functional changes to contractile proteins in the heart muscle.<sup>6,7</sup> These changes rarely lead to cell death, that might explain why the decrease in LVEF values is partly reversible when trastuzumab treatment is discontinued.<sup>5</sup> In addition, patients treated with trastuzumab are often pretreated with anthracyclines. Anthracyclines can irreversibly damage myocytes, possibly by generation of reactive oxygen species and lipid peroxidation of the cell membrane of cardiomyocytes.<sup>8</sup> A cumulative lifetime dose exceeding 550 mg/m<sup>2</sup> for doxorubicin and 950 mg/m<sup>2</sup> for epirubicin has been associated with increased incidence of heart failure.<sup>9,10</sup> These cumulative dose thresholds are therefore clinically applied to limit the risk for cardiac damage. Since both trastuzumab and anthracyclines can lead to cardiac dysfunction, it is not surprising that a higher incidence of cardiac dysfunction has been reported for patients treated with anthracyclines concomitantly or prior to trastuzumab.<sup>11</sup> However, a high variability in susceptibility to cardiotoxicity is seen for patients treated with anthracyclines and trastuzumab.

Cardiac function can be monitored during treatment using echocardiography or Multiple Gated Acquisition (MUGA) scan to determine the LVEF. Attempts have been made to optimize cardiac monitoring strategies, allowing for a better identification of patients that experience cardiotoxicity and decrease the number of LVEF measurements in low-risk patients.<sup>12</sup> Cardiac biomarkers such as troponin T and N-terminal-pro-brain natriuretic peptide (NT-proBNP) are molecular markers suggested to allow earlier detection of drug-induced cardiotoxicity compared to LVEF measurement.<sup>13</sup> Cardiac troponins are indicative

of myocyte damage and are suggested to predict patients at risk of cardiotoxicity during trastuzumab treatment who are pretreated with anthracyclines.<sup>14</sup> In addition, elevated baseline concentrations of troponin I and troponin T have been related to an increased risk of LVEF decrease.<sup>13</sup> NT-proBNP is a marker for heart failure. Currently, troponins and NT-proBNP are used as cardiac biomarkers for prognosis and diagnosis of myocardial infarction and heart failure, respectively.<sup>15</sup> However, no evidence exists for anti-cancer drug management based on abnormal cardiac biomarker concentrations. Development of a pharmacokinetic-pharmacodynamic (biomarker) model can give insight in the time course of cardiac biomarkers during treatment and help identify the optimal time point of cardiac biomarker assessment. In this analysis, we aim to quantify the kinetics and exposure-response relationship of LVEF, troponin T and NT-proBNP measurements, in patients with early breast cancer receiving anthracyclines followed by trastuzumab. Ultimately, the quantification of cardiac biomarkers could help identify patients at increased risk of developing cardiotoxicity and optimize clinical management of trastuzumab-induced cardiotoxicity.

## **METHODS**

### **Patients and data**

The analysis conducted in this study was based upon data from patients with HER2-positive early breast cancer from a previously conducted randomized, placebo-controlled clinical trial, investigating protection for trastuzumab-induced cardiotoxicity with angiotensin II-receptor inhibitor candesartan.

All patients received adjuvant treatment with anthracycline-containing chemotherapy, either doxorubicine or epirubicine, followed by trastuzumab treatment for 52 weeks. Patients were randomized to receive candesartan or placebo (1:1) daily, starting from the first trastuzumab administration until 26 weeks after the last trastuzumab administration. The trial demonstrated that concomitant candesartan treatment did not protect against decreases in LVEF during trastuzumab treatment.<sup>16</sup>

Repeated measurements for LVEF were available for all patients. LVEF was determined with MUGA scan or echocardiography. Autologous red blood cells (400 MBq Tc-99m labelled) were injected and acquisition was performed in 6 minutes with a large-field-of-view gamma camera with a low energy all-purpose parallel-hole collimator. Troponin T and NT-proBNP concentrations were available for 92% of patients and were measured in plasma samples using a sandwich immunoassay (Modular E system, Roche Diagnostics). The lower-limit of quantification (LLOQ) for NT-proBNP was 5 pg/mL and for (high sensitive) troponin T 3 ng/L. Troponin T and NT-proBNP measurements were scheduled at the following visits: before starting anthracycline treatment, at baseline before starting trastuzumab treatment and 3, 12, 24, 36, 52, 64, 78 and 92 after starting trastuzumab treatment. LVEF was evaluated at the same time points, except for the 3 week and 64 week visit since start trastuzumab treatment. Additionally, individual patient dosing records, including time of administration and dosages of anthracycline and trastuzumab were available. None of the patients received a cumulative dose above 550 mg/m<sup>2</sup> or 950 mg/m<sup>2</sup> for doxorubicin and epirubicin, respectively.

## Modeling cardiac biomarkers

### *Structural models*

Exposure to anthracyclines and trastuzumab were predicted using individual dosing records of the drugs and simulated using different approaches. A K-PD approach was applied for the anthracyclines (doxorubicin and epirubicin).<sup>17</sup> The trastuzumab PK profiles were obtained using fixed effect parameters from a previously published PK model for HER2-positive breast cancer patients.<sup>18</sup>

Exploratory plots were used to determine pharmacodynamic modeling starting points for the three cardiac biomarkers. The plots demonstrated an increase in troponin T during anthracycline treatment, and a gradual decrease of troponin T during trastuzumab treatment. Therefore, troponin T changes were assumed to be related to anthracycline treatment only. Troponin T samples were taken before anthracycline treatment, approximately 21 days after the last anthracycline dose and during trastuzumab treatment, with limited samples available during

anthracycline treatment. Therefore, direct and indirect effect models were evaluated to identify if the troponin T peak concentration occurred right after the last administration of anthracyclines or if the peak was delayed after treatment.

A previously published model by our group was used as a starting point for modeling trastuzumab-induced LVEF decrease.<sup>19</sup> In this model the LVEF decline was described by an effect compartment, demonstrating cardiac damage induced by trastuzumab treatment. The delay in LVEF decline in relation to trastuzumab treatment (the cardiac damage onset rate) was kept equal to the rate of recovery.

NT-proBNP changes were evaluated during anthracycline and trastuzumab treatment separately. A model that described NT-proBNP concentrations to be inversely associated with LVEF values was evaluated. In addition, NT-proBNP baseline values prior to initiation of either anthracycline or trastuzumab treatment were evaluated as covariates.

#### *Statistical models*

Between subject variability (BSV) was evaluated for all structural model parameters using an exponential error model:

$$P_i = P_{pop} \cdot \exp(\eta_i)$$

where  $P_i$  is the individual parameter estimate for individual  $i$ ,  $P_{pop}$  the population parameter estimate and  $\eta_i$  the individual value of between-subject variability for subject  $i$ , where  $\eta_i$  was assumed to be normally distributed with mean 0 and variance  $\omega^2$ . Off-diagonal elements of the variance-covariance (omega) matrix, were evaluated to identify covariances between the individual random effects. These covariances were used to derive the correlations between the random-effects. Residual unexplained variability was described as a proportional error model for all cardiac biomarkers:

$$C_{obs,ij} = C_{pred,ij} \cdot (1 + \varepsilon_{p,ij})$$

where  $C_{obs,ij}$  represents the observed concentration for individual  $i$  and observation  $j$ ,  $C_{pred,ij}$  represents the individual predicted concentration,  $\varepsilon_{p,ij}$  the proportional error distributed following  $N(0, \sigma^2)$ .

### Covariate analysis

Different covariates were included in the covariate analysis, based on physiological plausibility and clinical relevance. The following covariates were evaluated for the anthracycline-troponin T model and the trastuzumab-LVEF model: age, hypertension diagnosis and status, radiotherapy of the chest, laterality of radiotherapy and type of anthracycline administered. Additionally, type of anthracycline (epirubicin or doxorubicin) was evaluated as a covariate for the anthracycline-troponin T model, and baseline LVEF values (prior to initiation of trastuzumab) and time between last anthracycline dose and first trastuzumab dose for the trastuzumab-LVEF model. Since patients in this cohort were randomized to receive either placebo or candesartan to prevent or alleviate trastuzumab-induced cardiotoxicity, treatment group was evaluated as a covariate. In addition, the dose normalized cumulative dose of anthracycline and the predicted maximum concentration of troponin T reached by the previous anthracycline treatment were evaluated as a covariates. Binary covariates (previous radiotherapy, hypertension diagnosis, type of anthracycline administered) were implemented using the following equation:

$$P_i = P_{pop} \cdot (\theta_{cov})^{COV}$$

Where  $\theta_{cov}$  is the covariate effect parameter and COV the covariate value. Continuous covariates ( $COV_{cont}$ ) (time between last anthracycline dose and initiation of trastuzumab, maximum concentrations of troponin T) were normalized to the median value of the covariate ( $COV_{median}$ ) and implemented as follows:

$$P_i = P_{pop} \cdot \frac{COV_{cont}^{\theta_{cov}}}{COV_{median}}$$

Categorical covariates (laterality of radiotherapy and hypertension status) were implemented by estimating a separate parameter for each category. The selected physiologically plausible and clinically relevant covariates were evaluated using a forward inclusion and backward elimination method. A significance level of  $p < 0.01$  was set for the forward inclusion, corresponding to a decrease of OFV of  $> 6.63$ . For backward elimination, a significance level of  $p < 0.005$  was set, corresponding to an increase of OFV of  $> 7.88$ .

#### *Model evaluation*

Models evaluation was performed using general goodness-of-fit (GOF) plots, plausibility, stability and precision of parameter estimates and change in objection function value (OFV).<sup>20</sup> A  $p < 0.01$  was considered significant, meaning that an OFV drop of  $> 6.63$  for hierarchical models (degree of freedom = 1, chi-squared distribution) was considered as a significant improvement. Since troponin T samples were taken predominantly before anthracycline treatment and approximately 21 days after the last anthracycline dose, predicted troponin T concentrations at day 21 after the last anthracycline administration were also evaluated as a covariate. In addition, the final model for LVEF was evaluated for the placebo and the candesartan group, separately, in order to identify possible differences related to study treatment.

#### *Software*

Data management and graphical evaluation were performed using R (version 3.0.1).<sup>21</sup> Nonlinear mixed effects modeling was performed using NONMEM (version 7.3.0, ICON Development Solutions, Ellicott City, MD, USA) and Perl-speaks-NONMEM (version 4.4.8).<sup>22,23</sup> Piraña (version 2.9.2) was used as graphical user interface.<sup>24</sup> Models were estimated using First Order Conditional Estimation method with  $\eta$ - $\epsilon$  interaction (FOCE-I).

**Table 1 Patient characteristics**

	<b>MEDIAN [RANGE]</b>	<b>N</b>
Age at randomization (years)	50 [25-69]	-
Number of anthracycline cycles	4 [2-6]	-
<b>Absolute doses of anthracyclines</b>		
Doxorubicin (mg)	110 [75-150]	-
Epirubicin (mg)	170 [100-200]	-
Number of trastuzumab cycles	23 [5-46]	-
<b>Trastuzumab doses</b>		
3 weekly schedule	8 mg/kg - 6 mg/kg	62
weekly schedule	4 mg/kg - 2 mg/kg	144
Time between last anthracycline dose and first trastuzumab dose (days)	21 [14-217]	
	<b>No. of patients n=206</b>	<b>%</b>
<b>Measurements</b>		
LVEF measurements available	206	100
LVEF baseline - before anthracycline	173	84.0
LVEF baseline - before trastuzumab	205	99.5
Troponin T measurements available	190	92.2
NT-proBNP measurements available	190	92.2
<b>Type of anthracycline treatment</b>		
Doxorubicin	181	87.9
Epirubicin	25	12.1
<b>Clinically relevant decline in LVEF*</b>		
Yes	37	18
No	169	82
<b>Medical history</b>		
<b>Previous radiotherapy</b>		
Yes	112	45.6
No	94	54.4



**Table 1 continued**

<i>Laterality of radiotherapy</i>		
Left	58	28.2
Right	54	26.2
No radiotherapy	94	45.6
<i>Hypertension ever diagnosed</i>		
Yes	24	11.7
No	182	88.3
<i>Hypertension status</i>		
Past	5	2.4
Dormant	12	5.8
Active	7	3.4
No hypertension	182	88.3

*\*A decline in LVEF was assumed clinically relevant if LVEF values decreased with 15% or more from baseline or if a value of <45% was reached.*

## RESULTS

### Patients and data

In the final analysis, 206 patients were included. A total of 1444 LVEF measurements (96% by MUGA scan) were available for 206 patients with a median [range] of 8 [2-9] measurements per patient. Troponin T and NT-proBNP measurements were available for 190 patients, with a total of 1230 troponin T measurements,<sup>7</sup> [1-11] measurements per patient, and 1028 NT-proBNP measurements, 6 [1-10] measurements per patient. Concentrations below the LLOQ were divided by two in the final dataset (4.6% of the troponin T observations and 2.5% of NT-proBNP were below the LLOQ). Part of the patient characteristics are depicted in Table 1. The clinical data have been extensively described elsewhere.<sup>16</sup>

Data and models for the cardiac biomarkers troponin T, LVEF, and NT-proBNP were explored separately in relation to the anthracycline concentration-time profiles (troponin T and NT-proBNP) and to the trastuzumab concentration-time profiles (LVEF and NT-proBNP). The final model parameter estimates are summarized in Table 2.

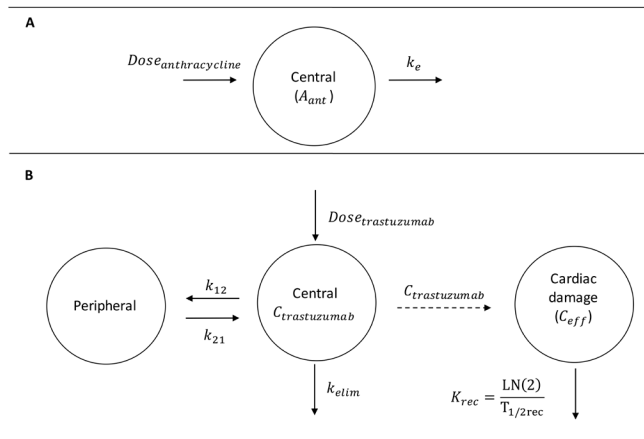


**Figure 1** Structural models for anthracycline and troponin T (K-PD) and trastuzumab and LVEF (PK-PD),  $K_e$  = elimination rate constant,  $A_{ant}$  = amount of anthracyclines,  $C_{eff}$  = the concentration in the effect compartment,  $K_{rec}$  = recovery rate constant,  $T_{1/2rec}$  = recovery half-life.

### Troponin T

Troponin T changes were best described by a direct effect model, where the troponin T concentration increased proportionally with the increment of simulated anthracycline concentrations (Figure 1A). The model was described by the following equations:

$$\frac{dA_{ant}}{dt} = -K_e \cdot A_{ant}$$

$$TRP = TRP_0 \cdot (1 + SLOPE \cdot A_{ant})$$

where  $A_{ant}$  is the amount of anthracyclines,  $K_e$  the elimination rate constant, TRP is troponin T,  $TRP_0$  is troponin T at baseline, before starting anthracycline treatment, SLOPE is the parameter that describes the proportional increase of troponin T from baseline. The goodness of fit plots (Figure 2A and Online Resource 1 Figure S1) showed that the anthracycline-troponin T underpredicted some of the observed

higher concentration of troponin T. However, the individual predictions were considered adequate. The VPC showed a slight overprediction of the declining troponin T concentrations in the 95th percentile (Figure 3), nevertheless, the higher concentrations are described adequately. NPDE plots did not show significant trends. In addition, an indirect effect model was evaluated. However, this model underpredicted the observed concentrations around day 21 post last anthracycline dose and also underpredicted the recovery rate of the troponin T peak.

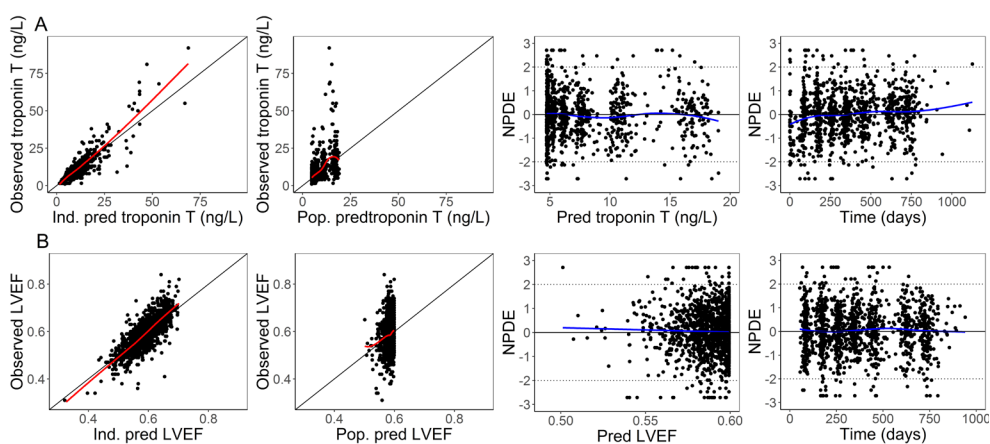


**Figure 2** Diagnostic plots for a. troponin T and b. left ventricular ejection fractions (LVEF), including individual and population predictions and normalized prediction distribution error (NPDE) over predictions and time.

**Table 2** Parameter estimates for cardiac biomarker models anthracycline-troponin T and trastuzumab-LVEF.

PARAMETER	UNIT	PARAMETER ESTIMATE	RSE (%)	SHRINKAGE (%)
<b>Anthracycline - troponin T model</b>				
Troponin T baseline ( $TRP_0$ )	ng/L	4.72	3.5	-
Elimination rate constant K-PD model ( $K_p$ )	day <sup>-1</sup>	8.49·10 <sup>-3</sup>	4.0	-
Proportional effect (anthracyclines-troponin T) (SLOPE)	ng <sup>-1</sup> ·L	8.84·10 <sup>-3</sup>	7.0	-
Proportional anthracycline-type effect on SLOPE		0.524	17.5	-
<b>Between-subject variability (%)</b>				
Slope effect on $TRP_0$ (SLOPE)	CV	57.7	23.3	31.0
Troponin T baseline ( $TRP_0$ )	CV	39.2	9.9	12.6
<b>Residual variability</b>				
Proportional residual error troponin T	%	30.1	4.2	11.2
<b>Trastuzumab - LVEF model</b>				
LVEF baseline value ( $LVEF_0$ )		0.599	0.6	-
Recovery half-life ( $T_{1/2rec}$ )	day	67.9	17.2	-
Sensitivity to LVEF decline ( $EC_{50}$ )	mg/L	2.18·10 <sup>5</sup>	23.4	-
Maximum troponin T effect on $EC_{50}$		-1.16	23.4	-
<b>Between-subject variability (%)</b>				
LVEF baseline value ( $LVEF_0$ )	CV	7.07	16.7	9.9
Sensitivity to LVEF decline ( $EC_{50}$ )	CV	82.9	43.1	26.0
Correlation $\omega LVEF_0 \sim \omega EC_{50}$ <sup>a</sup>	-	0.585		
<b>Residual variability</b>				
Proportional residual error LVEF	%	7.8	2.9	8.3

CV = coefficient of variation, SD = standard deviation, RSE = relative standard error.

<sup>a</sup>Correlation derived from the variance-covariance matrix of the random effects.

## LVEF

The previously published LVEF model, used as a modeling starting point, described the data well.<sup>19</sup> However, different models were evaluated to separate the delay in cardiac damage after trastuzumab administration and the recovery rate. In the final model, the cardiac damage was generated by cumulative trastuzumab concentrations and the recovery half-life was estimated. The structural model is depicted in Figure 1B. The model was described by the following equations:

$$\frac{dC_{eff}}{dt} = C_{trastuzumab} - \frac{\ln(2)}{T_{1/2rec}} \cdot C_{eff}$$
$$LVEF = LVEF_0 \cdot \left( 1 - \frac{C_{eff}}{C_{eff} + EC_{50}} \right)$$

where  $C_{eff}$  is the effect compartment concentration,  $C_{trastuzumab}$  the trastuzumab concentration in the central compartment,  $T_{1/2rec}$  the recovery half-life (where  $\ln(2) / T_{1/2rec}$  represents the recovery rate constant),  $LVEF_0$  the LVEF baseline value before the first administration of trastuzumab and  $EC_{50}$  the concentration at which 50% of the drug effect occurs. LVEF decline recovered after cessation of trastuzumab treatment with a recovery half-life of 68 days (RSE 17.2%). The BSV for both  $EC_{50}$  and recovery could not be identified, therefore the BSV on recovery was not included in the final model. The BSV in baseline LVEF was moderately positively correlated with the  $EC_{50}$  parameter ( $r=0.585$ ), indicating that patients with a low baseline LVEF tend to have a higher sensitivity to trastuzumab-induced LVEF decline (lower  $EC_{50}$ ). The model described the data adequately, however a slight underprediction was seen for the lower LVEF values (Figure 2B, Figure 3 and Online Resource 1 – Figure S1). This is expected to be the result of discontinuation of treatment in patients experiencing a significant decrease in LVEF, for whom follow up LVEF measurements were not available (e.g. Figure 4A and 4C). Therefore, the recovery to baseline in these patients was not supported by observations, but was predicted by the model.

A decrease in LVEF was classified as significant if LVEF dropped below 45% or when a decrease of 15% from baseline occurred. The final model was evaluated for the candesartan and placebo group separately. No major differences were found in magnitude of parameter estimates or model fit, as expected (data not shown).

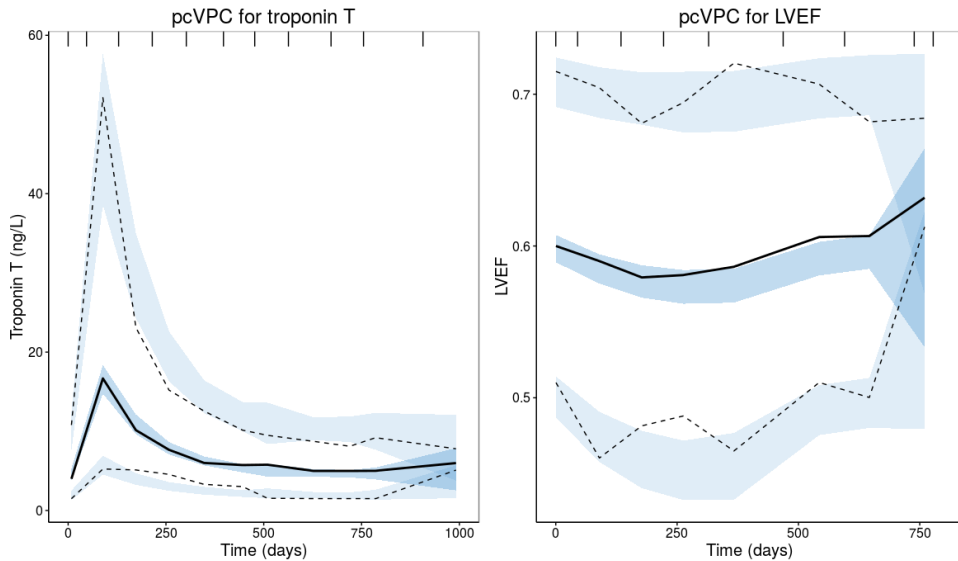


**Figure 3** Prediction corrected Visual Predictive Checks (pcVPCs) for troponin T and left ventricular ejection fractions (LVEF). The solid line represents the median of the observed data, the dashed lines represent the 5th and 95th percentiles of the observed data, the shaded areas represent the 95% confidence interval of the simulated data for the corresponding percentiles (n=500).

### NT-proBNP

NT-proBNP did not demonstrate a clear trend over time during anthracycline or trastuzumab treatment and NT-proBNP concentrations did not increase before LVEF decline occurred and did not behave as an inverse of LVEF decline. Therefore, the NT-proBNP baseline concentrations were evaluated as covariates in the LVEF model. These models were also evaluated for each treatment group separately (candesartan and placebo), leading to similar results.

However, high relative increases of NT-proBNP, approximately 27 weeks after the lowest LVEF value, were observed in 4 patients with a significant decline in LVEF and in 3 patients with no significant decline in LVEF (Online Resource 1, Figures S2 and S3). NT-proBNP increment could, therefore, be a delayed effect of previous LVEF decline, a sign of other underlying cardiac disease or a forecast of development of congestive heart failure, since these patients did not report an increase in heart failure symptoms (NYHA) at the time of the peak. Therefore, NT-proBNP was not included in the LVEF model.

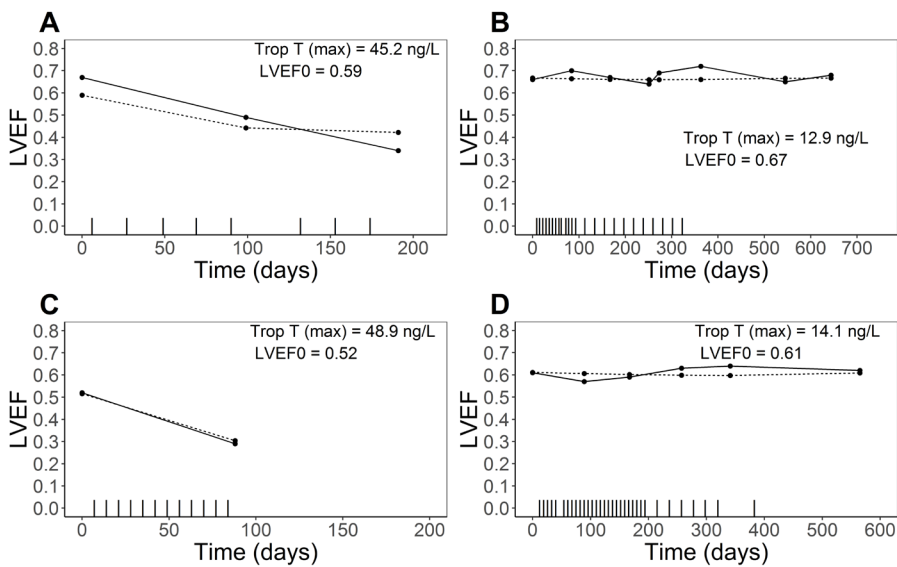


**Figure 4** Panels of individual plots for observed (solid line) and individual predicted (dotted line) left ventricular ejection fractions (LVEFs) over time for 4 different patients. Vertical dashes represent the trastuzumab administrations **A.** patient with maximum troponin T values in the higher range, relatively high baseline and a significant decline in LVEF value. **B.** patient with lower maximum concentration of troponin T, normal baseline and no significant decline in LVEF. **C.** patient with maximum troponin T values in the higher range, relatively low LVEF baseline and a significant decline in LVEF **D.** patient with maximum troponin T values in the lower range, relatively high LVEF baseline and no significant decline in LVEF.

## Covariates

The covariates were evaluated on the *SLOPE* parameter (anthracycline-troponin T model) and on the  $EC_{50}$  and recovery half-life parameter (trastuzumab-LVEF model). No covariates were identified that significantly improved model fit of the anthracycline-troponin T model, except for type of anthracycline on the *SLOPE* parameter. The *SLOPE*-parameter, was significantly affected by the type of anthracycline administered, as illustrated by 2-fold lower estimate for epirubicin compared to doxorubicin (anthracycline-type effect estimate of 0.524 (relative standard error (RSE) 17.5%). This means that, for example, administration of one dose of 100 mg doxorubicine leads to an increase in troponin T from 3 ng/L to 5.6 ng/L, where an equivalent dose of epirubicin would increase troponin T from 3 ng/L to 4.3 ng/L. Considering the LVEF-trastuzumab model, the sensitivity for LVEF decline ( $EC_{50}$  parameter) was significantly affected by the predicted maximum concentration of troponin T after anthracycline treatment. Sensitivity for LVEF decline was higher (decreased  $EC_{50}$  parameter) for patients with a high maximum concentration of troponin T, resulting in a more pronounced decline in LVEF during trastuzumab treatment (Figure 4), described by the following equation:

$$EC_{50i} = EC_{50pop} \cdot \frac{TRP_{max}}{18}^{-1.16}$$

where  $TRP_{max}$  is the peak concentration of troponin T. According to this equation, a peak concentration of 31 ng/L troponin T, would increase the sensitivity to LVEF decrease by a 2-fold (2-fold decrease in  $EC_{50}$ ). The maximum troponin T concentration reduced the between subject variability in sensitivity for LVEF decline from 98.0% in the base model (Online Resource 1, Table S1) to 82.9% in the covariate model. The sensitivity analysis demonstrated that the predicted concentration of troponin T at 21 days after the last anthracycline dose was an equally significant covariate on the  $EC_{50}$  parameter (Online Resource 1, Table S1). The other tested covariates did not significantly improve the model.



## DISCUSSION

The pharmacodynamics of troponin T and LVEF changes during anthracycline and trastuzumab treatment, respectively, were successfully described by the reported models. The maximum concentration of troponin T was a significant determinant of sensitivity to trastuzumab-induced cardiotoxicity, defined as a decline in LVEF values.

Baseline troponin T concentrations were directly affected by anthracycline concentrations. The type of anthracycline significantly affected the linear SLOPE parameter, showing that epirubicin had an approximately 2-fold lower proportional effect on baseline troponin T concentrations compared to doxorubicin. This finding is expected, since at equivalent doses, epirubicin demonstrates less cardiotoxicity than doxorubicin. Moreover, the cumulative lifetime anthracycline dose threshold, associated with increased incidence of heart failure, is also almost a 2-fold higher for epirubicin (950 mg/m<sup>2</sup>) compared to doxorubicin (550 mg/m<sup>2</sup>).<sup>9,10</sup> The anthracycline-troponin T model predicted maximum troponin T concentration at the day of the last anthracycline infusion. However most of the troponin T samples were drawn at approximately 21 days after the last anthracycline dose. To delay the troponin T peak to 21 days, a turnover model was evaluated. However, the recovery rate of troponin T was estimated to be slower than observed, indicating that the peak of troponin T occurs earlier after administration. This is supported by literature, reporting that myocyte damage induced by anthracyclines occurs within hours after administration.<sup>25</sup> In addition, an increase of troponin T within 1-3 days after doxorubicin infusion has been reported in the pediatric setting and an increase in troponin I within hours after high-dose chemotherapy has been reported for adults.<sup>26,27</sup>

The trastuzumab-LVEF model demonstrated a decline in LVEF values that improved after treatment cessation, demonstrated by a recovery of LVEF towards baseline. This analysis prospectively validated the model for LVEF developed in a previously published PK-PD analysis.<sup>19</sup> A high variability in susceptibility to LVEF decline and development of congestive heart failure has been reported in various clinical trials for patients treated with anthracyclines and trastuzumab.

High peak troponin T levels were proved to be predictive for this high sensitivity towards trastuzumab induced LVEF decline. The sensitivity analysis demonstrated that the concentration of troponin T at 21 days after the last anthracycline dose is predictive of sensitivity to trastuzumab-induced cardiotoxicity. In addition, the baseline value of LVEF showed to be moderately positive related to the  $EC_{50}$  parameter, indicating that patients with a low LVEF baseline tend to be more sensitive to trastuzumab-induced LVEF decrease.

Repeated NT-proBNP measurements were not integrated in the model, since NT-proBNP showed high variability. However, some patients experienced high relative increases of NT-proBNP, approximately 27 weeks after their nadir of the LVEF value. An increment in NT-proBNP could therefore possibly be a delayed effect of a prior decline in LVEF, which could be a sign of other cardiac comorbidities or a forecast of development of congestive heart failure. However, early time course data for NT-proBNP, during anthracycline treatment, was lacking for most patients, which could be a reason why NT-proBNP was not identified as an early cardiac biomarker in this cohort. Additionally, NT-proBNP baseline concentrations were not significantly related to anthracycline-induced troponin T increase nor to LVEF decline during trastuzumab treatment.

Age, cardiac history and interval between anthracycline treatment and initiation of trastuzumab treatment have been previously reported as risk factors for trastuzumab-induced cardiotoxicity.<sup>28</sup> In addition, age and pre-existing cardiac disease have been related to anthracycline-induced cardiotoxicity.<sup>29</sup> In this analysis none of these factors could be identified as covariates influencing either trastuzumab-induced cardiotoxicity or anthracycline-induced cardiotoxicity. This could be related to in- and exclusion criteria of the study, since only patients with favorable cardiac history and relatively low age were included, with a maximum age of 69 years and only 13% of patients being older than 60 years. In addition, for only 6% of patients the length of the interval between end of anthracycline and initiation of trastuzumab treatment was longer than 30 days, explaining why time between treatments could not be identified as a covariate in this analysis. Patients in this study were randomized to receive candesartan or placebo, initiated on the first day of trastuzumab treatment.

Therefore, we do not expect that the randomization affects the anthracycline-troponin T model. Candesartan showed no cardio-protective effects in the original study. Nevertheless, to evaluate potential differences between candesartan and placebo for the trastuzumab-LVEF model, treatment group was evaluated as a covariate on the  $EC_{50}$  and found not significantly different. In addition, no differences in parameter estimates or model fit were seen when the trastuzumab-LVEF model was evaluated for each treatment group separately.

The biomarker models were not estimated simultaneously. However, anthracyclines induce troponin T release by damaging cardiac cells, where trastuzumab is hypothesized to cause functional changes in contractile proteins, not associated with cell damage or troponin T changes.<sup>5-7</sup> Therefore, we do not expect that the LVEF changes affect the estimation of the anthracycline-troponin T model. In addition, we used the peak troponin T concentration as a covariate, because the amount of troponin T is expected to be a marker for the amount of damage caused by anthracyclines.

The established models can help evaluate the feasibility of using a cardiac biomarker (e.g. troponin T) to identify patients at risk of trastuzumab-induced LVEF decline. However, clinical applicability is challenged by unstandardized analytical assays for determination of cardiac biomarkers and algorithms to calculate LVEF, definition of the optimal sampling time point, identification of a cut-off value and subsequently determination of a proper strategy in case of identification of an abnormal cardiac value. In addition, subclinical LV dysfunction can be estimated using alternative methods, such as determination of LV diastolic dysfunction and myocardial strain. These parameters give insight in early changes in LV remodeling and have been recommended to monitor patients treated with cardio-toxic anti-cancer drugs.<sup>30</sup>

Although prospective validation is warranted, the developed models can be applied to evaluate cardiac monitoring strategies, such as previously described for LVEF.<sup>12</sup> Simulation of troponin T and LVEF profiles could aid development of adaptive cardiac monitoring protocols, possibly integrating troponin T as a potential biomarker and determination of optimal sampling time points.

Risk-stratified protocols could optimize adaptive dosing in high-risk patients, ensuring maximum possible exposure to trastuzumab, and reduce amount of LVEF measurements in low-risk patients.

In conclusion, to our knowledge this is the first PK-PD analysis that integrated longitudinal data of two cardiac biomarkers during anthracycline and trastuzumab treatment. In this cohort, changes in NT-proBNP could not be demonstrated to be related or predictive of anthracycline- or trastuzumab-induced cardiotoxicity. The analysis identified maximum troponin T concentration after anthracycline treatment as a significant determinant of subsequent trastuzumab-induced LVEF decrease.

## REFERENCES

1. Gianni, L. et al. Treatment with trastuzumab for 1 year after adjuvant chemotherapy in patients with HER2-positive early breast cancer: a 4-year follow-up of a randomised controlled trial. *Lancet Oncol.* 12, 236-244 (2011).
2. Slamon, D. J. et al. Use of chemotherapy plus a monoclonal antibody against HER2 for metastatic breast cancer that overexpresses HER2. *N. Engl. J. Med.* 344, 783-792 (2001).
3. Bang, Y. et al. Trastuzumab in combination with chemotherapy versus chemotherapy alone for treatment of HER2-positive advanced gastric or gastro-oesophageal junction cancer (ToGA): a phase 3, open-label, randomised controlled trial. *Lancet* 376, 687-697
4. Yu, A. F. et al. Trastuzumab interruption and treatment-induced cardiotoxicity in early HER2-positive breast cancer. *Breast Cancer Res. Treat.* 149, 489-495 (2015).
5. Suter, T. M. et al. Trastuzumab-associated cardiac adverse effects in the herceptin adjuvant trial. *J. Clin. Oncol.* 25, 3859-3865 (2007).
6. Ewer, M. S. & Lippman, S. M. Type II chemotherapy-related cardiac dysfunction: Time to recognize a new entity. *J. Clin. Oncol.* 23, 2900-2902 (2005).
7. Cote, G. M., Ph, D., Sawyer, D. B. & Chabner, B. a ERBB2 Inhibition and Heart Failure. *N. Engl. J. Med.* 367, 2150-2153 (2012).
8. Sawyer, D. B., Peng, X., Chen, B., Pentassuglia, L. & Chew, C. Mechanisms of anthracycline cardiac injury: can we identify strategies for cardio-protection? *Prog Cardiovasc Dis* 53, 105-113 (2010).
9. Swain, S. M., Whaley, F. S. & Ewer, M. S. Congestive Heart Failure in Patients Treated with Doxorubicin A Retrospective Analysis of Three Trials. *Cancer* 97, 2869-2879 (2003).
10. Conte, P. F., Gennari, A. & Landucci, E. Role of Epirubicin in Advanced Breast Cancer. *Clin. Breast Cancer* 1, S46-S51 (2000).
11. Seidman, A. et al. Cardiac dysfunction in the trastuzumab clinical trials experience. *J. Clin. Oncol.* 20, 1215-1221 (2002).
12. Hasselt, J. G. C. Van, Schellens, J. H. M., Gillavry, M. R. Mac, Beijnen, J. H. & Huitema, A. D. R. Model-based evaluation and optimization of cardiac monitoring protocols for adjuvant treatment of breast cancer with trastuzumab. *Pharm. Res.* 29, 3499-3511 (2012).

13. Zardavas, D. et al. Role of troponins I and T and N-terminal prohormone of brain natriuretic peptide in monitoring cardiac safety of patients with early-stage human epidermal growth factor receptor 2-positive breast cancer receiving trastuzumab: A herceptin adjuvant study ca. *J. Clin. Oncol.* 35, 878-884 (2017).
14. Cardinale, D. et al. Trastuzumab-induced cardiotoxicity: Clinical and prognostic implications of troponin I evaluation. *J. Clin. Oncol.* 28, 3910-3916 (2010).
15. Tian, S. et al. Serum biomarkers for the detection of cardiac toxicity after chemotherapy and radiation therapy in breast cancer patients. *Front. Oncol.* 4, 277 (2014).
16. Boekhout, A. H. et al. Angiotensin II-Receptor Inhibition With Candesartan to Prevent Trastuzumab-Related Cardiotoxic Effects in Patients With Early Breast Cancer: A Randomized Clinical Trial. *JAMA Oncol.* 2, 1030-7 (2016).
17. Jacqmin, P. et al. Modelling response time profiles in the absence of drug concentrations: Definition and performance evaluation of the K-PD model. *J. Pharmacokinet. Pharmacodyn.* 34, 57-85 (2007).
18. Bruno, R. et al. Population pharmacokinetics of trastuzumab in patients with HER2+ metastatic breast cancer. *Cancer Chemother. Pharmacol.* 56, 361-9 (2005).
19. Hasselt, J. G. C. van, Boekhout, A. H., Beijnen, J. H., Schellens, J. H. M. & Huitema, A. D. R. Population pharmacokinetic-pharmacodynamic analysis of trastuzumab-associated cardiotoxicity. *Clin. Pharmacol. Ther.* 90, 126-132 (2011).
20. Nguyen, T. H. T. et al. Model evaluation of continuous data pharmacometric models: Metrics and graphics. *CPT Pharmacometrics Syst. Pharmacol.* 6, 87-109 (2017).
21. R Core Team, 2018 R: A language and Environment for Statistical Computing. R Foundation for statistical computing, Vienna, Austria. at <<https://www.r-project.org/>>
22. Beal, S., Sheiner, L., Boeckmann, A. & Bauer, R. NONMEM 7.3.0 Users Guides. (1989-2013). ICON Development Solutions, Hanover, MD.
23. Lindbom, L., Ribbing, J. & Jonsson, E. N. Perl-speaks-NONMEM (PsN) - A Perl module for NONMEM related programming. *Comput. Methods Programs Biomed.* 75, 85-94 (2004).
24. Keizer, R. J., Karlsson, M. O. & Hooker, A. Modeling and Simulation Workbench for NONMEM: Tutorial on Pirana, PsN, and Xpose. *CPT pharmacometrics Syst. Pharmacol.* 2, e50 (2013).

25. Unverferth, D. V., Fertel, R. H., Talley, R. L., Magorien, R. D. & Balcerzak, S. P. The effect of first-dose doxorubicin on the cyclic nucleotide levels of the human myocardium. *Toxicol. Appl. Pharmacol.* 60, 151-154 (1981).
26. Lipshultz, S. E. et al. Predictive Value of Cardiac Troponin T in Pediatric Patients at Risk for Myocardial Injury. *Circulation* 2641-2648 (1997).
27. Cardinale, D. et al. Myocardial injury revealed by plasma troponin I in breast cancer treated with high-dose chemotherapy. *Ann. Oncol.* 13, 710-715 (2002).
28. Romond, E. H. et al. Seven-year follow-up assessment of cardiac function in NSABP B-31, a randomized trial comparing doxorubicin and cyclophosphamide followed by paclitaxel (ACP) with ACP plus trastuzumab as adjuvant therapy for patients with node-positive, human epidermal gr. *J. Clin. Oncol.* 30, 3792-3799 (2012).
29. Herrmann, J. et al. Evaluation and management of patients with heart disease and cancer: Cardio-oncology. *Mayo Clin. Proc.* 89, 1287-1306 (2014).
30. Plana, J. C. et al. Expert consensus for multimodality imaging evaluation of adult patients during and after cancer therapy: A report from the American society of echocardiography and the European association of cardiovascular imaging. *J. Am. Soc. Echocardiogr.* 27, 911-939 (2014).





## CHAPTER 3.3

# Neutropenia and docetaxel exposure in metastatic castration-resistant prostate cancer patients: a meta-analysis and evaluation of a clinical cohort

*Cancer Med. 2019 Feb 22 [Epub ahead of print]*

A.H.M. de Vries Schultink  
M.B.S. Crombag  
E. van Werkhoven  
H. Otten  
A.M. Bergman  
J.H.M. Schellens  
A.D.R. Huitema  
J.H. Beijnen

## **ABSTRACT**

### **Background**

The incidence of neutropenia in metastatic castration-resistant prostate cancer (mCRPC) patients treated with docetaxel has been reported to be lower compared to patients with other solid tumors treated with a similar dose. It is suggested that this is due to increased clearance of docetaxel in mCRPC patients, resulting in decreased exposure. The aims of this study were to i) determine if exposure in mCRPC patients is lower versus patients with other solid tumors by conducting a meta-analysis, ii) evaluate the incidence of neutropenia in patients with mCRPC versus other solid tumors in a clinical cohort and iii) discuss potential clinical consequences.

### **Methods**

A meta-analysis was conducted of studies which reported areas under the plasma concentration-time curves (AUCs) of docetaxel and variability. In addition, grade 3/4 neutropenia was evaluated using logistic regression in a cohort of patients treated with docetaxel.

### **Results**

The meta-analysis included 36 cohorts from 26 trials (n=1150 patients), and showed that patients with mCRPC had a significantly lower mean AUC versus patients with other solid tumors (fold-change [95% confidence interval (CI)]: 1.8 [1.5-2.2]), with corresponding AUCs of 1.82 and 3.30 mg·h/L, respectively. Logistic regression, including 812 patients, demonstrated that patients with mCRPC had a 2.2-fold lower odds of developing grade 3/4 neutropenia compared to patients with other solid tumors (odds ratio [95%CI]: 0.46 [0.31-0.90]).

### **Conclusion**

These findings indicate that mCRPC patients have a lower risk of experiencing severe neutropenia, possibly attributable to lower systemic exposure to docetaxel.

## INTRODUCTION

Docetaxel is a chemotherapeutic agent, currently approved for the treatment of various solid tumors, including breast cancer, head and neck cancer, gastric adenocarcinoma, non-small-cell lung cancer (NSCLC) and metastatic castration-resistant prostate cancer (mCRPC). The pharmacokinetic (PK) profile of docetaxel is best described by a three-compartment model with a rapid distribution of the drug and longer elimination half-life.<sup>1</sup> Docetaxel is for more than 90% protein-bound and binds mainly to  $\alpha$ 1-acid glycoprotein, albumin and lipoproteins. Docetaxel is metabolized in the liver by the CYP3A4 enzyme and eliminated via biliary excretion.<sup>2</sup> The clearance of docetaxel is affected by hepatic impairment,  $\alpha$ 1-acid glycoprotein and body surface area (BSA), explaining part of the variability in clearance.<sup>3</sup> Nevertheless, relatively high remaining unexplained variability in PK exists,<sup>1</sup> affecting both response and toxicity rates. Lower exposure to docetaxel has been related to shorter time to progression in patients with NSCLC.<sup>4</sup> Additionally, a 50% decrease in clearance has been related to a 4.3-fold increase in odds of developing grade 3/4 (severe/life-threatening) neutropenia.<sup>4</sup>

It has been reported that mCRPC patients experience less grade 3/4 neutropenia compared to patients with other solid tumors. Proportions of 32% and 16% have been reported for mCRPC patients treated with 75 mg/m<sup>2</sup> and 60-70 mg/m<sup>2</sup> docetaxel,<sup>5,6</sup> compared to 65% reported for patients with NSCLC receiving a comparable dose. Percentages between 61% and 68% have also been reported in different studies including non-castrated prostate cancer patients, receiving doses of 70-75 mg/m<sup>2</sup>.<sup>7-9</sup> A study by Franke et al. demonstrated a 2-fold lower area under the plasma concentration-time curve (AUC) in mCRPC patients compared to non-castrated prostate cancer patients<sup>10</sup>, which may explain the lower incidence of hematological toxicity in mCRPC patients treated with standard doses of docetaxel.

Extensive PK analyses have been conducted before docetaxel was approved for mCRPC in 2004.<sup>4</sup> In recent years, many independent clinical trials have been published, reporting PK characteristics of docetaxel in both mCRPC patients and patients with other solid tumors, enabling us to perform this meta-analysis.

In this study we aim i) to determine if mCRPC patients demonstrate lower exposure to docetaxel compared to patient with other solid tumors, by including data from literature in a meta-analysis, ii) to evaluate the incidence of neutropenia in patients with mCRPC versus patients with other solid tumors treated with docetaxel in clinical practice and iii) to evaluate the possible clinical implications of our findings.

## METHODS

### Meta-analysis

#### Data

PubMed was searched using the terms: “docetaxel AND (pharmacokinetics OR pharmacokinetic)”. Studies were included in the meta-analysis if an  $AUC_{0-inf}$  (hereafter AUC) was reported with a variance parameter, either standard deviation (SD) or coefficient of variation (CV). If AUC was not reported but clearance (L/h/m<sup>2</sup>) was reported with a variance parameter, the study was included and the AUC was calculated using the following equation:

$$AUC_{0-inf} = \frac{Dose}{Clearance}$$

The variance of AUC for these patients was then calculated based on the CV or SD of the clearance parameter, using the following equation:

$$CV = \frac{Standard\ deviation}{mean} \cdot 100\%$$

Studies that reported PK parameters for other solid tumors than mCRPC, were excluded if the PK parameters were reported for various tumor types, including prostate cancer patients, or if part of the tumor types included were unspecified, but could potentially be mCRPC based on inclusion criteria.

Of studies that reported AUCs for two cohorts, e.g. with and without another drug, only the monotherapy cohort was included. Combination cohorts were only

included if no drug interaction was to be expected. Additionally, if the same cohort of patients was sampled twice, the AUC for docetaxel monotherapy was included.

The following information was extracted from the publication: the AUC or clearance parameter with the corresponding variance parameter, number of patients for whom PK parameter was calculated, tumor type, dose level ( $\text{mg}/\text{m}^2$ ), time point at which the last sample was drawn, concurrent therapy, hepatic function, method used to calculate the AUC and allowance of co-medication affecting CYP3A4 metabolism.

Tumor type (mCRPC, yes/no) was evaluated as a covariate on AUC. Other covariates that were expected to influence AUC were included in the model. Firstly, the last time point at which a PK sample was taken was evaluated, to correct for differences in extrapolation of AUC to infinity. Studies in which a Bayesian PK approach was used, were classified as extrapolating from the last time point on which the Bayesian estimates were based, regardless of limited sampling strategy. Additionally, hepatic function was included as a covariate. A previous analysis demonstrated that patients with transaminases levels  $>1.5$  x the upper limit of normal (ULN) and alkaline phosphatase (AP)  $>2.5$  x ULN have a 27% reduction in docetaxel clearance<sup>3</sup>. Studies were classified based on these values reported in the ex- or inclusion criteria or in the patient characteristics table. A study was classified as having patients with adequate hepatic function, if patients with elevated transaminases or AP were excluded (either both or one of the two). If a study allowed patients with elevated transaminases and AP, this was classified as possibly inadequate hepatic function. If nothing on hepatic function was reported, though patients with liver metastases were included, this was classified as having patients with possibly inadequate. If a study stated that patients with adequate organ or liver function were included, without reference values, this study was classified as adequate hepatic function.

As previously reported, docetaxel exposure increases proportionally with dose.<sup>4</sup> AUC values were dose-normalized to  $75 \text{ mg}/\text{m}^2$ , the corresponding SD values were scaled by calculation of the CV.

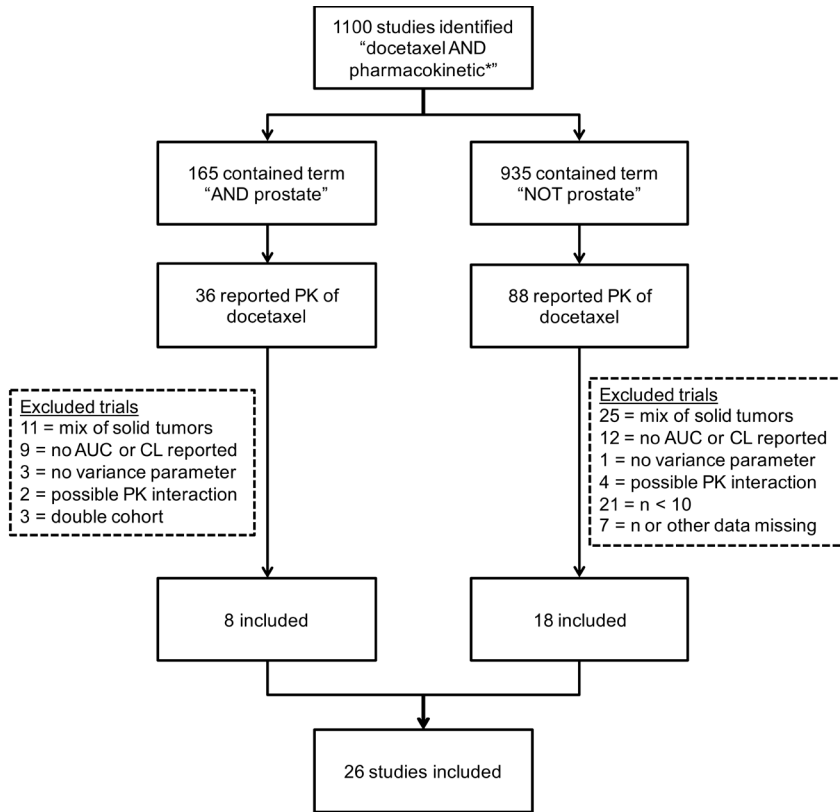


**Figure 1** Flowchart of study inclusion in the meta-analysis. Mix of solid tumors = trial included various solid tumor types including prostate cancer patients, and/or included unspecified or unknown tumor types, potentially being prostate cancer; n = number of patients for whom pharmacokinetic (PK) parameters were reported; AUC = Area under the plasma concentration-time curve extrapolated to infinity, CL = clearance in L/h/m<sup>2</sup>.

### Statistical analysis

The meta-analysis was conducted in R (version 3.4.3), using the metafor package (version 2.0-0).<sup>11,12</sup> A random effects model was used to analyze the data. The normalized AUC values were log-transformed in order to estimate a fold-change in AUC. Additionally, the sampling variance was calculated using the reported SDs:

$$V = \frac{SD^2}{\sqrt{n}} / AUC^2$$

Where  $V$  is the sampling variance and  $n$  the number of patients. Heterogeneity between studies was evaluated with the I-squared statistic.

### **Clinical cohort**

Patients treated with docetaxel between January 2006 and January 2016 at the Netherlands Cancer Institute or the Medical Center Slotervaart (both Amsterdam, the Netherlands) were eligible for inclusion. Docetaxel was either administered as monotherapy or in combination with chemotherapy or targeted therapies. All docetaxel-containing regimens were administered according to standard treatment protocols. Patients were excluded if neutrophil measurements were not available, BSA or per protocol dosage was not recorded or if the patient was enrolled in a clinical trial in which docetaxel treatment was part of the intervention. Patients >70 years were also excluded from the analysis, since increased neutropenia in elderly patients is more related to a deprived bone marrow reserve or increased sensitivity to docetaxel treatment, and not solely to exposure to docetaxel.<sup>4,13</sup> Patient characteristics, neutrophil counts at cycle 1, and underlying malignancies were extracted from patients' medical records. Neutropenia was graded according to the Common Terminology Criteria for Adverse Events (CTCAE) Version 4.03.<sup>14</sup>

### *Statistical analysis*

A multivariable logistic regression model was used to assess if grade 3/4 neutropenia was associated with mCRPC. Dose (classified as: <60 mg/m<sup>2</sup>, 60-75 mg/m<sup>2</sup> and 100 mg/m<sup>2</sup>) and concomitant administration of other chemotherapy (yes/no) were evaluated as predictors. Logistic regression was performed using R (Version 3.4.3), a two-sided  $p$ -value of <0.05 was considered significant.

Table 1 Study and cohort specific characteristics.

#1	COHORT <sup>a</sup>	STUDY	CO-MEDICATION	DOSE MG/M <sup>2</sup>	METHOD	TUMOR TYPE	AUC MG-H/L	AUC CALC.	SD	SD V
1	1	Franke 2010 <sup>10</sup>	dexa	75	NCA	mCRPC	4.27	yes <sup>b</sup>	1.86	yes <sup>f</sup>
2	1	Morris 2016 <sup>15</sup>	pred	75	NCA	mCRPC	2.00	-	0.7	yes <sup>g</sup>
3	1	Araujo 2012 <sup>16</sup>	pred	75	NCA	mCRPC	2.66	-	1.17	yes <sup>h</sup>
4	1	Tagawa 2016 <sup>17</sup>	pred	60	NCA	mCRPC	3.58	-	0.72	-
4	2	Tagawa 2016 <sup>17</sup>	pred	75	NCA	mCRPC	2.74	-	0.58	-
4	3	Tagawa 2016 <sup>17</sup>	pred	75	NCA	mCRPC	3.14	-	0.48	-
5	1	Tolcher 2005 <sup>18</sup>	pred+oblimerson	75	NCA	mCRPC	0.73	-	0.91	-
6	1	Tolcher 2004 <sup>19</sup>	dexa+oblimerson	60	NCA	mCRPC	0.87	-	0.41	-
6	2	Tolcher 2004 <sup>19</sup>	dexa+oblimerson	75	NCA	mCRPC	2.00	-	1.11	-
6	3	Tolcher 2004 <sup>19</sup>	dexa+oblimerson	75	NCA	mCRPC	1.96	-	0.61	-
6	4	Tolcher 2004 <sup>19</sup>	dexa+oblimerson	100	NCA	mCRPC	1.61	-	0.16	-
7	1	Bousquet 2011 <sup>20</sup>	pred+dexa	75	NCA	mCRPC	1.86	-	0.64	-
8	1	Hervonen 2003 <sup>21</sup>	ifosfamide+pre-med	40	Pop	mCRPC	1.08	-	0.15	-
1	2	Franke 2010 <sup>10</sup>	dexa	75	NCA	Prostate	8.25	yes <sup>b</sup>	2.42	yes <sup>f</sup>
9	1	Minami 2004 <sup>22</sup>	dexa+cisplatin	35	NCA	NSCLC	1.40	-	0.64	-
9	2	Minami 2004 <sup>22</sup>	dexa+cisplatin	20	NCA	NSCLC	0.79	-	0.34	-
10	1	Bruno 2001 <sup>3</sup>	-	75	Pop	Mix	3.64	yes <sup>c</sup>	1.22	yes <sup>h</sup>
11	1	Taylor 2015 <sup>23</sup>	-	75	NCA	Mix	2.47	-	0.91	-
12	1	Okamoto 2015 <sup>24</sup>	-	60	NCA	NSCLC	3.27	-	1.18	yes <sup>h</sup>
12	2	Okamoto 2015 <sup>24</sup>	-	75	NCA	NSCLC	3.81	-	0.88	yes <sup>h</sup>
13	1	Moulder 2012 <sup>25</sup>	dexa	75	NCA	Breast	3.46	yes <sup>d</sup>	1.06	-
14	1	Michael 2012 <sup>26</sup>	dexa	75	NCA	Mix	2.81	-	0.79	yes <sup>h</sup>
15	1	Cox 2006 <sup>27</sup>	dexa	30	NCA	Breast	1.34	-	0.70	-
16	1	Garland 2006 <sup>28</sup>	dexa	60	NCA	Mix	2.47	-	1.04	yes <sup>h</sup>



16	2	Garland 2006 <sup>28</sup>	dexa	75	NCA	Mix	3.03	-	0.97	yes <sup>h</sup>
17	1	Yamamoto 2005 <sup>29</sup>	-	60	Pop	NSCLC	2.71	-	0.4	-
18	1	Takigawa 2004 <sup>30</sup>	dexa	60	NCA	NSCLC	1.79	-	0.52	-
19	1	Freyer 2002 <sup>31</sup>	cortico	100	NCA	Breast	3.34	yes <sup>c</sup>	1.01	yes <sup>h</sup>
20	1	Rougier 2000 <sup>32</sup>	-	100	Pop	Pancreas	5.08	-	1.63	yes <sup>h</sup>
21	1	Soliman 2014 <sup>33</sup>	dexa+indoximod	60	NCA	Mix	4.08	-	2.61	-
22	1	Macaulay 2013 <sup>34</sup>	AVE1642+premed	75	NCA	Mix	4.59	-	4.2	-
23	1	Hor 2008 <sup>35</sup>	doxorubicin	75	NCA	Breast	3.80	-	2.2	-
24	1	Casanova 2016 <sup>36</sup>	cisplatin+d- exa+5-FU	75	Pop	Nasoph.	3.41	-	1.98	-
25	1	Chow 2008 <sup>37</sup>	dexa+PI-88	30	Pop	Mix	1.12	yes <sup>f</sup>	0.32	yes <sup>f</sup>
26	1	Nieto 2007 <sup>38</sup>	gemci+mephalan+ carbo	300	Pop	Mix	15.50	-	4.3	-
26	2	Nieto 2007 <sup>38</sup>	gemci+mephalan+ carbo	350	Pop	Mix	18.90	-	4.4	-

AUC = Area under the concentration-time curve extrapolated to infinity, AUC calc. = AUC is derived, requested or calculated (see footnotes), SD = standard deviation, SD calc. = SD is derived, requested or calculated (see footnotes), dexa = dexamethasone, pred = prednisone, premed = premedication, cortico = corticosteroids, 5-FU = fluorouracil, gemci = gemcitabine, carbo = carboplatin, NCA = non-compartmental analysis, Pop compartmental = population pharmacokinetic analysis, mCRPC = metastatic castration-resistant prostate cancer, NSCLC = non-small cell lung cancer, Mix various tumor types (excluding mCRPC), nasoph. = nasopharyngeal

<sup>a</sup>If PK of docetaxel was reported for multiple cohorts, characteristics were reported per cohort.

<sup>b</sup>AUC dose normalized by authors

<sup>c</sup>AUC calculated from clearance

<sup>d</sup>AUC calculated for each patients, dose normalized to 75 mg/m<sup>2</sup>

<sup>e</sup>Conversion nmol to mg

<sup>f</sup>SD provided by authors

<sup>g</sup>AUCs derived from plot, SD approximated

<sup>h</sup>SD calculated from CV

## RESULTS

### Meta-analysis

#### Data

The search identified 1100 studies. In total, 26 studies were included in the meta-analysis, reporting PK of docetaxel for 36 patient cohorts (n=1150).<sup>3,10,15-38</sup> A large number of papers were available for the other solid tumor group, where some reported PK for small patient cohorts. Therefore, cohorts of less than 10 patients were excluded from the analysis. The inclusion-overview is depicted in Figure 1.

Main trial characteristics were extracted from the articles and reported per cohort (Table 1). The dose-normalized AUCs and their confidence intervals are depicted in Figure 2.

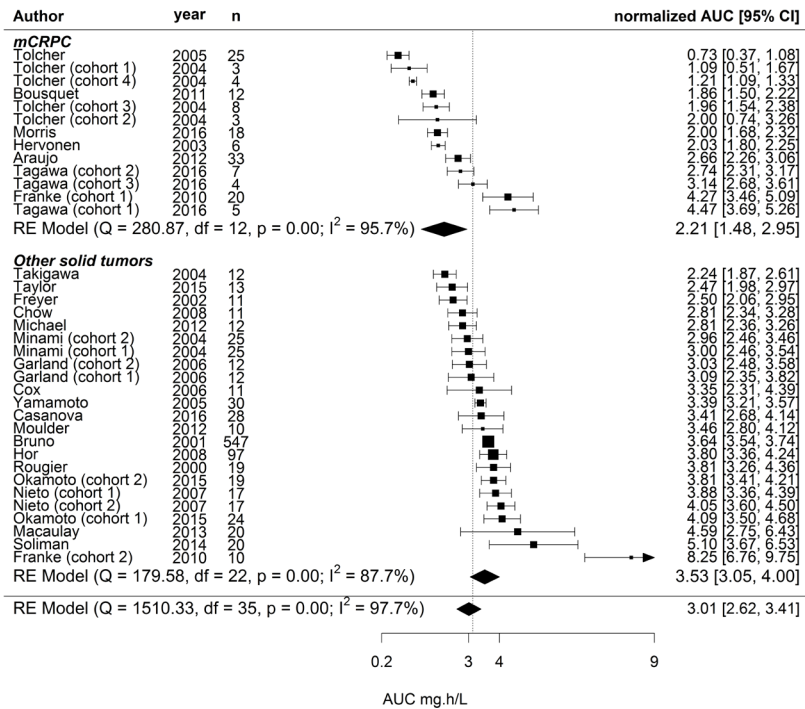


**Figure 2** Forest plot for all studies included in the meta-analysis; n amount of patient in cohort. AUC area under the plasma concentration-time, extrapolated to infinity and dose-normalized to 75 mg/m<sup>2</sup>.

## Statistical analysis

In the final model (Figure 3), patients with mCRPC had a 1.8-fold, 95% confidence interval (CI)[1.5-2.2] lower AUC than patients with other solid tumors ( $p < 0.0001$ ). Corresponding AUCs were 1.82 mg·h/L versus 3.30 mg·h/L extrapolated from 24 hours with adequate liver function, respectively. Patients for whom the AUC was extrapolated from a time point of 504 hours had a 2.4-fold higher AUC compared to extrapolation from 24 or 48 hours ( $p < 0.001$ ). There was no difference between extrapolation from 24 and 48 hours (1.01-fold,  $p > 0.05$ ). Lastly, studies that allowed inclusion of patients with elevated transaminases and AP had a 1.2-fold higher AUC than trials not including these patients, though this was not significant.

The residual heterogeneity in the final model remained high ( $I^2 = 91.7\%$ ), indicating that the differences in AUCs might be due to uncharacterized or unexplained underlying factors. Therefore, a sensitivity analysis was performed with a higher sampling error per cohort, which reduced the heterogeneity to low ( $I^2 = 18\%$ ).

In this analysis, mCRPC remained a significant determinant of having lower exposure to docetaxel, with a 1.6-fold difference and corresponding AUCs of 2.04 mg·h/L and 3.34 mg·h/L, for mCRPC versus other solid tumors.

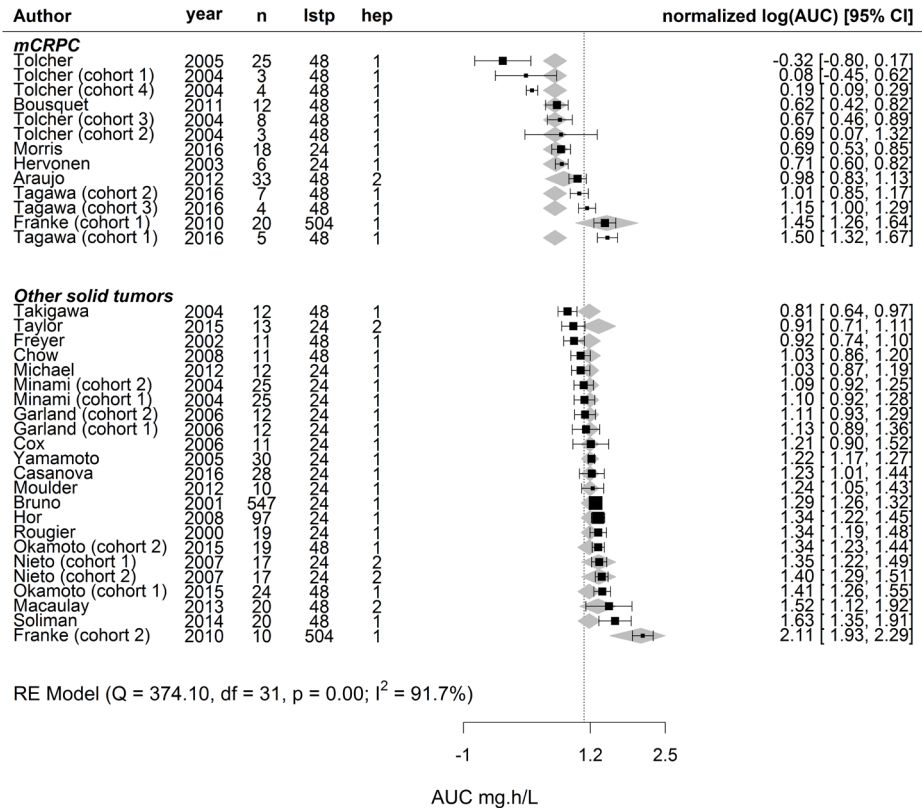


**Figure 3** Forest plot with log-transformed dose normalized AUC values and model predictions including covariates, n number of patients, lstp last measured time point, hep hepatic function (1 = only patients with normal liver enzymes included, 2 = patients with both normal and elevated liver enzymes included), 95% CI 95% confidence interval

**Clinical cohort**

In total, 812 patients were included in the analysis, 115 in the mCRPC group and 697 in the other solid tumors group. Patient characteristics are depicted in Table 2.

**Table 2 Patient characteristics clinical cohort.**

	MCRPC (N=115)	SOLID TUMORS (N=697)
<b>Units</b>	n (%)	n (%)
<i>Tumor type</i>		
Prostate	115 (100)	-
Breast	-	501 (71.9)
Lung	-	62 (8.9)
Gastric/esophagus	-	73 (10.5)
Head and neck	-	24 (3.4)
Other	-	37 (5.3)
<i>Dose (mg/m<sup>2</sup>)</i>		
<60	5 (4.4)	84 (12.1)
60-75	109 (94.8)	578 (82.9)
100	1 (0.8)	35 (5.0)
<i>Hospital</i>		
MC Slotervaart	4 (3.5)	72 (10.3)
Netherlands Cancer Institute	111 (96.5)	625 (89.7)

### Statistical analysis

Multivariable logistic regression demonstrated that after correction for dose, patients with mCRPC had a significantly lower risk of developing a grade 3/4 neutropenia than patients with other solid tumors (odds ratio [95% CI]: 0.46 [0.32-0.90],  $p = 0.035$ ). Neutropenia occurred in 16.5% of patients in the solid tumor group, compared to 7.8% in the mCRPC group. Patients who received a dose of 100 mg/m<sup>2</sup> docetaxel or more were also at increased risk of developing grade 3/4 neutropenia (Table 3). Including different tumor types in the logistic regression model as a categorical covariate instead of binary (mCRPC yes/no), did not demonstrate a significant different risk of developing grade 3/4 neutropenia for any of the other tumor types. Concomitant administration of other types of chemotherapy was not related to occurrence of grade 3/4 neutropenia and was excluded from the final model. Since most mCRPC patients were treated in the NKI, a sub-analysis was performed for only NKI patients. In this analysis mCRPC patients remained to have a significantly lower odds of developing a grade 3/4 neutropenia compared to patients with other solid tumors.

**Table 3 Odds ratios for experiencing grade 3/4 neutropenia.**

VARIABLE	ODDS RATIO [95%CI]	P-VALUE
Solid tumors <sup>A</sup>	1.00	-
mCRPC <sup>B</sup>	0.46[0.21-0.90]	0.035
Dose <60 mg/m <sup>2</sup>	0.72[0.34-1.39]	0.359
Dose 100 mg/m <sup>2</sup>	5.04[2.50-10.1]	<0.0001

<sup>A</sup>Reference group: patients with solid tumors receiving 60-75 mg/m<sup>2</sup>

<sup>B</sup>metastatic castration-resistant prostate cancer

## DISCUSSION

This meta-analysis demonstrated that patients with mCRPC had a significantly (1.8-fold) lower AUC than patients with other solid tumors. Furthermore, the analysis of our clinical patient cohort demonstrated that patients with mCRPC had a 2.2-fold lower odds of experiencing grade 3/4 neutropenia. These findings indicate that mCRPC patients experiencing more severe neutropenia, potentially attributable to lower systemic exposure to docetaxel.

The mechanism behind the decreased exposure to docetaxel in mCRPC patients remains to be elucidated. Possibly, castration levels of testosterone cause an increase in elimination and thus lower exposure of docetaxel. Franke et al. demonstrated a higher uptake of docetaxel in the liver in castrated rats. This higher uptake was concurrent with an increase in expression of rOat2, a transporter regulating the uptake of docetaxel from the circulation into hepatocytes. Several studies have demonstrated lack of association between castration and CYP3A4 activity: Franke et al. did not find an association between castration and elevated hepatic CYP3A4 activity and another study, investigating CYP3A4 activity before and 8 weeks after leuprolide or goserelin treatment in prostate cancer patients, did not find a difference in CYP3A4 activity.<sup>39</sup> In addition, Bruno et al. have previously demonstrated that  $\alpha$ 1-acid glycoprotein levels have a minor effect on clearance, where the free-fraction of docetaxel remained unchanged.<sup>3</sup> Therefore, it is not expected that CYP3A4 activity or  $\alpha$ 1-acid glycoprotein levels, are altered in patients with castration-levels of testosterone.

Prostate cancer patients receiving docetaxel treatment concurrent with androgen deprivation therapy in an early phase of the disease have castration levels of testosterone (<50 ng/dL). However, these patient experienced more toxicity compared to castration-resistant prostate cancer patients that received docetaxel in a later phase of disease.<sup>40</sup> Therefore, it is likely that the length of androgen-deprivation therapy is of importance in the mechanism behind the PK changes of docetaxel in mCRPC patients.

Regarding the covariates included in the meta-analysis, patients for whom AUC was extrapolated from a time point of 504 hours had a significantly higher AUC of docetaxel compared to extrapolation from 24 or 48 hours, due to a lower slope of the regression line, of the latter. Since the trials included both patients with elevated and normal liver enzymes, a less profound effect of elevated liver enzymes was found, in contrast to a previously demonstrated decrease in clearance of 27%.<sup>3</sup> In addition, the drug label recommends to not administer docetaxel to patients with elevated transaminases and AP.<sup>41</sup> Co-administration of CYP3A4 inhibitors or inducers could potentially affect the PK of docetaxel. Most trials did not specifically report if use of these drugs was allowed. However, the docetaxel label advices to avoid use of concomitant strong CYP3A4 inhibitors.

Our results should be interpreted considering several limitations. The meta-analysis demonstrated high variability between studies, regardless of using a random effects model, accounting for between-study variability. However, high heterogeneity is expected, since the majority of studies reported AUCs for either mCRPC or other solid tumors, whereas only one study conducted a head-to-head comparison.<sup>10</sup> The sensitivity analysis demonstrated that the differences in AUCs remained significant, with an increased sampling variance, that substantially reduced the heterogeneity and the risk of a false positive result.

Docetaxel is typically administered in combination with prednisone for mCRPC patients.<sup>6</sup> Prednisone is known to be an inducer of CYP3A4 and could therefore possibly increase the clearance of docetaxel. However, the TAX327 study demonstrated that co-administration of 5 mg prednisone administered twice daily did not affect the PK of docetaxel.<sup>6</sup>

Publication bias is not expected to be an issue, since PK parameters were often not the endpoints of the studies.

The absolute percentages of severe neutropenia reported in this study (7.6% versus 16.5%, for mCRPC and other solid tumors, respectively), were substantially lower than previously reported in literature (16% and 32% for mCRPC versus 61%-68% for other solid tumors). However, neutropenia in this study was evaluated in the first cycle and nadir values were not specifically monitored in the NKI. A sub-analysis was performed for only NKI patients and demonstrated a similar significant difference in odds between the groups.

A dose-response relationship for docetaxel in specifically mCRPC has not been previously reported. However, for patients with NSCLC the AUC in the first cycle was a significant predictor for the time to progression.<sup>4</sup> In general, chemotherapeutic agents, like docetaxel, are dosed at the maximum tolerated dose to achieve maximum effect. Therefore, mCRPC patients might benefit from a dose increment.

In conclusion, patients with mCRPC have a 1.8-fold lower docetaxel AUC compared to patients with other solid tumors as determined by our meta-analysis. This could explain the lower incidence of neutropenia reported in this patient population, which was confirmed in our clinical cohorts. Based on these results, patients with mCRPC, that are progressive on anti-androgen treatment and to be treated with docetaxel, could potentially benefit from a dose increment, considering that patients may be able to tolerate higher doses of the drug. The clinical implications of our findings need to be evaluated prospectively.



## REFERENCES

1. Bruno, R. et al. A population pharmacokinetic model for docetaxel (Taxotere): model building and validation. *J. Pharmacokinet. Biopharm.* 24, 153-172 (1996).
2. Clarke, S. J. & Rivory, L. P. Clinical pharmacokinetics of docetaxel. *Clin. Pharmacokinet.* 36, 99-114 (1999).
3. Bruno, R., Vivier, N., Veyrat-Follet, C., Montay, G. & Rhodes, G. R. Population pharmacokinetics and pharmacokinetic-pharmacodynamic relationships for docetaxel. *Invest. New Drugs* 19, 163-169 (2001).
4. Bruno, B. R. et al. Population Pharmacokinetics / Pharmacodynamics of Docetaxel in Phase II Studies in Patients With Cancer. *J. Clin. Oncol.* 16, 187-196 (1998).
5. Petrylak, D. P. et al. Docetaxel and estramustine compared with mitoxantrone and prednisone for advanced refractory prostate cancer. *N. Engl. J. Med.* 351, 1513-1520 (2004).
6. Tannock, I. F. et al. Docetaxel plus Prednisone or Mitoxantrone plus Prednisone for Advanced Prostate Cancer. *N Engl J Med* 351, 1502-1512 (2004).
7. Rathkopf, D. et al. Phase II trial of docetaxel with rapid androgen cycling for progressive noncastrate prostate cancer. *J. Clin. Oncol.* 26, 2959-2965 (2008).
8. Hussain, A. et al. Docetaxel followed by hormone therapy in men experiencing increasing prostate-specific antigen after primary local treatments for prostate cancer. *J. Clin. Oncol.* 23, 2789-2796 (2005).
9. Taplin, M. E. et al. Docetaxel, estramustine, and 15-month androgen deprivation for men with prostate-specific antigen progression after definitive local therapy for prostate cancer. *J. Clin. Oncol.* 24, 5408-5413 (2006).
10. Franke, R. M., Carducci, M. A., Rudek, M. A., Baker, S. D. & Sparreboom, A. Castration-dependent pharmacokinetics of docetaxel in patients with prostate cancer. *J. Clin. Oncol.* 28, 4562-4567 (2010).
11. Viechtbauer, W. Conducting Meta-Analyses in R with the metafor Package. *J. Stat. Softw.* 36, 1-48 (2010).
12. R Core Team, 2018 R: A language and Environment for Statistical Computing. R Foundation for statistical computing, Vienna, Austria. at <<https://www.r-project.org/>>

13. Lipschitz, D., Udupa, K., Milton, K. & Thompson, C. Effect of Age on Hematopoiesis in Man. *Blood* 63, 502–509 (1984).
14. Institute, N. cancer Common Terminology Criteria for Adverse Events (CTCAE) Common Terminology Criteria for Adverse Events v4.0 (CTCAE). (2009).
15. Morris, M. J. et al. Phase Ib study of enzalutamide in combination with docetaxel in men with metastatic castration-resistant prostate cancer. *Clin. Cancer Res.* 22, 3774–3781 (2016).
16. Araujo, J. C. et al. Dasatinib combined with docetaxel for castration-resistant prostate cancer: Results from a phase 1-2 study. *Cancer* 118, 63–71 (2012).
17. Tagawa, S. T. et al. Phase 1b Study of Abiraterone Acetate Plus Prednisone and Docetaxel in Patients with Metastatic Castration-resistant Prostate Cancer. *Eur. Urol.* 70, 718–721 (2016).
18. Tolcher, A. W. et al. A phase II, pharmacokinetic, and biological correlative study of oblimersen sodium and docetaxel in patients with hormone-refractory prostate cancer. *Clin. Cancer Res.* 11, 3854–3861 (2005).
19. Tolcher, A. W. et al. A phase I pharmacokinetic and biological correlative study of oblimersen sodium (Genasense, G3139), an antisense oligonucleotide to the Bcl-2 mRNA, and of docetaxel in patients with hormone-refractory prostate cancer. *Clin. Cancer Res.* 10, 5048–5057 (2004).
20. Bousquet, G. et al. Phase I study of BIBF 1120 with docetaxel and prednisone in metastatic chemo-naïve hormone-refractory prostate cancer patients. *Br. J. Cancer* 105, 1640–5 (2011).
21. Hervonen, P., Jekunen, A., Lefebvre, P. & Kellokumpu-Lehtinen, P. Docetaxel-ifosfamide combination chemotherapy in patients with metastatic hormone-refractory prostate cancer: A phase I pharmacokinetic study. *Int. J. Clin. Pharmacol. Res.* 23, 1–7 (2003).
22. Minami, H. et al. Comparison of pharmacokinetics and pharmacodynamics of docetaxel and cisplatin in elderly and non-elderly patients: Why is toxicity increased in elderly patients? *J. Clin. Oncol.* 22, 2901–2908 (2004).
23. Taylor, S. E. et al. Phase I study of intravenous (IV) docetaxel and intraperitoneal (IP) oxaliplatin in recurrent ovarian and fallopian tube cancer. *Gynecol. Oncol.* 138, 548–553 (2015).

24. Okamoto, I. et al. Tolerability of nintedanib (BIBF 1120) in combination with docetaxel: A phase 1 study in Japanese patients with previously treated non-small-cell lung cancer. *J. Thorac. Oncol.* 10, 346–352 (2015).
25. Moulder, S. et al. A phase 1 study of weekly everolimus (RAD001) in combination with docetaxel in patients with metastatic breast cancer. *Cancer* 118, 2378–2384 (2012).
26. Michael, M. et al. Docetaxel pharmacokinetics and its correlation with two in vivo probes for cytochrome P450 enzymes: The C14-erythromycin breath test and the antipyrine clearance test. *Cancer Chemother. Pharmacol.* 69, 125–135 (2012).
27. Cox, M. C. et al. Influence of garlic (*Allium sativum*) on the pharmacokinetics of docetaxel. *Clin. Cancer Res.* 12, 4636–4640 (2006).
28. Garland, L. L. et al. A phase I clinical and pharmacokinetic study of oral CI-1033 in combination with docetaxel in patients with advanced solid tumors. *Clin. Cancer Res.* 12, 4274–4282 (2006).
29. Yamamoto, N. et al. Randomized pharmacokinetic and pharmacodynamic study of docetaxel: Dosing based on body-surface area compared with individualized dosing based on cytochrome P450 activity estimated using a urinary metabolite of exogenous cortisol. *J. Clin. Oncol.* 23, 1061–1069 (2005).
30. Takigawa, N. et al. Clinical and pharmacokinetic study of docetaxel in elderly non-small-cell lung cancer patients. *Cancer Chemother. Pharmacol.* 54, 230–236 (2004).
31. Freyer, G. et al. Influence of amifostine on the toxicity and pharmacokinetics of docetaxel in metastatic breast cancer patients: A pilot study. *Clin. Cancer Res.* 8, 95–102 (2002).
32. Rougier, P. et al. A phase II study: Docetaxel as first-line chemotherapy for advanced pancreatic adenocarcinoma. *Eur. J. Cancer* 36, 1016–1025 (2000).
33. Soliman, H. H. et al. A first in man phase I trial of the oral immunomodulator, indoximod, combined with docetaxel in patients with metastatic solid tumors. *Oncotarget* 5, 8136–8146 (2014).
34. Macaulay, V. M. et al. Phase I study of humanized monoclonal antibody AVE1642 directed against the type 1 insulin-like growth factor receptor (IGF-1R), administered in combination with anticancer therapies to patients with advanced solid tumors. *Ann. Oncol.* 24, 784–791 (2013).
35. Hor, S. Y. et al. PXR, CAR and HNF4 $\alpha$  genotypes and their association with pharmacokinetics and pharmacodynamics of docetaxel and doxorubicin in Asian patients. *Pharmacogenomics J.* 8, 139–146 (2008).

36. Casanova, M. et al. International randomized phase 2 study on the addition of docetaxel to the combination of cisplatin and 5-fluorouracil in the induction treatment for nasopharyngeal carcinoma in children and adolescents. *Cancer Chemother. Pharmacol.* 77, 289–298 (2016).
37. Chow, L. Q. M. et al. A phase I pharmacological and biological study of PI-88 and docetaxel in patients with advanced malignancies. *Cancer Chemother. Pharmacol.* 63, 65–74 (2008).
38. Nieto, Y. et al. Phase I and Pharmacokinetic Study of Gemcitabine Administered at Fixed-Dose Rate, Combined with Docetaxel/Melphalan/Carboplatin, with Autologous Hematopoietic Progenitor-Cell Support, in Patients with Advanced Refractory Tumors. *Biol. Blood Marrow Transplant.* 13, 1324–1337 (2007).
39. Hutson, P. R. et al. Effect of medical castration on CYP3A4 enzyme activity using the erythromycin breath test. *Cancer Chemother. Pharmacol.* 62, 373–377 (2008).
40. James, N. D. et al. Addition of docetaxel, zoledronic acid, or both to first-line long-term hormone therapy in prostate cancer (STAMPEDE): Survival results from an adaptive, multiarm, multistage, platform randomised controlled trial. *Lancet* 387, 1163–1177 (2016).
41. US Food and Drug Administration, Official label Taxotere (docetaxel) NDA 020449. (2015). doi:[https://www.accessdata.fda.gov/drugsatfda\\_docs/label/2015/020449s075lbl.pdf](https://www.accessdata.fda.gov/drugsatfda_docs/label/2015/020449s075lbl.pdf)





## CHAPTER 3.4

Age-associated hematological toxicity  
in metastatic castration-resistant  
prostate cancer patients treated  
with docetaxel in clinical practice

*Drugs Aging. 2018 Feb 8 [Epub ahead of print]*

M.B.S Crombag  
A.H.M. de Vries Schultink  
J.G.C. van Doremalen  
H. Otten  
A.M. Bergman  
J.H.M. Schellens  
J.H. Beijnen  
A.D.R. Huitema

## ABSTRACT

### Background

Older patients with metastatic castration-resistant prostate cancer (mCRPC) may be more prone to chemotherapy-induced hematological toxicity, but tailored docetaxel dosing guidelines in older patients are lacking because of conflicting data.

### Objective

This study aims to evaluate the impact of older age on the incidence of hematological toxicity in mCRPC patients treated with docetaxel in daily clinical practice.

### Methods

mCRPC patients treated with docetaxel between January 2006-2016 at the Netherlands Cancer Institute and Medical Center Slotervaart were included, if dosing and hematological toxicity data were available from electronic patients' records. Impact of age on the incidence of grade 3 and 4 hematological toxicity was evaluated.

### Results

In total 175 patients treated with docetaxel were enrolled, with a median age of 67 years (range 47-86 years). Baseline hematological laboratory values were not age-related. After the first treatment cycle, hematological toxicity occurred significantly more frequently in the oldest age quartile (25%,  $p=0.02$ ) compared to the younger age quartiles (9%, 11%, and 7%, respectively for age quartiles 1, 2, and 3).

### Conclusion

A significantly higher risk of hematological toxicity was noted in the oldest age quartile compared to younger mCRPC patients treated with docetaxel in daily clinical practice.



## INTRODUCTION

Docetaxel is the cornerstone of chemotherapeutic treatment of patients with metastatic castration-resistant prostate cancer (mCRPC). Docetaxel is a highly toxic chemotherapeutic agent with a small therapeutic window.<sup>1</sup> Dose-limiting toxicity of docetaxel is hematological toxicity, including neutropenia and anemia.<sup>2,3</sup> The aged population was well represented in the pivotal clinical trial of docetaxel for mCRPC, which also predominantly occurs in older men. However, this trial included relatively fit older patients due to its strict exclusion criteria.<sup>4</sup> In the selected patient cohort of this clinical trial, drug-related infections and anemia occurred at a more than 10% higher rate in mCRPC patients aged 65 years or older compared to younger mCRPC patients.<sup>1,5</sup> The incidence of hematological toxicities may be even higher in routine clinical practice due to the heterogeneity of the treated patient population, including frail patients.<sup>6,7</sup>

Body composition changes with increasing age, which can be expected to influence the pharmacokinetics of lipophilic chemotherapeutic agents, such as docetaxel.<sup>8,9</sup> Moreover, multiple comorbidities and physiological changes with increasing age may lead to altered pharmacokinetics of docetaxel.<sup>10-12</sup> Due to these potential differences in pharmacokinetics with increasing age, tolerability of docetaxel may be altered in older patients. Furthermore, older people may be more susceptible to hematological toxicity due to a reduced bone marrow reserve or increased sensitivity of bone marrow to docetaxel treatment.<sup>13</sup>

Neither the FDA drug label nor the EMA Summary of Product Characteristics (SmPC) describe the need for dose adjustments in older patients,<sup>1,5</sup> but conflicting results have been published regarding the safety profile of docetaxel administered to the older mCRPC patient population in clinical trials and observational studies in routine clinical practice.<sup>14-17</sup> Thus far, there are no specific guidelines for treatment of older mCRPC patients with docetaxel, because of a lack of conclusive evidence to support tailored advice for this heterogeneous group of patients.<sup>18</sup>

Therefore, the objective of this multicenter retrospective study was to evaluate the impact of older age on the incidence of hematological toxicity in mCRPC patients treated with docetaxel. Furthermore, the influence of increasing age on tolerability of docetaxel in mCRPC patients was assessed by evaluating treatment discontinuation and dose intensity over multiple treatment cycles.

## **PATIENTS AND METHODS**

### **Inclusion and exclusion criteria**

Patients with mCRPC who were treated with docetaxel between January 2006 and January 2016 at the Netherlands Cancer Institute (NKI) or the Medical Center Slotervaart (MCS; Amsterdam, The Netherlands) were eligible for inclusion. Docetaxel was prescribed as monotherapy and was administered according to protocol, with fixed infusion rates, dose reduction guidelines, and anti-emetics treatment. The impact of older age was evaluated with age handled as an ordinal variable, divided into quartiles, and as a continuous variable.

Patients were excluded if no hematological laboratory measurements were available, only baseline measurements could be obtained, the per protocol dosage was not recorded, the patient's treatment period exceeded our study period, or if the patient was enrolled in a clinical trial in which docetaxel treatment was part of the intervention.

### **Data collection**

Patient characteristics, and laboratory values were extracted from (electronic) patients' records. The estimated glomerular filtration rate (eGFR) was calculated using the Modification of Diet in Renal Disease (MDRD) equation.<sup>19</sup> Data on docetaxel administrations was collected from the (electronic) patients' records and compounding protocols. Hematological toxicities were collected from (electronic) patients' records and comprised total leukocyte counts, neutrophil counts, platelet counts, and hemoglobin measurements.

## Study design and statistics

Hematological toxicities were graded according to the Common Terminology Criteria for Adverse Events (CTCAE) Version 4.03<sup>20</sup>, in which grade 3 toxicities are considered severe toxicities and grade 4 toxicities as potentially life-threatening toxicities. Primary endpoint of this study was the impact of age on the incidence of grade 3 and 4 hematological toxicity developed after the first treatment cycle of docetaxel. The risk of developing hematological toxicity was analyzed overall, and per type of hematological toxicity in older versus younger patients. Included types of toxicity were leukocytopenia, neutropenia, thrombocytopenia, and anemia. For these analyses, age was handled both as an ordinal variable, divided into quartiles, and as a continuous variable.

Secondary endpoint was treatment tolerability described as the proportion of patients per age quartile per received treatment cycle, dose intensity (DI), and relative dose intensity (RDI). The DI was defined as the actual administered docetaxel dose calculated in mg/m<sup>2</sup>/week. The RDI was defined as the administered dose intensity divided by the per protocol dose intensity, and was calculated over the median number of administered treatment cycles in our study cohort.<sup>21</sup>

Descriptive statistics were used to depict patient characteristics and baseline laboratory values. Fisher's exact test was used to compare the incidence of grade 3 and 4 hematological toxicities per age quartile, and to compare baseline laboratory values between age quartiles. Logistic regression was used to evaluate the impact of age as a continuous variable on hematological toxicity. The impact of age on DI and RDI was assessed using ANOVA.

Statistical analysis was performed using R (Version 3.3.1). A two-sided *p*-value of <0.05 for the different statistical tests was considered significant.

## RESULTS

### Patient population

A total of 195 patients was identified who received docetaxel between January 2006 and January 2016 at both hospitals. During further data collection, 20 patients were excluded, of whom the majority was excluded due to missing hematological laboratory data, as depicted in Fig. 1.

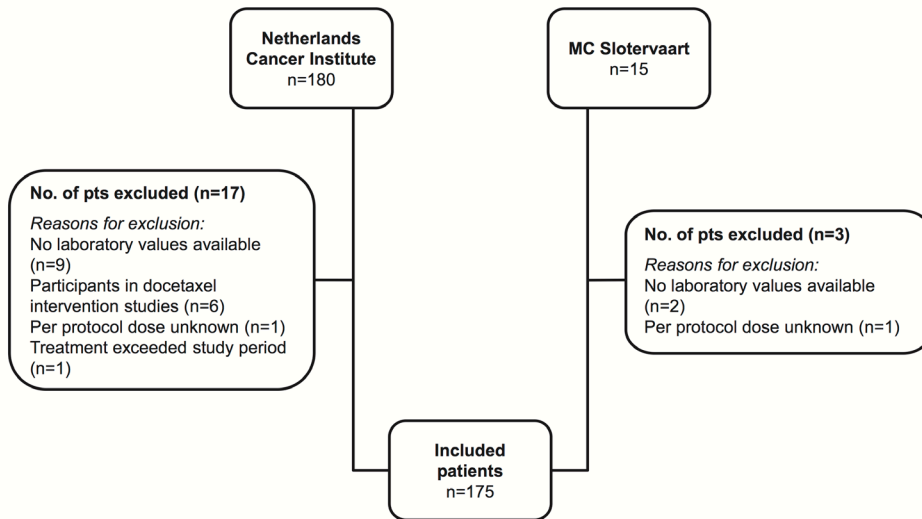


**Figure 1** Flowchart of patient inclusion of both hospitals.

Median age of the 175 remaining patients was 67 years, ranging from 47 to 86 years. There was no significant difference in the distribution of baseline laboratory values between age quartiles, as shown in table 1. Docetaxel was administered as monotherapy in a 3-weekly regimen, generally in a dose of 75 mg/m<sup>2</sup>.

**Table 1** Baseline patients' characteristics.

PARAMETER	AGE QUARTILE 1	AGE QUARTILE 2	AGE QUARTILE 3	AGE QUARTILE 4	P-VALUE
<b>Total, n (%)</b>	<b>44</b>	<b>44</b>	<b>43</b>	<b>44</b>	
Age, median [range]	59 [47-62]	65 [62-67]	69 [67-72]	76 [72-86]	
<b>Hospital, n (%)</b>					
NKI	43 (26)	42 (26)	41 (25)	37 (23)	
MC Slotervaart	1 (8)	2 (17)	2 (17)	7 (58)	
<b>Baseline hematological values</b>					
Leukocytes (109/L), median [IQR]	10 [8-12]	9 [7-14]	8 [6-11]	9 [7-12]	
≥4 (%)	100	97	98	100	1
<4 (%)	0	3	2	0	
Neutrophils (109/L), median [IQR]	8 [6-11]	8 [5-13]	7 [5-10]	8 [5-11]	
≥1.8 (%)	100	100	100	100	1
<1.8 (%)	0	0	0	0	
Platelets (109/L), median [IQR]	264 [219-309]	257 [232-306]	263 [222-320]	278 [208-317]	
≥150 (%)	100	97	95	92	0.34
<150 (%)	0	3	5	8	
Hemoglobin (mmol/L), median [IQR]	8 [8-9]	8 [7-8]	8 [7-9]	8 [7-9]	
≥8.5 (%)	47	23	35	31	0.13
<8.5 (%)	53	77	65	69	
<b>Baseline organ function</b>					
eGFR (mg/min/1,73 m <sup>2</sup> ), median [IQR]	95 [77-106]	95 [80-107]	97 [77-105]	82 [64-93]	
>60 (%)	92	87	85	87	0.82
≤60 (%)	8	13	15	13	
Bilirubin total (μmol/L), median [IQR]	5 [4-7]	5 [4-7]	6 [4-8]	6 [4-11]	
<16 (%)	97	100	97	100	0.49
≥16 (%)	3	0	3	0	

**Table 1 continued**

Alkaline phosphatase (IU/L), median [IQR]	149 [104-339]	176 [113-299]	161 [114-384]	127 [83-189]	
<115 (%)	41	28	25	47	0.13
≥115 (%)	59	72	75	53	
Albumin (109/L), median [IQR]	46 [42-47]	43 [42-47]	45 [42-47]	43 [39-45]	
≥35 (%)	97	94	91	94	0.81
<35 (%)	3	6	9	6	
ALT (IU/L), median [IQR]	30 [21-39]	27 [23-38]	23 [17-28]	22 [15-30]	
<45 (%)	81	88	97	95	0.07
≥45 (%)	19	12	3	5	
AST (IU/L), median [IQR]	26 [21-33]	29 [22-54]	25 [21-34]	28 [22-36]	
<35 (%)	78	64	74	73	0.59
≥35 (%)	22	36	26	27	
PSA (μg/L), median [IQR]	52 [17-244]	88 [33-215]	95 [52-253]	95 [34-195]	
<4 (%)	3	0	3	5	0.80
≥4 (%)	97	100	97	95	

Age quartiles 1-4: patients divided by age into 4 equally sized age groups, ALT = alanine aminotransferase, AST = aspartate aminotransferase, eGFR = estimated glomerular filtration rate, calculated using the Modification of Diet in Renal Disease (MDRD) equation, IQR = interquartile range 25%-75%, PSA = prostate-specific antigen.

## Hematological toxicity

A trend towards more grade 3 and 4 hematological toxicity after the first treatment cycle was observed with age treated as an ordinal variable, divided into age quartiles ( $p=0.08$ ). This difference was driven by the oldest age quartile ( $\geq 72$  years), in which a significantly higher risk of hematological toxicity was observed (25%,  $p=0.02$ ), compared to younger age quartiles (9%, 11%, and 7%, respectively for age quartiles 1, 2, and 3). The impact of age on grade 3 and 4 hematological toxicities remained significant when age was handled as a continuous variable ( $p=0.02$ , odds ratio 1.1, 95% confidence interval 1.01-1.14). For leukocytopenia, the impact of age either treated as an ordinal or as a continuous variable was significant ( $p=0.001$  and  $p=0.004$ , respectively).

For neutropenia, a trend towards a higher incidence of neutropenia was observed with age treated as an ordinal variable, which reached significance when age was handled as a continuous variable ( $p=0.08$  and  $p=0.02$ , respectively). In these separate analyses, patients in the oldest age quartile had a markedly higher risk of developing leukocytopenia and neutropenia compared to their younger counterparts, as depicted in Fig. 2.

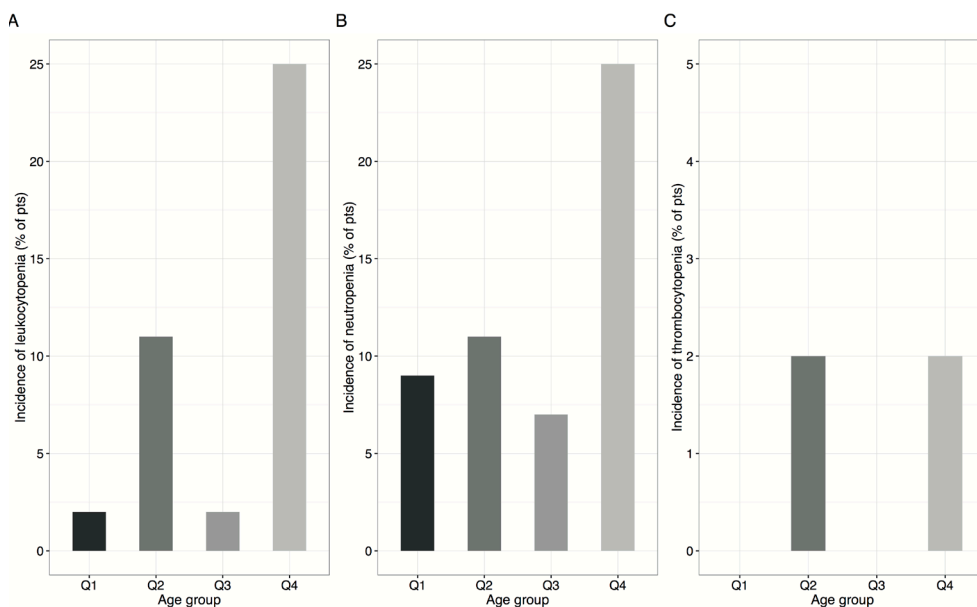


**Figure 2** Incidence of Grade 3/4 hematological toxicity in mCRPC patients. Incidence of (A) leukocytopenia, (B) neutropenia, and (C) thrombocytopenia after the first treatment cycle in patients with metastatic castration-resistant prostate cancer (mCRPC). Q1-Q4: age quartiles 1 to 4, with patients divided by age into four equally sized groups. No metastatic castration-resistant prostate cancer patients developed anemia after cycle 1.

### Dose intensity

After the first administered treatment cycle 7% of patients in the oldest age quartile ( $\geq 72$  years) discontinued treatment, whereas none in the youngest age quartile stopped docetaxel treatment after the first cycle ( $p=0.16$ ). In the total cohort, a median of six cycles of docetaxel was administered. The fraction of patients that received this median number of six treatment cycles was not significantly affected by age treated as an ordinal variable ( $p=0.07$ ). However, a significantly smaller fraction of patients in the oldest age quartile received six treatment cycles (45%,  $p<0.001$ ) compared to the three younger age quartiles (64%, 66%, and 72% for age quartiles 1-3, respectively). The mean DI over the first treatment cycle was not age-related ( $p=0.56$  and  $p=0.88$  for age treated as an ordinal or continuous variable, respectively).

Likewise, no age-related difference in RDI over the first treatment cycle was observed ( $p=0.97$  and  $p=0.37$  for age as an ordinal or continuous variable, respectively). Over the median number of six treatment cycles, mean DI and RDI were not significantly affected by age handled as an ordinal variable, divided into quartiles ( $p=0.16$  and  $p=0.22$ , respectively). However, in the oldest age quartile ( $\geq 72$  years) a significantly lower mean DI was observed compared to the three younger age quartiles ( $p=0.02$ ), with 23 mg/m<sup>2</sup>/week in oldest age quartile compared to 24 mg/m<sup>2</sup>/week in all three younger age quartiles. This difference remained significant when age was handled as a continuous variable ( $p=0.03$ ). Correspondingly, a significantly lower mean RDI over six treatment cycles was noted in patients in the oldest age quartile (73%,  $p=0.002$ ) versus their younger counterparts (82%, 80%, and 86% for age quartiles 1 to 3, respectively), as shown in Fig. 3. The impact of age as a continuous variable on RDI nearly reached significance ( $p=0.05$ ).



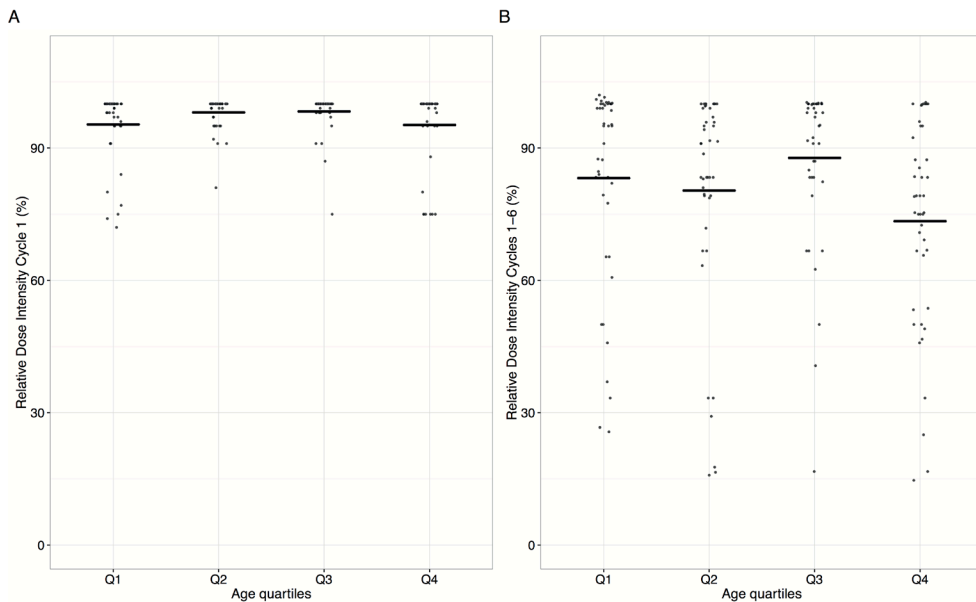


**Figure 3** Relative dose intensity. Relative dose intensity over (A) cycle 1 and (B) cycle 1 to 6 of docetaxel, with the crossbars representing the mean RDI per age quartile. Q1-Q4: age quartiles 1 to 4, with patients divided by age into four equally sized groups.

## DISCUSSION

The oldest fraction of mCRPC patients ( $\geq 72$  years) in our cohort developed significantly more hematological toxicity than their younger counterparts treated with docetaxel in daily clinical practice. The impact of age on hematological toxicity remained significant when age was handled as a continuous variable. No age-related difference in the first administered dose was noted, but after the median of six treatment cycles significantly lower absolute DI and RDI were observed in the oldest patient group. Furthermore, a significantly higher discontinuation rate was observed in the oldest patient group. More than half of patients in the oldest age group did not receive the median number of six treatment cycles, compared to approximately one-third of patients in the younger age quartile groups.

Although various previous studies showed that docetaxel could be safely administered to older mCRPC patients<sup>17,22</sup>, this was balanced by multiple other studies showing an increased risk of docetaxel-related hematological toxicity in older mCRPC patients<sup>14-16,23</sup>, which is also reported in the FDA drug label accordingly.<sup>5</sup> Our results support that hematological toxicity is increased in the oldest group of mCRPC patients treated in daily clinical practice. On the other hand, the relatively low incidence of hematological toxicity observed in younger mCRPC patients in this cohort may be caused by potentially higher clearance and thus lower docetaxel exposure in mCRPC patients compared to other solid tumors, as has previously been suggested for castrated prostate cancer patients.<sup>24</sup> Consequently, one may argue that instead of treating the oldest patients more vigilant, younger mCRPC patients may benefit from higher doses of docetaxel.

Baseline hematological values were not age-related, suggesting that the increased hematological toxicity in elderly is related to increased sensitivity of bone marrow or myeloid precursors to chemotherapy.<sup>13</sup> Besides, potential pharmacokinetic differences may partly explain why the oldest mCRPC patients have a higher risk of developing hematological toxicity compared to younger patients with mCRPC. The significantly lower absolute and relative docetaxel doses administered to these oldest mCRPC patients may also partly be ascribed to these lower nadirs, urging physicians to treat the oldest mCRPC patients more vigilant. The palliative intent of this highly toxic treatment may lower the threshold for dose reductions for all treated patients. This may explain why the observed difference in dose reductions over the different age quartiles is small. It should be kept in mind, however, that physicians' preference may recently have shifted towards more aggressive treatment of patients with metastatic prostate cancer following the results of improved survival with earlier docetaxel treatment.<sup>25,26</sup>

In the current analysis the impact of age was evaluated both as an ordinal variable, with patients divided into equally sized age groups, and as a continuous variable. A limitation of our study is its retrospective design. Data on performance status or geriatric assessments was not fully available.

Because we had no sound information on the administration of prophylactic intravenous granulocyte-colony stimulating factor (G-CSF) during docetaxel treatment in our cohort, only hematological toxicities after the first treatment cycle of docetaxel were included. Although an age of 65 years or older is considered a risk factor for developing neutropenia during chemotherapy treatment<sup>27</sup>, no prophylactic G-CSF administration was applied in either hospital during the first treatment cycle.

## **CONCLUSION**

Within the limits of a retrospective study, we conclude that the oldest ( $\geq 72$  years) mCRPC patients have a significantly higher risk of developing hematological toxicity than their younger counterparts treated in clinical practice. More prospective PK-PD research is warranted to optimize docetaxel treatment in mCRPC patients.

## REFERENCES

1. European Medicines Agency TAXOTERE (docetaxel). SmPC (2015).doi:10.2307/825086
2. European Medicines Agency Summary of Product Characteristics - Opdivo. (2017).
3. Ho, M. Y. & Mackey, J. R. Presentation and management of docetaxel-related adverse effects in patients with breast cancer. *Cancer Manag. Res.* 6, 253-259 (2014).
4. Tannock, I., Wit, R. de & Berry, W. Docetaxel plus prednisone or mitoxantrone plus prednisone for advanced prostate cancer. *N Engl J Med* 351, 1502-12 (2004).
5. Food and Drug Administration Official label - Taxotere, NDA 020449. (2015).
6. Xu, H. et al. Incidence of anemia in patients diagnosed with solid tumors receiving chemotherapy, 2010-2013. *Clin. Epidemiol.* 8, 61-71 (2016).
7. Bhatt, V. & Saleem, A. Review: Drug-induced neutropenia--pathophysiology, clinical features, and management. *Ann. Clin. Lab. Sci.* 34, 131-137 (2004).
8. Sweetman, S. C. *Martindale: the complete drug reference.* (Pharmaceutical press, 2014).
9. Klotz, U. Pharmacokinetics and drug metabolism in the elderly. *Drug Metab. Rev.* 41, 67-76 (2009).
10. Cusack, B. J. Pharmacokinetics in older persons. *Am. J. Geriatr. Pharmacother.* 2, 274-302 (2004).
11. Tan, J. J. L. et al. Age-Related Changes in Hepatic Function: An Update on Implications for Drug Therapy. *Drugs Aging* 32, 999-1009 (2015).
12. Hajjar, E. R., Cafiero, A. C. & Hanlon, J. T. Polypharmacy in elderly patients. *Am. J. Geriatr. Pharmacother.* 5, 345-351 (2007).
13. Lipschitz, D., Udupa, K., Milton, K. & Thompson, C. Effect of Age on Hematopoiesis in Man. *Blood* 63, 502-509 (1984).
14. Shigeta, K. et al. Predictive factors for severe and febrile neutropenia during docetaxel chemotherapy for castration-resistant prostate cancer. *Int. J. Clin. Oncol.* 20, 605-612 (2015).
15. Tije, A. J. ten et al. Prospective evaluation of the pharmacokinetics and toxicity profile of docetaxel in the elderly. *J. Clin. Oncol.* 23, 1070-1077 (2005).

16. Gerritse, F. L. et al. Analysis of docetaxel therapy in elderly ( $\geq 70$  years) castration resistant prostate cancer patients enrolled in the Netherlands Prostate Study. *Eur. J. Cancer* 49, 3176–3183 (2013).
17. Beer, T. M., Berry, W., Wersinger, E. M. & Bland, L. B. Weekly docetaxel in elderly patients with prostate cancer: efficacy and toxicity in patients at least 70 years of age compared with patients younger than 70 years. *Clin. Prostate Cancer* 2, 167–72 (2003).
18. Wong, H.-L., Lok, S. W., Wong, S., Parente, P. & Rosenthal, M. Docetaxel in very elderly men with metastatic castration-resistant prostate cancer. *Prostate Int.* 3, 42–46 (2015).
19. Jones, G. R. & Lim, E.-M. The National Kidney Foundation Guideline on Estimation of the Glomerular Filtration Rate. *Clin. Biochem. Rev.* 24, 95–98 (2003).
20. Institute, N. cancer Common Terminology Criteria for Adverse Events (CTCAE) Common Terminology Criteria for Adverse Events v4.0 (CTCAE). (2009).
21. Hryniuk, W. M. & Goodyear, M. The calculation of received dose intensity. *J. Clin. Oncol.* 8, 1935–1937 (1990).
22. Puisset, F. et al. Clinical pharmacodynamic factors in docetaxel toxicity. *Br. J. Cancer* 97, 290–6 (2007).
23. Horgan, A. M. et al. Tolerability and efficacy of docetaxel in older men with metastatic castrate-resistant prostate cancer (mCRPC) in the TAX 327 trial. *J. Geriatr Oncol* 5, 119–126 (2014).
24. Franke, R. M., Carducci, M. A., Rudek, M. A., Baker, S. D. & Sparreboom, A. Castration-dependent pharmacokinetics of docetaxel in patients with prostate cancer. *J. Clin. Oncol.* 28, 4562–4567 (2010).
25. Sweeney, C. J. et al. Chemohormonal Therapy in Metastatic Hormone-Sensitive Prostate Cancer. *N. Engl. J. Med.* 373, 737–46 (2015).
26. Vale, C. L. et al. Addition of docetaxel or bisphosphonates to standard of care in men with localised or metastatic, hormone-sensitive prostate cancer: A systematic review and meta-analyses of aggregate data. *Lancet Oncol.* 17, 243–256 (2016).
27. Aapro, M. S. et al. 2010 update of EORTC guidelines for the use of granulocyte-colony stimulating factor to reduce the incidence of chemotherapy-induced febrile neutropenia in adult patients with lymphoproliferative disorders and solid tumours. *Eur. J. Cancer* 47, 8–32 (2011).





# CHAPTER 4

CONCLUSIONS & SUMMARY





## CONCLUSIONS & PERSPECTIVES

In this thesis the application of modeling and simulation (M&S) methods to support drug development and to improve treatment with existing therapies in the area of oncology is described.

### **Pharmacokinetics and pharmacodynamics: Tamoxifen**

Different aspects of treatment optimization of tamoxifen in estrogen-receptor (ER)-positive breast cancer patients are described in the first chapter of this thesis. Tamoxifen has been the cornerstone treatment of endocrine breast cancer since the 1980s. Almost thirty years later, ways to further optimize tamoxifen treatment are still subject of investigation. Treatment individualization of this drug started by selecting patients with breast cancers expressing ERs to receive tamoxifen treatment. Tamoxifen is metabolized into different metabolites. The metabolites 4-hydroxy-tamoxifen and endoxifen have 30- to 100-fold higher potency in suppressing cell proliferations compared to tamoxifen itself.<sup>1,2</sup> Of these two metabolites, endoxifen is the most abundant and, therefore, known as the most important active metabolite of tamoxifen. Nowadays, research is focussed on further improving breast cancer recurrence rates by evaluating predictors of recurrence such as variability in exposure to endoxifen and variability in the activity of genes encoding enzymes important in bioactivation of tamoxifen

An overview of the literature is given in chapter 1.1, evaluating the effects of differences in pharmacogenetics on the pharmacokinetics (PK) and pharmacodynamics (PD) of tamoxifen and tamoxifen metabolites. This review demonstrates that alterations in genes encoding metabolizing enzymes are of minimal impact on the exposure to metabolites of tamoxifen, except for CYP2D6. The CYP2D6 genotype can explain part of the variability in endoxifen concentrations, however, the endoxifen concentration is not solely dependent on this genotype. Furthermore, effects of the CYP2D6 genotype on breast cancer outcome (PD) show conflicting results, where some studies demonstrated that indeed CYP2D6 poor metabolisers had worse recurrence-free survival while other studies did not.

The review described in chapter 1.1 concludes that the *CYP2D6* genotype is not an optimal predictor of breast cancer outcome in ER-positive breast cancer patients treated with tamoxifen, because it does not fully represent the exposure to endoxifen. Therefore, quantification of the true exposure by determination of endoxifen plasma concentrations is suggested to be the best way forward to individualize tamoxifen treatment. In this respect Therapeutic Drug Monitoring (TDM) of endoxifen can be applied by increasing the dose in patients with low endoxifen concentrations.

Chapter 1.2. evaluates whether an anti-estrogenic activity score (AAS), based on plasma concentrations of tamoxifen and three metabolites, is a better predictor for recurrence-free survival than only endoxifen concentrations. The AAS integrates the anti-estrogenic activity of tamoxifen and three metabolites (4-hydroxy-tamoxifen, *N*-desmethyl-tamoxifen and endoxifen) with their abundancies in blood. The results demonstrated that the AAS is a predictor for recurrence-free survival, though not better than only endoxifen concentrations. Therefore, it can be concluded that endoxifen can serve as a proxy for the anti-estrogenic effect of tamoxifen and three of its metabolites. Based on the evaluation of literature and the evaluation of the AAS on breast cancer recurrence a viewpoint is shared in chapter 1.3. This viewpoint states that TDM of endoxifen is the best way forward to individualize tamoxifen treatment. The *CYP2D6* genotype can only explain part of the variability in endoxifen concentrations and is, therefore, not a good predictor of the endoxifen concentration. The problem with implementing TDM of endoxifen in clinical practice is the lack of prospective validation of the endoxifen concentration threshold and its effect on recurrence-free survival. The relationship between an endoxifen concentration threshold and breast cancer recurrences has been reported in a retrospective trial including 1370 ER-positive breast cancer patients that were followed for an average of 7.3 years after inclusion. This analysis demonstrated that patients with endoxifen concentrations  $>5.97$  ng/mL have 26% decreased risk of developing breast cancer recurrence compared to patients with lower endoxifen concentrations.<sup>3</sup> However, different prospective studies were not able to reproduce these findings, albeit with less patients and shorter follow up time. In clinical trial simulations, reported in the last part of this chapter, the feasibility of prospective observational and randomized controlled trials was evaluated.

These simulations demonstrated that for an observational design at least 1500 patients and 15 years of intended follow up are needed to be able to detect a decreased risk of recurrence of 29% in patients with concentrations  $>5.97$  ng/mL, with a power of 80% ( $p < 0.05$ ). None of the performed retrospective or prospective studies had this power. Therefore, a conclusive answer on whether or not TDM of endoxifen is indicated is not yet available. However, these simulations demonstrated that the retrospective trial by Madelensky et al.<sup>3</sup> has a power of around 62% to detect a difference in breast cancer recurrence between patients with low and high endoxifen concentrations. In conclusion, TDM of endoxifen still seems the best way forward for individualising tamoxifen treatment. This simulation demonstrates the added value of using a model-based approach in interpreting previously conducted trials and supporting development of future clinical trials.

### **Pharmacokinetics and pharmacodynamics in drug development: MCLA-128**

Population PK analysis was initially used to solve problems regarding the clinical application of drugs. However, it has become an important tool in drug development as well.<sup>4</sup> It has been a pivotal component of many submissions to the Food and Drug Association, aiming to get regulatory approval for new drugs.<sup>5</sup> Chapter 2 demonstrates how PK-PD modeling can be useful for the translation from preclinical to clinical research in early drug development. These analyses can be used to support decision making regarding dosage and dose schedules for different phases in clinical drug development. In this chapter the application of (translational) PK-PD modeling in the development of MCLA-128, a bispecific monoclonal antibody targeting the HER2 and HER3 receptor, is described.

In chapter 2.1 a preclinical PK-PD model is described, which was developed based on toxicity studies in cynomolgus monkeys and mice. This PK-PD model was able to characterize the PK and PD properties of MCLA-128 and resulted in the prediction of a safe starting dose and efficacious clinical dose for the First-in-Human trial. In this analysis, all available relevant PK and PD data before start of the First-in-Human trial were combined in a comprehensive framework to fully evaluate a safe starting dose and predicted an efficacious dose range.

This analysis shows that translational modeling approaches are very useful for characterization of PK and PD properties of new drugs in animals and is able to make predictions for human use. Subsequently, this type of modeling can support the choice of dosing regimens for First-in-Human trials.

In chapter 2.2 a clinical PK model for MCLA-128 was developed based on data from the First-in-Human trial. The PK model was used to characterize the clinical PK properties of MCLA-128 and to evaluate feasibility of a flat dose in patients with solid tumors. The PK model adequately described the PK characteristics of MCLA-128 over a range of doses. Simulations demonstrated that the effect of body size parameters on the disposition of MCLA-128 was minimal and that flat dosing of the drug is appropriate for patients with solid tumors. This analysis also allowed the evaluation of the predictive value of the preclinical model. The PK model structure for the preclinical and the clinical model were similar. The predictions of the preclinical model, slightly overpredicted the lower MCLA-128 plasma concentrations observed in humans. This was mainly attributable to the difference in variability of target expression in humans compared to cynomolgus monkeys where cynomolgus monkeys express far less HER2 receptors than human patients with HER2 expressing tumors. This analysis illustrates that a preclinical PK model is able to predict clinical exposure to a new drug, not yet evaluated in humans. This analysis also demonstrates that usefulness of a (preclinical) model should always be interpreted given the underlying assumptions of a model, for example the quality of the data and the limitations of an animal model. Transparency on the impact of these assumptions is pivotal for interpreting and using these results to support drug development.

### **Pharmacokinetics and pharmacokinetics: Toxicity**

Adverse effects are a major problem in the treatment with both cytotoxic drugs and newer targeted therapies. Toxicity of anti-cancer drugs can cause dose reductions, dose delays and treatment cessation and can, therefore, negatively affect response to treatment and outcome. Chapter 3 describes how mathematical modeling of adverse effects can be a helpful tool to improve clinical management of anti-cancer drugs.

Chapter 3.1 reports an overview of existing toxicity modeling approaches and reports several model structures that describe relationships between drug concentrations and toxicities, including myelosuppression, cardiovascular adverse effects and ordered categorical adverse effects, such as hand-foot syndrome, proteinuria, diarrhoea and rash. Established PK-PD models can help predict clinical scenarios, to find optimal relationships between exposure and safety. The overview in chapter 3.1 shows that mathematical modeling can provide insight in how toxicities evolve over time and if or what patient-related factors can impact this time course. A longitudinal modeling approach can make efficient use of all available data. For example neutropenia can be categorized as severe or life threatening neutropenia (grade 3 or grade 4). However, using longitudinal data of blood counts (multiple measurements of blood counts over time, per patient), includes all available data, minimizes loss of information and allows for evaluation of changes of toxicity over time.

Trastuzumab is associated with cardiotoxicity, manifesting as a decrease in left-ventricular ejection fraction (LVEF). High-sensitive troponin T is a molecular marker that may allow for earlier detection of drug induced cardiotoxicity. In chapter 3.2 the kinetics and exposure-response relationships of LVEF and troponin T in breast cancer patients receiving anthracyclines and trastuzumab, are quantified. Anthracycline pretreatment has previously been related to the slope of LVEF decline after receiving trastuzumab.<sup>6</sup> In this analysis it was demonstrated that within the group of patients receiving anthracyclines, sensitivity of LVEF decline during trastuzumab treatment is related to peak levels of troponin T during anthracycline treatment. This indicates that patients with higher troponin T peaks during anthracycline treatments experienced more cardiac damage and are, therefore, more sensitive for LVEF decline under trastuzumab treatment. Troponin T levels could potentially be used as a biomarker to predict LVEF decline and improve cardiac monitoring schedules in this patient population.

Cytotoxic anti-cancer drugs are notorious for causing hematological toxicity. Severe neutropenia is known as the major dose limiting toxicity for many of these drugs, including docetaxel. In chapter 3.3, a meta-analysis is described to evaluate the differences in neutropenia and exposure to docetaxel between

patients with metastatic castration-resistant prostate cancer (mCRPC) versus patients with other solid tumors. The incidence of neutropenia in mCRPC patients treated with docetaxel has been reported to be lower compared to patients with other solid tumors treated with a similar dose. It has been suggested that this is due to increased clearance of docetaxel in mCRPC patients, resulting in decreased exposure.<sup>7</sup> The current meta-analysis included 26 trials and 36 cohorts (n=1150) and used a random effects model to evaluate the data. Patients with mCRPC had a significantly (1.8-fold) lower mean area under the concentration-time curve than patients with other solid tumors. A logistic regression analysis showed that patients with mCRPC and treated with docetaxel in clinical practice had a 2.2-fold lower odds of developing grade 3/4 neutropenia compared to patients with other solid tumors. These findings indicate that mCRPC patients have a lower risk of experiencing severe neutropenia, possibly attributable to lower systemic exposure to docetaxel. In chapter 3.4 the effect of age on docetaxel-induced neutropenia is evaluated in patients with mCRPC, and demonstrated that older patients ( $\geq 70$  years) have a significantly higher risk of developing hematological toxicity than younger patients, probably due to deprived bone marrow reserve or increased sensitivity to docetaxel treatment and less to exposure.<sup>8,9</sup>

In conclusion, this thesis describes different examples of applying M&S methods to improve current treatments and support development of new drugs in oncology. It demonstrates that pharmacometrics provides a powerful technique to answer (clinical) pharmacological questions that are much more difficult to answer using conventional statistical methods. It allows for clinical trial simulations beyond the setting of an experimental design and can, therefore, contribute to efficient development of future clinical trials. In early drug development, population PK-PD modeling can support translational questions from preclinical to the clinical setting, predicting exposure and response in humans and support selection of safe and efficacious clinical dose schedules. At the same time discrepancies between predictions based on preclinical data and eventual clinical data improve our understanding of and/or can confirm mechanistic and pathophysiological differences between animal models and humans, in a quantitative way.

Additionally, pharmacometric models are able to integrate all available data and add a time component, minimizing loss of information and allowing evaluation of changes over time. Model-based evaluation of PK-PD relationships is also vital when concentration or dose-response relationships are not straightforward, for example when drug response shows a delay in relation to drug exposure.

The examples of applying pharmacometrics in this thesis, are applied to the therapeutic area of oncology, though can in part also be applied to pharmacological questions in other therapeutic fields and contribute to better and safer drug treatment in patients.

## REFERENCES

1. Lim, Y.C., Desta, Z., Flockhart, D.A. & Skaar, T.C. Endoxifen (4-hydroxy-N-desmethyl-tamoxifen) has anti-estrogenic effects in breast cancer cells with potency similar to 4-hydroxy-tamoxifen. *Cancer Chemother. Pharmacol.* 55, 471-8 (2005).
2. Johnson, M. D. et al. Pharmacological characterization of 4-hydroxy- N -desmethyl tamoxifen, a novel active metabolite of tamoxifen. *Breast Cancer Res. Treat.* 85, 151-159 (2004).
3. Madlensky, L. et al. Tamoxifen metabolite concentrations, CYP2D6 genotype, and breast cancer outcomes. *Clin. Pharmacol. Ther.* 89, 718-25 (2011).
4. Derendorf, H. et al. Pharmacokinetic/pharmacodynamic modeling in drug research and development. *J. Clin. Pharmacol.* 40, 1399-1418 (2000).
5. Lee, J. et al. Impact of pharmacometric analyses on new drug approval and labelling decisions: A review of 198 submissions between 2000 and 2008. *Clin. Pharmacokinet.* 50, 627-635 (2011).
6. Hasselt, J.G.C. van, Boekhout, A.H., Beijnen, J.H., Schellens, J.H.M. & Huitema, A.D.R. Population pharmacokinetic-pharmacodynamic analysis of trastuzumab-associated cardiotoxicity. *Clin. Pharmacol. Ther.* 90, 126-132 (2011).
7. Franke, R.M., Carducci, M.A., Rudek, M.A., Baker, S.D. & Sparreboom, A. Castration-dependent pharmacokinetics of docetaxel in patients with prostate cancer. *J. Clin. Oncol.* 28, 4562-4567 (2010).
8. Lipschitz, D., Udupa, K., Milton, K. & Thompson, C. Effect of Age on Hematopoiesis in Man. *Blood* 63, 502-509 (1984).
9. Bruno, B.R. et al. Population Pharmacokinetics / Pharmacodynamics of Docetaxel in Phase II Studies in Patients With Cancer. *J. Clin. Oncol.* 16, 187-196 (1998).







## SUMMARY

This thesis describes the application of pharmacometrics to optimize treatment with existing therapies and to support development of novel drugs in the area of oncology. In the field of pharmacometrics, data on pharmacokinetic (PK) and pharmacodynamic (PD) properties of drugs are characterized using a combination of mathematical and statistical models. These properties give insight in the fate of a drug in the body (PK) and in its desired and undesired (toxic) effects (PD). Quantification of PK-PD relationships in mathematical and statistical models allows for understanding the characteristics of a drug. Additionally, these models can help answer questions to improve clinical application of drugs and supports decision making in drug development.

### **Pharmacokinetics and pharmacodynamics: tamoxifen**

Different aspects of treatment optimization for tamoxifen in estrogen-receptor (ER)-positive breast cancer patients are described in the first chapter of this thesis. Tamoxifen is bioactivated by cytochrome P450 (CYP) enzymes, resulting in the formation of metabolites, e.g. 4-hydroxy-tamoxifen and endoxifen. These metabolites have a much higher anti-estrogenic activity compared to tamoxifen. Chapter 1.1 reviews published data on the effect of various genetic polymorphisms in CYP encoding genes on the PK and PD of tamoxifen. Review of the data demonstrated no clear associations between genetic alterations and PK and PD outcome measures, except for CYP2D6. A clear gene-exposure effect was found for alterations in the *CYP2D6* genotype. This genotype explained part of the interindividual variability in plasma concentrations of the pharmacologically most active metabolite endoxifen. However, a clear gene-response effect for the *CYP2D6* genotype remained controversial. This controversy and the partial contribution of genotype in explaining interindividual variability in plasma concentrations of, in particular, endoxifen, imply that tailored tamoxifen treatment may not be fully realized through pharmacogenetics of metabolizing enzymes alone.

In a retrospective analysis, endoxifen concentrations of > 5.97 ng/mL have been associated with improved breast cancer recurrence in tamoxifen-treated patients.

However, as previously described, tamoxifen itself and other metabolites also show anti-estrogenic anti-tumor activity. Therefore, the aim of chapter 2.2. was to develop a comprehensive Antiestrogenic Activity Score (AAS) and subsequently, to evaluate if this score is a better predictor for recurrence-free survival compared to only endoxifen concentrations. The AAS integrates the anti-estrogenic activity of tamoxifen and three metabolites with their abundancies in blood. The anti-estrogenic activities of tamoxifen, endoxifen, 4-hydroxytamoxifen and N-desmethyltamoxifen were determined in a cell proliferation assay. Tamoxifen and metabolite concentrations and recurrence-free survival data were available from 1370 patients. The results demonstrated that the AAS is a predictor for recurrence-free survival, though not better than the endoxifen PK target concentration of 5.97 ng/mL. Therefore, it can be concluded that endoxifen can serve as a proxy for the anti-estrogenic effect of tamoxifen and three of its metabolites.

The findings in chapter 1.1 and 1.2 support the viewpoint on treatment individualization of tamoxifen, described in chapter 1.3. Regardless of the controversial findings regarding a gene-response relationship for the *CYP2D6* genotype and recurrence-free survival, the debate on what the best strategy is for treatment individualisation of tamoxifen remains. In chapter 1.3 Therapeutic Drug Monitoring (TDM) of endoxifen is highlighted to be the preferred methodology for treatment optimization of tamoxifen compared to *CYP2D6* genotyping. The *CYP2D6* genotype can only explain part of the inter-individual variability in endoxifen concentrations and is, therefore, not an optimal predictor of the endoxifen concentration. TDM of endoxifen can help improve treatment outcome, by increasing the dose of tamoxifen from 20 mg/day to 40 mg/day for patients with endoxifen concentrations below the PK target concentration of 5.97 ng/mL.

Although an exposure-response relationship between endoxifen and treatment outcome has been established, the challenge of implementing TDM of endoxifen in clinical practice remains. This is partly explained by subsequent studies where such a relationship could not be identified. Additionally, the benefits of TDM have not been shown prospectively. Appropriately designed prospective clinical trials will be necessary to be able to demonstrate the potential benefits of TDM.

In chapter 1.4 it is evaluated whether such trials are feasible and which design would be needed. The feasibility of prospective observational and randomized controlled trials was evaluated. These simulations demonstrated that for an observational design to detect an exposure-response relationship at least 1500 patients and 15 years of intended follow up are needed, where patients with endoxifen concentrations  $>5.97$  ng/mL have 29% lower risk of experiencing breast cancer recurrence, with a power of 80% ( $p < 0.05$ ). None of the performed retrospective or prospective studies had this power. Therefore, a conclusive answer on whether or not TDM of endoxifen is indicated is not yet available. However, these simulations demonstrated that the previously reported large retrospective trial has a power of around 62% to detect a difference in breast cancer recurrence between patients with low and high endoxifen concentrations. The simulations in this study demonstrated that prospective evaluation of TDM of endoxifen could be feasible, though would require a large sample size and long follow up time. Additionally, these simulations demonstrate the added value of using a model-based approach in interpreting previously conducted trials and supporting development of future clinical trials.

### **Pharmacokinetics and pharmacodynamics in drug development: MCLA-128**

Chapter 2 demonstrates how PK-PD modeling can be used to support decision making regarding dosage and dose schedules for different phases in clinical drug development. In this chapter the application of (translational) PK-PD modeling in drug development of MCLA-128, a bispecific monoclonal antibody targeting the HER2 and HER3 receptor, is described.

In chapter 2.1 a translational PK-PD model was developed based on data from preclinical studies in cynomolgus monkeys and mice. The model was used to characterize the PK and PD properties of MCLA-128. Subsequently, the model allowed to predict a safe starting dose and efficacious clinical dose for the First-In-Human study, based on area under the concentration-time curves (AUCs), receptor occupancies and PK-PD model simulations. This analysis predicted that a flat dose of 10 to 480 mg MCLA-128, administered every 3 weeks (q3wk) was suitable as starting dose for a First-in-Human study. Flat doses  $\geq 360$  mg q3wk were expected to be efficacious in human.

In chapter 2.2 the data from the First-in-Human trial were used to develop a population PK model for MCLA-128 to characterize its clinical PK properties and to evaluate feasibility of a flat dose of MCLA-128. The PK model adequately described the PK characteristics of MCLA-128 over a range of doses. Simulations demonstrated that dosing based on body size parameters resulted in similar AUC, maximum and trough concentrations of MCLA-128, compared to fixed dosing. This analysis demonstrated that the PK of MCLA-128 exhibits similar disposition characteristics as other therapeutic monoclonal antibodies and that a fixed dose of MCLA-128 in patients with various solid tumors would be appropriate. This analysis also allowed the evaluation of the predictive value of the preclinical model. The PK model structure for the preclinical and the clinical model were similar. Considering some assumptions, the preclinical PK model was able to predict clinical exposure to a new drug, not yet evaluated in humans.

The analyses described in chapter 2 showed that translational modeling approaches are very useful for characterization of PK and PD properties of new drugs in animals and enable predictions for human use. Subsequently, this type of modelling can support the choice of dosing regimens for First-in-Human trials.

### **Pharmacokinetics and pharmacokinetics: toxicity**

Adverse effects of treatment with both cytotoxic drugs and newer targeted therapies can affect patients' quality of life. In addition, adverse effects can impact the proposed dosing regimen by causing dose reductions, dose delays and treatment cessation. Therefore, toxicity of these drugs can affect response to treatment and outcome. In chapter 3 quantitative models are described that relate drug exposure to the dynamics of adverse effects and shows how these models can be instrumental to optimize dosing schedules. In addition the relation between docetaxel exposure and toxicity for patients with metastatic castration-resistant prostate cancer (mCRPC) is reported.

Chapter 3.1 provides a perspective of how adverse effects of these drugs can be modelled and reports model structures that describe relationships between drug concentrations and toxicities, including: myelosuppression, cardiovascular adverse effects and ordered categorical adverse effects, such as hand-foot syndrome, proteinuria, diarrhoea and rash. Established PK-PD models can help predict clinical scenarios, to find optimal relationships between exposure and safety. A longitudinal modeling approach includes all available data, minimizes loss of information and allows for evaluation of changes of toxicity over time.

Chapter 3.2 reports a PD model for cardiac biomarkers in breast cancer patients treated with anthracycline and trastuzumab containing regimens. Trastuzumab is associated with cardiotoxicity, manifesting as a decrease in left-ventricular ejection fraction (LVEF). Administration of anthracyclines prior to trastuzumab increases risk of cardiotoxicity. High-sensitive troponin T and N-terminal-pro-brain natriuretic peptide (NT-proBNP) are molecular markers that may allow earlier detection of drug-induced cardiotoxicity. PD models for troponin T and LVEF were successfully developed and identified the maximum troponin T concentration (an indicator for cardiac damage) after anthracycline treatment as a significant determinant for trastuzumab-induced LVEF decline. These models can help identify patients at risk of drug-induced cardiotoxicity and can potentially optimize cardiac monitoring strategies.

Severe neutropenia is known as the major dose limiting toxicity for many cytotoxic anti-cancer drugs, including docetaxel. In chapter 3.3, a meta-analysis is described to evaluate the differences in neutropenia and exposure to docetaxel between docetaxel-treated patients with mCRPC versus patients with other solid tumors. The incidence of neutropenia in mCRPC patients treated with docetaxel has been reported to be lower compared to patients with other solid tumors treated with a similar dose. This analysis demonstrated that patients with mCRPC had a significantly (1.8-fold) lower mean AUC than patients with other solid tumors. Additionally, patients with mCRPC treated with docetaxel in clinical practice had a 2.2-fold lower odds of developing grade 3/4 neutropenia compared to patients with other solid tumors.

These findings indicate that mCRPC patients have a lower risk of experiencing severe neutropenia, possibly attributable to lower systemic exposure to docetaxel.

Lastly, in chapter 3.4 the effect of age on docetaxel-induced neutropenia is evaluated in patients with mCRPC, to support selection of patients in chapter 3.3. The analysis in chapter 3.4 demonstrated that older patients have a significantly higher risk of developing hematological toxicity than younger patients in daily clinical practice. This is assumed to be caused by a deprived bone marrow reserve or increased sensitivity to docetaxel treatment.

In conclusion, this thesis describes various examples of applying modeling and simulation methods to improve current treatments and support development of new drugs in oncology. It demonstrates that pharmacometrics provides powerful techniques to answer (clinical) pharmacological questions that are often impossible to answer using conventional statistical methods. The examples in this thesis, are applied to the therapeutic area of oncology, though can in part also be applied to answer pharmacological questions in other therapeutic fields and contribute to improved and safer drug treatment in patients.







## NEDERLANDSE SAMENVATTING

Dit proefschrift omschrijft de toepassing van farmacometrische technieken om behandeling met bestaande oncologische geneesmiddelen te verbeteren en om geneesmiddelontwikkeling van nieuwe oncologische middelen te ondersteunen. Binnen de farmacometrie worden farmacokinetische en farmacodynamische eigenschappen van geneesmiddelen gekarakteriseerd, wiskundige en statistische modellen worden ontwikkeld op basis van (patiënten) data. Deze eigenschappen geven inzicht in de processen die een geneesmiddel ondergaat in het lichaam (de PK) en de effecten en bijwerkingen van een geneesmiddel (de PD). Het kwantificeren van deze zogenaamde PK-PD relaties in wiskundige en statistische modellen biedt de mogelijkheid om de karakteristieken van een geneesmiddel te begrijpen. Daarnaast kunnen deze modellen helpen bij het verbeteren van de klinische toepasbaarheid van geneesmiddelen en kunnen ze nuttig zijn voor het maken van beslissingen tijdens de ontwikkeling van een geneesmiddel.

### **Farmacokinetiek en farmacodynamiek: Tamoxifen**

Verschillende aspecten van het optimaliseren van de behandeling met tamoxifen voor patiënten met oestrogeen-receptor positieve borstkanker, worden beschreven in het eerste hoofdstuk van dit proefschrift. Tamoxifen wordt gemetaboliseerd door cytochroom P450 (CYP) enzymen, wat leidt tot de formatie van metabolieten zoals, 4-hydroxy-tamoxifen en endoxifen. Hoofdstuk 1.1 is een review van de gepubliceerde data naar het effect van verschillende genetische polymorfismen, in genen die CYP-enzymen coderen, op de PK en PD van tamoxifen. Een review van deze literatuur liet zien dat er geen duidelijke associatie is tussen genetische afwijkingen en de PK en PD uitkomstmaten, behalve voor het *CYP2D6* genotype. Een duidelijke relatie tussen genotype en blootstelling werd gevonden voor het *CYP2D6* genotype. Dit genotype kon een deel van de interindividuele variabiliteit in plasma concentraties van endoxifen, de farmacologisch meest actieve metaboliet van tamoxifen, verklaren. Echter, voor een relatie tussen genotype en response werden tegenstrijdige resultaten gevonden.

Deze controversie en daarnaast de partiele bijdrage van het genotype aan de variabiliteit van de plasma concentraties van endoxifen, impliceren dat dosis individualisatie van tamoxifen niet gerealiseerd kan worden met behulp van farmacogenetische afwijkingen van metaboliserende enzymen.

In een retrospectieve analyse, werd aangetoond dat endoxifen concentraties van  $>5.97$  ng/mL geassocieerd zijn met een verbeterde borstkanker uitkomst in patiënten behandeld met tamoxifen. Echter, zoals eerder beschreven, hebben tamoxifen zelf en andere metabolieten ook anti-oestrogene activiteit. Hoofdstuk 2.2. beschrijft de ontwikkeling van een anti-oestrogene activiteitsscore (AAS) score. In dit hoofdstuk wordt onderzocht of deze score een betere predictor is voor recurrence vrije overleving dan endoxifen concentraties. De AAS integreert de anti-oestrogene activiteit van tamoxifen en drie metabolieten met hun concentraties in bloed. De anti-oestrogene activiteit van endoxifen, 4-hydroxy-tamoxifen en N-desmethyltamoxifen werden bepaald in een cel-proliferatie experiment. Tamoxifen en metaboliet concentraties en recurrence vrije overlevingsdata waren beschikbaar voor 1370 patiënten. De resultaten van de analyse lieten zien dat de AAS een voorspeller is van recurrence vrije overleving, echter was de AAS niet beter in het voorspellen van recurrence dan de endoxifen target concentratie van  $5.97$  ng/mL. Hieruit kan geconcludeerd worden dat endoxifen een proxy is voor het totale anti-oestrogene effect van tamoxifen en drie metabolieten.

De bevindingen in hoofdstuk 1.1 en 1.2 ondersteunen de point of view m.b.t. dosis individualisatie van tamoxifen omschreven in hoofdstuk 1.3. Ongeacht de controversiële bevindingen wat betreft een genotype-response relatie voor CYP2D6 en recurrence vrije overleving, blijft de discussie over de beste therapie voor de individualisatie van tamoxifen behandeling bestaan. In hoofdstuk 1.3 wordt omschreven waarom Therapeutic Drug Monitoring (TDM) van endoxifen de voorkeur heeft in vergelijking met CYP2D6 genotypen. Het CYP2D6 genotype kan enkel een deel van de interindividuele variabiliteit in endoxifen concentraties verklaren, en is om die reden geen optimale voorspeller voor de endoxifen concentratie. TDM van endoxifen kan helpen om behandelingsuitkomsten te verbeteren door patiënten met endoxifen concentraties van  $5.97$  ng/mL of lager een dosis verhoging te geven van  $20$  mg/dag naar  $40$  mg/dag tamoxifen.

Ondanks de bewijsvoering voor een relatie tussen endoxifen concentraties en verbeterde borstkanker recurrence cijfers, blijft het een uitdaging om TDM van endoxifen te implementeren in de klinische praktijk. Dit komt omdat vervolgstudies een dergelijke relatie niet konden identificeren. Daarnaast zijn de voordelen van TDM niet prospectief bewezen effectief. Goed ontwikkelde trials zijn nodig om de voordelen van TDM aan te tonen. In hoofdstuk 1.4 wordt de haalbaarheid van prospectieve observationele en gerandomiseerde studies geëvalueerd. Simulaties lieten zien dat voor een observationele studies op zijn minst 1500 patiënten en een intentionele follow up van 15 jaar nodig zijn om een effect van endoxifen concentraties  $>5.97$  ng/mL op borstkanker recurrence (hazard ratio 0.71) te laten zien met een power van 80% ( $p < 0.05$ ). Geen van de eerder uitgevoerde retrospectieve of prospectieve studies hebben een dergelijke power. De simulaties lieten zien dat de eerder gerapporteerde retrospectieve studie een power van ongeveer 62% had om dit verschil in recurrence tussen patiënten met hoge en lage endoxifen concentraties te kunnen laten zien. De simulaties in deze studie laten zien dat de prospectieve evaluatie van TDM van endoxifen haalbaar is, maar dat hiervoor grote patiënten aantallen en een lange follow up tijd nodig zijn. Daarnaast laten deze simulaties zien dat een benadering op basis van modellen nuttig is in het interpreteren van uitgevoerde studies en in het ontwikkelen van nieuwe studies in de toekomst.

### **Farmacokinetiek en farmacodynamiek: MCLA-128**

Hoofdstuk 2 laat zien hoe PK-PD modeleren gebruikt kan worden om beslissingen te maken met betrekking tot dosering en doseringsschema's voor verschillende fases van klinische geneesmiddelontwikkeling. In dit hoofdstuk wordt de toepasbaarheid van (translationele) PK-PD modelering in de ontwikkeling van MCLA-128, een bispecifiek antilichaam met de HER2 en HER3 receptoren als target, omschreven.

In hoofdstuk 2.1 wordt een translationeel PK-PD model ontwikkeld gebaseerd op data uit preklinische studies met cynomolgus apen en muizen. Het model werd gebruikt om de PK en PD eigenschappen van MCLA-128 te karakteriseren. Vervolgens kon met dit model een veilige start dosering en klinisch effectieve dosering voor de First-in-Human studie worden voorspeld.

Deze predictie was gebaseerd op de area under the concentration-time curves (AUC), receptorbezetting en PK-PD model simulaties.

Deze analyse voorspelde dat een gefixeerde dosering van 10 tot 480 mg MCLA-128, toegediend elke 3 weken (q3wk) geschikt was als start dosering voor de First-in-Human studie. Gefixeerde doseringen van 360 mg of meer, q3wk zullen naar verwachting effectief zijn in mensen.

In hoofdstuk 2.2 werd de data van de First-in-Human trial gebruikt om een populatie PK model te ontwikkelen voor MCLA-128 om de klinische PK eigenschappen te karakteriseren en om te evalueren of een gefixeerde dosering geschikt is. Het PK model kon de PK eigenschappen van MCLA-128 voor verschillende doseringen adequaat omschrijven. Simulaties lieten zien dat doseringen aangepast op gewichtsparemeters resulteerde in een vergelijkbare AUC, maximale en minimale concentratie van MCLA-128, in vergelijking met gefixeerde doseringen. Deze analyse laat zien dat de PK van MCLA-18 vergelijkbare dispositie eigenschappen heeft als andere monoklonale antilichamen en dat een gefixeerde dosering gepast is voor patiënten met solide tumoren. De analyse kon ook de voorspellende waarde van het preklinische model onderzoeken. De structuur van het PK model was vergelijkbaar voor het preklinische en klinische model. Wanneer enkele aannames in overweging worden genomen, kan het preklinische PK model de klinische blootstelling aan een nieuw geneesmiddel voorspellen, zonder dat het daarvoor in mensen is geëvalueerd.

De analyses beschreven in hoofdstuk 2 laten zien dat translationele modellen nuttig kunnen zijn in het karakteriseren van PK en PD eigenschappen van nieuwe geneesmiddelen in dieren en dat deze modellen voorspellingen kunnen doen voor toepasbaarheid in mensen. Daarnaast kan dit type modelering de keus voor een bepaald doseringsregime voor een First-in-Human studie, ondersteunen.

## **Farmacokinetiek en farmacodynamiek: toxiciteit**

Cytotoxische anti-kanker geneesmiddelen en meer target-specifieke therapieën hebben beiden bijwerkingen. Deze bijwerkingen kunnen de kwaliteit van leven van patiënten beïnvloeden. Daarnaast kunnen bijwerkingen invloed hebben op de voorgestelde dosering, doordat ze leiden tot dosis reducties, uitstellen van doseringen en stoppen van behandelingen. Toxiciteit kan daardoor het effect van het geneesmiddel dwarsbomen. In hoofdstuk 3 worden kwantitatieve modellen beschreven die de blootstelling aan een geneesmiddel linken aan de dynamiek van bijwerkingen. Dit hoofdstuk laat zien hoe deze modellen nuttig kunnen zijn in het optimaliseren van doseringsschema's. Daarnaast wordt in dit hoofdstuk de relatie tussen de blootstelling aan docetaxel en toxiciteit voor patiënten met gemetastaseerde castratie-resistente prostaatacarinomen (mCRPC) gerapporteerd.

Hoofdstuk 3.1 omschrijft hoe bijwerkingen van anti-kanker geneesmiddelen in een model kunnen worden gekwantificeerd. Daarnaast worden in dit hoofdstuk verschillende modelstructuren gerapporteerd die de relatie tussen geneesmiddelconcentraties en toxiciteit beschrijven, zoals: myelosuppressie, cardiovasculaire bijwerkingen en categorisch geclassificeerde bijwerkingen, zoals hand voet syndroom, proteïnurie, diarree en uitslag. Gerapporteerde PK-PD modellen kunnen klinische scenario's voorspellen, met als doel de optimale balans te vinden tussen blootstelling en veiligheid. Hierbij wordt gebruikt gemaakt van longitudinale data, waarbij alle beschikbare data wordt meegenomen in het model. Hierdoor gaat geen informatie verloren en kan er een inschatting worden gemaakt van de veranderingen in mate van toxiciteit over de tijd.

Hoofdstuk 3.2 beschrijft een PD model voor cardiale biomarkers in borstkanker patiënten die behandeld worden met antracyclines en trastuzumab. Trastuzumab is geassocieerd met cardiotoxiciteit, wat zich manifesteert als een daling in de links-ventriculaire ejectie fractie (LVEF). Het toedienen van antracyclines voor start met trastuzumab heeft een verhoogd risico op cardiotoxiciteit tot gevolg. High-sensitive troponin T en N-terminal-pro-brain natriuretic peptide (NT-proBNP) zijn moleculaire markers die mogelijk in een vroeg stadium geneesmiddel-geïnduceerde cardiotoxiciteit kunnen detecteren.

PD modellen voor troponine T en LVEF werden ontwikkeld en identificeerden dat de maximale troponine T concentratie (een indicatie voor hartschade) na behandeling met antracyclines een significante determinant is voor trastuzumab-geïnduceerde afname in LVEF. Deze modellen kunnen patiënten identificeren die een risico hebben op geneesmiddel-geïnduceerde cardiotoxiciteit en kunnen mogelijk protocollen voor cardiale monitoring optimaliseren.

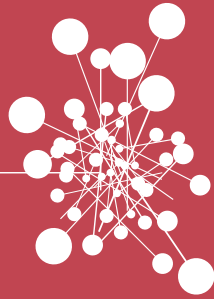
Ernstige neutropenie is een bekende dosis-limiterende toxiciteit voor vele cytotoxische anti-kanker geneesmiddelen, zoals docetaxel. Hoofdstuk 3.3 betreft een meta-analyse waarin de verschillen in neutropenie en blootstelling aan docetaxel tussen patiënten met solide tumoren versus patiënten met mCRPC worden geëvalueerd. De incidentie van neutropenie in patiënten met mCRPC, behandeld met docetaxel, is lager vergeleken met patiënten met solide tumoren, die behandeld werden met een vergelijkbare dosering docetaxel. De analyse in hoofdstuk 3.3 laat zien dat patiënten met mCRPC een significant (1.8x) lagere gemiddelde blootstelling (AUC) hebben dan patiënten met andere solide tumoren. Daarnaast hadden patiënten met mCRPC, behandeld met docetaxel, een 2.2 maal lagere kans om graad 3/4 neutropenie te krijgen in vergelijking met patiënten met andere solide tumoren. Deze bevindingen indiceren dat mCRPC patiënten een lager risico op ernstige neutropenie hebben, wat waarschijnlijk te wijden is aan lagere systemische blootstelling aan docetaxel.

Tot slot, in hoofdstuk 3.4, wordt het effect van leeftijd op docetaxel-geïnduceerde neutropenie geëvalueerd in patiënten met mCRPC. Deze analyse ondersteund de selectie van patiënten in hoofdstuk 3.3. De analyse in hoofdstuk 3.4 laat zien dat oudere patiënten een significant hoger risico hebben op het ontwikkelen van hematologische toxiciteit in vergelijking met jongere patiënten, in de dagelijkse klinische praktijk. De resultaten suggereren dat dit verhoogde risico wordt veroorzaakt doordat ouderen patiënten minder reserve aan bloedcellen hebben in het beenmerg of dat ouderen gevoeliger zijn voor de bijwerkingen van docetaxel.



In conclusie, dit proefschrift omschrijft verschillende voorbeelden van het toepassen van modelering en simulatiemethoden om huidige oncologische therapieën te verbeteren en geneesmiddelontwikkeling van nieuwe oncologische geneesmiddelen te ondersteunen. Het proefschrift laat zien dat een farmacometrische benadering van data een krachtige techniek is om (klinisch) farmacologische vragen te beantwoorden. Dit soort vragen zijn vaak onmogelijk om te beantwoorden met behulp van alleen conventionele statistische methoden. De voorbeelden in dit proefschrift zijn toegepast op de oncologische setting, echter kunnen deze modellen deels ook toegepast worden op andere therapeutische aandachtsgebieden. Deze modellen kunnen bijdragen aan verbeterde en veiligere therapieën voor patiënten.





# APPENDICES



## AUTHOR AFFILIATIONS

### At time of publications

<i>Xanthippi Alexi</i>	Division of Molecular Pathology, Netherlands Cancer Institute-Antoni van Leeuwenhoek, Amsterdam, the Netherlands
<i>Alexander B.H. Bakker</i>	Merus N.V., Utrecht, the Netherlands
<i>Jos H. Beijnen</i>	Department of Pharmacy & Pharmacology, Netherlands Cancer Institute-Antoni van Leeuwenhoek, Amsterdam, the Netherlands; Department of Clinical Pharmacology, Netherlands Cancer Institute-Antoni van Leeuwenhoek, Amsterdam, the Netherlands; Utrecht Institute of Pharmaceutical Sciences, Utrecht University, Utrecht, the Netherlands
<i>Andries M. Bergman</i>	Department of Medical Oncology, Netherlands Cancer Institute-Antoni van Leeuwenhoek, Amsterdam, the Netherlands
<i>Kees Bol</i>	Merus N.V., Utrecht, the Netherlands
<i>Annelies H. Boekhout</i>	Division of Pharmacology, Netherlands Cancer Institute-Antoni van Leeuwenhoek, Amsterdam, the Netherlands

<i>Artur M. Burylo</i>	Division of Pharmacology, Netherlands Cancer Institute-Antoni van Leeuwenhoek, Amsterdam, the Netherlands
<i>Marie-Rose B.S. Crombag</i>	Department of Pharmacy & Pharmacology, Netherlands Cancer Institute-Antoni van Leeuwenhoek, Amsterdam, the Netherlands
<i>Robert P. Doornbos</i>	Merus N.V., Utrecht, the Netherlands
<i>Jacobine G.C. van Doremalen</i>	Utrecht Institute of Pharmaceutical Sciences, Utrecht University, Utrecht, the Netherlands
<i>Thomas P.C. Dorlo</i>	Department of Pharmacy & Pharmacology, Netherlands Cancer Institute-Antoni van Leeuwenhoek, Amsterdam, the Netherlands
<i>Shirley W. Flatt</i>	Moore's Cancer Center, University of California San Diego, United States
<i>Cecile Geuijen</i>	Merus N.V., Utrecht, the Netherlands
<i>Jourik A. Gietema</i>	Department of Medical Oncology University Medical Center Groningen, University of Groningen, Groningen, the Netherlands

<i>Alwin D.R. Huitema</i>	Department of Pharmacy & Pharmacology, Netherlands Cancer Institute-Antoni van Leeuwenhoek, Amsterdam, the Netherlands; Department of Clinical Pharmacy, University Medical Center Utrecht, Utrecht, the Netherlands
<i>J.G. Coen van Hasselt</i>	Division of Systems Biomedicine and Pharmacology, Leiden Academic Centre for Drug Research, Leiden University, Leiden, the Netherlands
<i>Sabine C. Linn</i>	Division of Molecular Pathology, Netherlands Cancer Institute-Antoni van Leeuwenhoek, Amsterdam, the Netherlands; Department of Pathology, University Medical Center, Utrecht, the Netherlands
<i>Lisa Madlensky</i>	Moore's Cancer Center, University of California San Diego, United States
<i>Loki Natarajan</i>	Moore's Cancer Center, University of California San Diego, United States
<i>David Maussang</i>	Merus N.V., Utrecht, the Netherlands
<i>Hans-Martin Otten</i>	Department of Medical Oncology, MC Slotervaart, Amsterdam, Netherlands
<i>Barbara A. Parker</i>	Moore's Cancer Center, University of California San Diego, United States

<i>John P. Pierce</i>	Moore's Cancer Center, University of California San Diego, United States
<i>Jan H.M. Schellens</i>	Department of Medical Oncology, Netherlands Cancer Institute-Antoni van Leeuwenhoek, Amsterdam, the Netherlands; Department of Clinical Pharmacology, Netherlands Cancer Institute-Antoni van Leeuwenhoek, Amsterdam, the Netherlands; Utrecht Institute of Pharmaceutical Sciences, Utrecht University, Utrecht, the Netherlands
<i>Mark Throsby</i>	Merus N.V., Utrecht, the Netherlands
<i>Ernesto Wasserman</i>	Merus N.V., Utrecht, the Netherlands
<i>Alan H.B. Wu</i>	Laboratory Medicine, University of California, San Francisco, United States
<i>Erik van Werkhoven</i>	Department of Biometrics, Netherlands Cancer Institute-Antoni van Leeuwenhoek, Amsterdam, the Netherlands
<i>Wilbert Zwart</i>	Division of Molecular Pathology, Netherlands Cancer Institute-Antoni van Leeuwenhoek, Amsterdam, the Netherlands





## DANKWOORD

Dit boek is af! Graag wil ik iedereen bedanken die hieraan een bijdrage hebben geleverd.

Allereerst wil ik alle patiënten bedanken die hebben meegedaan aan de studies waarop dit proefschrift is gebaseerd. Zonder hun bereidheid om te participeren in deze studies is het doen van klinisch wetenschappelijk onderzoek onmogelijk.

Daarnaast wil ik mijn promotores Alwin Huitema en Jos Beijnen bedanken. Alwin, bedankt voor het vertrouwen dat je mij vanaf het begin hebt gegeven. Met veel plezier heb ik de afgelopen jaren aan mijn onderzoek met jou gewerkt. Dat jij mijn promotor ipv copromotor werd tijdens dit traject is meer dan verdiend, en ik ben dan ook trots om mij een oio van prof. Alwin te mogen noemen. Jos, bedankt voor de mogelijkheid om mijn onderzoek in jouw gerenommeerde onderzoeksgroep te doen. Je betrokkenheid bij de endoxifen en docetaxel projecten heb ik erg gewaardeerd, net zoals je input voor mijn andere manuscripten. Jan, bedankt dat ik mijn opleiding tot klinisch farmacoloog in het AvL kon volbrengen.

Thomas Dorlo, bedankt dat jij in de laatste fase van mijn onderzoek er altijd was voor de technische vragen en waardevolle feedback op mijn manuscripten. Uiteraard ook voor al je werk met betrekking tot de nieuwe research HPC! Beiden hebben bijgedragen aan de snelheid van mijn analyses.

Ik wil graag de leden van de leescommissie, prof. Ronette Gehring, prof. Mirjam Kretzschmar, prof. Catherijne Knibbe, prof. Aukje Mantel en prof. Wilbert Zwart, bedanken voor het doorlezen van mijn leesmap.

Graag wil ik alle medewerkers van de CRU (artsen, verpleegkundigen, VSen), het trialbureau, pathologie en het priklab van het AvL bedanken voor de ondersteuning van het klinische onderzoek in dit proefschrift. Jullie zijn onmisbaar in de praktische uitvoering van de vele studies in het ziekenhuis.

*Huixin and Coen, thank you for inspiring me to do a PhD in this field. Without your introduction into the subject during my internship, I would have completely missed out on this opportunity!*

*Muchas gracias Iñaki, for welcoming me in Pamplona. My stay in your group was a great experience and I am very grateful for the knowledge I have gained in those couple months. Mijn onderzoeksstage in Pamplona werd financieel ondersteund door de René Vogels Stichting NVvO, waarvoor veel dank.*

Daarnaast wil ik Kees Bol, Lex Bakker en Robert Doornbos van Merus bedanken voor de prettige samenwerking van de afgelopen jaren en voor de mogelijkheid die het mij heeft gegeven om inzicht te krijgen in de vele facetten van de geneesmiddelontwikkeling. Erik van Werkhoven, bedankt dat je altijd tijd voor mij had om over de statistiek te praten. Annelies Boekhout, bedankt voor de samenwerking van het cardiotoxiciteit model en voor het delen van de data van de Candy-trial. *Xanthippi Alexi, thank you for the collaboration and for updating the cell proliferation experiments for the AAS-analysis. Prof Pierce and dr. Madlensky, thank you for the collaboration and for sharing your valuable endoxifen data.*

Wat een geweldige tijd heb ik gehad in de Keet, wat later het O-gebouw en daarna H3 werd. Alle OIOs en in het bijzonder de Keet-bewoners, kamergenoten van de notoire room 5 en de harde kern van de koffieclub, bedankt voor de mooie borrels, oio-weekenden, kerstdiners, straaljagers en natuurlijk voor de kritische inzichten. Gedeelde smart is halve smart.

Lieve Rose en Chris, bedankt dat jullie mijn paranimfen willen zijn!

Dierbare vrienden en familie bedankt voor de mentale support, jullie interesse in mijn onderzoek en uiteraard voor de nodige afleiding!

Lieve Thomas, bedankt dat je er altijd voor mij bent. Jouw humor, positieve instelling en ratio hebben mij meerdere malen op de been gehouden tijdens dit traject. Lieve papa en mama, Eem en Do, bedankt voor jullie onvoorwaardelijke support en liefde. Jullie maken mij een gelukkig mens.

## LIST OF PUBLICATIONS

**de Vries Schultink AHM**, Dorlo TPC, Madlensky L, Pierce JP, Beijnen JH, Huitema ADR. Prospective evaluation of Therapeutic Drug Monitoring of Endoxifen: feasibility of observational and randomized trials. *To be submitted*

**de Vries Schultink AHM**, Bol K, Wasserman E, Dorlo TPC, Schellens JHM, Beijnen JH, Huitema ADR. Populations pharmacokinetics of MCLA-128, a HER2/HER3 bispecific monoclonal antibody, in patients with solid tumors. *Submitted*

**de Vries Schultink AHM**, Crombag MBS, van Werkhoven E, Otten H, Bergman AM, Schellens JHM, Huitema ADR, Beijnen JH. Neutropenia and exposure to docetaxel in metastatic castration resistance prostate cancer patients: a meta-analysis. *Cancer Med.* 2019 Feb 22 [Epub ahead of print]

Crombag MBS, **de Vries Schultink AHM**, van Doremalen JGC, Otten H, Bergman AM, Schellens JHM, Beijnen JH, Huitema ADR. Age-associated hematological toxicity in patients treated with docetaxel or docetaxel containing regimens. *Cancer Med.* 2019 Feb 22 [Epub ahead of print]

Crombag MBS, **de Vries Schultink AHM**, Koolen SLW, Wijngaard S, Joerger M, Schellens JHM, Dorlo TPC, van Erp NP, Mathijssen RHJ, Beijnen JH, Huitema ADR. Impact of Older Age on the Exposure of Paclitaxel: a Population Pharmacokinetic Study. *Pharm Res.* 2019 Jan 7;36(2):33.

**de Vries Schultink AHM**, Koomen J, van Triest B, Hendriks JJMA, Haanen JBAG, Beijnen JH, Huitema ADR. Vemurafenib and dabrafenib in combination with radiotherapy and the risk of aggravated radiotoxicity. *Pharmaceutisch weekblad.* 2018 April 153(14):22-27

**de Vries Schultink AHM**, Doornbos RP, Bakker ABH, Bol K, Throsby M, Geuijen C, Maussang D, Schellens JHM, Beijnen JH, Huitema ADR. Translational PK-PD modeling analysis of MCLA-128, a HER2/HER3 bispecific monoclonal antibody, to predict clinical efficacious exposure and dose. *Invest New Drugs.* 2018 Dec;36(6):1006-1015.

**de Vries Schultink AHM**, Huitema ADR, Beijnen JH. Therapeutic Drug Monitoring of endoxifen as an alternative for CYP2D6 genotyping in individualizing tamoxifen therapy. *Breast.* 2018 Aug 22;42:38-40.

van Nuland M, Vreman RA, Ten Ham RMT, **de Vries Schultink AHM**, Rosing H, Schellens JHM, Beijnen JH, Hövels AM. Cost-effectiveness of monitoring endoxifen levels in breast cancer patients adjuvantly treated with tamoxifen. *Breast Cancer Res Treat.* 2018 Jul 13. [Epub ahead of print]

**de Vries Schultink AHM**, Boekhout AH, Gietema JA, Burylo AM, Dorlo TPC, van Hasselt JGC, Schellens JHM, Huitema ADR. Pharmacodynamic modeling of cardiac biomarkers in breast cancer patients treated with anthracycline and trastuzumab regimens. *J Pharmacokinet Pharmacodyn*. 2018 Jun;45(3):431-442.

Bastida C, Ruiz-Esquide V, Pascal M, **de Vries Schultink AHM**, Yagüe J, Sanmartí R, Huitema ADR, Soy D. Fixed dosing of intravenous tocilizumab in rheumatoid arthritis. Results from a population pharmacokinetic analysis. *Br J Clin Pharmacol*. 2018 Apr;84(4):716-725.

van Andel L, Fudio S, Rosing H, Munt S, Miguel-Lillo B, González I, Tibben MM, de Vries N, **de Vries Schultink AHM**, Schellens JHM, Beijnen JH. Pharmacokinetics and excretion of (14)C-Plitidepsin in patients with advanced cancer. *Invest New Drugs*. 2017 Oct;35(5):589-598.

**de Vries Schultink AHM**, Alexi X, van Werkhoven E, Madlensky L, Natarajan L, Flatt SW, Zwart W, Linn SC, Parker BA, Wu AH, Pierce JP, Huitema AD, Beijnen JH. An Antiestrogenic Activity Score for tamoxifen and its metabolites is associated with breast cancer outcome. *Breast Cancer Res Treat*. 2017 Feb;161(3):567-574.

**de Vries Schultink AHM**, Suleiman AA, Schellens JH, Beijnen JH, Huitema AD. Pharmacodynamic modeling of adverse effects of anti-cancer drug treatment. *Eur J Clin Pharmacol*. 2016 Jun;72(6):645-53.

**de Vries Schultink AHM**, Zwart W, Linn SC, Beijnen JH, Huitema AD. Effects of Pharmacogenetics on the Pharmacokinetics and Pharmacodynamics of Tamoxifen. *Clin Pharmacokinet*. 2015 Aug;54(8):797-810.

Abdulla A, van Leeuwen RW, **de Vries Schultink AHM**, Koch BC. Stability of colistimethate sodium in a disposable elastomeric infusion device. *Int J Pharm*. 2015;486(1-2):367-9.

Crombag MR, **de Vries Schultink AHM**, Schellens JH, Beijnen JH, Huitema AD. Incidence of hematologic toxicity in older adults treated with gemcitabine or a gemcitabine-containing regimen in routine clinical practice: a multicentre retrospective cohort study. *Drugs Aging*. 2014 Oct;31(10):737-47.



## **CURRICULUM VITAE**

Aurelia de Vries Schultink was born on January 16th 1988 in Rotterdam, the Netherlands. After graduating from high school at the Adelbert College Wassenaar, she went on to study Pharmacy at the University of Utrecht. During her Masters she performed a scientific internship at the Netherlands Cancer Institute – Antoni van Leeuwenhoek and the Slotervaart Hospital, where she worked on a project looking into the hematological toxicity of gemcitabine in elderly patients. A short second scientific internship followed at the Pharmacometrics group of the University of Uppsala, in Uppsala, Sweden, working on time-to-event modeling. After receiving her PharmD in 2014, she started her PhD research at the Department of Pharmacy & Pharmacology of the Netherlands Cancer Institute – Antoni van Leeuwenhoek, under the supervision of prof. dr. Alwin Huitema, prof. dr. Jos Beijnen and dr. Thomas Dorlo. Her PhD research resulted in this thesis. During her PhD she spent 4 months in the Pharmacometrics & Systems Pharmacology research group at the University of Navarra in Pamplona, Spain. This fellowship was financially supported by a travel grant received from the René Vogels Foundation / Dutch Society for Oncology. In 2017, Aurelia became a board certified clinical pharmacologist of the Dutch Society for Clinical Pharmacology & Biopharmacy. As of July 2018, she started as a resident in St. Antonius hospital in Nieuwegein to become a hospital pharmacist.





